

X. Grigoris

## Stability Optimisation of the top armour row of a breakwater with Xbloc<sup>Plus</sup> units





# Stability Optimisation of the top armour row of a breakwater with Xbloc<sup>Plus</sup> units

By

X. Grigoris

in partial fulfilment of the requirements for the degree of

**Master of Science**  
in Civil Engineering

at the Delft University of Technology,  
to be defended publicly on Thursday June 27, 2019 at 15:00.

Thesis committee: Prof. Dr. ir. S.G.J. Aarninkhof, TU Delft  
Assoc. Prof. Dr.ir. B. Hofland, TU Delft  
Assis. Prof. Dr. ir. A. Antonini, TU Delft  
Ir. B. Reedijk, BAM Infraconsult

An electronic version of this thesis is available at <https://repository.tudelft.nl/>.



**List of trademarks used:**

Delta Marine Consultants [DMC] is a trademark of BAM Infraconsult B.V., with registered office at H.J. Nederhorststraat 1, Gouda, The Netherlands.

Xbloc is a registered trademark of Delta Marine Consultants.

Xbloc<sup>Plus</sup> is a registered trademark of Delta Marine Consultants.

*The use of trademarks in any publications of Delft University of Technology does not imply any endorsement or disapproval of this product by the University.*

## Preface

This thesis is the final step towards the completion of my MSc in Hydraulic Engineering at Delft University of Technology and was performed in cooperation with BAM Infraconsult from September 2018 to June 2019. It would not have been possible without the support of many people.

First, I would like to thank my thesis committee members for their valuable contribution and guidance. Especially, Stefan Aarninkhof, for his enthusiasm and positive attitude, Bas Hofland, for taking my ideas further and attention to detail, Alessandro Antonini for his comments, and Bas Reedijk, for proposing this interesting topic and guiding me on a regular basis.

I would also like to express my gratitude to my colleagues of BAM Infraconsult for the enjoyable working climate, pleasant atmosphere during the lunch breaks the last 10 months and their interest in my topic.

My almost 3-year period at Delft University of Technology was definitely the most demanding experience of my life so far. I would not have been able to complete this journey without the amazing support of my friends and family, to whom I cannot express with words how thankful I am, but I will make an effort. Maria, thank you for all your advice and “trolling” the past 10 years, especially the past year in Utrecht. Vassia, thank you for all the moments we spent together during our studies in Athens and Delft and for the motivation during our numerous “study hours”. Nancy, thank you for all the laughs and for always cheering me up. Sonia, thank you all the deep conversations (no matter the time zone difference) during hectic periods and for all the relaxing summer moments. I would also like to thank the new friends that I made at Delft, with whom we shared easy and difficult moments: Matteo, Alexia, Alejandra, Vaso, Lina, Teni and Vaggy.

Finally, I would like to express my immense love to my parents, Marianna and George, who have mentally and practically supported my endeavours, but, most importantly, who are so difficult to surpass role models.

This thesis is dedicated to the memory of my grandmother, who, for 27 years, was the most caring and giving person in my life.

*Xenofon Grigoris*

*Utrecht, June 2019*

## Abstract

The Xbloc<sup>Plus</sup> (referred to as Xbloc+) is a new, uniformly placed single layer armour unit, developed by Delta Marine Consultants (BAM Infraconsult). Although a breakwater armour layer with Xbloc<sup>Plus</sup> combines material saving and easy placement with increased stability, the transition between the armour layer and the crest is not adequately stable. The Xbloc<sup>Plus</sup> units of the top armour row (crest units) become easily displaced. In this research, several solutions to this problem are investigated through physical modelling, in order to determine the best one.

Firstly, tests are performed on a breakwater with single, Xbloc<sup>Plus</sup> crest elements without rear support, in order to determine the most important parameters and mechanisms contributing to failure. The criterion for initiation of failure for the top armour row is 10%, so when 1 of the 10 crest units fails. Failure of a unit is defined as the condition where contact with the units of the row underneath is lost under at least one of the two wings.

During wave run-up, under the forces resulting from the wave velocities, the Xbloc<sup>Plus</sup> crest units initially rotate and, subsequently, make a combined motion consisting of rotation, vertical and horizontal translation. The main parameters of influence to this movement are the crest freeboard ( $R_c/D_n$ ) and wave steepness ( $s_{op}$ ): for  $R_c/D_n \geq 1.7$ , stability increases for increasing  $R_c/D_n$  and for increasing  $s_{op}$  (from 2% to 4%). For zero freeboard, wave impact forces at breaking proved to be an important mechanism in the case of  $s_{op}=4\%$ , where collapsing breakers occurred. Failure and partial displacement were initiated at stability numbers ( $N_s=H_s/(\Delta D_n)$ ) of 1.39 and 0.74, respectively, for  $R_c/D_n \leq 1.7$ , which are much lower than the stability number for displacement of the armour layer ( $N_s > 3.88$ ).

A second set of tests was conducted, in order to investigate a way of optimising the stability of the transition area between the armour layer and the crest. Under the most critical conditions of the first tests, 7 crest configurations, based on their potential ability to resist the failure mechanisms, were investigated: 2 orientations of the Xbloc+ crest units (with the tail or nose tilted upwards), 2 different ways of placement of Xbloc at the crest, placement of Xbloc with a concrete crown wall element, underlayer rock material at the crest and underlayer rock material with a concrete crown wall element.

From the above "trial and error" approach, it was concluded that the most effective way of increasing stability (optimised configuration) is the provision of a backwards support, which fulfils the criteria of no erosion and no uplift and resists rotation by bringing the rotation point of the Xbloc+ crest elements further to the back.

The form of this concept tested was the placement of underlayer material between the Xbloc+ crest units and under their tails and a concrete element behind, which functions as backwards support to prevent erosion of the rock fill. No displacement of the Xbloc+ crest elements occurred for  $R_c/D_n \leq 1.7$ ,  $2\% \leq s_{op} \leq 4\%$  and no failure happened for  $R_c/D_n=0$ ,  $s_{op}=4\%$  for a stability number up to 3.55. Rocking was decreased to zero. Failure and rocking of 10% happened only at the case of  $R_c/D_n=1.7$ ,  $s_{op}=2\%$  for  $N_s \geq 2.78$ , due to the erosion of the fill, resulting from the uplift of the supporting crest element, with the final damage (at  $N_s=3.49$ ) being repairable and limited at the 4 upper rows of the breakwater.

---

# Table of Contents

Preface

Abstract

Table of Contents .....	1
1. Research Objective and Literature Review .....	1
1.1 Introduction.....	1
1.1.1 Xbloc+ Armour Unit Development .....	1
1.1.2 Top Row of an Armour Layer with Xbloc+ .....	2
1.1.3 Thesis Outline .....	3
1.2 Research Objective .....	4
1.2.1 Problem Definition .....	4
1.2.2 Research Questions .....	4
1.2.3 Research Methodology.....	4
1.3 Literature Review .....	6
1.3.1 Breakwaters.....	6
1.3.1.1 Rubble Mound Breakwater .....	6
1.3.1.2 Failure Mechanisms of the Armour Layer .....	6
1.3.1.3 Loading of the Armour Layer .....	7
1.3.1.4 Concrete Armour Units.....	9
1.3.1.5 Stability of an Armour Layer with Concrete Armour Units .....	10
1.3.1.6 Stability of Low Crested Breakwaters.....	11
1.3.2 Wave Characteristics .....	13
1.3.2.1 Linear Wave Theory.....	13
1.3.2.2 Wave Breaking.....	13
1.3.2.3 Wave-Structure Interaction.....	14
1.3.3 Stability of Breakwater Crest.....	16
1.3.3.1 Classification of Breakwaters based on Crest Height .....	16
1.3.3.2 Parameters of Influence to Crest Stability.....	17
1.3.4 Current Research on Xbloc+ .....	20
1.3.4.1 Stability of the Top Row of an Armour Layer with Xbloc+ .....	20
1.3.4.2 Research on Other Topics Regarding Xbloc+.....	21
1.3.5 Physical Modelling.....	22
1.3.5.1 Similitude in Physical Modelling.....	22
1.3.5.2 Froude Scaling .....	23

1.3.5.3.	Reynolds Scaling .....	23
1.3.5.4.	Stability Scaling .....	24
1.3.5.5.	Permeability Scaling .....	24
1.3.5.6.	Scale Effects .....	24
1.3.5.6.1.	Viscous Scale Effects .....	24
1.3.5.6.2.	Surface Tension Scale Effects .....	25
1.3.5.6.3.	Aeration effects .....	25
1.3.5.6.4.	Friction scale effects .....	25
2.	Physical Model Set-up .....	26
2.1	Wave Flume Configuration .....	26
2.1.1	Wave Gauges .....	26
2.1.2	Foreshore .....	27
2.1.3	Water Level in the Flume .....	27
2.2	Model Breakwater Scaling .....	28
2.2.1	Xbloc+ Model Armour Units .....	28
2.2.2	Underlayer .....	29
2.2.3	Core .....	30
2.2.4	Toe .....	30
2.2.5	Crest .....	30
2.2.6	Rear Slope .....	30
2.2.7	Model Breakwater Cross-section .....	30
2.3	Wave Generation .....	32
2.3.1	Wave Characteristics .....	32
2.3.2	Test Duration .....	32
2.4	Test Program .....	33
2.4.1	1 <sup>st</sup> Test Set .....	33
2.4.2	2 <sup>nd</sup> Test Set .....	34
2.4.3	3 <sup>rd</sup> test set .....	37
2.4.4	Overview – All tests .....	37
2.5	Test Execution .....	39
2.5.1	Methodology .....	39
2.5.2	Visual Observations .....	40
2.5.3	Units’ Movement Definitions .....	40
3.	Results – Tests on Single Xbloc+ Crest Units .....	42
3.1	Failed Units – Single Xbloc+ (1 <sup>st</sup> Test Set) .....	42



3.1.1	Comparison between Initial and Repetition Test Series on the Single Xbloc+ elements (1 <sup>st</sup> Test Set) .....	44
3.2	Rocking units – Single Xbloc+ (1 <sup>st</sup> Test Set) .....	46
3.2.1	Rocking Before Failure Units .....	47
3.2.2	Rocking After Failure units .....	48
3.2.2.1.	Comparison between Rocking Before Failure and Rocking After Failure Units 49	
3.3	Start of Movement – Single Xbloc+ .....	51
3.4	Total Damage to the 4 Upper Rows of the Armour Layer – Single Xbloc+ (1 <sup>st</sup> Test Set) 53	
3.5	Underlayer Effect.....	55
4.	Results – Tests on Crest Configurations and Optimised Configuration (2 <sup>nd</sup> & 3 <sup>rd</sup> Test Sets) 58	
4.1	Results of Tested Crest Configurations (2 <sup>nd</sup> Test Set).....	58
4.2	Results of the Additional Tests on the Optimised Configuration (3 <sup>rd</sup> Test Set).....	61
5.	Failure Mechanisms.....	67
5.1	Xbloc+ Crest Units Motions .....	67
5.2	Influence of Freeboard and Wave Steepness on the Xbloc+ Crest Units Failure Mechanisms.....	70
5.2.1	Wave impact.....	70
5.2.2	Wave run-up velocities.....	71
5.2.3	Conclusions on Failure Mechanisms and Effect of Optimised Configuration .	72
6.	Conclusions and Recommendations .....	74
6.1	Conclusions.....	74
6.2	Recommendations.....	76
6.2.1	Recommendations for further research on the single Xbloc+ crest units.....	76
6.2.2	Recommendations for further research on the optimised configuration.....	76
References	78	
	Appendix A. Literature Review .....	A-1
	Appendix B. Failure Development in Time .....	B-1
	Appendix C. Rocking Before and After Failure Units.....	C-1
	Appendix D. Standard Deviation (for formulas of freeboard influence on critical stability number).....	D-1
	Appendix E. Theoretical Background of the Failure Mechanisms.....	E-2
	Appendix F. Wave Parameters .....	F-1
	Appendix G. Observations during the Experiments .....	G-1
	Appendix H. Experiment Photos.....	H-1

Table of Figures .....i  
Table of Tables.....iii

# 1. Research Objective and Literature Review

## 1.1 Introduction

### 1.1.1 Xbloc+ Armour Unit Development

In 2003 Delta Marine Consultants (BAM Infraconsult) launched an interlocking, randomly placed armour unit, the Xbloc, which has been used in many projects worldwide. Despite the Xbloc's known advantages, such as lower concrete consumption (approximately 10% lower than competitor armour units), there was the need for further optimization. The first reason is that uniform placement, which creates a smooth, more aesthetically attractive surface, is a growing clients' demand, as in the case of the Afsluitdijk renovation. The Xbloc can be placed in such a set-up, but in this way each unit's effectiveness is decreased by 30%, which requires denser packing and, consequently, higher concrete consumption than in the case of random placement. Another reason is that although random placement is prescribed, crane operators tend to place the units in a uniform, repetitive way, leading to less interlocking than calculated in the design and, thus, lower strength than expected.

Therefore, to resolve the above mentioned problems, Delta Marine Consultants developed a new, uniformly placed armour unit, the Xbloc+. An Xbloc+ has the same concrete consumption, but is larger than the equivalent Xbloc (used for the same wave conditions). This results in larger surface coverage on the breakwater slope per Xbloc+ compared to the Xbloc and, thus, lower overall concrete consumption, since fewer units are needed (approximately 30% less units than competitor units for the coverage of the same area). The latter makes the Xbloc+ a very attractive alternative, not only because of the aesthetic result, but also because of its cost-effectiveness.

The shape of the Xbloc+ unit can be seen in Figure 1.1.

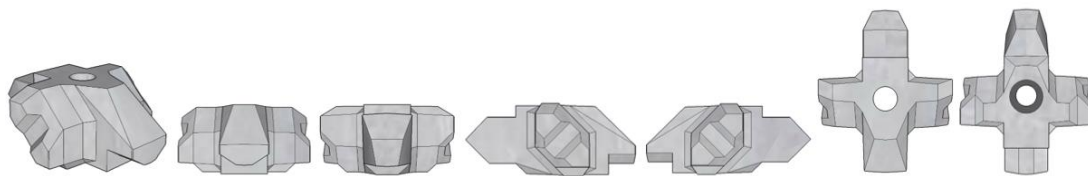


Figure 1.1: Left to right: 3D, Front, Back, Left, Right, Top and Bottom view of the Xbloc+ (Delta Marine Consultants)

The characteristic dimension of the unit is the width ( $D$  or  $L2$  in Figure 1.2).

The following relations hold between the width, the length ( $L$  or  $L3$  in Figure 1.2) and the height ( $H$  or  $L1$  in Figure 1.2) of the Xbloc+ unit:

$$L = 1.27D$$

$$H = 0.50D$$

Other dimensions that follow from the width are: horizontal placement distance:  $D_x = 1.10D$ ; up-slope placement distance:  $D_y = 0.63D$ ; armour layer thickness:  $t_a = 0.80D$ .

The Xbloc+ is horizontal when placed at a breakwater slope of  $35.3^\circ$ . At slopes of  $33.7^\circ$  (2:3) and  $36.8^\circ$  (3:4), it is a bit tilted backwards and forward respectively.

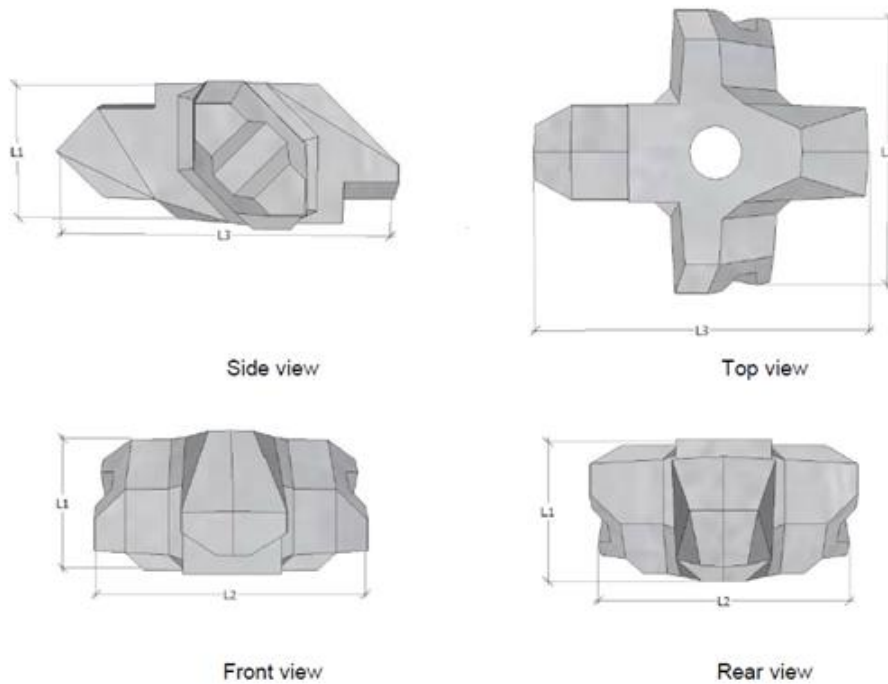


Figure 1.2: Main dimensions of Xbloc+ (DMC Guidelines for Xbloc Concept Design, 2018)

The Xbloc+ has 9 contact surfaces in total. The first contact surface is with the underlayer and is located at the bottom and below the tail of the Xbloc+. The other 8 are with the neighbouring Xbloc+ armour units and are located in the following positions: 2 below the nose (front part) at the left and right side, 1 below and 1 above each of the two wings and 2 on top of the tail at the left and right side.

The Xbloc+ element, when placed at the top row of the armour layer, has only 4 contact surfaces with the neighbouring units, 2 of which are below the nose and 1 below each of the two wings. Contact with the underlayer can occur only at the bottom or both at the bottom and below the tail of the unit, depending on the placement of the underlayer.

### 1.1.2 Top Row of an Armour Layer with Xbloc+

The stability of the Xbloc+ at the top row of the armour layer (crest element) still remains an issue to be investigated further. It is known that the Xbloc+ is not sufficiently stable, when placed at the crest without any shape or material modifications. For this reason, for the renovation of the Afsluitdijk, the first project, where Xbloc+ will be applied, a special crest element is designed. The element, the concept of which is shown in Figure 1.3, achieves higher stability as a result of its increased own weight.

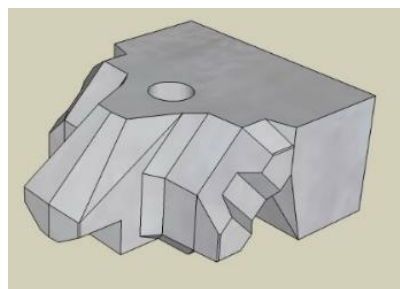


Figure 1.3: Xbloc+ crest element concept for the Afsluitdijk

However, such a special element is not intended to be generally used for other projects, as it introduces additional moulds and, therefore, increases the cost at site locations, that are often remote. Consequently, it is desirable to investigate alternative ways to increase the stability of the Xbloc+ crest element, without modifying its shape or material.

### 1.1.3 Thesis Outline

In this thesis, the stability of the top row of an armour layer with Xbloc+ is examined, the governing parameters and mechanisms are researched and an optimised configuration of the crest to increase the stability is proposed. The outline of the thesis is presented in Figure 1.4.

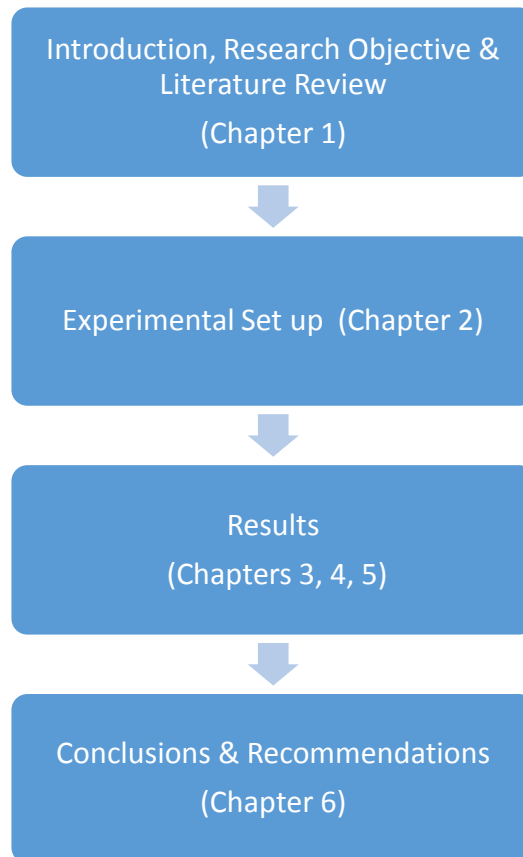


Figure 1.4: Thesis Outline

## 1.2 Research Objective

In this section, the problem addressed, the questions answered and the methodology followed in this research are presented.

### 1.2.1 Problem Definition

The single Xbloc+ units of the top row of the armour layer (Xbloc+ crest units) achieve a lower stability number compared to the units of the other rows of the armour layer, which achieve a stability number higher than 3.88 (Berg, 2018). Therefore, the crest units have inadequate stability and become easily displaced, without the presence of rear support.

The fact that no additional armour layer rows are present above the top row results in fewer contact points with neighbouring units for the crest Xbloc+ units (5 points), compared to units located at the other rows of the breakwater (9 points). The stabilising effect resulting from the additional weight of overlying rows is also absent. As a result, the crest elements have low friction, almost no interlocking and their own weight is not enough to keep them in stable position under wave loading. During wave run-up, they rotate and can be easily extracted from the armour layer.

Consequently, it is necessary to seek a solution that leads to sufficient stability of the top armour row. It is preferred that the shape and material of the Xbloc+ unit is kept unchanged and an appropriate crest configuration results in the increase in stability. Such a promising optimisation for the transition between the slope and the crest still remains a concept, that has not been investigated.

The objective of this research is to get insight into the parameters and mechanisms that influence the stability of the top row of an armour layer with Xbloc+ (crest elements). Additionally, based on the aforementioned insight, to determine ways of increasing the stability.

### 1.2.2 Research Questions

The research objective can be analysed into three research questions:

1. What is the relation of the stability of the Xbloc+ crest elements with the parameters: crest freeboard and wave steepness?
2. How do the parameters, crest freeboard and wave steepness, affect the failure mechanism of the crest elements?
3. How can different crest configurations increase the stability of the crest elements?

### 1.2.3 Research Methodology

To answer the research questions, numerical or physical modelling can be chosen to be applied.

From the research by Latham et al (2014) on the application of numerical modelling to simulate the interaction between water and rubble mound breakwaters, it was concluded that numerical modelling is possible, but requires increased computational resources and non-practical run-times.

Janssen (2018), during his research on the stability of Xbloc+ crest elements, attempted to apply a 3 dimensional multi-phase model, but did not manage to make it stable. The conclusion was that constructing such a model is “very time consuming and has a high numerical effort”.

On the other hand, physical modelling is much less time-consuming and, thus, very attractive for testing various parameters, as well as many test configurations, in the search for the optimised configuration. Finally, the practical reason that BAM has existent in-house facilities, as well as experience in physical modelling further strengthens the choice. Therefore, physical modelling is chosen over numerical modelling,

In order to acquire answers for the research questions, the physical modelling is planned in the following manner. First, a set of tests on the single Xbloc+ crest element (without rear support) is performed. The results of this test set are expected to provide insight into the parameters and mechanisms that govern the stability of the Xbloc+ crest elements (1<sup>st</sup> and 2<sup>nd</sup> research questions), as well as to determine the most critical conditions (combination of freeboard and wave steepness) for the stability.

Subsequently, another set of tests is performed, with the aim to investigate ways of optimising the transition between the crest and the armour layer, thus, answering the second research question by proposing a configuration that will lead to increased stability of the Xbloc+ crest elements. The most critical conditions for stability (output of the first test set) constitute the boundary conditions (input) for the second test set. The acquired insight into the failure mechanisms is expected to function as a “thinking basis” for a solution that can effectively resist them. Finally, additional tests are performed, at the optimised configuration.

The research methodology is schematised in Figure 1.5.

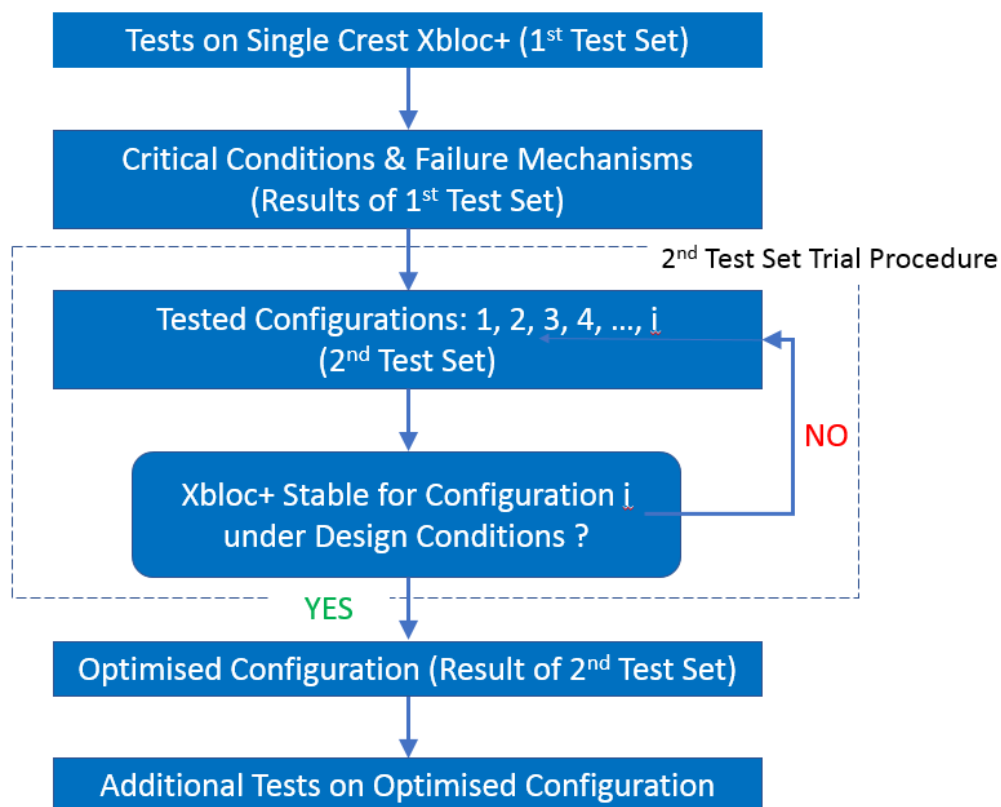


Figure 1.5: Methodology for physical modelling

## 1.3 Literature Review

### 1.3.1 Breakwaters

Breakwaters are coastal structures with primary function the protection of their leeward area by decreasing the incoming wave energy, through dissipation and reflection (CEM, 2002). Breakwaters can also be part of the hard measures used for coastline stabilization. They can be distinguished in different categories depending on different criteria, as presented in Appendix A.1.1.

The most commonly constructed type of breakwater is the rubble mound, which is typically preferred over the other types, in case of waves with heights over 4.5 m and periods larger than 15 s.

#### 1.3.1.1. Rubble Mound Breakwater

A rubble mound breakwater's cross section consists of different layers of material. The main parts of a rubble mound breakwater are: armour layer, underlayer, filter layer (if present), core, toe and crown superstructure (if present). A typical cross section (Hald, 1998) is shown in Figure 1.6. More details about the main parts and dimensions are included in Appendix A.1.2.

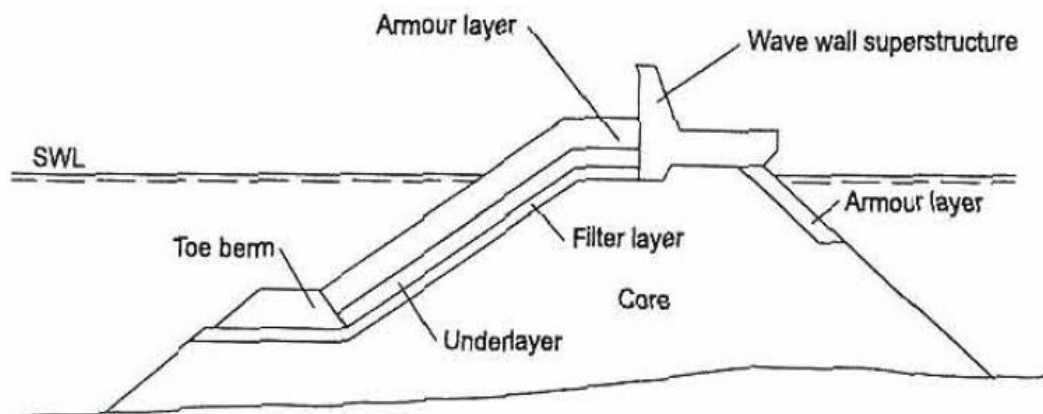


Figure 1.6: Typical cross section of a rubble mound breakwater without filter layer and crown superstructure (Hald, 1998)

#### 1.3.1.2. Failure Mechanisms of the Armour Layer

Rubble mound breakwaters have different failure modes, all of which are important to consider, since failure often happens, because one of the failure modes was not taken into account in the design. The failure modes of a rubble mound breakwater (Burcharth, 1994) are presented in Figure 1.7.

One of the most critical modes is the failure of the armour layer. An armour layer unit can fail in different ways, as seen in Figure 1.8 (Hald, 1998):

- During wave run-up and run-down, an armour unit can rock. Rocking is the continuous and regular movement of an armour unit (van der Linde et al, 2009). When a unit is rocking, it is "tilting" up and down during wave run-up and run-down respectively, but without being displaced from its original position. More information about the importance of rocking as a failure mechanism is presented in Appendix A.1.3).



- A unit rotates and, subsequently, gets out of position and rolls up or down the slope in the cases of wave run up or run down respectively.
- More than one units slide down the slope during wave run-down.

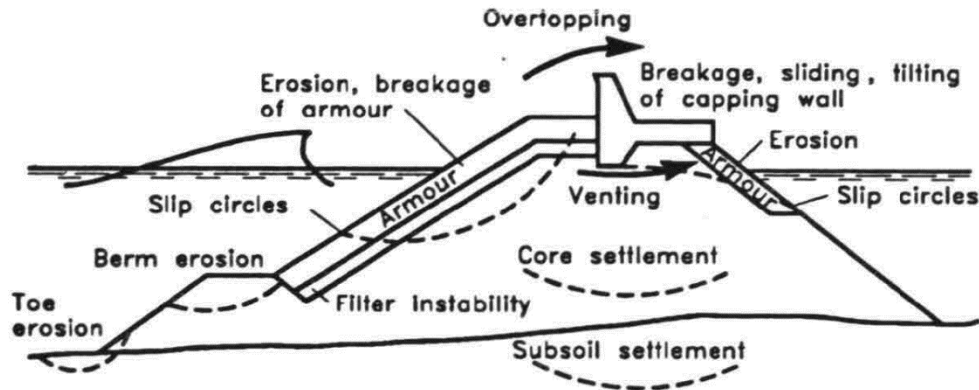
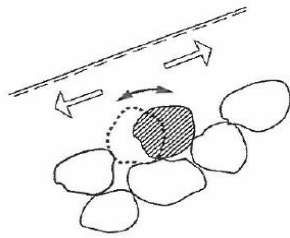
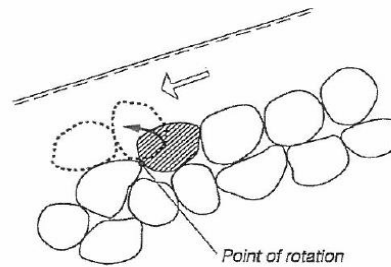


Figure 1.7: Failure modes of a rubble mound breakwater with crown superstructure (Burcharth, 1994)

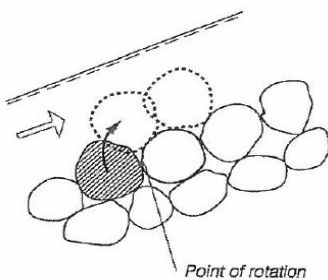
Rocking of unit during up- and down-rush



Rotation and subsequent down-slope displacement of unit during down-rush



Rotation and subsequent up-slope displacement of unit during up-rush



Sliding of several armor units (armor layer) during down-rush

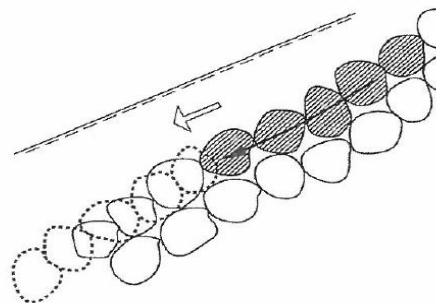


Figure 1.8: Armour layer failure modes (Hald, 1998)

### 1.3.1.3. Loading of the Armour Layer

During the wave action on the breakwater's slope, the following forces (Figure 1.9) act on the armour layer units (Hald, 1998):

$F_G = (\rho_s - \rho_w) * V * g$  : submerged weight.

$F_L \approx C_L * \rho_w * u^2 * A_L$  : lift force, which is approximately normal to the slope and "outwards" directed.

$F_D \approx C_D * \rho_w * u^2 * A_D$  : drag force, which is approximately parallel to the slope and has the direction of the flow (upslope during run-up and downslope during run-down).

$F_I \approx C_M * \rho_w * V * \frac{du}{dt}$  : inertia force, which has the same direction as the drag force.

$F_s$  : seepage force, caused by the hydrostatic pressure build-up and the outward directed flow velocities inside the breakwater.

$F_s$ : seepage force, caused by the hydrostatic pressure build-up and the outward directed flow velocities inside the breakwater.

Frictional forces at the points of contact with the “neighbouring” armour units.

With,

V: volume of the stone ( $m^3$ )

g: acceleration of gravity ( $\frac{m}{s^2}$ )

$\rho_s, \rho_w$ : armour unit and water densities ( $\frac{kg}{m^3}$ )

$C_L, C_D, C_M$ : coefficients depending on armour unit shape and flow regime (–)

$A_L, A_D$ : cross – sectional areas subject to lift or drag ( $m^2$ )

u: wave velocity

The vectoral sum of  $F_L, F_D$  and  $F_I$  constitutes the total wave force,  $F_w$ .

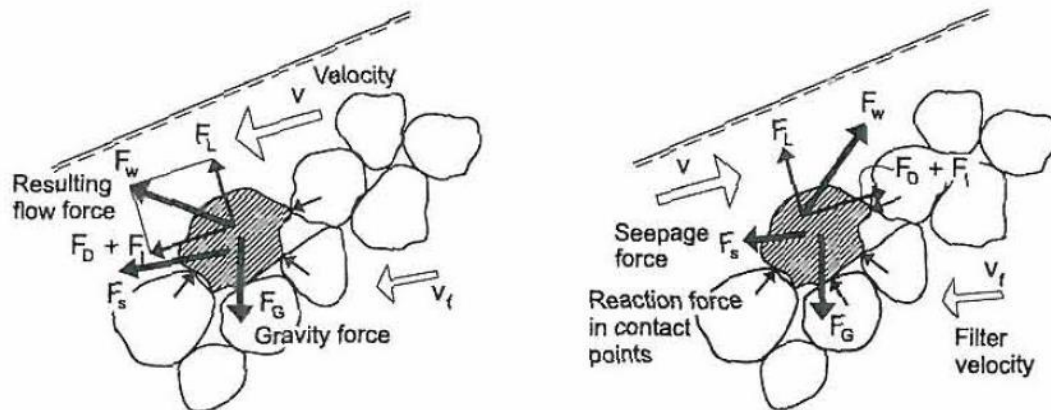


Figure 1.9: Forces acting on a stone at slope during wave run-down (left) and run-up (right) (Hald, 1998)

The failure modes are the result of the loading acting on the armour layer units. The loading is dynamic, as all the forces, except for gravity, are not constant neither in size nor in direction. When the destabilising become higher than the stabilising forces, a unit is no longer stable and is set into motion.

Hald (1998) concluded that at the armour layer part below the still water level, the forces are predominantly caused by the phenomenon of down-rush, as well as by the flow reversal at the interface between the down-rush caused by the previous wave and the uprush of the next incoming wave. At the part of the armour layer, where the latter happens, the resulting wave

force is maximum. At the armour layer part above still water level, the loading is predominantly caused by the wave up-rush. Based on the above, it is expected that for a unit located high at the armour layer, failure is most likely to happen because of the occurring loads during wave uprush in the following way: the unit rocks, rotates and, finally, gets displaced towards the upslope direction.

#### 1.3.1.4. Concrete Armour Units

Rock traditionally was the material used at the armour layer of breakwaters. However, because of decreasing local availability and increasing transport cost of larger rock sizes (which are necessary in case of severe wave conditions), concrete armour units started to become a very popular alternative (Dupray et al, 2010). The units can be distinguished into different categories based on different criteria: placement on a double or single layer; placement in a random or uniform manner; shape ranging from compact (bulky) to slender or from simple to more complex.

Concrete armour units gain their stability from three different mechanisms: own weight, interlocking and friction, each of which contributes to a lesser or higher degree to the overall stability, which depends on the characteristics of the armour unit and the properties of the structure, such as the slope angle. For complex interlocking armour units, the contribution of interlocking and friction is increasing with increasing slope angle, whereas the contribution of own weight is decreasing. For bulky types, the same trend is followed, however, in this case, the maximum stability is achieved at milder slope angles, as shown in Figure 1.10.

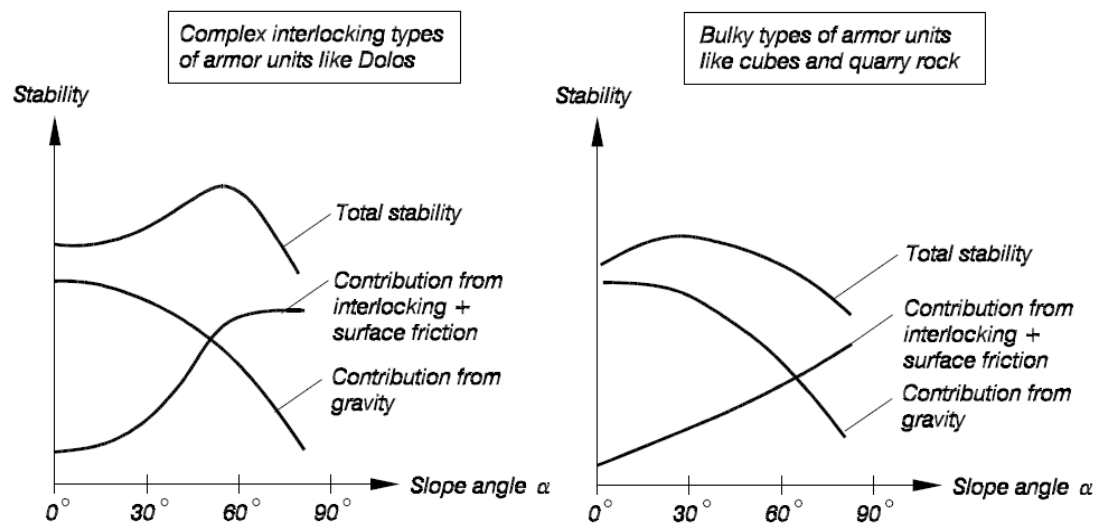


Figure 1.10: Contribution of interlocking, friction and own weight to stability plotted against the structure's slope angle for complex interlocking armour units (left) and bulky units (right). (CEM, 2002)

Placement and shape of units determine the degree to which the mechanisms contribute to the total stability of the unit. Randomly placed units rely more on own weight and interlocking rather than friction. Units with simple bulky shape rely primarily on own weight, whereas units with slender shape rely primarily on interlocking, which becomes higher, as shape becomes more complex. Uniformly placed units, which are placed in one layer, mainly rely on the friction between them and the unit weight. The variability of friction is lower than the variability of interlocking as a mechanism, therefore, uniformly placed units require narrower safety bandwidths, which leads to smaller sizes. This in combination with single layer placement generates savings in material cost and facilitates ease of placement. Adding the

higher aesthetic result to the above, uniformly placed units are gaining increasing potential compared to their randomly placed competitors. However, special attention is required to transitions at the tow and the crest, at curved sections of the breakwaters, as well as for applications to severe wave conditions.

When choosing and designing a concrete armour unit, it is crucial to ensure both hydraulic stability and structural strength. The former guarantees that displacements of the units remain within the predefined limits resulting from the design, whereas the second guarantees that there is sufficient internal resistance against the external stresses that develop during placement or during lifetime.

A summary of the main categories in which the most common concrete armour units can be distinguished can be seen in Figure 1.11.



















Randomly placed armour units				Uniformly placed armour units			
Double layer placement		Own weight and interlocking		Single layer placement		Interlocking	
Stability factor: Own weight		Own weight and interlocking		Interlocking		Friction	
Cube 	Tetrapode France, 1950 	Accropode France, 1980 	Cob UK, 1969 	Modified Cube USA, 1959 	Akmon NL, 1962 	Core-loc® USA, 1996 	Diahitis Ireland, 1998 
Antifer Cube France, 1973 	Tribar USA, 1958 	A-Jack USA, 1998 	Seabee Australia, 1978 	Haro Belgium, 1984 	Stabit UK, 1961 	Xbloc NL, 2003 	Shed UK, 1982 
Tripod NL, 1962 	Dolos South Africa, 1963 						

Figure 1.11: Concrete Armor Units Categories (Muttray and Reedijk, 2008)

### 1.3.1.5. Stability of an Armour Layer with Concrete Armour Units

Various researchers have investigated the stability of rock armour layer and have produced formulas, the most important of which are presented in Appendix A.1.4. The stability of concrete armour units is presented in this section. A summary of the most important findings of the research on the stability of concrete blocks was given by Babak et al (2009), some of which are summarised below.

Regarding concrete units placed in a double layer, Van der Meer (1988b) has proposed formulas for cubes and tetrapods. The formulas describe the relation between the stability number ( $H_s/(\Delta D_n)$ ) and the following parameters: relative damage level ( $N_{od}$ ), wave steepness ( $s_{om}$ ) and number of waves ( $N$ ). To obtain the required concrete unit size, expressed by the nominal diameter ( $D_n$ ), a choice upon the value of  $N_{od}$  is made. If no damage is allowed,  $N_{od}$  is set to zero and the unit size increases considerably. Thus, normally the “start of damage” criterion is used, which corresponds to  $N_{od}=0.5$ .

Regarding single layers concrete units, they are more complex in shape, in order to achieve higher interlocking. Single layer blocks achieve higher stability numbers than double layer ones, but if the stage of “start of damage” occurs, then a quick and abrupt “failure” can happen. The stability numbers corresponding to “start of damage” are much lower than those corresponding to “failure”. The stability number to be used in the design is even lower, in order to allow a required safety margin and avoid the sudden failure of the armour layer mentioned above. The damage definitions and stages of damage are described in Appendix A.1.5.

For the stability of the Xbloc+ armour unit, the following formula is used by Delta Marine Consultants for design:

$$V_{\text{Xbloc+}} = \left(\frac{H_s}{2.5\Delta}\right)^3$$

Where,

V: unit volume (m<sup>3</sup>)

H<sub>s</sub>: design significant wave height (m)

$\Delta = \frac{\rho_c - \rho_w}{\rho_w}$ : relative concrete density (-)

$\rho_c$ : concrete density ( $\frac{\text{kg}}{\text{m}^3}$ );  $\rho_w$ : water density ( $\frac{\text{kg}}{\text{m}^3}$ )

It can be seen that the quotient  $\frac{H_s}{\Delta D_{n50}}$  is central in the description of stability. This quotient is known as “stability number”. It shows the relationship between the loading (expressed by the wave height, H<sub>s</sub>) and the armour resistance (expressed by the parameters of buoyant relative density (Δ) and armour stone diameter (D<sub>n50</sub>)). The higher the value of the stability number, the higher the wave loads that can be resisted by a unit. The design stability number of the Xbloc+ has been chosen to be 2.5, providing a large safety margin, since the stability number resulting from physical model tests is higher than 3.88.

#### 1.3.1.6. Stability of Low Crested Breakwaters

The van der Meer and Hudson formulas are applicable for non-overtopped structures. At low crested breakwaters, there is frequent overtopping and wave transmission, which lead to a smaller fraction of the incoming wave energy being dissipated at the seaward slope. Thus, the stability of the seaward armour layer as a whole increases and, consequently, the required stone size can be reduced (Taveira-Pinto, 2005).

The required size of the armour layer units, resulting from the Van der Meer formula for a non-overtopped structure, can be reduced in the case of a statically stable low-crested structure with crest above the still water level. A reduction factor, used to multiply the diameter D<sub>n50</sub>, was proposed by Van der Meer and Pilarczyk (1990):

$$\frac{1}{1.25 - 4.8R_p^*} \quad \text{for} \quad 0 < R_p^* < 0.052 \quad \text{and} \quad R_p^* = \frac{R_c}{H_s \sqrt{\frac{S_{op}}{2\pi}}}$$

Where,

$R_c$ : freeboard (m)

$H_s$ : significant wave height (m)

$s_{op} = \frac{2\pi H_s}{gT_p^2}$ : wave steepness (-)

$T_p$  = peak period (s)

From the formula, it can be seen that reduction factor increases for decreasing freeboard. The lower the crest becomes, the more stable the front armour layer as a whole becomes. The maximum value for the reduction factor is 1 (i.e. no reduction) and the minimum is 0.8 at  $R_c/H_s=0$ .

### 1.3.2 Wave Characteristics

Waves in nature are short-crested and random, which means that they have different directions, heights and periods. The distribution of those characteristics can be described either by statistical or spectral analysis, which are presented in Appendices A.2.1 and A.2.2 respectively.

Waves can be divided into two categories, based on their steepness: wind with typical steepness of 4-6% and swell with 2%. The former are found near the wind source, thus, they represent “young” sea states, whereas the later more far away. When travelling away from their source, the phenomena of direction and frequency dispersion take place, which means that different waves travel in different directions and waves with different periods travel at different speeds. Consequently, far away from the source of generation, strong grouping is created, so swell waves are more uniform.

#### 1.3.2.1. Linear Wave Theory

Linear Wave Theory can accurately describe the behaviour of waves, under certain limitations, the most important of which is the assumption that the wave amplitude is negligible over the water depth. Accordingly, waves follow the dispersion relation:

$$\omega^2 = g * k * \tanh(kh)$$

Where,

$$\omega = 2\pi f = \frac{2\pi}{T} : \text{radian frequency } \left(\frac{\text{rad}}{\text{s}}\right); f: \text{frequency } (\text{s}^{-1}); T: \text{period}(\text{s})$$

$$g: \text{gravitational acceleration } \left(\frac{\text{m}}{\text{s}^2}\right)$$

$$k = \frac{2\pi}{L} : \text{wave number } \left(\frac{\text{rad}}{\text{m}}\right)$$

L: wave length (m)

h: water depth (m)

The linear wave theory is applicable in deep waters. When propagating at intermediate and shallow waters, waves become strongly non-linear and their shape changes. This is the result of increasing steepness, because of increasing wave height due to shoaling, until the point of breaking. Breaking is also a highly non-linear procedure. At those cases, other theories, such as the cnoidal or solitary wave theory are applicable.

To distinguish between deep, intermediate and shallow waters, the relative depth criterion ( $h/L$ ) is used: for  $h/L > 0.5$ ,  $0.05 < h/L < 0.5$  and  $h/L < 0.05$ , deep, intermediate and shallow waters are defined respectively.

#### 1.3.2.2. Wave Breaking

Waves can break either in deep water, when steepness exceeds a certain value (white-capping phenomenon), or in shallow water, when depth gets limited. The criteria  $H/L > 0.142$  and  $H/h > 0.88$  (Miche’s breaking limit) apply respectively.

To describe wave breaking on a slope, the surf-similarity parameter ( $\xi$ ) is used. It is the quotient:

$$\xi = \frac{\tan\alpha}{\sqrt{s_0}}$$

Where,

$\tan\alpha$ : seaside slope of the coastal structure

$s_0 = \frac{H}{L_0}$ : fictitious wave steepness

$L_0 = \frac{gT^2}{2\pi}$ : deep water wave length

H: wave height at the toe of the structure (m)

T: wave period at deep water (s)

In deep waters, the fictitious wave steepness is the same as the real wave steepness (equal to  $H_0/L_0$ ). However, in shallow waters the wave period changes and, therefore, the fictitious and real wave steepness are different. Different definitions are used for the wave steepness, depending on the definitions chosen for the wave height and period. More information is provided in Appendix A.2.3.

### 1.3.2.3. Wave-Structure Interaction

Run-up, overtopping, transmission and reflection of waves are the main wave-structure interactions defining the design of the different parts of a breakwater (CEM, 2002). Those processes are shown in Figure 1.12, summarised below and described in more detail in Appendix A.2.4.

#### **Run-up**

The wave tongue goes up and down at the breakwater's slope, reaching a maximum and a minimum vertical elevation with respect to the mean water level. The former is called run-up ( $R_u$ ), whereas the latter run-down ( $R_d$ ).

#### **Overtopping**

In the case that the run-up tongue exceeds the top level of the breakwater, waves pass over the crest to the lee side of the structure, a phenomenon called overtopping.

#### **Reflection**

The incoming wave energy is partly dissipated on the breakwater's armour layer, partly reflected and partly transmitted. The portion of the energy that reflects back increases, when the permeability and roughness of the armour layer decrease and/or the seaward slope of the breakwater increases (CEM, 2002).

#### **Transmission**

Wave energy can be transmitted from the sea to the lee-side of a breakwater. Most of the energy passes through the armour layer and the crest, the permeability of which is an important factor in this process.



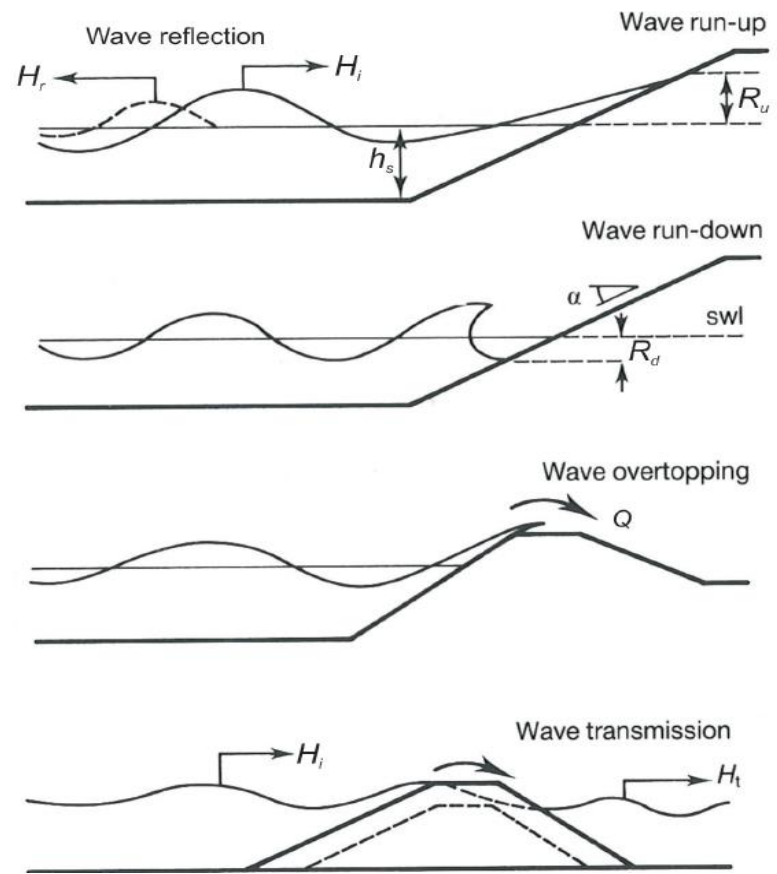


Figure 1.12: Main wave-structure hydraulic interactions (*The Rock Manual*, 2007)

The phenomena of run-up, overtopping, reflection and transmission determine which percentages of the incoming wave energy dissipate on the slope, reflect or get transmitted to the lee side. In the case of allowing minimal run-up and overtopping, the top part of the armour layer and the crest area will be very rarely impacted by the incoming wave energy, thus, suffering minimal damage. However, in the case of allowing considerable run-up and, subsequently, overtopping, a large portion of the incoming wave energy will be concentrated at the transition zone between the armour layer and the crest, therefore, causing more damage there.

Run-up and overtopping depend on many parameters, related both to the incoming waves (wave height, steepness, obliqueness) and the structure's characteristics (slope surface roughness, slope permeability, presence of a berm, breakwater crest's configuration). A particularly important parameter used in the overtopping calculations is the freeboard ( $R_c$ ), which influences the volume of water that overtops the breakwater, since an increasing freeboard leads to decreasing water volumes passing over the crest of the structure.

### 1.3.3 Stability of Breakwater Crest

#### 1.3.3.1. Classification of Breakwaters based on Crest Height

The freeboard, denoted as  $R_c$ , is the vertical distance from the still water level to the top of the breakwater crest, as shown in Figure 1.13. In case of a crown wall, the top is defined at this level, whereas in its absence, it is defined at the top of the armour stone (or concrete unit) at the crest. The freeboard is given by:

$$R_c = h_c - h$$

With,

$R_c$ : freeboard (m)

$h_c$ : height of the structure (m)

$h$ : water depth at the structure (m)

The freeboard can be made dimensionless by dividing with the median rock diameter or with the significant wave height, resulting in the quotients  $R_c/D_{n50}$  or  $R_c/H_s$  respectively.

The level of the crest, as described in The Rock Manual (2007), is mainly determined by the allowed overtopping volumes and, subsequently, the resulting stability requirements for the seaside and leeside armour layer and the crest. Constructability limitations can also restrict the crest level. Other considerations, such as settlements and sea-level rise, are also taken into account.

Depending on the freeboard, breakwaters can be distinguished in the following 2 main categories (Verhagen and van den Bos, 2018):

- High crested, when the crest is high enough for the rear slope not to be seriously impacted by the overtopping waves, which are fairly limited in number. Typically, when  $R_c/H_s > 1$ , the breakwater can be characterized high crested.
- Low crested, where there are many waves passing over the crest and impacting the rear slope.

Van der Meer (1994) divides the low crested structures in 3 subcategories:

- Dynamically stable reef breakwaters, which can be reshaped. The crest is constructed just above the still water level, but, after wave action, it becomes lower.
- Statically stable low-crested breakwaters with crest above the still water level, but still allowing more overtopping than the high crested breakwaters.
- Statically stable submerged breakwaters, that are overtopped by all the waves. In this category, the crest is always under the still water level.

For high crested breakwaters, the wave attack is mainly concentrated at the sea-side slope, whereas for low crested, a considerable portion of damage is inflicted at the crest and rear slope.

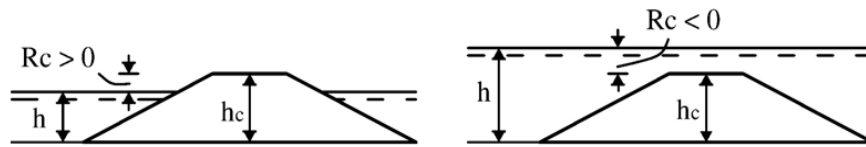


Figure 1.13: Freeboard for emerged (left) and submerged (right) breakwater (Burcharth et al, 2005)

### 1.3.3.2. Parameters of Influence to Crest Stability

Previous research has been conducted on the influence of the freeboard in the stability of low crested breakwaters with rock armour. Burcharth et al (2005), besides their own research, have summarized the most important findings of other researchers. The most interesting conclusions are presented in this section.

Vidal et al (1992, 1995) conducted research on the stability of different breakwater parts under non-depth-limited waves perpendicular to the breakwater trunk. In those experiments, the crest included the upper parts of the front and rear slope of the structure. It was observed that the crest shows minimum stability when it is slightly submerged (Figure 1.14) with the stability number being lower than 1.75 for  $-0.75 < R_c/D_{n50} < 0.50$ . Stability increases as  $R_c/D_{n50}$  increases in absolute value, namely when the breakwater becomes more emerged or submerged.

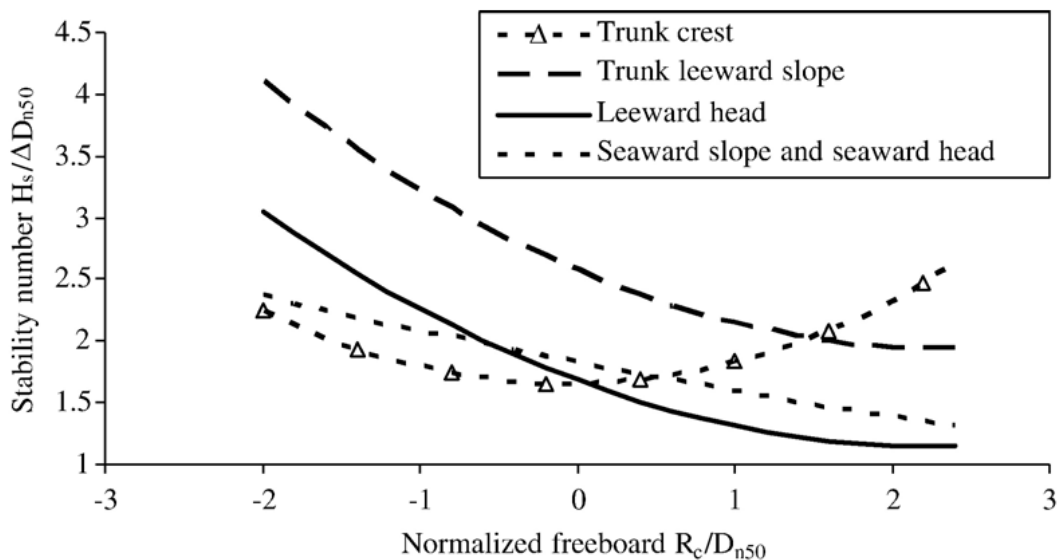


Figure 1.14: Stability number of different parts of a breakwater trunk and head as a function of the normalised freeboard. (From Vidal et al. (1992, 1995). (Burcharth et al, 2005)

Burger (1995), who did additional experiments and reanalysed data from Van der Meer et al (1988) and Vidal et al (1992), concluded that, in conditions of non-depth-limited waves, the stability number for the crest of the breakwater trunk is the lowest when the crest is around the still water level and slightly emerged. As seen in Figure 1.15, the stability number for the crest remains under 1.5, when  $-0.25 < R_c/D_{n50} < 2$ . Also evident is the tendency that, as the freeboard increases in absolute magnitude, the stability of the crest also increases. This can be explained by the fact that in the case of positive freeboard, as the crest level becomes higher, fewer waves reach up the crest, whereas, in the case of negative freeboard, as the crest level becomes more submerged, more waves pass “undisturbed” over the crest without interacting with it.

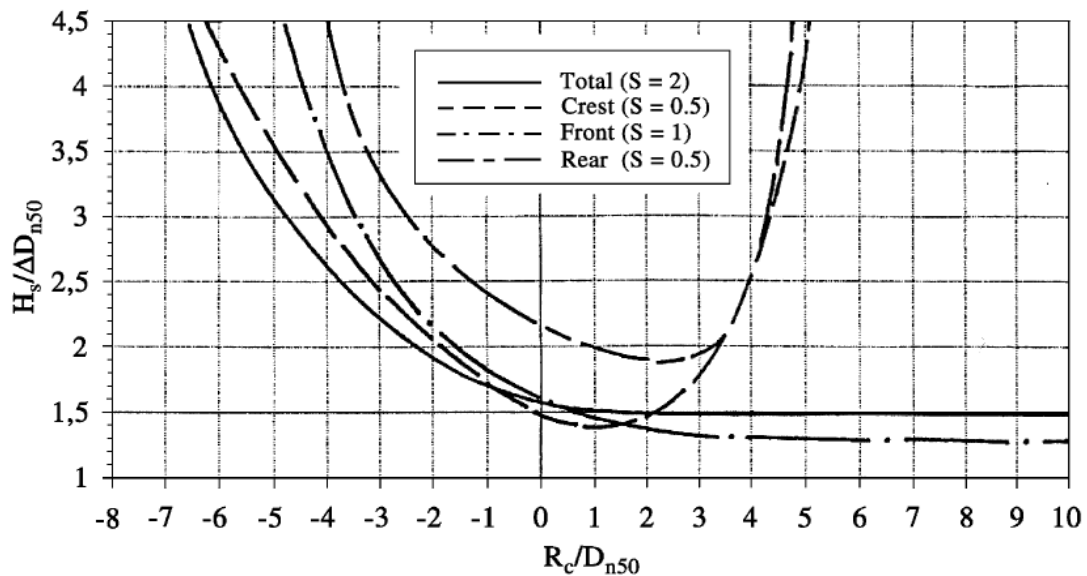


Figure 1.15: Stability number of different parts of a breakwater trunk as a function of the normalised freeboard, from Burger (1995). (Burcharth et al, 2005)

For the experimental configurations tested, the crest width, wave steepness and angle of wave attack were found to have minor influence on the stability of the crest in rock armoured breakwaters.

Kramer and Burcharth (2003) studied depth-limited short crested waves and verified the strong correlation between the crest freeboard and the stability number of the crest by concluding that the case in which the crest is around the still water level and slightly emerged results is the minimum stability. The stability number for the crest was found to be under 2 for values of the freeboard normalized with the median rock diameter between -2 and 2 ( $N_s < 2$  for  $-2 < R_c/D_{n50} < 2$ ). A narrower (width equal to  $3D_{n50}$ ) and a wider (width equal to  $8D_{n50}$ ) crest were tested, but no strong influence of the crest width on stability was concluded.

Muttray et al (2012) & van den Bosch et al (2012) processed data of physical modelling conducted by Van der Linde (2009) on the stability of a low-crested breakwater with Xbloc armour units and front and rear slope of 3:4. The average stability number for the crest units proved lower for positive than for negative relative freeboards ( $N_s = 3.5$  for  $R_c/H_s > 0$  against  $N_s > 4$  for  $R_c/H_s < 0$ ) and attained a minimum value of  $N_s = 3$  for  $R_c/H_s = 0$  (case of crest at still water level). In the case of positive relative freeboards, the mainly landward displacements of the crest units in combination with the settlements of the armour layer created gaps at the transition between the seaward slope and the crest, making it the most prone to damage part. This was also the same part of the structure, where most of the rocking units was located, but rocking followed a different trend, being more significant for submerged than for emerged conditions (2% of the units against 1%). No clear correlation between rocking and displacement of units was defined, so rocking could not be characterized as a reliable factor to forecast damage. The above results can be explained by the fact that more space between the units is created, thus, a larger area of the Xblocs becomes exposed to the wave forces, while, at the same time, the interlocking and friction with the armour rows beneath the crest is decreased (Van der Linde, 2009). It was also concluded that steepness had an important effect on stability, since  $s_{op} = 2\%$  ( $\xi_p = 5.3$ ) led to 20% lower stability numbers for the armour

layer as a whole compared to  $s_{op}=4\%$  ( $\xi_p=3.75$ ). No clear effect of the packing density on the rocking or displacements of units could be identified. Regarding the crest width, the narrower crest tested was more stable for crest level near the still water level ( $-1.5 < R_c/D_n < 0.5$ ), while the wider crest (3 times wider) was more stable outside this range. Nevertheless, all in all, the crest width did not prove to have a considerable influence in stability.

From the existing literature review, it can be concluded that there is strong dependency between the crest stability and the crest freeboard. When the crest is at the still water level, its stability is minimum, because the wave attack is focused there. This is impaired by the fact that, at the same time, no units are present above the top row of the armour layer, so the positive contribution to stability of the mechanisms of interlocking, friction and additional overlying weight is decreased. Wave steepness has also influence on the crest stability, whereas the crest width and packing density are of far lesser importance.

### 1.3.4 Current Research on Xbloc+

Extensive research on the Xbloc+ armour unit has been conducted by Delta Marine Consultants, including over 600 physical model tests. The main findings are summarized in this section.

#### 1.3.4.1. Stability of the Top Row of an Armour Layer with Xbloc+

Regarding the stability of the Xbloc+ units at the armour layer's top row (crest elements), Janssen (2018) studied the physical processes that lead to lower stability. From physical modelling, he distinguished that a combination of two types of failure occurs. First type is the two-dimensional failure: the unit rotates, when the overturning moment caused during the wave uprush surpasses the stabilising moment caused by the unit's own weight. The rotation causes a threefold destabilising effect on the unit: firstly, the area exposed to the flow and, thus, the destabilizing drag force on the unit increases. Secondly, the contact area with the underlying units and the underlayer decreases. This leads to lower stabilizing frictional forces at the unit, so it is much easier for the unit to slide backwards as a result of the wave action. Lastly, during rotation the centre of gravity of the unit moves closer to the point of rotation, which decreases the stabilizing moment of the own weight. Second type is the three-dimensional failure: as the Xbloc+ is rotating during wave uprush, its tail is making contact and is relying for support at the underlayer, which is not even due to irregularities. This causes the element to turn over sideways.

From the limited physical modelling data, it was concluded that an Xbloc+ element at the top row of the armour layer with 1:1.5 slope under wave conditions of 4% steepness, achieves the following stability numbers ( $N_s$ ):

$$N_s = 1.72, \text{ for } R_c/H_{m0,d} = 1.0 - N_s = 1.21, \text{ for } R_c/H_{m0,d} = 0.5 - N_s = 1.26, \text{ for } R_c/H_{m0,d} = 0.0$$

To enhance the stability number, two crest configurations were tested: the first was the placement of three crest units next to each other, which did not produce the expected results and the second was the placement of a stiff element behind the Xbloc+ crest elements' tails, which resulted in enhanced stability.

From the numerical modelling, it was concluded that the Xbloc+ crest element has very low rotational and vertical stability. Thus the primary failure mechanisms are the rotation due to the destabilising moment caused by the wave forces combined with lifting due to the wave lift force. The final stage of failure happens, once the wave drag forces entrain the unit away. The most unfavourable load situation was found to be the stage of wave run-up. More specifically, the ratios of overturning moments to stabilizing moments, vertical loading over vertical resistance and horizontal loading over horizontal resistance were estimated at 0.16, 0.81 and 4.76 respectively. Therefore, the overturning moment is the most critical phenomenon that leads to failure. Uplift is also important, as the upward pressures are higher than the downward pressures, leading to pressure differences.

Regarding potential optimisations that would make the Xbloc+ crest unit stable, it was proposed that adding rock backfill could contribute to avoiding failure, so it is a solution worth investigating further. An increase in the density of the material could only work if the material used would have a density of  $15000 \text{ kg/m}^3$ , which is an extreme value, so such a solution does not seem practical and feasible. Likewise, applying rock at the top of the Xbloc+ tail does not seem promising, as the rock backfill should reach a height of approx. 7 m, which is too high.

#### 1.3.4.2. Research on Other Topics Regarding Xbloc+

Vos (2017) investigated the failure mechanisms of an initial version of the Xbloc+, called Xbloc+v1, by conducting both dry pull-out and hydraulic tests. She concluded that the more armour rows are present above a unit, the higher the required average pull-out force becomes. This shows that the units at the top rows of the armour layer can be much more easily displaced than the units at the bottom. Thus, the top row of the armour layer has minimum stability compared to the other rows for the same loading conditions. Additionally, it was concluded that Xbloc+ gains its stability mainly from its own weight and friction and at a lesser degree from interlocking. Uplift was identified as a much more critical failure mechanism for the Xbloc+ than for its previous version, the Xbloc. The main reason is that the overall porosity is smaller for the Xbloc+. Thus, uplift forces build up and contribute to the extraction of armour units during wave run-down.

Optimizations were made to the version Xbloc+v1, resulting in an altered version, the Xbloc+v2. The main difference between the two versions was the drilling of a funnel shaped hole in the unit, in order to relieve the pressure differences between the top and bottom of the unit.

By testing the variances Xbloc+v1 and Xbloc+v2, Mora (2017) also concluded that uplift is the main failure mechanism for the armour layer. Although damage was initiated at a lower stability number in the case of the milder slope (1:2), it progressed faster and more extensively in the case of the steeper slope (3:4) tested. Damage also proved to be worse under swell (2% steepness) compared to wind (4% and 6% steepness) wave conditions.

Jimenez's (2017) research revealed that overtopping depends on various factors. Overtopping volumes increase at the cases that structure slope, breaker parameter or wave period increase and in the cases that relative freeboard, wave steepness or slope roughness decrease. Corrections to existing overtopping formulas were proposed, whereas the roughness coefficient ( $\gamma_r$ ) of the Xbloc+ armour unit was determined.

The influence of irregularities of the underlayer on the armour layer's stability was researched by Van den Berg (2018). The results showed that a convex shape in cross shore direction and an S-shaped profile in the cross shore direction are the most critical shapes of the underlayer, with the latter leading to sudden and abrupt failure.

### 1.3.5 Physical Modelling

Physical modelling is essential for testing of the hydraulic and structural response of coastal structures. The main reason is that, compared to analytical, empirical or numerical methods, physical models include fewer simplifications and, thus, can represent more aspects of local boundary conditions and in a more complete way (Wolters et al, 2010). However, when applying physical modelling, it is inevitable that certain errors occur. Those errors result from model, measurement and scale effects and lead to distortions of the physical modelling results (Burcharth et al, 2009).

#### Model effects

Model effects result from errors in reproducing the prototype structure, geometry, waves and currents or from the boundary conditions at the laboratory's wave flume, such as wave paddle and side walls (EurOtop II, 2016). According to Burcharth et al (2009), model effects result from differences between the prototype and the model in: deviations in wave kinematics, the methods for wave recording and analysis, the geometrical differences, the lack of wind and currents.

#### Measurement effects

Measurement effects are caused by the difference in the measurement devices between the prototype and model (EurOtop II, 2016).

#### 1.3.5.1. Similitude in Physical Modelling

When choosing the scale of a model, it is important to make sure that all wave conditions and structural parameters of interest are reproduced to an adequate degree and that a sufficient measuring accuracy is guaranteed (Wolters et al, 2007). The scale of the model can be chosen based on geometric, kinematic or dynamic similitude.

#### Geometric similitude

Geometric similitude implies that all geometric lengths in the prototype ( $L_p$ ) have a constant relation with the corresponding lengths in the model ( $L_m$ ):

$$N_L = \frac{L_p}{L_m}$$

#### Kinematic similitude

Kinematic similitude means that time-dependent processes in the model ( $t_p$ ) have a constant time relation with the processes ( $t_m$ ) in the prototype:

$$N_t = \frac{t_p}{t_m}$$

#### Dynamic similitude

Dynamic similitude implies that the forces in the prototype ( $F_p$ ) and the model ( $F_m$ ) have a constant ratio:

$$N_t = \frac{F_p}{F_m}$$



Various ratios between forces exist. Each ratio is quantified by a scale number and is of relevance for the description of a different phenomenon of the ones present in the interaction between waves and rubble mound breakwaters (Burcharth et al, 2007). The most important ratios are summarised in Table 1.1.

Scale Number	Forces Ratio	Quantification	Phenomenon of relevance
Froude	$\frac{\text{Inertia}}{\text{Gravity}}$	$\frac{U}{\sqrt{gL}}$	Surface waves
Reynolds	$\frac{\text{Inertia}}{\text{Viscosity}}$	$\frac{UL}{\nu}$	Flow
Cauchy	$\frac{\text{Inertia}}{\text{Elasticity}}$	$\frac{\rho U^2}{E}$	Wave slamming
Weber	$\frac{\text{Inertia}}{\text{Surface tension}}$	$\frac{\rho U^2 L}{\sigma}$	Air content

Table 1.1: Forces' Ratios and Scale Numbers

Where,

U: characteristic velocity (m/s)

g: acceleration of gravity (m/s<sup>2</sup>)

L: characteristic length (m)

$\nu$ : kinematic viscosity of water (10<sup>-6</sup> m<sup>2</sup>/s)

E: modulus of elasticity (N/m<sup>2</sup>)

$\rho$ : water density (kg/m<sup>3</sup>)

$\sigma$ : surface tension (N/m)

#### 1.3.5.2. Froude Scaling

The Froude number expresses the relative importance of inertia over gravity. According to Froude scaling, the Froude number should be the same in the model and the prototype:

$$\left(\frac{U}{\sqrt{gL}}\right)_P = \left(\frac{U}{\sqrt{gL}}\right)_M$$

Froude scaling is applied, when the inertial forces are predominantly balanced by gravitational forces (Wave Flume Manual – Hydraulic Model Testing, Delta Marine Consultants, 2017).

#### 1.3.5.3. Reynolds Scaling

The Reynolds number expresses the relative importance of inertia over viscosity. According to Reynolds scaling, the Reynolds number should be the same in the model and the prototype:

$$\left(\frac{UL}{\nu}\right)_P = \left(\frac{UL}{\nu}\right)_M$$

Reynolds scaling is applied, when the inertial forces are predominantly balanced by viscous forces (Wave Flume Manual – Hydraulic Model Testing, Delta Marine Consultants, 2017).

#### 1.3.5.4. Stability Scaling

Stability scaling entails that the stability number should be the same in the model and the prototype and is applied for the scaling of the armour layer and the toe.

#### 1.3.5.5. Permeability Scaling

Whereas geometric scaling is suitable for the armour layer, it might create viscous scale effects (Wolters et al, 2014), when applied for the underlayer and core of the model breakwater. If geometric scaling is applied for the core material diameter, the resulting permeability of the model core may become too low. The flow regime inside the model core becomes laminar, which is not in agreement with the partly turbulent flow regime (known as “Forchheimer” flow regime) in the prototype core. Consequently, the inflow and outflow in the core decrease, which leads to higher run-up and overtopping, as well as lower transmission and armour layer stability compared to the prototype (Vanneste et al, 2012).

Alternatively, permeability scaling is applied, which implies that the core stone size is scaled according to the resulting velocities in the core. In this way, sufficient permeability is achieved. The application of core scaling has been studied extensively and still remains a very challenging topic. Many different approaches have been proposed by different researchers, a brief summary of which is presented in Appendix A.3.

#### 1.3.5.6. Scale Effects

Scale effects result from the incorrect reproduction of ratios between forces in the model and the prototype. In order to obtain dynamic similarity, when modelling rubble mound breakwaters, the Froude, Reynolds and Weber numbers should be the same in the model and the prototype. However, since this is not possible, in short-wave hydrodynamic models, it is assumed that gravity is the dominant force that balances the inertia (Wolters et al, 2007). Thus, Froude scaling is applied, but, this leads to scale effects on viscosity, elasticity and surface tension.

##### 1.3.5.6.1. Viscous Scale Effects

Viscous scale effects happen when the viscous forces are higher in the model than in the prototype. In order to avoid viscous scale effects, the Reynolds number in the model should be above a certain threshold. Different thresholds have been proposed by different researchers, an overview of which is given in Table 1.2.

In order to avoid viscous scale effects in the model armour layer and, thus, maintain turbulent flow conditions, Wolters et al (2010) proposed that the minimum Reynolds number should be  $3 \cdot 10^4$ .

Researcher	Reynolds number
Dai and kamel (1969)	$3 \cdot 10^4$
Jensen and Klinting (1983)	$6 \cdot 10^3$
Oumeraci (1984)	$3 \cdot 10^4$
Shimada et el (1986)	$4 \cdot 10^5$
Van der Meer (1988)	$4 \cdot 10^4$
Jensen (1989) for core	$5 \cdot 10^3$
Jensen (1989) for armour layer	$4 \cdot 10^4$

Table 1.2: Reynolds number above which no viscous scale effects occur (Hughes (1993), obtained from an internal document of Delta Marine Consultants)

#### 1.3.5.6.2. Surface Tension Scale Effects

Surface tension and, therefore, the associated scale effects can be disregarded, when the following rules apply in the physical model (Wolters et al, 2007):

$L > 2$  cm (L: wave length)

$T > 0.35$  s (T: wave period)

$d > 2$  cm (d: water depth)

#### 1.3.5.6.3. Aeration effects

The air bubbles in breaking waves are not in similitude in small scale models compared to the prototype. The bubbles in the model are larger than in the prototype, which is the result of not satisfying the similitude in the Weber number. The energy dissipation is larger in the model, which influences wave run-up and overtopping.

#### 1.3.5.6.4. Friction scale effects

The friction forces between units may not be in similitude with the prototype. It is usual practice to try to reduce the roughness of the units in the model by applying colour. Alternatively, plastic instead of concrete units can be used. All in all, the friction scale effects are considered to have a negligible effect.

## 2. Physical Model Set-up

### 2.1 Wave Flume Configuration

The physical modelling was conducted in the wave flume of Delta Marine Consultants in Utrecht (Figure 2.1). The flume has the following dimensions: length of 25 m, width of 0.6 m and height of 1 m. The maximum water depth is restricted to 0.7 m, whereas the maximum wave height to 0.3 m. The flume walls are made of glass, which facilitates observations during the experiments. The flume is equipped with the Edinburgh Designs piston wave generator, which can generate regular and irregular waves and is able to correct the paddle motion to absorb the reflected wave.

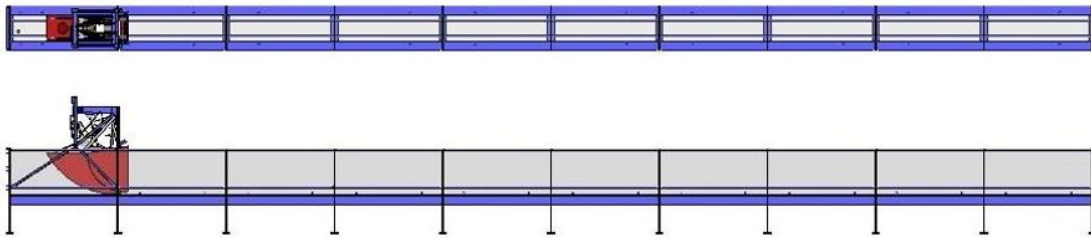


Figure 2.1: Top (top of image) and side view (bottom of image) of wave flume (Delta Marine Consultants)

The section in front of the wave maker should extend at a length larger than 3-5 times the water depth at the wave paddle, in order to ensure that the evanescent wave modes generated by the wave paddle have disappeared. Additionally, the array of wave gauges should fit in this length, allowing for the necessary spacing between them (Wolters et al, 2010). The depth was larger than 3 times the generated wave height.

#### 2.1.1 Wave Gauges

The wave gauges measure the surface elevation. The measured wave train is separated into its incident and reflected wave components, so that the model response is related to the parameters of the incident wave train. The signal from the wave gauges is analysed with the program WaveLab software, which is developed by Aalborg University. The program uses the method of Mansard & Funke (1980) for the reflection analysis of irregular waves. The method is based on least squares and requires a simultaneous measurement of the waves at three positions in the flume in reasonable proximity to each other and on a line parallel to the wave propagation. The principles of this method are applied in configuring the wave gauges's separation distances in the physical model. Considering the irregular waves produced by the wave generator as a linear superposition of a number of monochromatic waves, each of which travelling with its own celerity, the incident and reflected spectra can be distinguished by establishing three measurement positions in a horizontal array perpendicular to the incident wave crest. Let  $X_{1-2}$  and  $X_{1-3}$  be the distances between wave gauges 1,2 and 1,3 respectively, then the following rules should be applied in the model:

$$X_{1-2} = L_p/10$$

$$L_p/6 < X_{1-3} < L_p/3 \quad \& \quad X_{1-3} \neq L_p/5 \quad \& \quad X_{1-3} \neq 3L_p/10$$

$L_p$ : Wave length corresponding to the peak frequency of the spectrum

The peak wave length differs throughout the tests, but the spacing of the wave gauges is kept constant. There is no spacing that can satisfy all the above mentioned conditions for all the different peak wave lengths occurring during the tests. Spacing of 0.3 m between the first and second gauge and a spacing of 0.7 between the first and third gauge is chosen (Wave Flume Manual – Hydraulic Model Testing, Delta Marine Consultants, 2017).

The chosen spacing fulfils the following criteria: the distance  $X_{1-2}$  should be between the lower and upper boundaries (Vos-Jansen (2018) after Wenneker and Hofland (2014)):

$$\varepsilon L_{\max} < X_{1-2} < E L_{\min}$$

Where,

$L_{\max}$ : maximum wave length

$L_{\min}$ : minimum wave length

$$\varepsilon = 0.04, E = 0.95$$

With  $L_{\max}=6.94$  m and  $L_{\min}=1.49$  m being the maximum and minimum wave lengths expected to be generated during the experiment, the resulting distance  $X_{1-2}$  should be between the following limits:

$$0.28 < X_{1-2} < 1.41$$

Additionally, the wave gauges should be placed at least  $1L_p$  away from the wave paddle to allow the wave to be fully developed and  $0.4L_p$  away from the breakwater toe, in order for the fluctuations of the incident and the reflected wave heights to be as minimum as possible at the location of the gauges. In view of the absence of a foreshore, no changes in wave characteristics are expected. Therefore, only 1 set of wave gauges is chosen to be placed. The peak wave length is  $L_p = 4.96$  m (corresponding to  $100\%H_{m0,d}$  wave conditions &  $s_{op}=2\%$ ). Thus, the wave gauges should be placed at minimum distances of 4.96 m and 1.98 m from the wave paddle and the structure respectively. Eventually, the wave gauges are placed such that the first wave gauge is located 5 m after the wave paddle and the third 2.17 m from the structure.

### 2.1.2 Foreshore

A foreshore is chosen not to be constructed. Without a foreshore, there is no wave breaking due to limited depth, thus, energy dissipation is minimum. Therefore, more and higher waves will reach the structure, which makes the conditions under which the crest elements stability is studied more conservative. An additional more practical reason of choosing to conduct the tests in “deep water” is that similarity in wave conditions between the test series is ensured, when the water depth is varied during the experiments.

### 2.1.3 Water Level in the Flume

The water depth throughout the flume is constant during each test series, because no foreshore is used. It should be kept at least 3 times higher than the maximum significant wave height generated during all tests (Wave Flume Manual – Hydraulic Model Testing, Delta Marine Consultants, 2017)) and lower than 70 cm, due to flume restrictions.

It is assumed that the maximum wave height expected to be generated is 13.88 cm (corresponding to  $140\%H_{m0,d}$ ;  $H_{m0,d}$ : design significant wave height), thus, the water level should be at least 41.64 cm. Between the test series, the freeboard is varied by adjusting the

water level. The minimum occurring water level is 48.6 cm (corresponding to  $R_c/H_{m0,d}=1.5$ ) and the maximum is 63.5 cm (corresponding to  $R_c/H_{m0,d}=0$ ). The experimental set-up is shown in Figure 2.2.

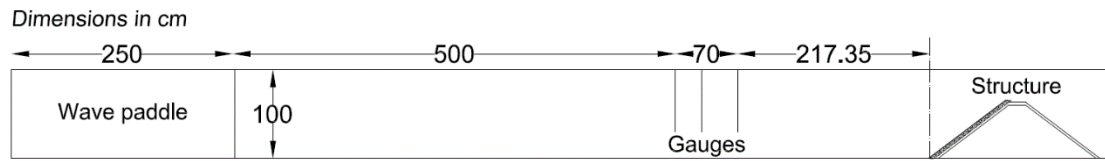


Figure 2.2: Experimental set-up cross section

## 2.2 Model Breakwater Scaling

### 2.2.1 Xbloc+ Model Armour Units

The Xbloc+ model armour units are placed on a slope of 3:4, which is the most common in practice, because the interlocking and friction contribution to the total stability and material saving are increased compared to milder slopes. Moreover, less dissipation of wave energy during wave run-up is expected, thus, more wave energy will reach the crest, making the conditions more conservative.

Armour units are scaled based on stability scaling, which requires the stability number ( $N_s$ ) of the model to be equal to the prototype. The units do not correspond to a real prototype, but can be assumed to correspond to Xbloc+ prototype units with volume of  $3 \text{ m}^3$ , when applying a scaling factor of 1:49. The units used are readily available at the lab. Their dimensions are summarised in Table 2.1.

Notation	Dimension	Value	Unit
L	Length	6.1	cm
H	Height	2.4	cm
D	Width	4.8	cm
$D_n$	Nominal Diameter	2.91	cm
W	Weight	58.5	gr
$\rho_c$	Density	2360	$\text{kg/m}^3$
$D_x$	Horizontal placement distance	5.28	cm
$D_y$	Up-slope placement distance	3.02	cm
$t_a$	Armour layer thickness	3.84	cm

Table 2.1: Dimensions of Xbloc+ model units

The material of the Xbloc+ model units is plastic. According to Vos (2017), plastic Xbloc+ units achieve slightly lower stability numbers than their concrete counterparts, which can be attributed to the lower friction between the units. Thus, the result is expected to be more conservative.

The nominal diameter of the model units is calculated from the relation:

$$D_n = \sqrt[3]{\frac{W}{\rho_c}} = \sqrt[3]{\frac{58.4 \cdot 10^{-3}}{2360}} = 0.0291 \text{ m} = 2.91 \text{ cm}$$

The following relations hold between the width (D), the length (L) and the height (H) of the Xbloc+ unit:  $L=1.27D$ ;  $H=0.50D$ . Other dimensions also follow from the width: Horizontal

placement distance:  $D_x=1.10D$ ; Up-slope placement distance:  $D_y=0.63D$ ; Armour layer thickness:  $t_a=0.80D$ .

In total, 367 Xbloc+ units in 35 rows are placed. Xbloc+ has been found to be less sensitive to settlements within the armour layer than other single layer armour units. Thus, there is no strict limitation in the maximum number of rows, as in the case of Xbloc, where 20 is the maximum number of rows. The Xbloc+ units are placed in a staggered grid: 10 units are placed at the bottom row, 11 at the subsequent row etc, which leads to 10 units at the top row (crest row). At the sides of the flume, there are gaps between the Xbloc+ and the glass walls, which lead to decreased stability of those units due to the boundary effect of no friction and interlocking. To counteract this, the gaps are filled with rock of grading 11.2 – 16 mm and two chains are placed on and parallel to the slope.

### 2.2.2 Underlayer

Based on the assumption that the model armour units correspond to prototype units with volume of 3 m<sup>3</sup> (with scaling factor 1:49), the recommended underlayer (Guidelines for Xbloc Concept Design, 2018) is 300-1000 kg. This corresponds to an average weight  $W_{50}=650$  kg and a nominal diameter  $D_{n50}=0.626$  m in the prototype. The resulting values for the model are  $W_{50}=5.371$  gr and  $D_{n50}=1.3$  cm.

The following standard grading (available at the laboratory) is chosen:

Diameter range: 11.2 – 16 mm

Weight range: 2.21 gr – 6.43 gr

The underlayer thickness is  $f=26$  mm ( $=2D_{n50\text{underlayer}}$ ).

Van den Bos and Verhagen (2018) recommend that the weight ratio between the armour layer and the underlayer should be between 10 and 25 ( $d_{n50}$  ratio between 2 and 3), in order to obtain a “geometrically impermeable” filter. In the model:

$$\frac{D_{n50\text{underlayer}}}{D_{n50\text{armourlayer}}} = 2.24$$

Which conforms to the above rule.

Regarding the placement of the underlayer under the crest Xbloc+ elements, the underlayer is placed until the horizontal level defined by the bottom of the Xbloc+ crest elements. After the underlayer is placed, it is smoothed with a trowel to create an even surface. The matching of the placed underlayer (thickness and profile) with the design drawn in the 2 side glass walls of the flume is checked.

However, complete matching of the constructed and design profile cannot be achieved. Deviations from the design are always expected to occur as a result of irregularities caused by the natural roughness and the additional roughness of the underlayer’s rock material (Brouwer, 2013). The former implies that not all top levels of the rocks in the chosen grading can be located at the same plane, whereas the later is the result of the inaccuracies of placement during the construction of the model. When the underlayer stones protrude above the line of intended placement (case of positive placement tolerance), a larger area of the bottom of of the Xbloc+ crest element’s tail can be supported than in the case, when the stones’ top is below the line of intended placement (negative placement tolerance).

### 2.2.3 Core

As a rule of thumb, the core material should be smaller than the underlayer material and larger than the result of geometrical scaling, which leads to an upper limit of 12.66 mm and a lower limit of 7.77 mm. The application of the Burcharth (1999) approach for  $D_{n50}=9.6$  mm results in an average velocity of  $2.1 * 10^{-2}$  m/s in the model core. The target velocity, resulting from Froude scaling of the prototype core velocity, is  $1.89 * 10^{-2}$  m/s. In the absence of a real prototype, quarry run 1-300 kg is assumed (one grading lower than the prototype underlayer material). It should be noted that the target velocity is subject to change depending on the assumptions made for the prototype. Nevertheless, the two velocities are close to each other. The corresponding Reynolds number is 177, which is lower than the threshold Reynolds number of 300 proposed by Andersen and Burcharth (1995) for turbulent flow in coarse granular material. Therefore, the flow in the model core will be more laminar than in the prototype and viscous scale effects are expected. The model core is less permeable and, thus, more conservative for the armour layer stability. Standard grading 8 – 11.2 mm is chosen to be applied.

### 2.2.4 Toe

When designing and constructing the toe of the model breakwater, it is important to ensure that the toe is stable and will not slide during testing. Sliding of the toe could cause sliding of the bottom Xbloc+ row and subsequent downward movements and settlements of the lower armour rows, negatively affecting the stability of the armour row as a whole. Therefore, and because the toe is not part of this study, it is chosen to be fixed. This is achieved by placing a rectangular concrete slab ( $58.5 * 15 * 3$  cm) with weight of 6.165 kg in front of the bottom armour row. No considerable wave impact is expected at the toe, since the damage is expected to be concentrated in an area  $1.5H_s$  below the still water level (Vos, 2017). This distance is 15 cm for design conditions, whereas the toe is located 44 cm below the lowest water level in the flume.

### 2.2.5 Crest

The crest width is set at 20 cm, in order to allow sufficient space for the different crest configurations to be tested.

### 2.2.6 Rear Slope

In order to prevent erosion due to overtopping waves, the rear slope is covered with glued rock and gabions, placed on top of the core material, since no underlayer material is present at the rear slope. Furthermore, 2 sets of 2 bricks on top of each other are placed next to each other (total weight of 8.631 kg) at the rear toe to prevent sliding of the rear slope.

### 2.2.7 Model Breakwater Cross-section

The model breakwater cross-section is shown in Figure 2.3.



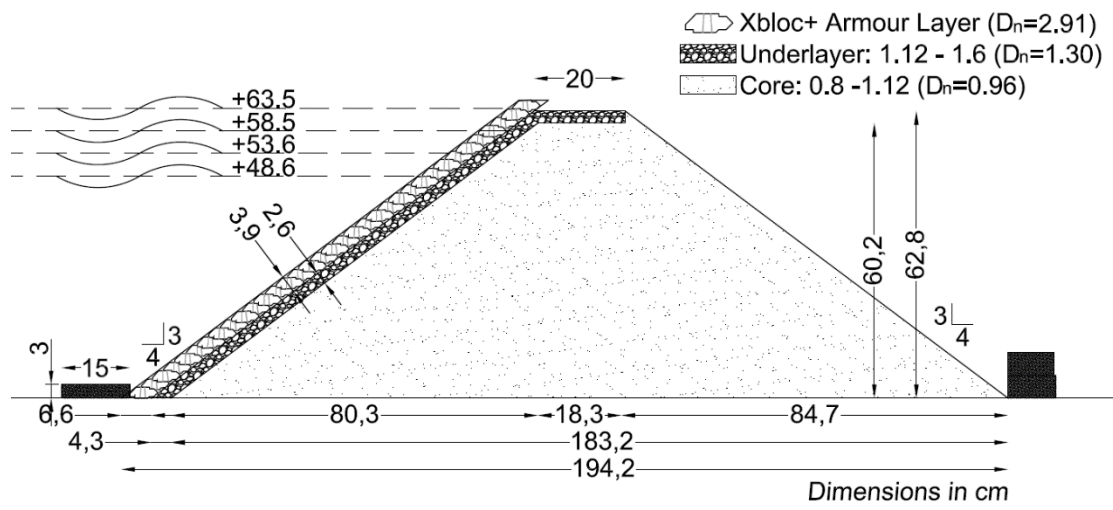


Figure 2.3: Model breakwater cross section

## 2.3 Wave Generation

For wave generation, acquisition and processing of the wave data, the software WaveLab, developed by Aalborg University is used. To generate the target waves in deep water, a file is created, in which information, such as significant wave height, peak period, spectrum characteristics and test duration are contained. To record the time series of water level elevations, a frequency of 32 Hz is used.

### 2.3.1 Wave Characteristics

The formula used by Delta Marine Consultants for the stability of the Xbloc+ is based on a design stability number of  $N_{s,d} = 2.5$ . In order to obtain the design significant wave height,  $H_{s,d}$  (corresponding to 100% wave conditions), this formula is used for the Xbloc+ model units:

$$H_{s,d} = 2.5 * \Delta * D_n = 9.91 \text{ cm}$$

Where,

$$\Delta = \frac{\rho_c - \rho_w}{\rho_w} = 1.36: \text{relative density (-)}$$

$$\rho_c = 2360 \text{ kg/m}^3: \text{model units density}$$

$$\rho_w = 1000 \text{ kg/m}^3: \text{water density}$$

In order to avoid viscous scale effects in the armour layer, turbulent flow conditions should be present in the armour layer (Wolters et al, 2010). This is ensured, when the Reynolds number for the armour layer is above a certain threshold. Many different thresholds have been proposed in the literature by various researchers. The Reynolds number for the model armour layer is given by:

$$Re_{\text{armour}} = \frac{\sqrt{gH_s} D_n}{\nu} = \frac{\sqrt{9.81 \frac{\text{m}}{\text{s}^2} * 9.91 \text{cm} * 2.91 \text{cm}}}{10^{-6} \frac{\text{m}^2}{\text{s}}} = 28730$$

The resulting Reynolds number for the model armor layer can be considered high enough to neglect scale effects at the armor layer, as it is approximately equal to  $3 * 10^4$ .

Having calculated the target design significant wave height ( $H_{s,d}=H_{m0,d}$ ), the significant wave heights and peak periods, corresponding to the 2 different values for the steepness ( $s_{op}=2\%$ ,  $s_{op}=4\%$ ), for all the tests are calculated for the waves generated in deep water.

To create irregular waves, a standard Jonswap spectrum with the following parameters is used:  $\gamma=3.3$ ,  $\sigma_a=0.07$  and  $\sigma_b=0.09$ ,  $\alpha=0.0081$ .

### 2.3.2 Test Duration

It can be assumed that after 1000 waves, the Jonswap spectrum is fully developed. Also, it is known that most of the damage to armour units has already happened after 1000 waves, which corresponds to a 3 hour storm with waves of 10s in reality. Thus, it is chosen that each test consists of 1000 waves, in order to gain statistically reliable results (Wolters et al, 2007).

## 2.4 Test Program

The test program is divided into 3 test sets. Each test set is divided into test series, each of which is characterized by a specific combination of wave steepness and relative freeboard. Each test series is divided into tests, each of which is characterized by a different significant wave height.

The test sets are the following:

- 1<sup>st</sup> test set: performed on the single (without rear support) Xbloc+ crest elements. Initially 8 test series were performed, 5 of which were repeated, resulting in 13 test series in total.
- 2<sup>nd</sup> test set: testing of different crest configurations to determine an optimal one.
- 3<sup>rd</sup> test set: additional testing on the on the optimal configuration.

The 1<sup>st</sup> test set aims to answer the 1<sup>st</sup> and 2<sup>nd</sup> research question:

*What is the relation of the stability of the crest elements with the following parameters: relative crest freeboard and wave steepness?*

*How do those parameters affect the failure mechanism?*

The 2<sup>nd</sup> and 3<sup>rd</sup> test sets aim to answer the 3<sup>rd</sup> research question:

*How can different crest configurations increase the stability of the crest elements?*

### 2.4.1 1<sup>st</sup> Test Set

The 1<sup>st</sup> test set is performed on the single crest elements, which means that the upper armour row of the Xbloc+ is placed on top of the second upper row, without any rear support. The 1<sup>st</sup> test set is subdivided into 13 test series, of which 8 were conducted first (initial test series), whereas 5 were conducted after the 2<sup>nd</sup> and 3<sup>rd</sup> test sets and constitute repetition of 5 of the initial test series, as explained below.

During the execution of the 1<sup>st</sup> test set, it was noticed that, at certain test series, movement of the crest units started already from the test with the lowest significant wave height performed (first test of the test series). Thus, in order to find the critical stability number for which movement started, those tests were repeated, starting from lower stability numbers. The latter, in combination with the 10% increment in increasing the wave height between tests leads to much larger total duration of a repetition test series. The repetition of those test series also serves as a way to check the reliability of experiments. Finally, the distances between the unit and the underlayer were measured, in order to examine the effect of the underlayer on the way that units get partially displaced.

Each test series is subdivided into a number of tests with the same combination of freeboard and wave steepness. As wave steepness, the peak steepness of the spectrum,  $S_{op}$ , is used. The freeboard can be made dimensionless either by dividing with the significant design wave height of each test series ( $H_{s,d} = 9.91$  cm) or by dividing with the nominal diameter of the Xbloc+ unit ( $D_n = 2.91$  cm). Both formulations of the relative freeboards are presented in Table 2.2.

Freeboard – $R_c$ (cm)	Relative Freeboard – $R_c/H_{s,d}$ (-)	Relative Freeboard – $R_c/D_n$ (-)
0.00	0.0	0.0
4.95	0.5	1.7
9.91	1.0	3.4
14.85	1.5	5.1

Table 2.2: Relative freeboard formulations

Between tests of each test series, the wave height is gradually increasing. For the 8 initial test series, the significant wave height starts from  $0.60H_{s,d}$  ( $H_{s,d} = 9.91$  cm being the design height, corresponding to a stability number of  $N_s=2.5$ ). By initially applying lower waves, the start of storm is simulated and the structure is enabled to settle and become more compact (Wolters et al, 2007). Subsequently, from one test to another, the wave height is increased by increments of  $0.2H_{s,d}$  until  $1.00H_{s,d}$  and, subsequently,  $0.1H_{s,d}$  until  $1.20H_{s,d}$ , after which testing is stopped. For the 5 repetition test series, the significant wave height starts from the value that causes no movement and increase by increments of  $0.1H_{s,d}$  until  $1.20H_{s,d}$ .

From one test series to another, the relative freeboard ( $R_c/D_n$ ) and/or the wave steepness ( $s_{op}$ ) is changed: 4 different cases for the relative freeboard ( $R_c/D_n = 0, 1.7, 3.4, 5.1$ ) and 2 for the wave steepness ( $s_{op}=2\%$  - typical for swell waves – and  $4\%$  - typical for wind waves) are tested.

#### 2.4.2 2<sup>nd</sup> Test Set

The aim of the 2<sup>nd</sup> test set is to find an optimized configuration, that would prevent the Xbloc+ crest units from failing. The different configurations are tested for the combination of  $R_c/D_n = 0.0$  and  $s_{op} = 4\%$ , which caused the most units to fail during the initial test series of the 1<sup>st</sup> test set. Furthermore, wind waves (typical steepness of  $4\%$ ) are expected to be more common in project locations compared to swell waves (typical steepness of  $2\%$ ). In total, 7 different configurations are tested, which are described below:

##### Test series 2.2.1 - Different orientations of unit: Tail tilted upwards & Nose tilted upwards

For this test series, half of the units of the top armor row (5 left units) are placed with their tail tilted upwards, whereas the other half (5 right units) are placed with their nose tilted upwards. In both cases, contact is no longer made between the bottom of the wings of the crest unit with the horizontal part of the tail of the two neighboring units of the row beneath. In the first case, contact is made between the crest unit wings' bottom and the top (highest horizontal surface) of the left and right units of the row beneath. Underlayer material is placed below the now inclined bottom of the crest units to enable this placement. In the second case, contact is made between the crest unit wings' bottom and the top of the left and right elements of the second row and, also, the "tip" of the Xbloc+ crest unit tail makes contact with the underlayer.



Figure 2.4: Test series 2.2.1 Crest configuration

### Test series 3.2.1 – Xblocs A

For this test series, 21 Xblocs in total are placed behind and in between the Xbloc+ crest units, in order to increase friction and interlocking. For 2 neighbouring Xbloc+, 5 Xblocs are placed: one at the left side of the left unit, one at the right side of the right unit, one in the gap between the 2 Xbloc+ units and 2 behind the tail of each of the Xbloc+ units. The orientation and distances between the Xblocs are random, but they are placed in such a way that: two neighboring Xblocs interlock by having at least one contact area and, particularly, the Xbloc behind the tail touches the Xbloc+ there.



Figure 2.5: Test series 3.2.1 Crest configuration

### Test series 4.2.1 – Xblocs B

For this test series, the Xblocs are closer to each other (higher packing density), but occupy a larger area of the crest both in horizontal and vertical direction, as 3 rows of Xblocs are used and also additional Xblocs are placed on top of the first row to increase the packing density. In total, 76 Xblocs are used, the characteristics of which are shown in Table 2.3.

D (Height) (cm)	$D_n$ (Nominal Diameter) (cm)	V (Volume) (cm <sup>3</sup> )	M (Mass) (gr)	$\rho$ (Density) (gr/cm <sup>3</sup> )	$H_{s,d,Xbloc}$ (Design wave height) (cm)
4	2.8	21.33	49	2.30	9.96

Table 2.3: Characteristics of Xblocs used for configurations



Figure 2.6: Test series 4.2.1 Crest configuration

### Test series 5.2.1 – Xblocs & Crown Wall

For this test series, 21 Xblocs are placed in the same manner, as in test series 3.2.1, but closer to each other. Behind the Xblocs, 8 elements, with an average mass of 304 gr each are placed,

in order to function as a crown wall. The purpose of the latter is to prevent the Xblocs from moving and, subsequently, creating more space for the Xbloc+ units to move. The Xblocs are placed in such a way that friction and interlocking is increased behind and above the Xbloc+ units and, additionally, weight is added at the top. Underlayer material is used to fill the crest area behind, as well as between the edge crown wall elements and the glass flume, in order to ensure that there are no gaps that could cause moving or settlements of the crown wall elements.



Figure 2.7: Test series 5.2.1 Crest configuration

#### Test series 6.2.1 - Underlayer Filling & Crown Wall

For this test series, underlayer material is used to fill the gaps between the Xbloc+ crest units. In combination, a concrete element is placed 1 cm behind edges of the tails of the Xbloc+. This element is aimed to prevent the underlayer material from moving, eroding and spreading over the crest area. The gap between the tails and the concrete crest element is also filled with underlayer material. To construct this configuration, the below procedure is followed:

- Stones (from the underlayer material) are placed below the tails of the Xbloc+ crest units, so that they are almost horizontal and make full contact with the row below.
- The gaps between the Xbloc+ are filled with underlayer material. (11.2-16 mm).
- The placed material is pressed with a spatula.
- The crown wall element is placed at 1 cm behind the tails' edges of the Xbloc+ elements. This element has 48 cm length, 15 cm width, 2 cm height and weighs 3 kg.
- The gap between the Xblocs+ and the crown element, as well as other visible gaps are filled with underlayer material.
- The placed material is again pressed with a spatula and fingers to make sure that there are no gaps.
- The gaps between the crown element and the glass flume walls are filled with 16 – 22 material, which is also compacted with the spatula. Two pieces of glued rock are placed over this material. A gabion is placed behind the crown wall element to cover the rest of the crest. In the above described way, it is ensured that the crown element at the crest will not move.



Figure 2.8: Test series 6.2.1 Crest configuration

### Test series 7.2.1 - Underlayer filling at the top of the crest

In this tested configuration, the whole crest area is filled with underlayer stones, which are compacted with a spatula. The difference with Test series 6.2.1 is that there is no crown wall element, which is stiff. The goal is to determine whether only filling with underlayer material could make the crest Xbloc+ units stable without eroding.



Figure 2.9: Test series 7.2.1 Crest configuration

### 2.4.3 3<sup>rd</sup> test set

To test if the optimised configuration resulting from the 2<sup>nd</sup> test set is also a feasible solution for other conditions except for the most critical conditions of the 1<sup>st</sup> test set ( $R_c/D_n = 0$ ,  $s_{op} = 4\%$ ), 3 additional tests are performed for:  $R_c/D_n = 0$  &  $s_{op} = 2\%$ ,  $R_c/D_n = 1.7$  &  $s_{op} = 2\%$ ,  $R_c/D_n = 1.7$  &  $s_{op} = 2\%$ .

### 2.4.4 Overview – All tests

In this section, an overview of all tests is presented in Table 2.4.

More information about the theoretical and generated parameters are included in Appendix F.

Test Set	Test Series	Crest Configuration	Wave steepness $S_{op}$	Relative Freeboard $R_c/D_n$
1 <sup>st</sup>	1.1.1	Initial - Single Xbloc+	2%	0.0
1 <sup>st</sup>	1.1.2	Initial - Single Xbloc+		1.7
1 <sup>st</sup>	1.1.3	Initial - Single Xbloc+		3.4
1 <sup>st</sup>	1.1.4	Initial - Single Xbloc+		5.1
1 <sup>st</sup>	1.2.1	Initial - Single Xbloc+	4%	0.0
1 <sup>st</sup>	1.2.2	Initial - Single Xbloc+		1.7
1 <sup>st</sup>	1.2.3	Initial - Single Xbloc+		3.4
1 <sup>st</sup>	1.2.4	Initial - Single Xbloc+		5.1
1 <sup>st</sup>	1.1.1	Repetition - Single Xbloc+	2%	0.0
1 <sup>st</sup>	1.2.2	Repetition - Single Xbloc+	4%	0.0
1 <sup>st</sup>	1.1.2	Repetition - Single Xbloc+	2%	1.7
1 <sup>st</sup>	1.2.2	Repetition - Single Xbloc+	4%	1.7
1 <sup>st</sup>	1.1.3	Repetition - Single Xbloc+	2%	3.4
2 <sup>nd</sup>	2.2.1 - Orientation with Tail upwards	Tested configuration	4%	0.0
2 <sup>nd</sup>	2.2.1 - Orientation with Nose upwards	Tested configuration	4%	0.0
2 <sup>nd</sup>	3.2.1 – Xblocs A	Tested configuration	4%	0.0
2 <sup>nd</sup>	4.2.1 – Xblocs B	Tested configuration	4%	0.0
2 <sup>nd</sup>	5.2.1 – Xblocs & Crown Wall	Tested configuration	4%	0.0
2 <sup>nd</sup>	6.2.1 – Underlayer filling & Crown Wall	Tested configuration & Optimised Configuration (Solution)	4%	0.0
2 <sup>nd</sup>	7.2.1 – Underlayer filling at top of crest	Tested configuration	4%	0.0
3 <sup>rd</sup>	6.1.1 – Underlayer filling & Crown Wall	Optimised Configuration (Solution)	2%	0.0
3 <sup>rd</sup>	6.1.2 – Underlayer filling & Crown Wall	Optimised Configuration (Solution)	2%	1.7
3 <sup>rd</sup>	6.2.2 – Underlayer filling & Crown Wall	Optimised Configuration (Solution)	4%	1.7

Table 2.4: All tests overview



---

## 2.5 Test Execution

### 2.5.1 Methodology

In this section, the methodology followed for the model set up and the execution of the tests is described.

For the model set-up, the below steps are followed:

1. One drawing of the cross-section in each side of the glass flume is created by making sure that both drawings are exactly at the same location.
2. The core material is first washed and then placed. Correct placement is checked, as per the drawn cross sections.
3. The underlayer material is washed and placed at the front slope and the crest. During placement, it is flattened with a spatula in order to be as smooth and level as possible and without rocks protruding.
4. Gabions and glued rock are placed at the rear slope. The toe at the rear side is also placed.
5. The Xbloc+ units of the armour layer are placed. After the first (bottom) row is placed, the concrete element, that functions as a toe, is placed in front of them. Once all Xbloc+ rows are in place, the gaps between the sides and the glass walls of the flume are filled with underlayer material and the chains are placed on top.
6. The wave gauges are placed.
7. Two cameras are placed. The first is located on top of the flume and is looking perpendicular at the slope, while focusing on the top rows of the armour layer. The second is at the side of the glass flume and is looking perpendicular at the top row, to record the wave motions. The cameras are kept in the same position during each test series, so the pictures taken before and after each test are comparable.

For the tests' execution, the following steps are followed:

1. The flume is filled up to the required water level for each test series and the wave gauges are calibrated. The wave gauges are recalibrated regularly during each day.
2. Calibration runs of 10 minutes duration are conducted for all tests of the test series to ensure that the generated wave parameters are close to the theoretical ones.
3. After calibration, the wave generation files for the duration of the actual experiments are created. The files are revised to ensure that the correct input parameters are present.
4. A picture is taken before the start of the test (1.1.1.1.1.Appendix H. ). The videos are also started.
5. The actual test take place.
6. After the test finishes, a picture is taken after and the videos are stopped.
7. The wave acquisition file, that is created during the test, is checked to ensure that the recorded wave data from the gauges match with the target wave characteristics in the input files and that there are no other errors.
8. Any damage that happened during the test series in the cross-section is repaired.

Steps 4 – 7 are repeated for each test of a test series. Steps 1-3 and 8 take place before and after each test series respectively.

## 2.5.2 Visual Observations

During the tests, visual observations are made and recorded in a notebook. To facilitate the observations, the 10 crest elements are referred to as: 1L, 2L, 3L, 4L, 5L, 5R, 4R, 3R, 2R, 1R. “L” stands for left and “R” for right, when looking at the cross section from the side of the incoming waves.

The items observed are:

- Rocking units. The observations regarding rocking units are cross-checked with the videos to confirm if a unit actually rocked during a test.
- Time of failure of each unit.
- Damage to the other rows of the breakwater (2<sup>nd</sup> row from the top etc).
- Movement/Erosion of the underlayer rock at the crest.
- Other phenomena that happen, but have not been predicted.

The visual observations made during the testing can be found in Appendix G. .

## 2.5.3 Units’ Movement Definitions

The movements that the Xbloc+ crest units make during the experiments are distinguished in the following categories:

### 1. Rocking

Rocking is the rotational movement, during which the unit is “tilting” up and down during wave uprush and rush-down respectively, but, eventually, is returning to its initial position. Rocking can happen before or/and after a unit fails.

### 2. Partial Displacement

Partial displacement is defined as the situation in which a unit is displaced from its original position, but contact is still maintained under both wings of the unit. More specifically, the left (and right) wing of the unit still makes contact with the horizontal part at the top of the tail of the “neighbouring” unit of the row below located at the left (and right) of the crest unit in question. Partial displacement can be distinguished in the three stages below:

- Partial displacement – Stage 1: When a unit only rotates, but does not move backwards. The unit’s nose is tilted up, so it does not make contact with the top of the wings of the two units of the below row.
- Partial displacement – Stage 2: When only one of the two wings of the unit moves backwards, but the other remains at its original position. The unit ends up displaced sideways.
- Partial displacement – Stage 3: When both wings of the unit move backwards.

The three stages of partial displacement are shown in Figure 2.10:



Figure 2.10: Top left: Stable unit; Top right: Stage 1 of partial displacement; Bottom left: Stage 2 of partial displacement; Bottom right: Stage 3 of partial displacement

### 3. Failure

An element is considered failed, when at least one of its wings loses contact with the top horizontal part of the tail of the beneath unit. Some examples of failed units are given in Figure 2.11:



Figure 2.11: Examples of failed units

#### Criterion for Failure and Partial Displacement

During testing, it was observed that, when one unit of the top armour row fails, it is very likely to subsequently rock and change positions at the crest, thus, creating additional damage. Furthermore, the failure of one unit provides more space for the two neighbouring units of the 2<sup>nd</sup> from the top row to be displaced. Thus, the failure (or partial displacement) of one units is considered failure (or partial displacement) for the top armour row, 10% criterion. Regarding failure of the armour layer as a whole, it did not occur, since, the final damage during all tests, is considered repairable.

### 3. Results – Tests on Single Xbloc+ Crest Units

In this chapter, the results from the performed physical model tests on the single Xbloc+ crest elements (1<sup>st</sup> test set - Initial & Repetition) are presented. The tests on the single Xbloc+ elements were performed, in order to get insight into the influence of the freeboard and wave steepness on the stability and failure mechanisms of the Xbloc+ crest elements. In total, 13 test series were executed: 8 test series were performed first (referred to as “Initial”), 5 of which were performed again after (referred to as “Repetition”).

During the initial execution of the test series with  $R_c/D_n=0$  and  $s_{op}=4\%$  (Test series 1.2.1 - Initial), all units failed, whereas during the repetition, 20% fewer units failed, although the testing duration was more than double and the final test with the highest significant wave height was repeated. On the contrary, for the other 4 test series repeated, 20% more units failed during the repetition. A possible explanation for the difference in behaviour is that the initial experiment with  $R_c/D_n=0$ ,  $s_{op}=4\%$  was the first conducted, so the underlayer must have been placed in a way that it provided less support to the Xbloc+ crest units compared to the rest of the experiments. Based on this, the results of test series 1.2.1 - Initial are excluded from the analysis, thus, the results of 12 test series are presented.

#### 3.1 Failed Units – Single Xbloc+ (1<sup>st</sup> Test Set)

In this section, the failed units of the 12 test series on the single Xbloc+ are compared. For a certain test (corresponding to a certain stability number), a unit might have failed during that test or before. In Figure 3.1, the failed units (as percentage of the 10 crest units) with respect to the stability number ( $N_s=H_s/(\Delta D_n)$ ) on the single Xbloc+ are shown for all test series (Initial and Repetition). The following results are derived.

##### **Influence of Freeboard and Wave Steepness on Failed Units**

The conditions leading to most failed units are the following:

$R_c/D_n=1.7$  and  $s_{op}=2\%$

$R_c/D_n=0$  and  $s_{op}=4\%$

$R_c/D_n=0$  and  $s_{op}=2\%$

During the initial testing, the condition with  $R_c/D_n=1.7$ ,  $s_{op}=2\%$  caused 10% more failed units compared to  $R_c/D_n=0$ ,  $s_{op}=2\%$ , whereas during the repetition testing, the former condition caused 10% more failed units compared to  $R_c/D_n=0$ ,  $s_{op}=2\%$  and  $R_c/D_n=0$ ,  $s_{op}=4\%$ . A difference of 10% (1 unit) can be justified by the result of the different conditions during testing, such as underlayer irregularities, and, thus, cannot be considered determining. Therefore, all 3 above conditions are considered critical.

The conditions with  $R_c/D_n=1.7$ ,  $s_{op}=4\%$  and  $R_c/D_n=3.4$ ,  $s_{op}=2\%$  follow and cause the same number of failed units, but 30% fewer, both during the initial and repetition tests.

Another observation is that waves of 2% steepness acting at a specific relative freeboard cause the same or more failed units compared to waves of 4% steepness acting at  $1.7D_n$  lower relative freeboard. This holds for:

$R_c/D_n=1.7$ ,  $s_{op}=4\%$  and  $R_c/D_n=3.4$ ,  $s_{op}=2\%$

$R_c/D_n=0$ ,  $s_{op}=4\%$  and  $R_c/D_n=1.7$ ,  $s_{op}=2\%$

This phenomenon can be explained by the largest run-up of 2% waves compared to 4% waves, which leads to more waves reaching and acting on the crest units, despite the lower freeboard.

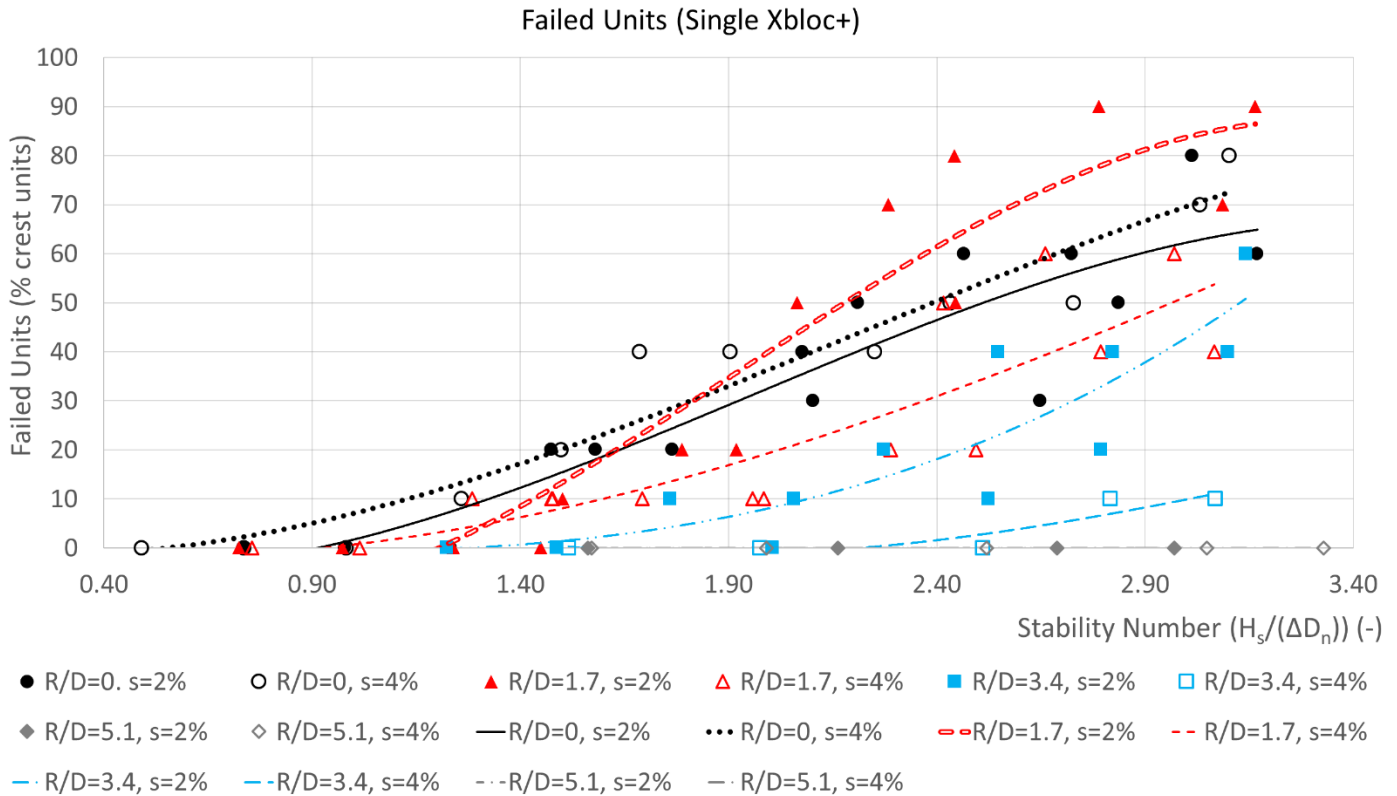


Figure 3.1: Failed units - Initial & Repetition tests on the single Xbloc+ (1<sup>st</sup> test set)

### Influence of Freeboard on Failed Units (for constant Wave Steepness)

For 2% steepness waves, failed crest units increase, as relative freeboard increases from  $R_c/D_n=0$  to  $R_c/D_n=1.7$ , are maximum at  $R_c/D_n=1.7$  and, subsequently, decrease constantly, as relative freeboard increases further. This decrease is evident from  $R_c/D_n=3.4$  onwards.

For 4% steepness waves, the maximum failure at the crest row is observed, when the still water level is at the crest level, but as the water level decreases, failure also decreases.

### Influence of Wave Steepness on Failed Units (for Constant Freeboard)

In general, 2% steepness waves create more failure than 4% steepness waves, when the relative freeboard ( $R_c/D_n$ ) is higher than 1.7, whereas, at conditions of zero freeboard, failure is the same. More specifically:

For zero freeboard, no conclusion on the influence of the wave steepness on failed units can be drawn, as both 2% and 4% steepness cause the same failed units during the repetition tests and the initial test series with zero freeboard and 4% steepness in excluded from the analysis. For relative freeboard ( $R_c/D_n$ ) equal to 1.7, 2% steepness waves cause more failed units than 4% steepness waves and the difference is 30% at both the initial and repetition tests. For  $R_c/D_n=3.4$ , 2% steepness waves result in 30% more failed units than 4%, which is based on the

initial tests, because the test series with 4% steepness was not repeated. For  $R_c/D_n=5.1$ , crest units did not fail, for neither 2% nor 4% wave steepness.

### Failure Development in Time

During testing, the time of failure of each of the Xbloc+ crest units was noted down and confirmed from the recorded videos. The majority of the units failed at the time interval between the end of the test with significant wave height equal to 50% of the design wave height and the end of the test with the design wave height. More information can be found in Appendix B.

#### 3.1.1 Comparison between Initial and Repetition Test Series on the Single Xbloc+ elements (1<sup>st</sup> Test Set)

The total number of failed units at the end of the initial and repetition test series on the single Xbloc+ crest elements are compared (only test series with the same combination of relative freeboard and wave steepness) in Figure 3.2. The number of failed units during the repetition is 20% higher than the corresponding initial test series.

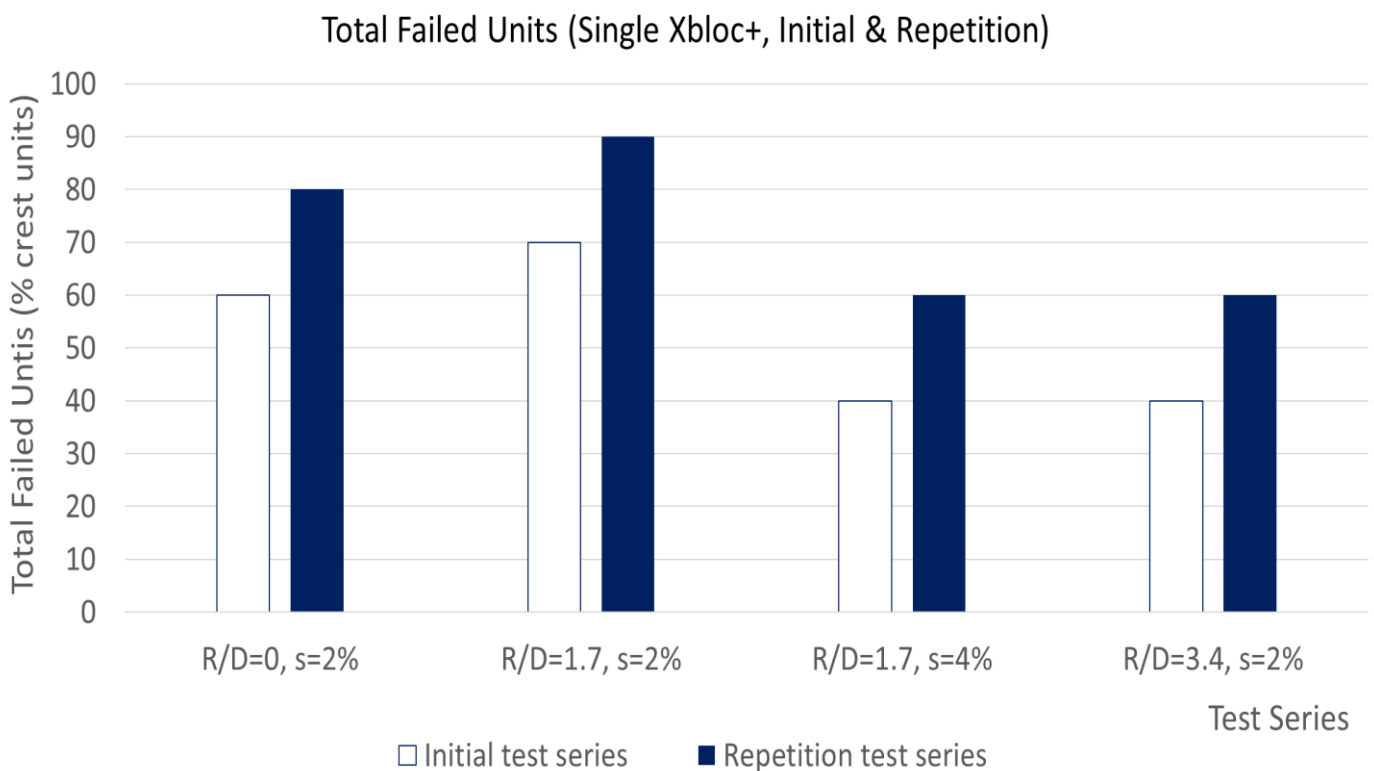


Figure 3.2: Failed units at the end of each test series on the single Xbloc+ – Initial and Repetition

The more failed units can be explained by the larger duration of the repetition test series: additional tests with significant wave height lower than  $0.60H_{s,d}$  were conducted, in order to find the wave conditions that cause the initial movement of the Xbloc+ crest units. Furthermore, from one test to the next, the significant wave height was increased by 10% (compared to 20% initially). As seen in Table 3.1, the duration of the repetition test series is

minimum 1.49 times higher than initial, whereas the number of failed units is minimum 1.29 times higher.

Test series	Duration Ratio (Repetition/Initial) (-)	Failed Units Ratio (Repetition/Initial) (-)
1.1.1 - $R_c/D_n=0$ - $s_{op}=2\%$	1.76	1.33
1.1.2 - $R_c/D_n=1.7$ - $s_{op}=2\%$	2.28	1.29
1.2.2 - $R_c/D_n=1.7$ - $s_{op}=4\%$	1.76	1.50
1.1.3 - $R_c/D_n=3.4$ - $s_{op}=2\%$	1.49	1.50

Table 3.1: Duration ratio and Failed units ratio (Repetition/Initial)

### 3.2 Rocking units – Single Xbloc+ (1<sup>st</sup> Test Set)

During the experiments on the single Xbloc+ elements, a number of units were rocking. The rocking of units was assessed visually during the experiment, so if a unit was observed to be rocking (“tilting” up and down at wave uprush and rush-down respectively, but, eventually, returning to its initial position), it was noted down. After the experiments, the recorded videos were reviewed, in order to confirm if the unit was actually rocking or not. A unit is considered to have rocked, if it has been observed to rock at least once during the test series.

Units were rocking before failing, after failing or at both cases. In the laboratory, the used plastic Xbloc+ units do not break and return to their initial position, after the experiment is finished, and, thus, no damage is visible. However, in reality, it is possible that rocking concrete units break and, additionally, collide with neighbouring units, causing the latter also to break, which, eventually, creates “weaker spots” in the armour layer, where the underlayer can become exposed. For example, if a failed unit located very close to units of the top or the 2<sup>nd</sup> from the top armour layer row rocks, it can collide with the neighbouring units and result in their breakage. Broken units are impossible to repair.

#### Influence of Freeboard and Wave Steepness on Rocking Units

In Figure 3.3, the influence of the relative freeboard and wave steepness on the rocking units is presented. The total number of units that rocked at the end of each test series - both Initial (“In.”) and Repetition (“Rep.”) - is shown in the Y axis. A unit is considered “rocking”, if it rocked at least once, either before or after failure, whereas units rocking both before and after failure are accounted only once.

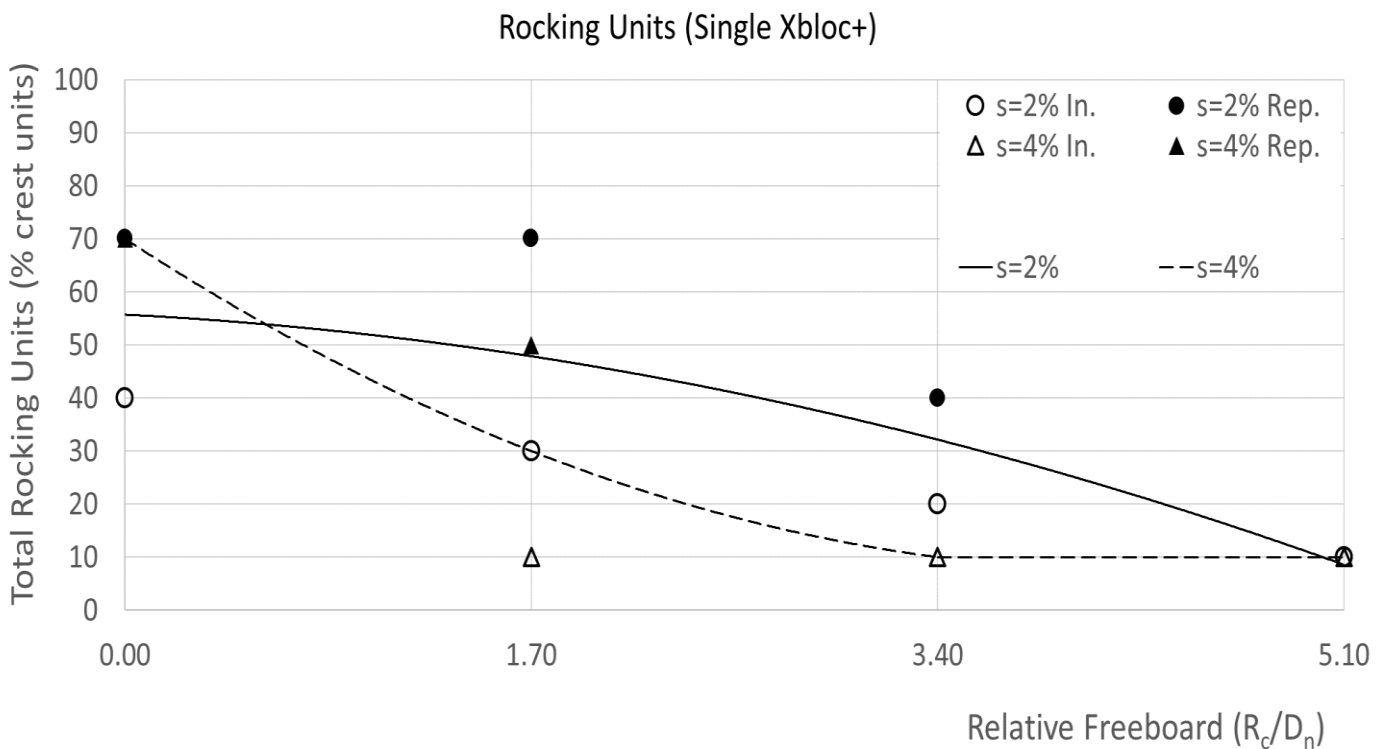


Figure 3.3: Rocking units - Initial & Repetition tests on the Single Xbloc+ (1<sup>st</sup> test set)



The conditions causing the most rocking units are the following:

$R_c/D_n=1.7$  and  $s_{op}=2\%$

$R_c/D_n=0$  and  $s_{op}=4\%$

$R_c/D_n=0$  and  $s_{op}=2\%$

All 3 conditions caused the same number of rocking units (70% of crest units) during the repetition testing. The condition with  $R_c/D_n=1.7$  and  $s_{op}=4\%$  follows with 20% fewer rocking units both during the initial and repetition testing.

The same conclusions are drawn when examining the influence of the freeboard and wave steepness on the rocking before and after failure units, separately, and the corresponding graphs are included in 1.1.1.1.1.Appendix C.

#### **Influence of Freeboard on Rocking Units (for constant Wave Steepness)**

An increase in the relative freeboard ( $R_c/D_n$ ) results in a decrease in rocking units, for both 2% and 4% steepness. The decrease is evident at  $R_c/D_n=3.4$  and  $1.7$  for 2% and 4% steepness respectively. The more gradual decrease in the case of 2% steepness waves and the fact that they cause the same number of rocking units for  $R_c/D_n=0$  and  $R_c/D_n=1.7$  (observed during the repetition testing) can be attributed to their higher run-up, compared to 4% steepness waves.

#### **Influence of Wave Steepness on Rocking Units (for constant Freeboard)**

In general, 2% steepness waves result in more rocking units than 4% steepness waves, when the relative freeboard ( $R_c/D_n$ ) is higher than 1.7, whereas, at conditions of zero freeboard, the number of rocking units is the same. More specifically:

For zero freeboard, no conclusion on the influence of the wave steepness on failed units can be drawn, as the result is the same for both steepness during the repetition test, whereas the initial test series with zero freeboard and 4% steepness is excluded from the analysis. For relative freeboard ( $R_c/D_n$ ) equal to 1.7, 2% steepness waves cause more failed units than 4% steepness waves and the difference is 20% at both the initial and repetition tests. For  $R_c/D_n=3.4$ , 2% steepness waves result in 10% more failed units than 4%, based on the initial tests (the test series with 4% steepness was not repeated). For  $R_c/D_n=5.1$ , only 1 unit rocked (10%) for both steepness.

#### **Rocking Units Comparison between Initial and Repetition Test Series**

The total number of rocking units is larger during the repetition than the initial testing for the 4 test series compared (5 out of 8 tests series repeated and test series with  $R_c/D_n=0$  &  $s_{op}=4\%$  excluded from analysis). More specifically, the difference is 30%, 40%, 40%, 20% for test series with  $R_c/D_n=0$  &  $s_{op}=4\%$ ,  $R_c/D_n=0$  &  $s_{op}=4\%$ ,  $R_c/D_n=0$  &  $s_{op}=4\%$ ,  $R_c/D_n=0$  &  $s_{op}=4\%$  respectively. This increase, which is also present when examining the rocking before and after failure units separately (Appendix C. ), is attributed to the larger duration of the repetition series.

### **3.2.1 Rocking Before Failure Units**

Three categories of units in terms of rocking before failure are distinguished: units that have rocked before failing, units that have not rocked before failing and units that have rocked, but did not fail.

In Table 3.2, the rocking before failure units with respect to the failed units are presented.

Test Series	Rocking before failure units (% failed units)
$R_c/D_n=0 - s_{op}=2\%$ - Initial	33
$R_c/D_n=1.7 - s_{op}=2\%$ - Initial	14
$R_c/D_n=1.7 - s_{op}=4\%$ - Initial	25
$R_c/D_n=3.4 - s_{op}=2\%$ - Initial	25
$R_c/D_n=3.4 - s_{op}=4\%$ - Initial	0
$R_c/D_n=5.1 - s_{op}=2\%$ - Initial	No failure
$R_c/D_n=5.1 - s_{op}=4\%$ - Initial	No failure
$R_c/D_n=0 - s_{op}=2\%$ - Repetition	38
$R_c/D_n=0 - s_{op}=4\%$ - Repetition	50
$R_c/D_n=1.7 - s_{op}=2\%$ - Repetition	33
$R_c/D_n=1.7 - s_{op}=4\%$ - Repetition	17
$R_c/D_n=3.4 - s_{op}=2\%$ - Repetition	17

Table 3.2: Relation of Rocking before failure and Failed units (All test series)

The following remarks are made:

- The units that rock, and, subsequently, fail, are always less than 50% of the total failed units, except for one test series, where exactly half of the failed units rocked before failing.
- During 1 of the 12 test series, none of the units rocked before failing.
- During 3 of the 12 test series, the rocking before failure units were less than 40% of the failed units.
- During 5 of the 12 tests series, the rocking before failure units were less than 25% of the failed units.

Therefore, although rocking before failure happens and is important for damage, it cannot be characterised as a reliable indicator of failure. This means that it is more possible that a unit fails without rocking before, rather than rocking and failing.

### 3.2.2 Rocking After Failure units

Failed Xbloc+ units from the top armour row lose contact with the units of the row below (2<sup>nd</sup>) and are displaced at the crest. At their new position, they are either rocking or not. In Table 3.3, the rocking after failure units with respect to the failed units are presented.

During the initial tests the percentage of rocking after failure units is in all cases lower than 50% of the total failed units. However, during the repetition tests the percentage is always higher than 67%. Therefore, Xbloc+ crest units are likely to rock at their new positions at the crest. Rocking causes breakage of the units and, furthermore, collision and subsequent breakage of neighbouring units.

The phenomenon of increased rocking after failure reinforces the 10% criterion for start of failure, because even at the case that 1 unit (out of 10) fails, it will most probably not remain still at the same position, but rock or move to new positions at the crest, thus, causing additional damage to the structure.

Test Series	Rocking after failure units (% failed units)
$R_c/D_n=0 - s_{op}=2\%$ - Initial	50
$R_c/D_n=1.7 - s_{op}=2\%$ - Initial	43
$R_c/D_n=1.7 - s_{op}=4\%$ - Initial	25
$R_c/D_n=3.4 - s_{op}=2\%$ - Initial	25
$R_c/D_n=3.4 - s_{op}=4\%$ - Initial	0
$R_c/D_n=5.1 - s_{op}=2\%$ - Initial	No failure
$R_c/D_n=5.1 - s_{op}=4\%$ - Initial	No failure
$R_c/D_n=0 - s_{op}=2\%$ - Repetition	75
$R_c/D_n=0 - s_{op}=4\%$ - Repetition	75
$R_c/D_n=1.7 - s_{op}=2\%$ - Repetition	67
$R_c/D_n=1.7 - s_{op}=4\%$ - Repetition	67
$R_c/D_n=3.4 - s_{op}=2\%$ - Repetition	67

Table 3.3: Relation of Rocking after Failure and Failed units (All test series)

### 3.2.2.1. Comparison between Rocking Before Failure and Rocking After Failure Units

In Figure 3.5, the total percentages of rocking before failure units (incl. units that rock, but do not fail) and rocking after failure units for all test series are presented. If a unit rocks both before and after failure, then it is counted twice i.e. at both categories. It is evident that the number of units rocking after failing is larger than the number of units rocking before failing. This conclusion is valid for 7 out of 12 cases, with the following 5 exceptions:

$R_c/D_n=1.7$  and  $s_{op}=4\%$  (Initial),  $R_c/D_n=3.4$  and  $s_{op}=2\%$  (Initial),  $R_c/D_n=3.4$  and  $s_{op}=4\%$ ,  $R_c/D_n=5.1$  and  $s_{op}=2\%$ ,  $R_c/D_n=5.1$  and  $s_{op}=4\%$ . The latter exception can be explained by the fact that no failure occurred for  $R_c/D_n=5.1$ , whereas the failure for the other 3 cases was only 10%, not allowing for an increased number of rocking after failure units.

The difference between rocking before and after failure units is the result of two phenomena. Firstly, units that have failed are subject to more severe wave action than units that have not failed. This is mainly the result of the fact that, in most cases, failed units on the crest acquire positions that constitute a larger area of the unit exposed to wave action. An example of such a unit is shown in Figure 3.4. This unit was rocking continuously for approximately 6 minutes immediately after it failed. A second reason is that failed units have decreased stability, because the friction with the units of the 2<sup>nd</sup> upper row is lost and the friction with the underlayer is decreased.



Figure 3.4: Failed unit at position that facilitates rocking

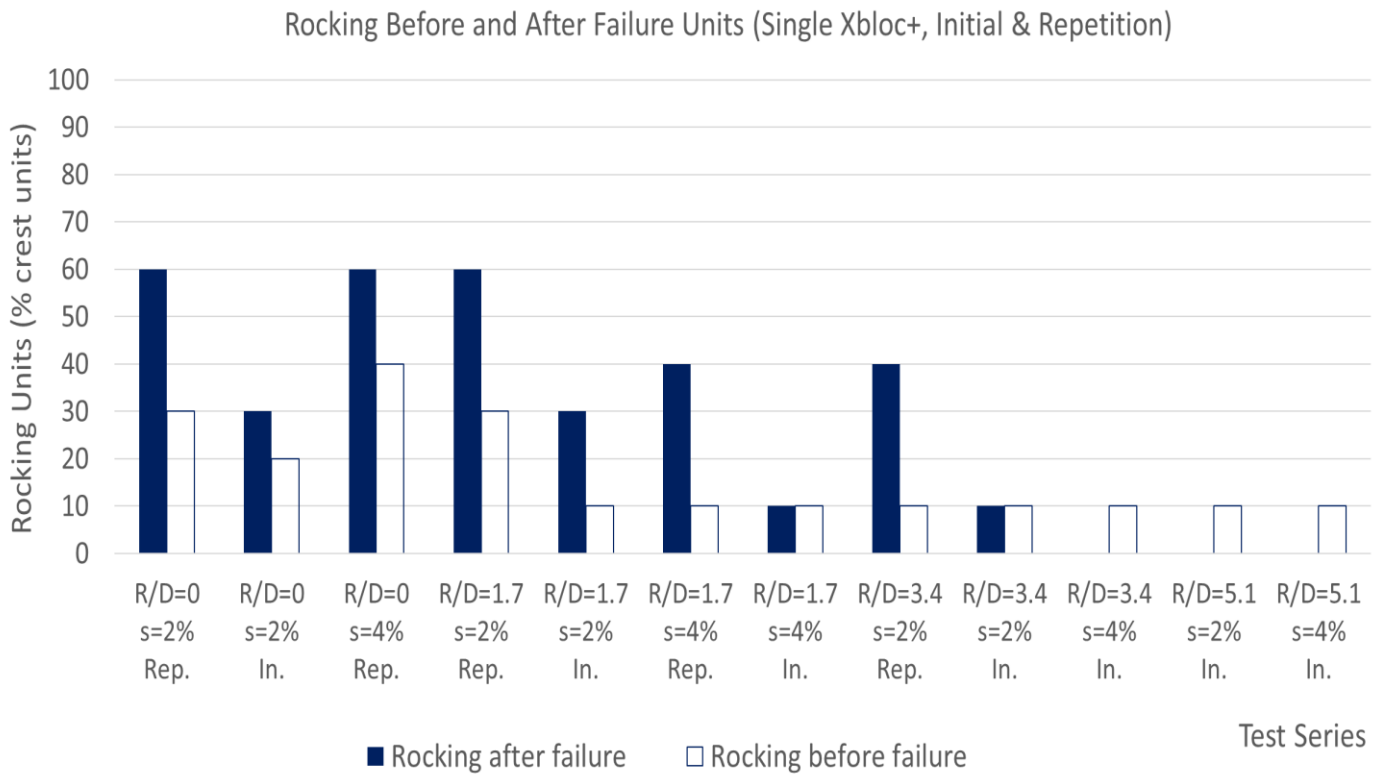


Figure 3.5: Total number of Rocking Before failure and Rocking After failure units per test series - Initial and Repetition tests on the single Xbloc+ (1<sup>st</sup> test set)

### 3.3 Start of Movement – Single Xbloc+

During the initial tests on the single (without rear support) Xbloc+ crest element, it was observed that damage (partial displacement or failure) occurred already from the first test (lowest wave height tested) of most test series. This was the case for the following 5 out of the 8 test series performed: 1.1.1, 1.2.1, 1.1.2, 1.2.2, 1.1.3. Therefore, those test series were repeated, in order to find the critical stability number, at which movement (failure or partial displacement) at the top armour row started (threshold of movement). The data from the repetition of those 5 test series, as well as the initial data from test series 1.2.3, 1.1.4 and 1.2.4 are used for the results of this section.

The combined effect of the relative freeboard and wave steepness on the start of failure (rectangular marker) and partial displacement (circular marker) is shown in Figure 3.6. The critical stability number ( $H_{s,c}/(\Delta D_n)$ ) is plotted in the Y axis, the relative freeboard ( $R_c/D_n$ ) in the X axis, whereas 2% and 4% wave steepness is shown with “solid” and “blank” marker respectively.

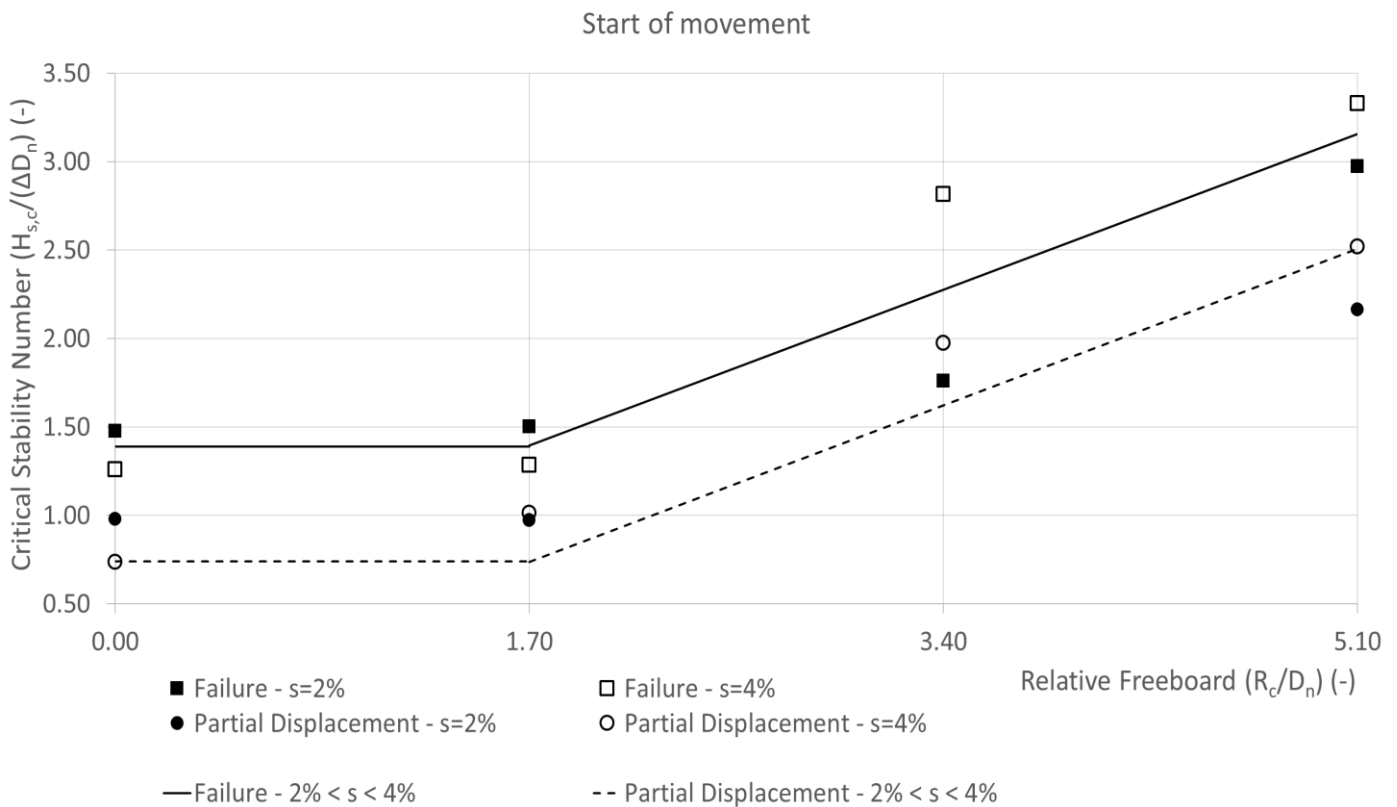


Figure 3.6: Influence of Freeboard & Wave Steepness on Start of Movement

Failure and partial displacement for the top armour row are initiated at critical stability numbers of 1.39 and 0.74, respectively, which occur for  $R_c/D_n \leq 1.7$ . The stability numbers are much lower than the one for displacement of the armour layer ( $>3.88$ ).

For  $0 \leq R_c/D_n \leq 1.7$ , partial displacement is initiated at equal critical stability numbers, for  $2\% \leq s_{op} \leq 4\%$ . Increasing the relative freeboard causes the critical stability number to increase, which is more considerable, when  $R_c/D_n$  increases from 1.7 to 3.4 (0.79 (81%) for  $s_{op}=2\%$  and 0.97 (96%) for  $s_{op}=4\%$ ), than when  $R_c/D_n$  increases from 3.4 to 5.1 (0.40 (23%) for  $s_{op}=2\%$  and

0.54 (27%) for  $s_{op}=4\%$ ). No considerable influence of the wave steepness in this trend can be concluded.

In the same manner as partial displacement, failure is initiated at equal critical stability numbers, for  $0 \leq R_c/D_n \leq 1.7$  and  $2\% \leq s_{op} \leq 4\%$ . However, the critical stability number for  $R_c/D_n=3.4$  and  $s_{op}=2\%$  is not considerably higher than the one for  $R_c/D_n=1.7$  (17% difference), so this condition is considered equally important for the initiation of failure. Based on the fact that the condition with  $R_c/D_n=3.4$  and  $s_{op}=4\%$  results in an increase in the stability number of 1.06 (60%) compared to the condition with  $R_c/D_n=3.4$  and  $s_{op}=2\%$ , it can be concluded that higher wave steepness results in later initiation of failure for  $R_c/D_n=3.4$ . Increasing  $R_c/D_n$  to 5.1 causes the critical stability number to increase further.

The influence of the relative freeboard ( $R_c/D_n$ ) on the critical stability number ( $N_{s,c}$ ) is described by the following formulas:

#### Partial Displacement

$$N_{s,c- \text{ Partial Displacement}} = \begin{cases} 0.74, & 0 \leq \frac{R_c}{D_n} \leq 1.7 \quad \text{with } \sigma = 0.11 \\ 0.52 \frac{R_c}{D_n} - 0.15, & 1.7 < \frac{R_c}{D_n} \leq 5.1 \quad \text{with } \sigma = 0.18 \end{cases}$$

#### Failure

$$N_{s,c- \text{ Failure}} = \begin{cases} 1.39, & 0 \leq \frac{R_c}{D_n} \leq 1.7 \quad \text{with } \sigma = 0.03 \\ 0.52 \frac{R_c}{D_n} + 0.52, & 1.7 < \frac{R_c}{D_n} \leq 5.1 \quad \text{with } \sigma = 0.29 \end{cases}$$

From the formulas and Figure 3.6, it is observed that the difference between the trends of the critical stability numbers for failure and partial displacement can be approximated by a constant number, thus, the formulas can alternatively become:

#### Partial Displacement

$$N_{s,c- \text{ Partial Displacement}} = \begin{cases} 0.74, & 0 \leq \frac{R_c}{D_n} \leq 1.7 \quad \text{with } \sigma = 0.11 \\ 0.52 \frac{R_c}{D_n} - 0.15, & 1.7 < \frac{R_c}{D_n} \leq 5.1 \quad \text{with } \sigma = 0.18 \end{cases}$$

#### Failure

$$N_{s,c- \text{ Failure}} = \begin{cases} N_{s,c- \text{ Partial Displacement}} + 0.65, & 0 \leq \frac{R_c}{D_n} \leq 1.7 \quad \text{with } \sigma = 0.03 \\ N_{s,c- \text{ Partial Displacement}} + 0.37, & 1.7 < \frac{R_c}{D_n} \leq 5.1 \quad \text{with } \sigma = 0.29 \end{cases}$$

Where,  $\sigma$  is the standard deviation, the derivation of which is provided in Appendix D.

### 3.4 Total Damage to the 4 Upper Rows of the Armour Layer – Single Xbloc+ (1<sup>st</sup> Test Set)

Except for the 1<sup>st</sup> (top row, where the Xbloc+ crest units are located), the damage to the 2<sup>nd</sup>, 3<sup>rd</sup> and 4<sup>th</sup> upper rows was assessed, in order to check its extent at the upper area of the armour layer. In Figure 3.7, the total failed units at the 1<sup>st</sup>, 2<sup>nd</sup>, 3<sup>rd</sup> and 4<sup>th</sup> upper rows at the end of a test series are shown, as a percentage of the total units of the 4 upper rows.

It is observed that most of the failed units are located at the top row and their number decreases substantially at the 2<sup>nd</sup> row, whereas no units at the 3<sup>rd</sup> and 4<sup>th</sup> row failed.

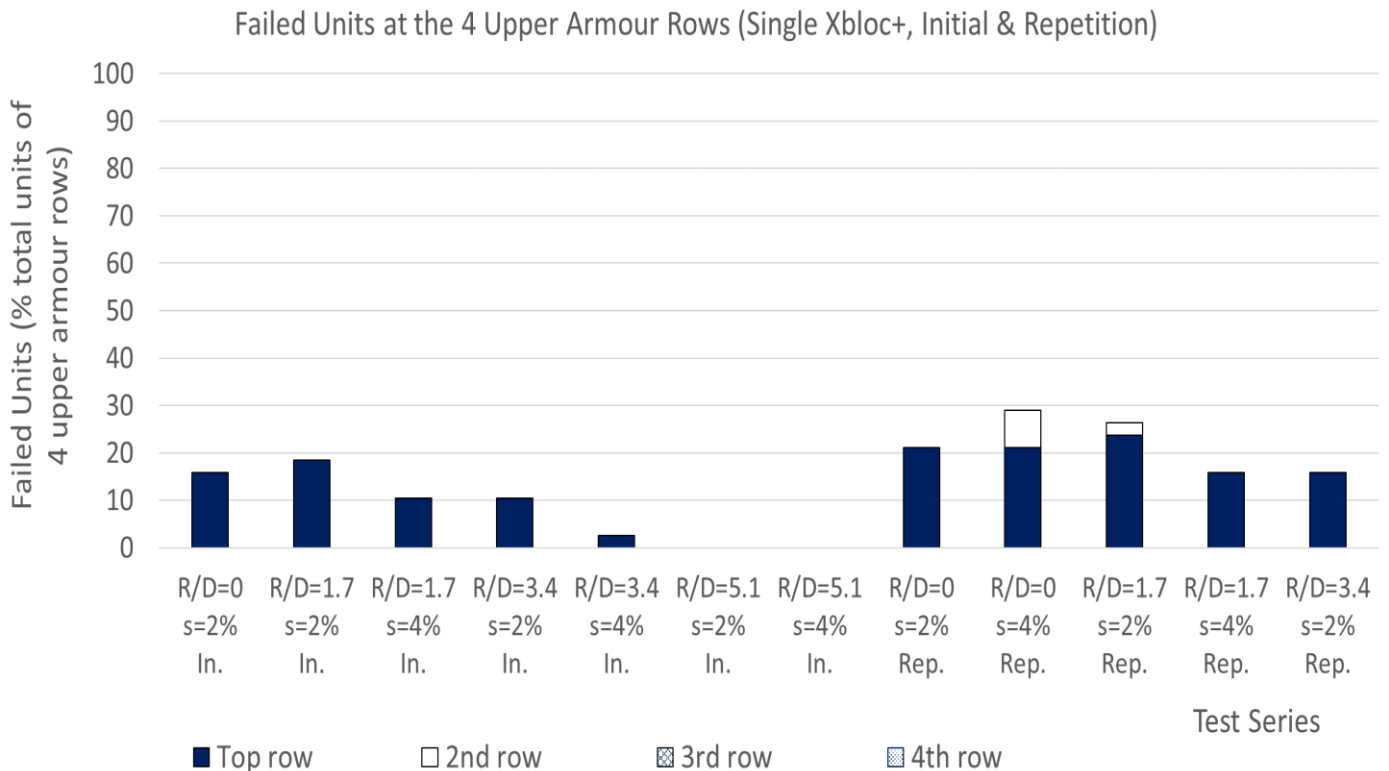


Figure 3.7: Failed units at 1<sup>st</sup>, 2<sup>nd</sup>, 3<sup>rd</sup>, 4<sup>th</sup> upper rows - Initial and Repetition tests on the Single Xbloc+ (1<sup>st</sup> test set)

In Figure 3.8, the total displaced units are presented, which include both failed units and partially displaced units. Most of the displaced units are located at the 1<sup>st</sup> and 2<sup>nd</sup> row, whereas the number of displaced units is decreased considerably at the 3<sup>rd</sup> row. All units of the 4<sup>th</sup> row are stable.

The displacement of the Xbloc+ units at the part of the armour layer near the crest did not result in extensive damage in the armour layer and did not jeopardise the integrity of the structure as a whole. An example is given in Figure 3.9, where the armour layer at the end of the repetition of test series 1.1.2 ( $R_c/D_n=0.5$ ,  $s_{op}=2\%$ ) - condition with most damage - is shown.

Concerning damage to other parts of the breakwater, only limited erosion of the underlayer at the crest occurred, as some stones were dragged by the waves.

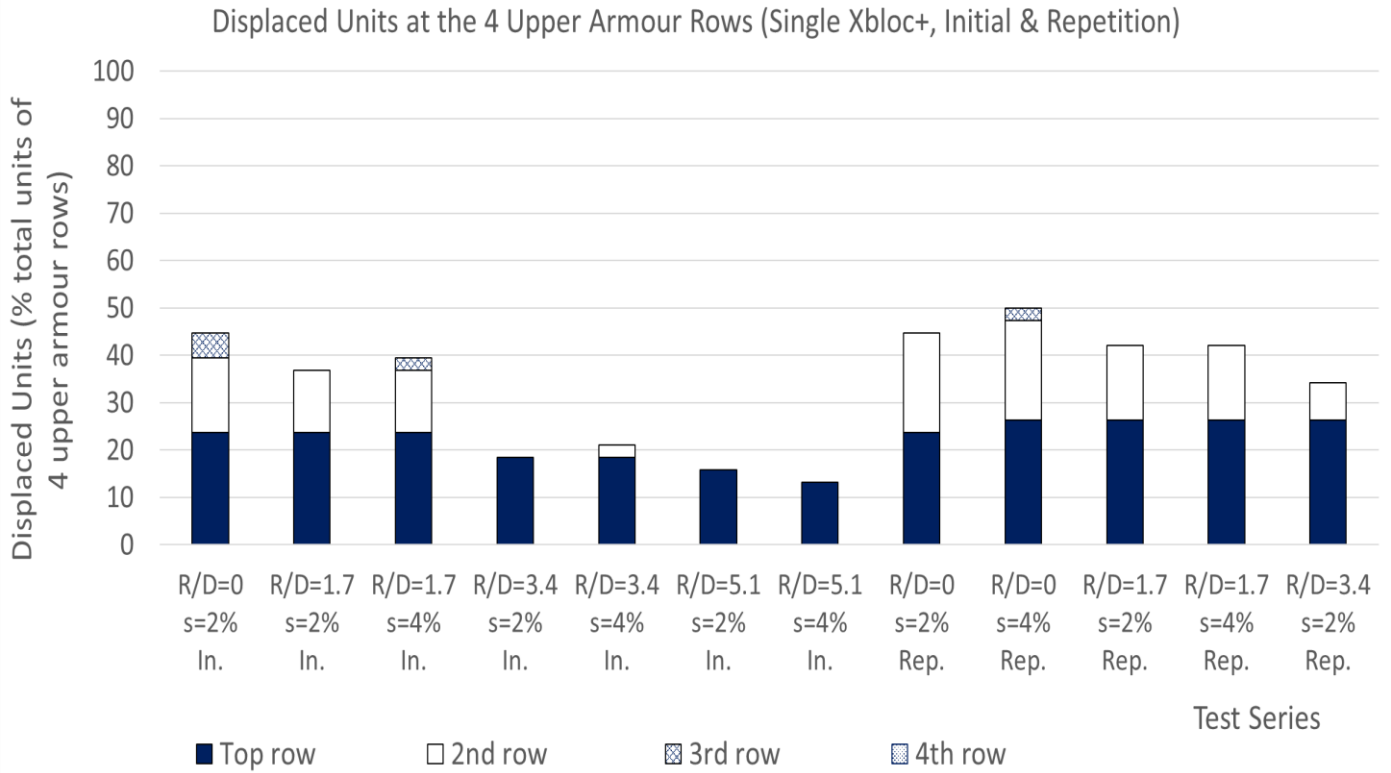


Figure 3.8: Displaced units at 1<sup>st</sup>, 2<sup>nd</sup>, 3<sup>rd</sup>, 4<sup>th</sup> upper rows - Initial and Repetition tests on the single Xbloc+

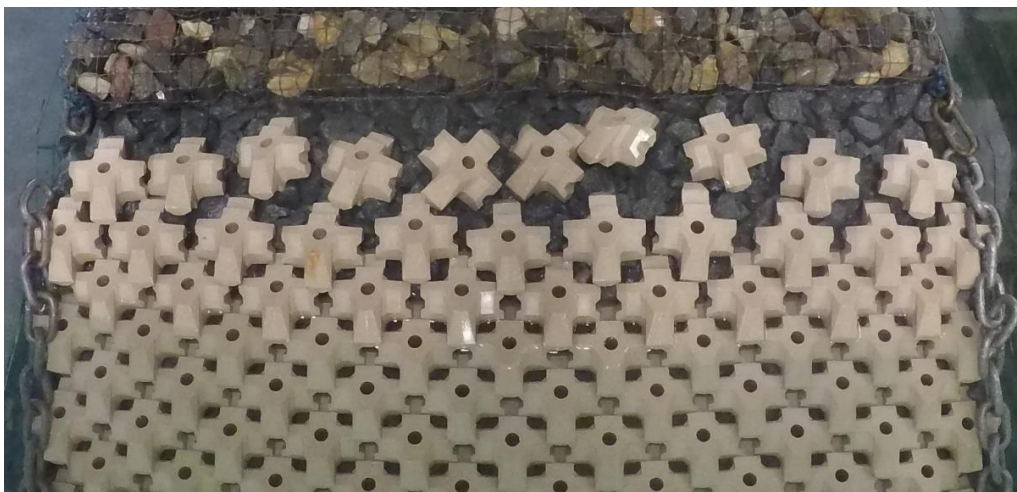


Figure 3.9: Armour layer at the end of test series 1.1.2 – Repetition



### 3.5 Underlayer Effect

During the initial tests on the single Xbloc+ crest units, it was observed that for the same conditions of relative freeboard ( $R_c/D_n$ ), wave steepness ( $s_{op}$ ) and significant wave height ( $H_s$ ), the Xbloc+ crest elements get partially displaced or fail at different stability numbers ( $N_s$ ).

A factor that was assumed to be of influence to the time of failure and, thus, explanatory of the above described different behaviour is the underlayer. In practice, the underlayer is never completely smooth and even, so some stones protrude more than others, thus, providing unequal support to the tail of the Xbloc+ element. It is assumed that the more a unit's tail is supported by the underlayer, the more difficult it is for it to get partially displaced or fail. In order to test this hypothesis, the distance from each of the 10 Xbloc+ crest units to the underlayer was measured. The measurements were taken at three points of the unit's tail before the start of testing at each of the 5 test series, that were repeated. The three distances and the measurement locations are shown in Figure 3.10 and Figure 3.11.

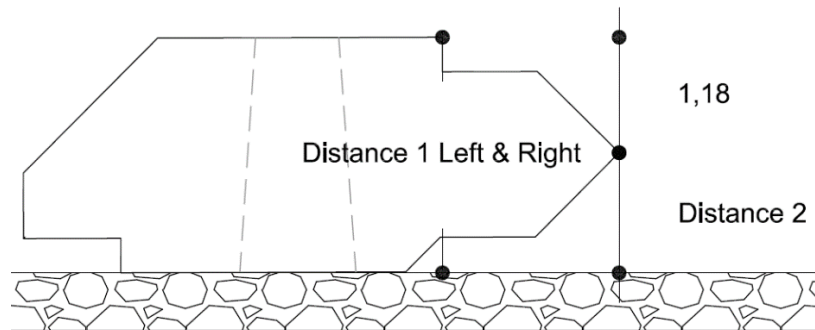


Figure 3.10: Distances from unit to the underlayer measured before the repetition of the test series on the single Xbloc+ crest elements (dimension in cm)

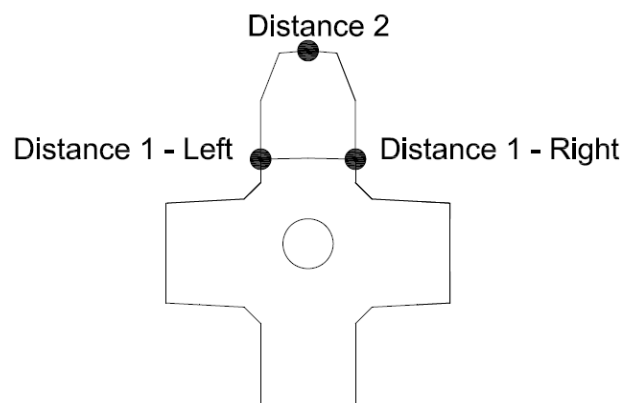


Figure 3.11: Points at which the distances from unit to the underlayer were measured

The vertical distance between the horizontal plane where the top measurement point for “Distance 1 – Left” (or “Distance 1 – Right”) is located and the horizontal plane where the top measurement point for “Distance 2” is located is 1.18 cm. The latter is subtracted from “Distance 1 – Left” and “Distance 1 – Right”, in order to have the same reference, and the three distances are averaged.

In Figure 3.12 and Figure 3.13, the stability number ( $N_{s,c}$ ), at which each unit failed or initially became partially displaced, respectively, is plotted against the average distance from the unit to the underlayer. In the cases that no failure occurred, the maximum stability number of each test series is used in Figure 3.12, while in the case that a unit did not get partially displaced, but failed directly, it is excluded from this analysis in Figure 3.13. The stability number is normalised by dividing with the “expected” value resulting from the formulas for the influence of the relative freeboard ( $R_c/D_n$ ) on the critical stability number ( $N_{s,c}$ ). The average distance from the underlayer to the tail of the unit is divided with the maximum average measured distance.

There is the tendency that a unit fails at a higher stability number, when the average distance from the underlayer to its tail is smaller. The reason is that the smaller this distance, the more the underlayer stones protrude, thus, making contact with the unit’s tail at more points. This leads to increased support of the units: the stabilising effect of the friction forces becomes higher and the backwards horizontal movement of the units is hindered by protruding underlayer stones at the tail.

A similar, but less pronounced tendency, is observed for the initial partial displacement, since, the more the underlayer is protruding at the tail of the units, the later the units get partially displaced.

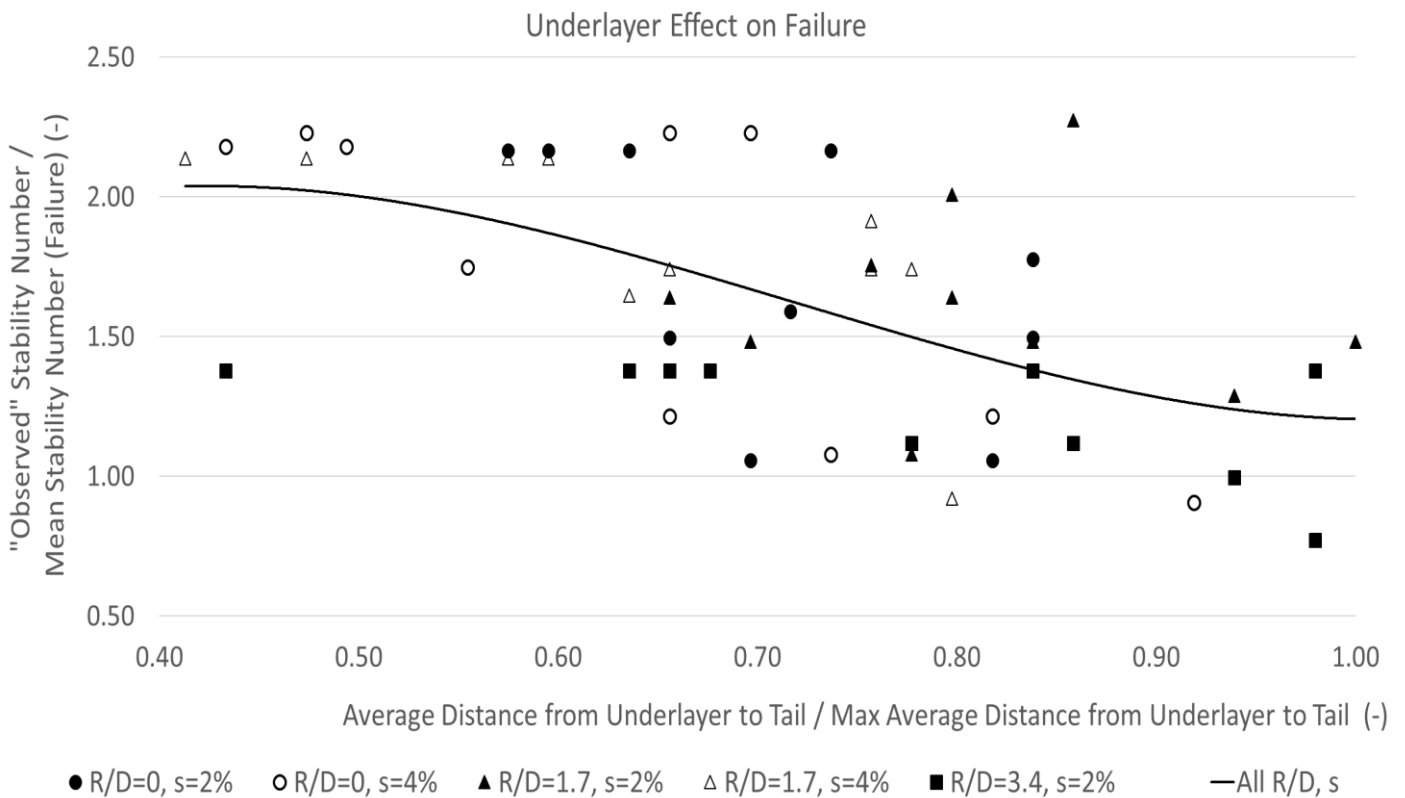


Figure 3.12: Stability Number at Failure and Distance from Underlayer

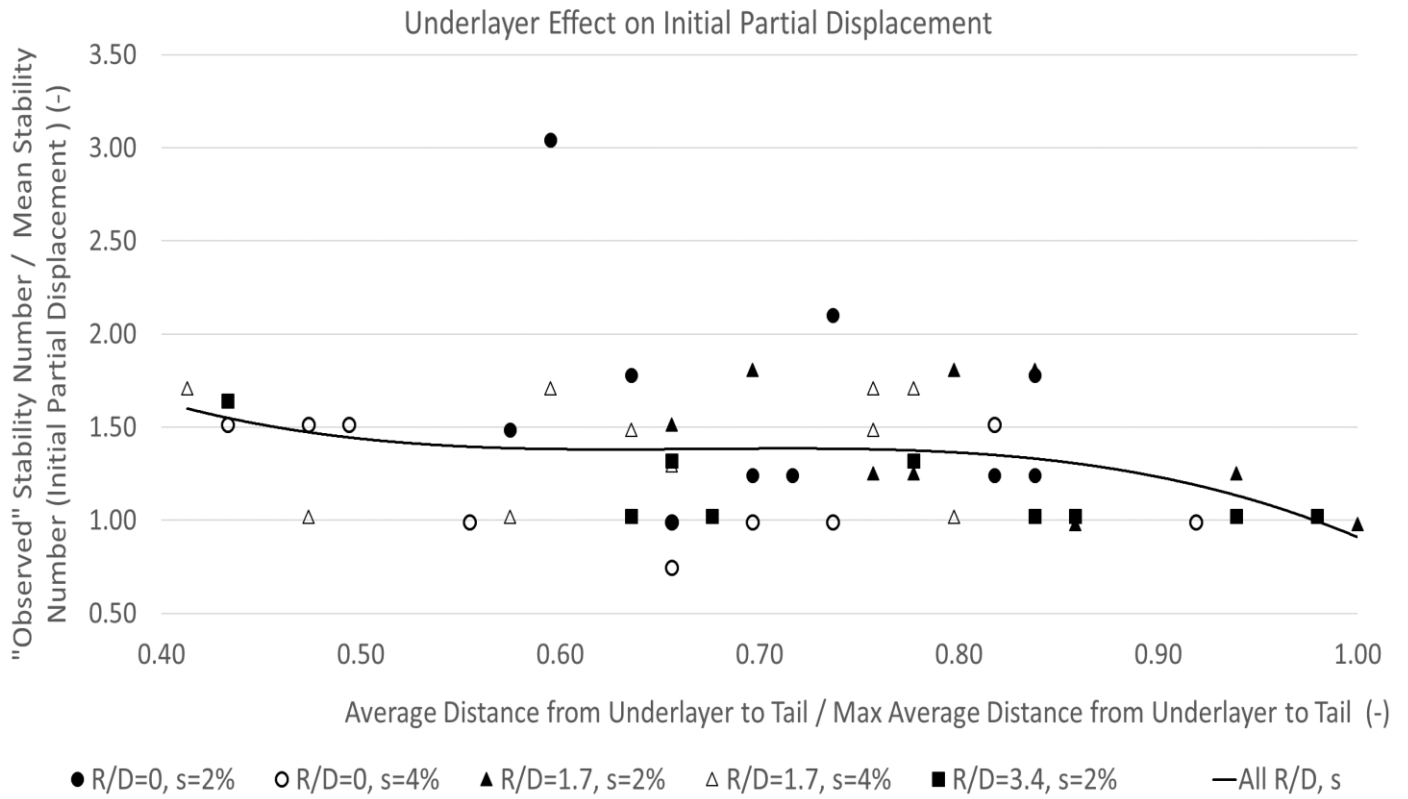


Figure 3.13: Stability Number at Initial Partial Displacement and Distance from Underlayer

## 4. Results – Tests on Crest Configurations and Optimised Configuration (2<sup>nd</sup> & 3<sup>rd</sup> Test Sets)

The results of the tested crest configurations (2<sup>nd</sup> test set) and the additional testing performed on the optimised crest configuration (3<sup>rd</sup> test set) are presented in this section.

The 2<sup>nd</sup> test set includes 7 test series, at each of which a different test configuration was tested, in order to investigate which of the configurations is the optimised one, that enhances the stability of the Xbloc+ crest elements. All test series were conducted under the same conditions:  $R_c/D_n=0$  and  $s_{op}=4\%$ , which proved to be the most critical conditions for failure of the crest Xbloc+ during the initial testing on the single Xbloc+ crest elements. After the repetition testing on the single Xbloc+ crest elements, it was decided to exclude this series from the analysis, but the tests on the crest configurations were conducted before that, therefore, the relative freeboard and wave steepness of that series were applied.

### 4.1 Results of Tested Crest Configurations (2<sup>nd</sup> Test Set)

In this section, the failed and rocking units of the top armour row and the displaced units at the 4 top armour rows for the tested crest configurations are presented.

#### Failed Units

In Figure 4.1, the failed units with respect to the stability number are shown for the 7 different crest configurations tested. It is concluded that the optimal configuration is the underlayer fill and placement of a crown wall element behind the Xbloc+ crest units, since no units failed up to a stability number of 3.52 (corresponding to  $1.41H_{s,d}$  overload conditions).

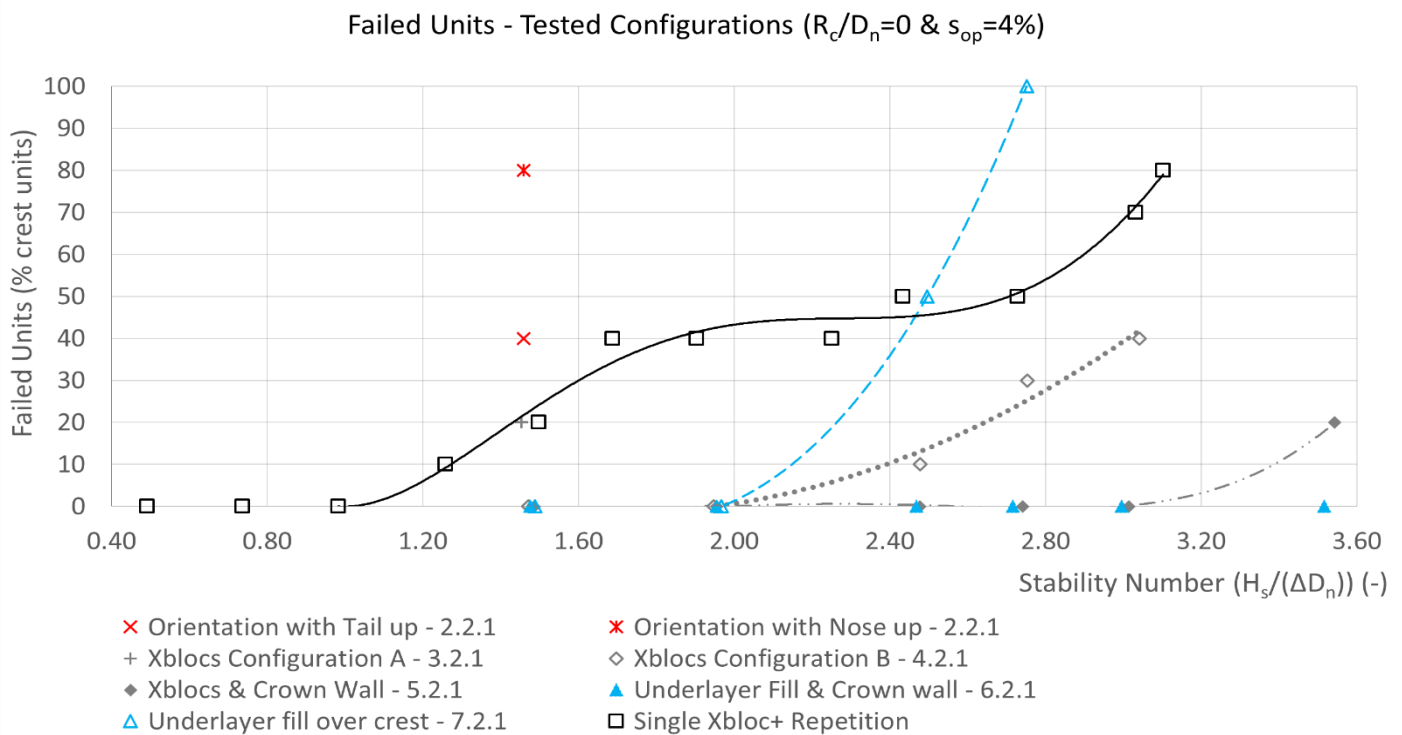


Figure 4.1: Failed units during the Tested Configurations

### Damage to the 4 upper armour rows

The occurring failure and displacement to the upper 4 armour rows during testing on the different crest configurations is presented in Figure 4.2 & Figure 4.3.

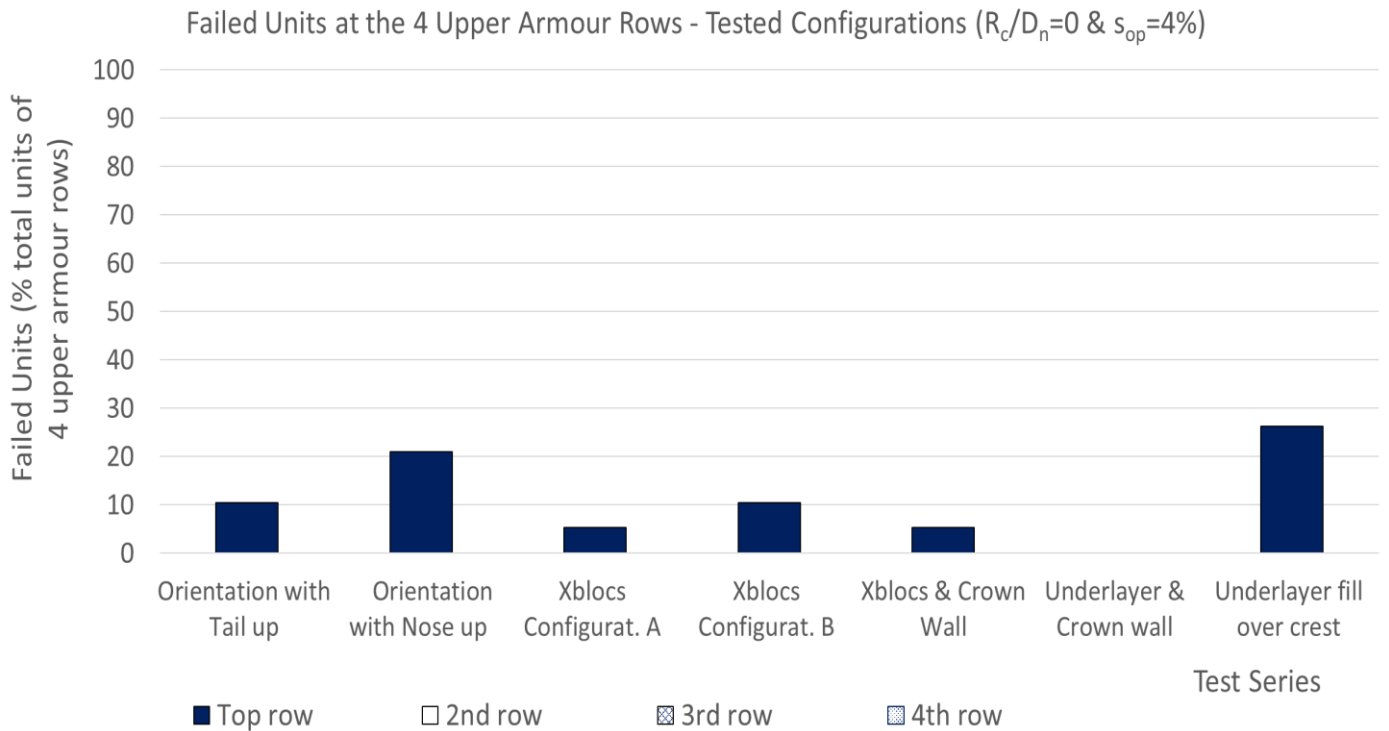


Figure 4.2: Failed units at 1<sup>st</sup>, 2<sup>nd</sup>, 3<sup>rd</sup>, 4<sup>th</sup> upper rows during the Tested Configurations

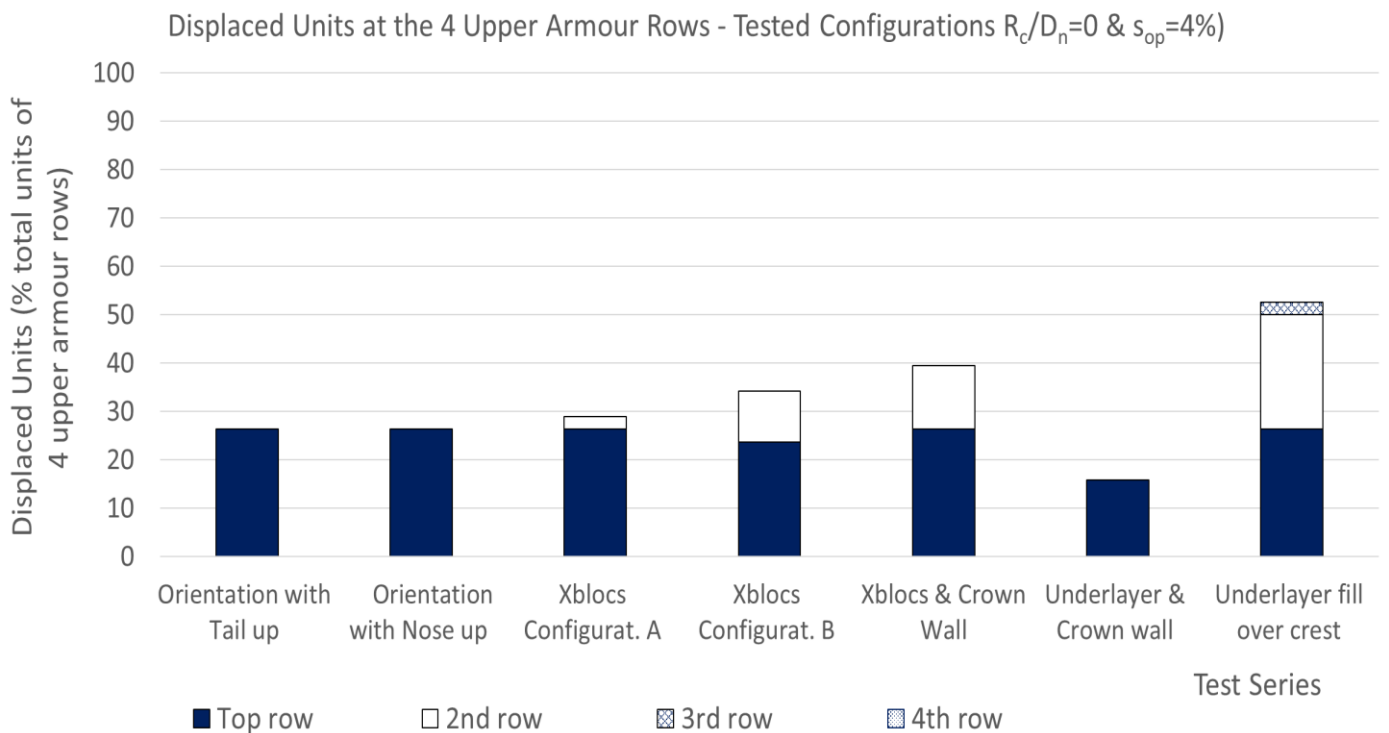


Figure 4.3: Displaced units at 1<sup>st</sup>, 2<sup>nd</sup>, 3<sup>rd</sup>, 4<sup>th</sup> upper rows during the Tested Configurations

The failed units are located only at the top row, where the majority of the displaced units are also located. Damage progressed up to the 2<sup>nd</sup> row and all the units of the 3<sup>rd</sup> row were stable for all tested configurations, except for the one with “Underlayer fill over the crest” (Test series 7.2.1), where very minor damage occurred. The optimised configuration did not cause any failed units at the upper part of the armour layer and only caused partially displaced units at the top row. All the units at the 2<sup>nd</sup>, 3<sup>rd</sup> and 4<sup>th</sup> upper armour rows remained stable.

During the testing on the configuration that proved to be the optimised, some stones of the underlayer material moved, but those movements were limited. On the other hand, during testing of the other configurations, considerable damage was inflicted to the parts of the configurations, apart from the upper armour rows. More specifically: during the configurations with Xblocs, all Xblocs moved from their initial positions, whereas, during the configuration with only underlayer material over the crest, the latter showed extensive erosion.

### Rocking Units

In Figure 4.4, the rocking units for all tested configurations are presented. It is concluded that no units rock during the testing on the configuration with underlayer fill and placement of a crown wall element behind the Xbloc+ crest units.

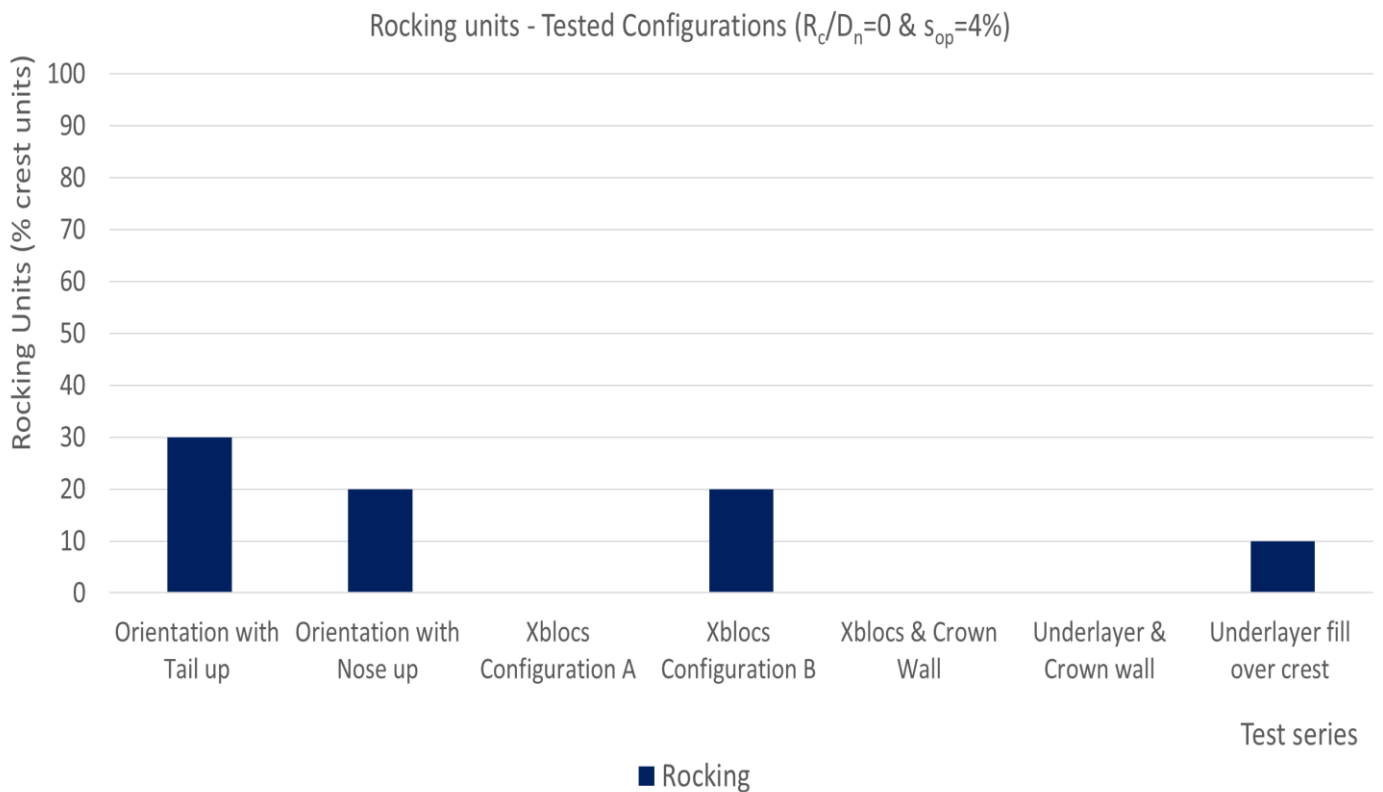


Figure 4.4: Rocking units during the Tested Configurations

## 4.2 Results of the Additional Tests on the Optimised Configuration (3<sup>rd</sup> Test Set)

In Section 4.1, the testing on different crest configurations, in order to find the one that increases the stability of the Xbloc+ units of the top armour row was described.

The optimised configuration proved to be the following: filling the gaps between the Xbloc+ units with underlayer material, placing underlayer material below and behind the Xbloc+ tails and, finally, a concrete element on the crest to avoid displacement and resist the erosion of the underlayer material. The concrete element is not required for structural support, but for erosion control, because, in its absence, first the erosion of the underlayer material at the crest happened and, subsequently, the Xbloc+ crest units moved, as was observed during Test series 7.2.1 – “Underlayer material over crest”.

The optimised configuration is shown in Figure 4.5.



Figure 4.5: Optimised configuration from 2<sup>nd</sup> test set

With this configuration, for  $R_c/D_n=0$  &  $s_{op}=4\%$ , there was no failure and rocking of the Xbloc+ units of the top armour row. Additionally, only 16% (6 out of the 38) of the units of the 4 upper armour rows were displaced and none failed.

The optimised configuration was initially tested for  $R_c/D_n=0$  and  $s_{op}=4\%$ . In order to get further insight into the behaviour of the optimised configuration under different combinations of freeboard and steepness, 3 additional test series were conducted. Finally, 4 in total test series were performed on the optimised configuration:

Test series 6.1.1:  $R_c/D_n=0$ ,  $s_{op}=2\%$

Test series 6.2.1:  $R_c/D_n=0$ ,  $s_{op}=4\%$

Test series 6.1.2:  $R_c/D_n=1.7$ ,  $s_{op}=2\%$

Test series 6.2.2:  $R_c/D_n=1.7$ ,  $s_{op}=4\%$

The results are presented in this section.

### Failed units

In Figure 4.6, the failed units with respect to the stability number during the additional test series on the optimised configuration are shown. No failure occurs for 3 out of 4 conditions:

$R_c/D_n=1.7$ ,  $2\% \leq s_{op} \leq 4\%$  and for  $R_c/D_n=0$ ,  $s_{op}=4\%$ . The only test series, where failure occurs, is  $R_c/D_n=0$ ,  $s_{op}=2\%$ . Nevertheless, the first unit failed at overload conditions (test with  $N_s=2.78$ ), no units failed after the test with  $N_s=3.05$  and 6 additional units failed abruptly during the final test with  $N_s=3.49$ . When comparing with the initial and repetition test series on the single Xbloc+ units, the failed units are decreased by 30% and 60% respectively, for design conditions ( $N_s=2.50$ ).

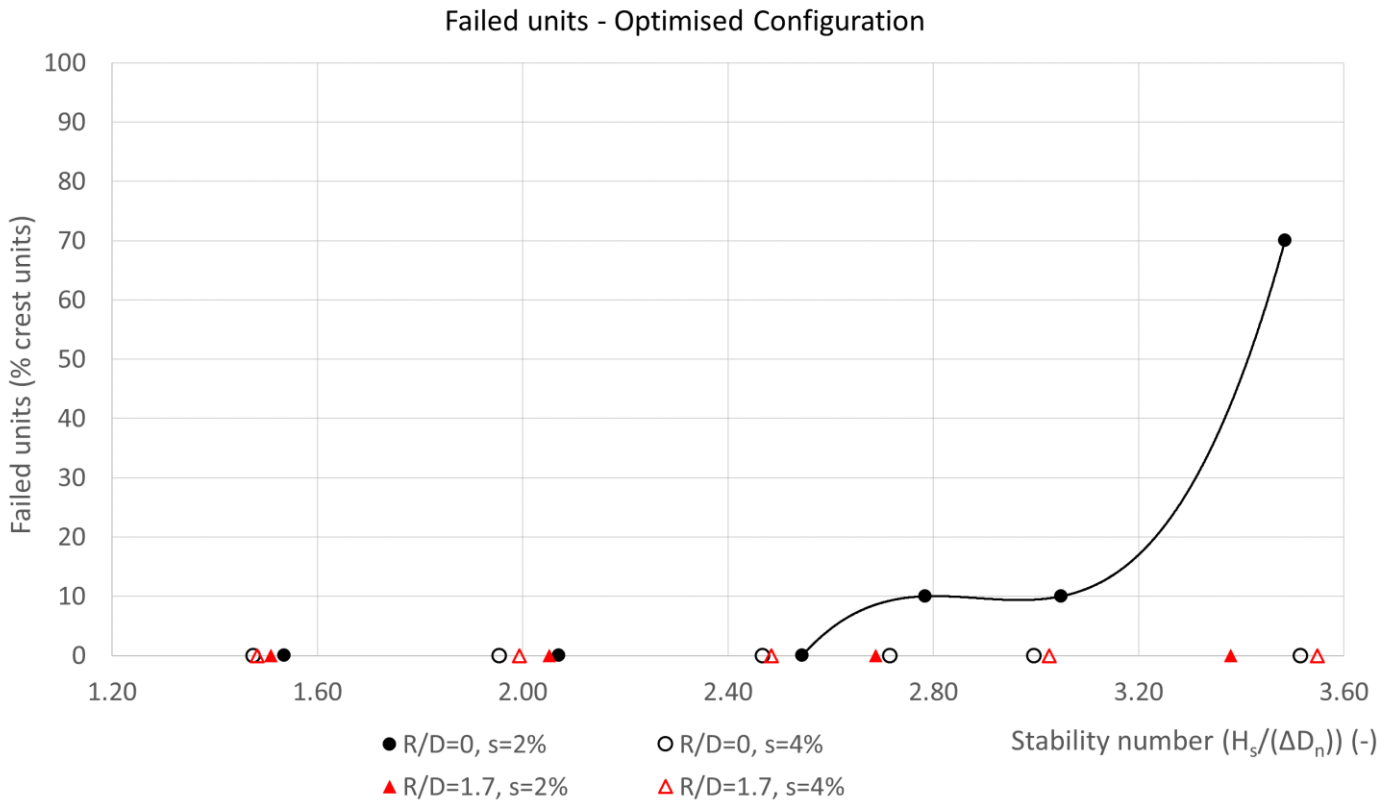


Figure 4.6: Failed units during testing on the Optimised Configuration

The abrupt failure is attributed to the uplift of the concrete crown wall element, most likely caused by the increased under-pressure. This movement happened during the test with  $N_s=2.54$  (design conditions), as seen in Figure 4.7. In this way, more space was created for the underlayer filling to spread and, thus, for the Xbloc+ crest units to move.

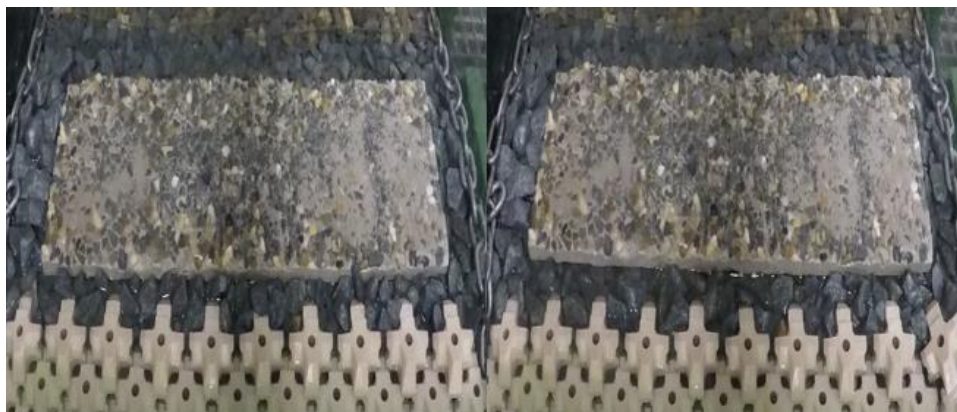


Figure 4.7: Crown Element Before movement (Left) and After movement (Right)



The failed units (% crest units) at the end of the test series on the optimised configuration, as well as the initial and repetition testing on the single Xbloc+ are presented in Table 4.1.

Failed units (% crest units)	Optimised Configuration	Single Xbloc+ Initial	Single Xbloc+ Repetition
$R_c/D_n=0, s_{op}=2\%$	70	60	80
$R_c/D_n=0, s_{op}=4\%$	0	Excluded	80
$R_c/D_n=1.7, s_{op}=2\%$	0	70	90
$R_c/D_n=1.7, s_{op}=4\%$	0	40	60

Table 4.1: Failed units - Optimised Configuration & Single Xbloc+

The optimised configuration decreases failed units to zero, except for the test series with  $R_c/D_n=0$  and  $s_{op}=2\%$ , where there is an increase of 10%.

### Stable Units

The stable units (% crest units) at the end of the test series on the optimised configuration, as well as the initial and repetition testing on the single Xbloc+ are presented in Table 4.2. Stable are the units that have remained at their initial position, after a test series (might have rocked or not during the test series). Increase in stable units is desirable, because it results in decrease in the cost and duration of repair after a severe storm.

Stable units (% crest units)	Optimised Configuration	Single Xbloc+ Initial	Single Xbloc+ Repetition
$R_c/D_n=0, s_{op}=2\%$	20	10	10
$R_c/D_n=0, s_{op}=4\%$	40	Excluded	0
$R_c/D_n=1.7, s_{op}=2\%$	100	10	0
$R_c/D_n=1.7, s_{op}=4\%$	100	10	0

Table 4.2: Stable units - Optimised Configuration & Single Xbloc+

From Table 4.2, it is concluded that the optimised configuration substantially increases stable units, except for the test series with  $R_c/D_n=0$  and  $s_{op}=2\%$ , where considerable failure occurred. More specifically, for relative freeboard equal to 1.7, all Xbloc+ crest units remained stable, compared to only 10% and no stable units at the end of the initial and repetition test series on the single Xbloc+, respectively. The increase in stability is 40% in the case of zero relative freeboard and 4% wave steepness.

### Rocking Units

In Figure 4.8, the rocking units for the additional tests on the optimised configuration are presented. Rocking did not occur, except for the case with  $R_c/D_n=0$  and  $s_{op}=2\%$ , where only 1 unit rocked after failure.

The rocking units (% crest units) at the end of the test series on the optimised configuration, as well as the initial and repetition testing on the single Xbloc+ are presented in Table 4.3.

Rocking units (% crest units)	Optimised Configuration	Single Xbloc+ Initial	Single Xbloc+ Repetition
$R_c/D_n=0, s_{op}=2\%$	10	40	70
$R_c/D_n=0, s_{op}=4\%$	0	Excluded	70
$R_c/D_n=1.7, s_{op}=2\%$	0	30	70
$R_c/D_n=1.7, s_{op}=4\%$	0	10	50

Table 4.3: Rocking units - Optimised Configuration & Single Xbloc+

The optimised configuration results in considerable decrease in rocking units for all 4 conditions tested.

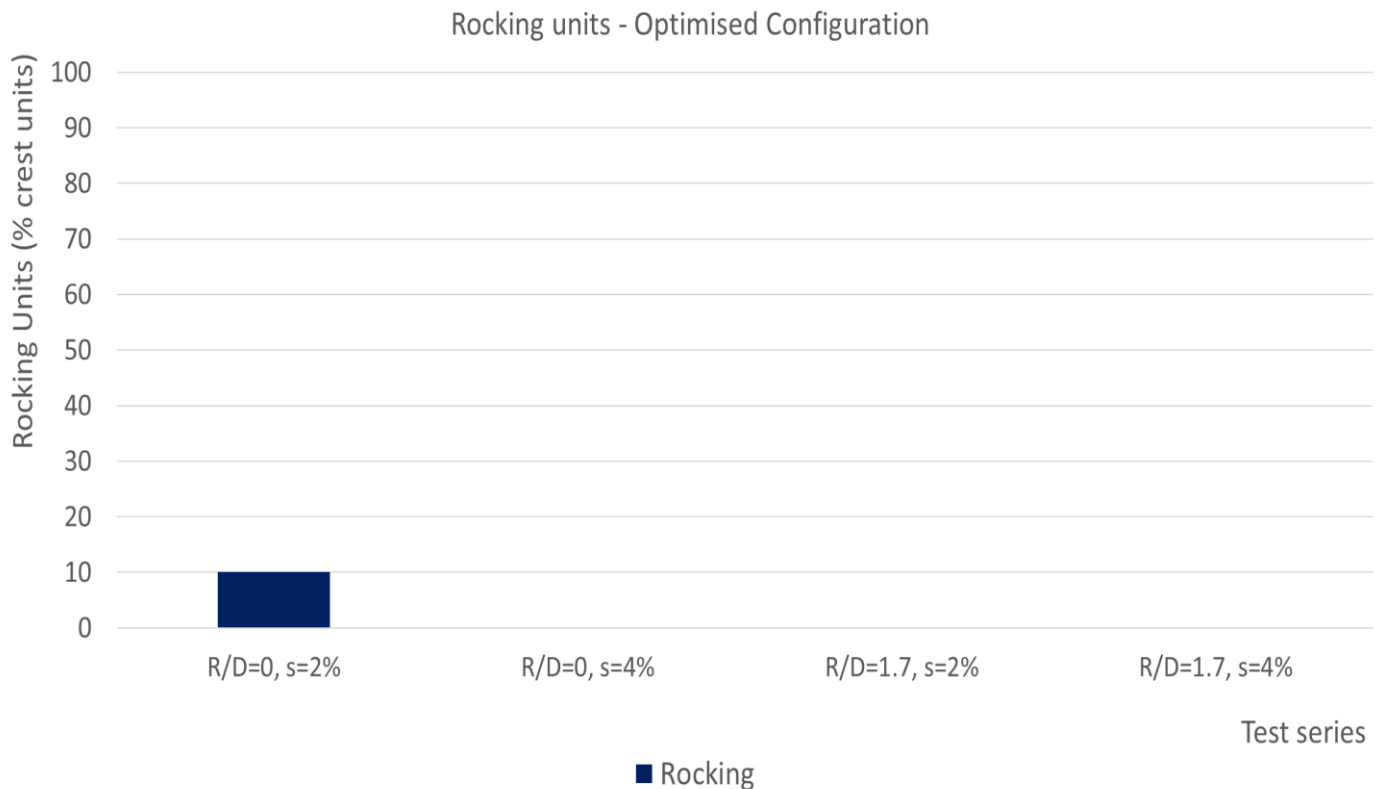


Figure 4.8: Rocking units during testing on the Optimised configuration

#### Damage to the 4 upper armour rows

The occurring failure and displacement to the upper 4 armour rows during the additional tests performed on the optimised configuration are presented in Figure 4.9 and Figure 4.10 respectively.

Failed units at the 4 upper rows occurred only during the test series with zero relative freeboard and 2% steepness, however, they were mostly concentrated at the top row.

Regarding displaced units, they were located at all 4 upper armour rows during the test series. More specifically, during the conditions with zero relative freeboard and 4% steepness, there were partially displaced units at the top row, whereas units at the other rows were stable. The conditions with relative freeboard of 1.7 result in much fewer partially displaced units at the upper armour layer. The most damage (60%) occurred at the condition with zero relative freeboard and 2% wave steepness, however, as seen in Figure 4.11, the damage was concentrated at a specific area (at the left of the picture), and, although severe, it was not extensive and did not endanger the stability of the whole armour layer.

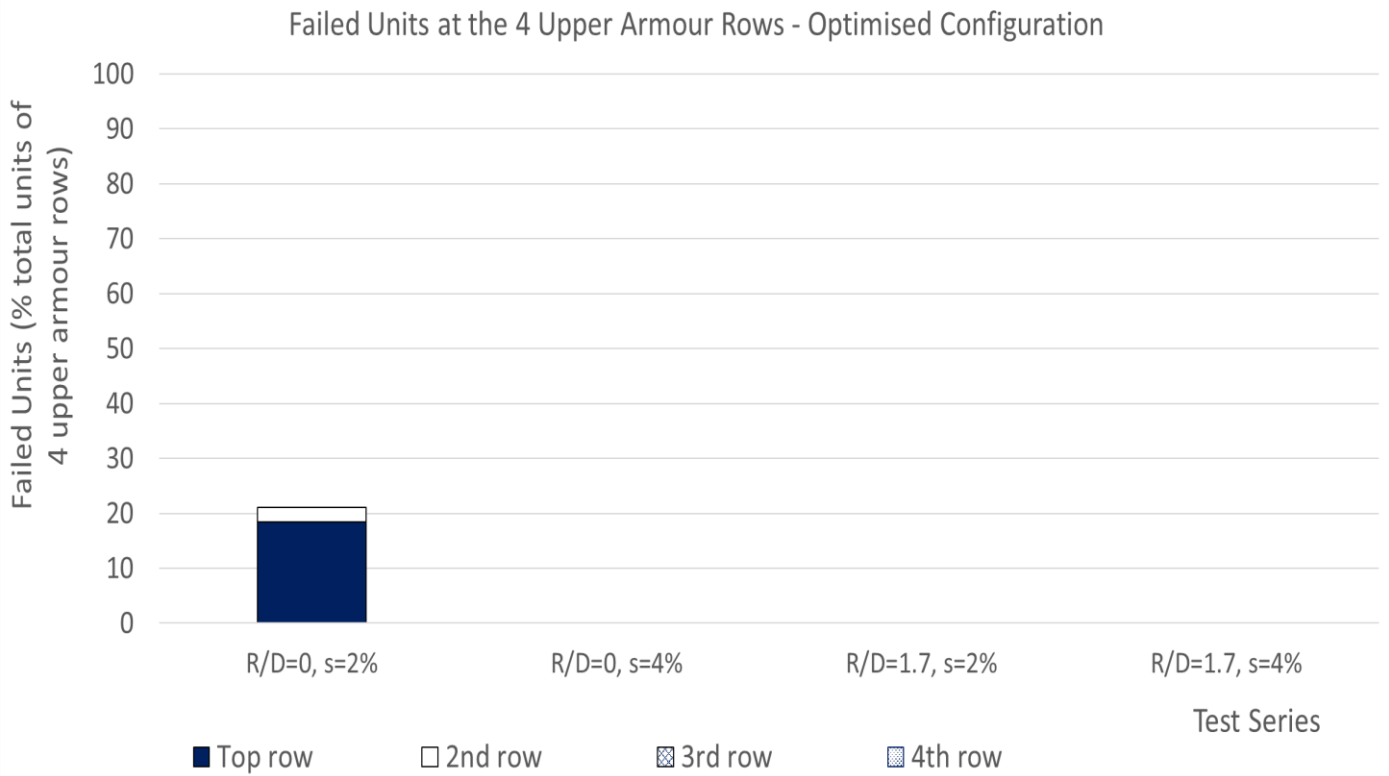


Figure 4.9: Failed units at 1<sup>st</sup>, 2<sup>nd</sup>, 3<sup>rd</sup>, 4<sup>th</sup> upper rows - Optimised Configuration

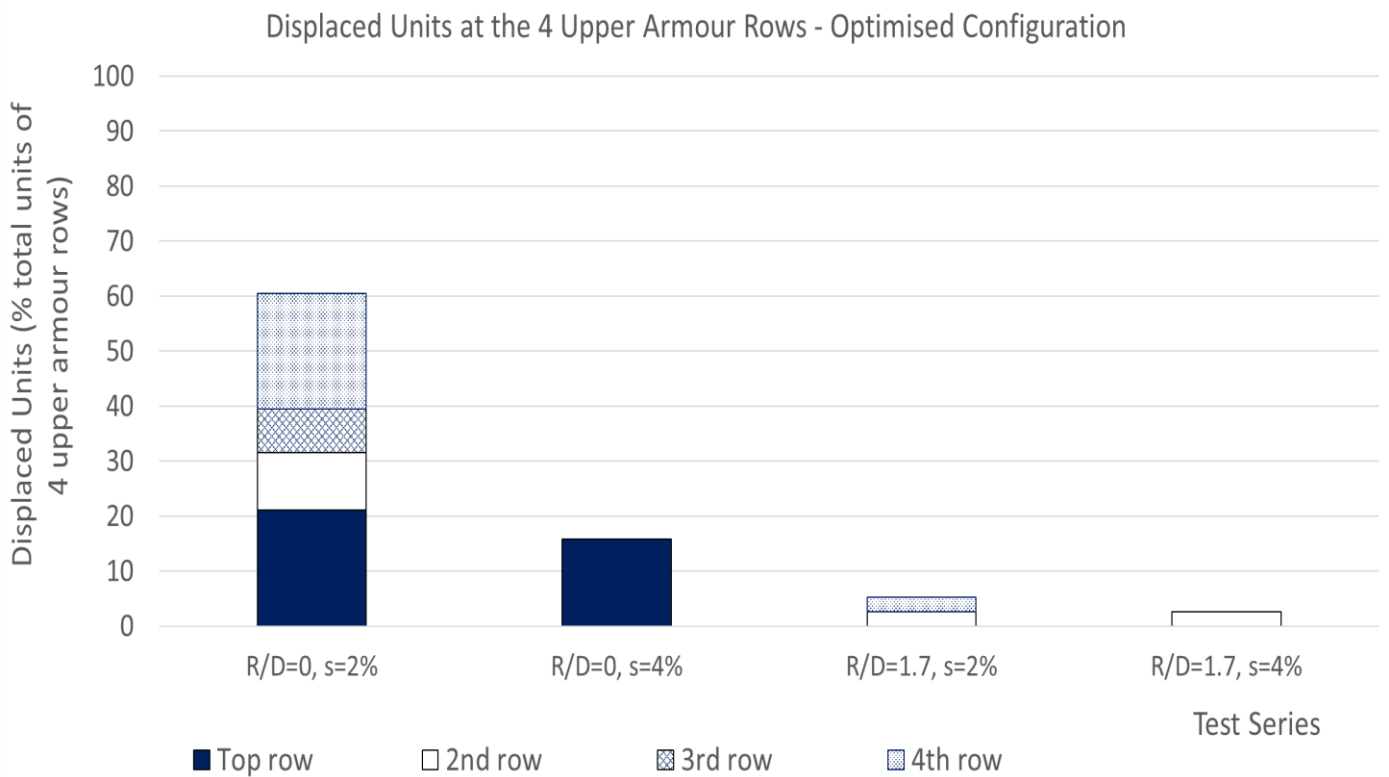


Figure 4.10: Displaced units at 1<sup>st</sup>, 2<sup>nd</sup>, 3<sup>rd</sup>, 4<sup>th</sup> upper rows - Optimised Configuration



Figure 4.11: Armour layer at the end of test series 6.1.1

## 5. Failure Mechanisms

In this section the mechanisms that lead to the failure of the Xbloc+ units of the top armour row of a breakwater (crest Xbloc+'s) are discussed. The influence of the wave steepness, relative freeboard and wave height on the failure mechanisms is also presented.

### 5.1 Xbloc+ Crest Units Motions

The stages of the interactions between the waves and the breakwater is described below:

1. Initially, before waves start acting on the structure, the water level is undisturbed.
2. Subsequently, waves start acting on the breakwater: A wave breaks on the structure and runs up the slope. The incoming wave energy can: be dissipated on the slope during run-up, be reflected back to the sea side, be transmitted through the armour layer, underlayer and core of the breakwater to the lee side or pass over the crest through overtopping.
3. If the run-up height is lower than the freeboard, then overtopping does not occur, and the incoming wave energy is dissipated on the slope, transmitted to the lee side and reflected to the sea side.
4. If the run-up height is higher than the freeboard, overtopping occurs, during which waves pass over the crest and interact with the upper part of the armour row, the crest and the rear slope. Although part of the energy is again dissipated on the slope, reflected and transmitted, a substantial part is dissipated on the crest and rear slope.
5. During the final stage, the wave runs-down the slope, where it meets the next incoming wave, which, subsequently, runs-up the slope.

For the Xbloc+ crest units, Stage 4 proves to be the most critical for movement and, thus, damage or failure. During testing, it was observed that the units' first movement from stable position happened during wave run-up. The sequence of motions, that an Xbloc+ crest unit makes is shown in Figure 5.1, Figure 5.2, Figure 5.3 and Figure 5.4 and described below:

1. Before waves start acting on the slope, the Xbloc+ crest unit is stable, making contact with the two underneath units of the 2<sup>nd</sup> armour row (from the top) and the underlayer (Figure 5.1).
2. In the case that the wave run-up reaches the crest, it interacts with the Xbloc+ crest unit. First, the front part of the unit is subject to the wave action, followed by the rest of the unit, as the wave is passing. The first and primary movement the unit makes is rotation, as seen in Figure 5.2. This motion ranges from rocking to larger rotations. In the former case, the unit is rotating during wave uprush, but returns to its original position during wave rush-down. In the latter cases, the unit does not return to its original position. It is possible that a unit does not rotate at all (stable unit), only rocks without being displaced or both rocks and gets displaced.

3. Next, the rotating unit is also moving upwards, as a result of the uplift force and, backwards, as a result of the drag force. In the end, the unit is making a combined motion: rotation, vertical and horizontal translation (Figure 5.3).
4. At the end of this combined motion, the unit is displaced. In Figure 5.4, a unit at fully displaced position (failed) is shown.

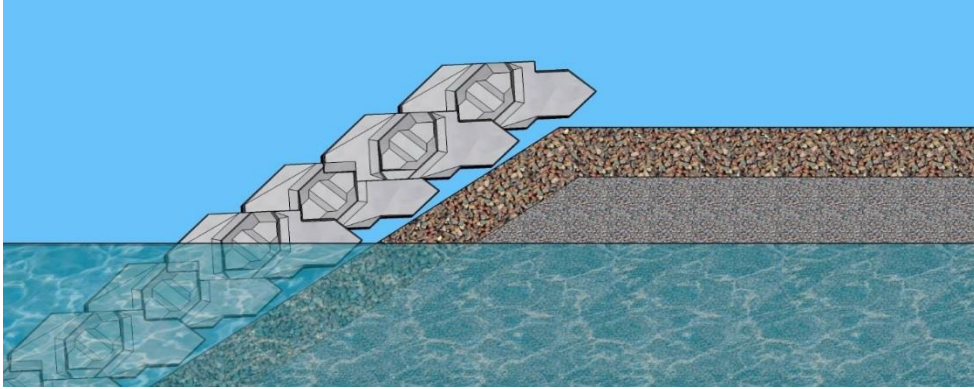


Figure 5.1: Crest Xbloc+ at stable position, prior to wave action.

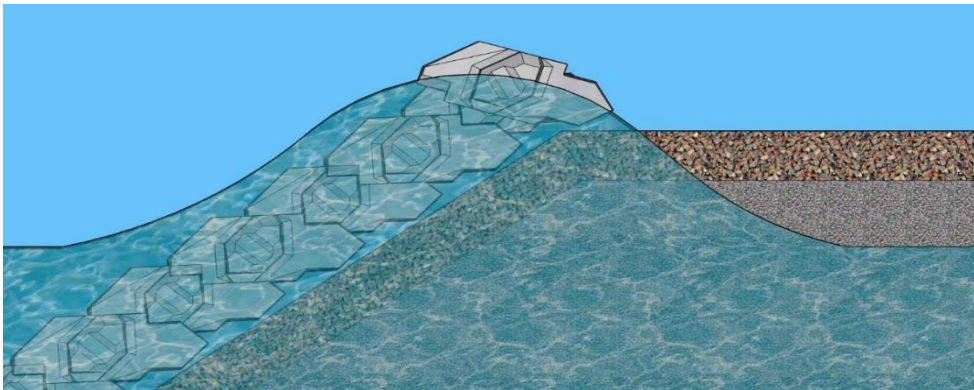


Figure 5.2: Crest Xbloc+ during the initial rotational movement.

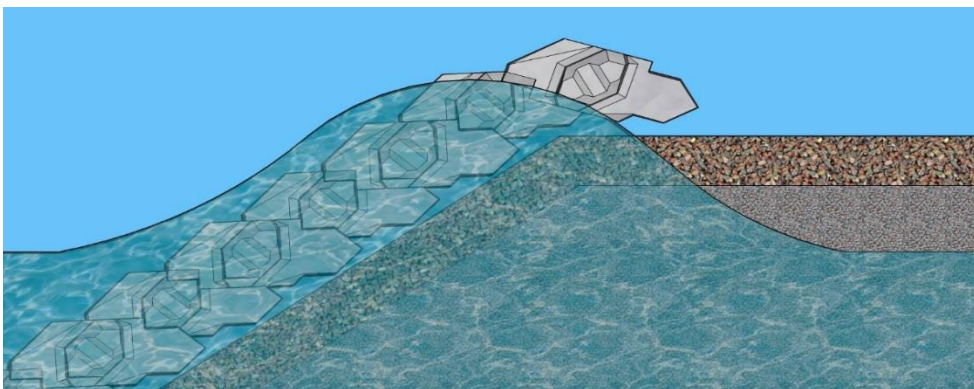


Figure 5.3: Crest Xbloc+ during the combined rotational, vertical and horizontal movement.

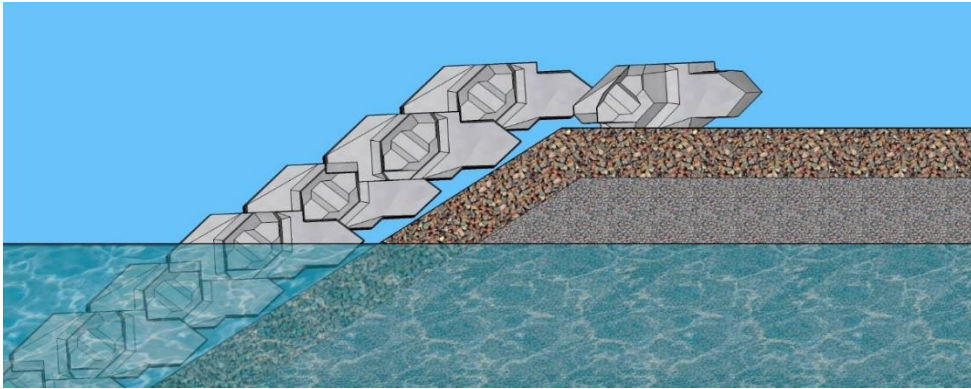


Figure 5.4: Crest Xbloc+ at final failed position, after wave action.

A displaced unit can be partially displaced, in the case that contact is maintained under both wings with the 2 units underneath or fully displaced, in the case that contact is lost under at least one of the two wings. During testing, displaced units, at their majority, did not remain at the first position into which they found themselves immediately after the initial displacement. Nevertheless, they made additional motions on the crest. Partially displaced units continued making combined motions, until, most of them, failed. Regarding failed units, they rocked, i.e. making a rotational motion after which they returned to their initial failed position or made combined motions after which they found themselves into new failed positions. The sequence of rocking at the initial failed position, combined movement to a new failed position, rocking at the new failed position and so on was quite a common phenomenon observed during testing.

The above described motions result in several final failed positions acquired by the Xbloc+ crest units, after a test series was finished, an overview of which is shown in Figure 5.5. From left to right the following positions of the 10 failed units can be observed: Stable unit, Failed unit dragged over the crest to the rear slope (not shown), Stable unit, Unit flipped 180°, Stable unit, Unit that lost contact under one wing (right), Stable unit, Unit dragged backwards horizontally, Stable unit, Unit dragged backwards non-horizontally because of underlayer irregularities.

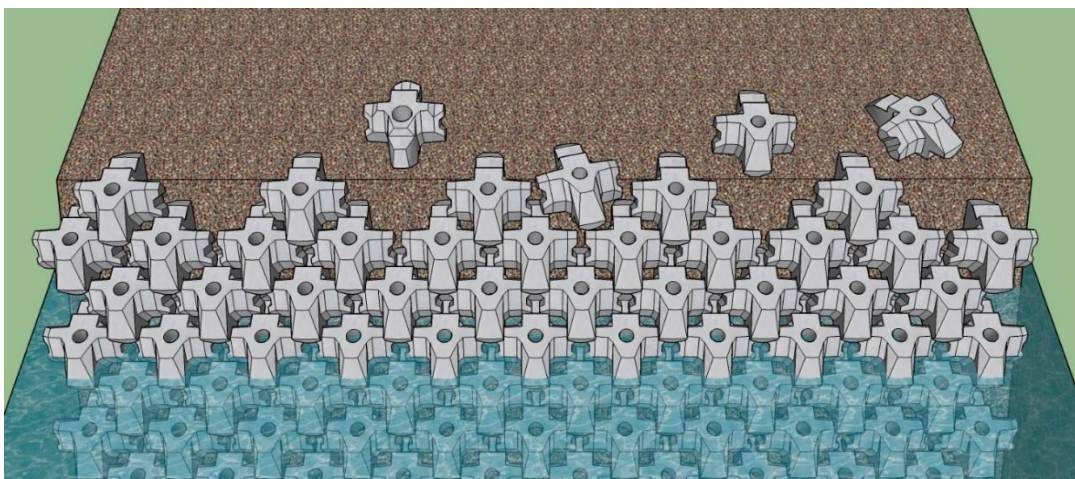


Figure 5.5: Various positions acquired by failed units.

## 5.2 Influence of Freeboard and Wave Steepness on the Xbloc+ Crest Units Failure Mechanisms

In this section the influence of the freeboard ( $R_c$ ) and wave steepness ( $s_{op}$ ) on the failure mechanisms of the single Xbloc+ crest element is presented. The most relevant loads exerted by the waves, during their interaction with the Xbloc+ units of the top armour row are the wave velocities during run-up and the wave impact load. More information about the other wave loads is given in Appendix Appendix E. .

### 5.2.1 Wave impact

The freeboard influences the location of wave breaking and impact on the structure slope. For high still water level, waves break higher at the slope and exert the high impact load near the Xbloc+ crest units. For low still water level, the wave impact and breaking does not happen close to the Xbloc+ crest units, thus, not influencing them.

The wave steepness is very important for the wave impact load, since it affects the breaking type. During testing, two types of wave breakers occurred: surging and collapsing. The most critical between the two is the collapsing breaker, as there are simultaneous high velocities and accelerations (Hald, 1998), that are higher than the surging breaker. The breaker parameter was theoretically calculated for all tests, based on the wave height with probability of exceedance 1% ( $H_{1\%}$ ) and the peak period ( $T_p$ ). The theoretical results showed that the majority of wave breakers are surging ( $\xi > 3$ ), but there is the possibility of 9 collapsing breakers (per 1000 breakers of test) for the 4 following tests:  $R_c/D_n=0$ ,  $s_{op}=4\%$ ,  $H_{m0}=0.0598$  m (Initial) &  $R_c/D_n=1.7$ ,  $s_{op}=4\%$ ,  $H_{m0}=0.0586$  m (Initial) &  $R_c/D_n=0$ ,  $s_{op}=4\%$ ,  $H_{m0}=0.0292$  m (Repetition) &  $R_c/D_n=1.7$ ,  $s_{op}=4\%$ ,  $H_{m0}=0.03$  m (Repetition).

The presence of 9 collapsing waves (out of 1000) was confirmed by the recorded video from the test:  $R_c/D_n=0$ ,  $s_{op}=4\%$ ,  $H_{m0}=0.0292$  m (Repetition). An example of such a breaker at the top armour row is shown in Figure 5.6. Regarding the corresponding test with 2% steepness, all waves were surging.



Figure 5.6: Collapsing breaker at the top armour row



### 5.2.2 Wave run-up velocities

For the specific conditions under which the physical modeling on the Xbloc+ crest units was performed, the breaker parameter:

$$\xi_{m-1,0} = \frac{\tan\alpha}{\sqrt{\frac{2\pi H_{m0}}{gT_{m-1,0}^2}}}$$

was within the range from 3.31 to 5.23. Therefore, the run-up height is given by:

$$R_{u2\%} = 0.51 \frac{H_{m0}}{\sqrt{S_{op}}}$$

The run-up velocity is approximated by:

$u_{A,2\%} = 6.40(R_{u2\%} - R_c)^{0.5}$ , based on the formula by Schüttrumpf and Van Gent (2004) and taking into account the roughness of the Xbloc+ ( $\gamma_r=0.45$ ). The formula is for impermeable, smooth dike slopes, but it can give an indication for the parameters' influence in this case. The theoretical derivation for the run-up height and velocity is presented in Appendix E.2.

The run-up velocity exerts the following forces on the Xbloc+ armour units:

- Lift force ( $F_L$ ), which is approximately normal to the slope and directed “outwards” (destabilising).
- Drag force ( $F_D$ ), which is approximately parallel to the slope and is directed upslope during wave run-up (destabilising). According to Janssen (2018), the Xbloc+ crest units are first lifted by the sum of the vertical load, whereas the horizontal loads on the Xbloc+ crest units are relatively small. Therefore, the drag and inertia force is not taken into account.

The following forces also act on the Xbloc+ armour units:

- Submerged own weight of the unit ( $F_G$ ). (stabilising)
- Friction forces from the contact with the underlayer and the 2 underneath neighbouring units, that are approximated with a horizontal and normal force at the rotation point and disregarded for the moment balance.

The relevant forces are given by:

$$F_L \sim C_L * \rho_w * u^2 * A_L \quad F_G \sim (\rho_c - \rho_w) * V * g$$

Where,

$C_L$ : lift coefficients (–)

$A_L$ : cross sectional areas subject to lift  $\approx D_n^2$  (m<sup>2</sup>)

$\rho_c, \rho_w$  : concrete and water densities (kg/m<sup>3</sup>)

$V$ : armor unit volume (m<sup>3</sup>)

$g$ : gravitational acceleration ( $\text{m/s}^2$ )

$u = u_{A,2\%}$ : run – up velocity ( $\text{m/s}$ )

The lift force is proportional to the square of the run-up velocity:  $F_L \propto u_{A,2\%}^2$

The run-up velocity is influenced by the run-up height ( $R_u$ ) and the freeboard ( $R_c$ ): An increase in the run-up height, for constant freeboard, causes an increase in the run-up velocity. Decrease in the freeboard, for constant run-up height, leads to an increase in the run-up velocity, since the Xbloc+ crest elements are located closer to the still water level.

The run-up height increases, as the wave steepness ( $s_{op}$ ) decreases. A wave with lower steepness results in higher run-up height compared to a wave with higher steepness, same height, and still water level. Thus, in the case of 2% steepness waves, more waves reach the crest and the Xbloc+ units are subject to more frequent and intense wave action compared to the case of 4% steepness. Hence, the run-up velocity and, thus, the drag and lift forces, and the resulting destabilizing moments are increased. The above theoretically explain the observed larger failure caused by 2% steepness waves compared to 4%, for relative freeboards larger than 1.7 ( $R_c/D_n > 1.7$ ), as well as the phenomenon that 2% steepness waves acting at a certain water level lead to more failure compared to 4% steepness waves, acting at  $1.7D_n$  higher water level. During the experiments with the same freeboard and significant wave height, it was also observed that more waves were reaching the crest at the case of 2% steepness waves compared to 4%.

Increasing the freeboard leads to a decrease in failed units, because larger freeboard means higher required run-up height for the waves to reach the crest units. Furthermore, even in the case that waves reach the crest, their run-up velocity is smaller. In fact, the freeboard can become enough for failure not to occur, as observed for the case of  $R_c/D_n > 5.1$ . So, the freeboard influences the number of waves acting on the top armour row.

### 5.2.3 Conclusions on Failure Mechanisms and Effect of Optimised Configuration

In conclusion, two failure mechanisms are substantially contributing to the failure of the Xbloc+ crest elements:

- The run-up velocities and the resulting forces. The influence of the parameters on this mechanism is the following:
  - 2% wave steepness increases this loading compared to 4% steepness.
  - Decreasing freeboard increases this loading, as well as the frequency of its occurrence on the Xbloc+ crest units.
- The wave impact, which depends on the breaker type and is worse for collapsing waves, which occurred for 4% steepness. This type of loading becomes critical for low freeboards, especially zero freeboard (crest at still water level), where wave breaking occurs at the Xbloc+ crest units.

The optimized crest configuration positively influences the stability of the Xbloc+ crest units. The underlayer fill behind the Xbloc+ crest units moves the center of rotation towards the

back of the unit, which increases its distance from the center of gravity and, therefore, the stabilizing moment of the unit's own weight. Furthermore, the unit, in order to lose contact with the underneath units, must move over the underlayer fill, which is difficult. The purpose of the crown wall element is the resistance against erosion of the underlayer fill. The crown wall element functions as backwards support, whose passive resistance prevents the underlayer from spreading. Alternatively, larger rocks or grouted rocks can be applied, provided that they remain in position.

The (simplified) force balance for the single Xbloc+ and the optimised configuration is schematised in Figure 5.7, where the positions of the centre of gravity (COG) and centre of rotation (COR) - from Janssen (2018) - are shown.  $F_G$  is applied at COG, whereas  $F_L$  is assumed to be applied at the first point subject to wave action and furthest point of the COR (conservative assumption).

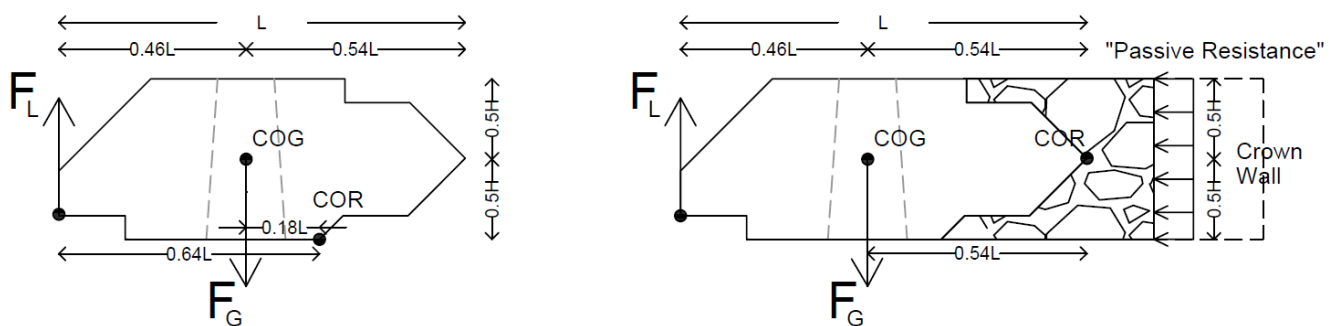


Figure 5.7: Forces during Wave run-up. Single Xbloc+ (left) and Optimised Configuration (right)

The optimised configuration leads to an increase of the critical stability number ( $N_{s,c}$ ) of 40%, resulting from the movement of the COR to the back of the Xbloc+ unit. The passive resistance additionally contributes to the unit to remaining stable.

## 6. Conclusions and Recommendations

In this chapter, the conclusions of this research and recommendations for further research are discussed. All tests were performed on a model breakwater with 3:4 slope and no foreshore ("deep water" conditions). Tests with the following combinations of freeboard:  $R_c/D_n=0, 1.7, 3.4, 5.1$  and wave steepness:  $s_{op}=2\%$  and  $4\%$  were performed.

### 6.1 Conclusions

The conclusions constitute the answers to the research questions, therefore, each research question is repeated, followed by the relevant conclusions.

1. *What is the relation of the stability of the Xbloc+ crest elements with the parameters: crest freeboard ( $R_c/D_n$ ) and wave steepness ( $s_{op}$ )?*

- Two types of displacement of the top armour row were defined: partial displacement, when 1 out of the 10 Xbloc+ units is displaced without losing contact under the two wings with the units of the row below and failure, when 1 unit loses contact at least under one wing (10% criterion). Both movements are initiated at critical stability numbers ( $N_{s,c}=H_{s,d}/(\Delta D_n)$ ) much lower than the armour layer, where no damage was observed up to  $N_{s,c}>3.88$ . Failure and partial displacement start at  $N_{s,c}\leq 1.50$  and  $N_{s,c}\leq 1.01$ , respectively, for  $R_c/D_n\leq 1.7$  and  $s_{op}\leq 4\%$ . Increasing further the freeboard results in increase (with a linear trend) in the critical stability numbers. The following formulas describe the influence of  $R_c/D_n$  on  $N_{s,c}$ :

#### Partial Displacement

$$N_{s,c- \text{ Partial Displacement}} = \begin{cases} 0.74, & 0 \leq \frac{R_c}{D_n} \leq 1.7 \quad \text{with } \sigma = 0.11 \\ 0.52 \frac{R_c}{D_n} - 0.15, & 1.7 < \frac{R_c}{D_n} \leq 5.1 \quad \text{with } \sigma = 0.18 \end{cases}$$

#### Failure

$$N_{s,c- \text{ Failure}} = \begin{cases} N_{s,c- \text{ Partial Displacement}} + 0.65, & 0 \leq \frac{R_c}{D_n} \leq 1.7 \quad \text{with } \sigma = 0.03 \\ N_{s,c- \text{ Partial Displacement}} + 0.37, & 1.7 < \frac{R_c}{D_n} \leq 5.1 \quad \text{with } \sigma = 0.29 \end{cases}$$

- The critical stability numbers for failure and partial displacement decrease, when the distance of the Xbloc+ tail from the underlayer increases, as support becomes less.
- Failure of the top armour layer is maximum, when  $R_c/D_n\leq 1.7$  and  $s_{op}\leq 2\%$  and at the case of  $R_c/D_n=0$  and  $s_{op}=4\%$ . Increase in freeboard results in increase in stability, which is evident for  $R_c/D_n\geq 1.7$  and  $R_c/D_n\geq 3.4$  for  $s_{op}=4\%$  and  $2\%$  respectively, whereas no failure occurs for  $R_c/D_n\geq 5.1$ . Concerning the influence of wave steepness,  $s_{op}=2\%$  increases failure compared to  $s_{op}=4\%$ , at conditions of  $R_c/D_n\geq 1.7$
- Damage is limited predominantly to the upper two armour rows and is repairable for  $N_s\leq 3.17$ .

- The Xbloc+ crest units rock considerably. Rocking cannot be characterised as a reliable indicator of failure, because the majority of the units fail without rocking before. However, rocking after failure proves to be pronounced and frequent, thus, more important. The conclusions for rocking units are the same as the ones for failed units.

2. *How do the parameters, crest freeboard and wave steepness, affect the failure mechanism of the crest elements ?*

Under wave loading, the Xbloc+ crest units initially rotate and, subsequently, perform a combined motion of rotation, vertical and horizontal translation. Two failure mechanisms mainly contribute to failure:

- The wave impact, which becomes particularly important for the initiation of displacement at  $R_c/D_n=0$ , when waves break at the Xbloc+ crest units. This loading is further increased in the presence of waves with  $s_{op}=4\%$  due to the occurrence of collapsing breakers, which are more energetic than the surging breakers of waves with  $s_{op}\leq 2\%$ .
- The wave run-up velocities and the resulting forces, for the conditions with  $R_c/D_n\geq 1.7$ . This loading's magnitude and frequency of occurrence increase when: wave steepness decreases ( $s_{op}\leq 4\%$ ); freeboard decreases.

3. *How can different crest configurations increase the stability of the crest elements?*

- The most effective way of increasing stability is the provision of an unerodable and permeable backwards support, which brings the rotation point of the Xbloc+ crest elements further to the back, thus, resisting rotation. The form of this concept tested was the placement of underlayer material between the Xbloc+ crest units and under their tails and a concrete element behind. The latter functions as backwards support to prevent erosion of the rock fill, a phenomenon that occurs before the failure of the Xbloc+ units, in the case that only underlayer fill is applied.
- For a stability number up to 3.55, the optimised crest configuration resulted in no partial displacement of the Xbloc+ crest elements for  $R_c/D_n\geq 1.7$  and  $s_{op}\leq 4\%$ , whereas no failure occurred at the case of  $R_c/D_n=0$  and  $s_{op}=4\%$ . Rocking decreased to zero. Failure and rocking of 10% happened only at the case of  $R_c/D_n=1.7$ ,  $s_{op}=2\%$  for  $N_s\geq 2.78$ , due to the erosion of the fill, resulting from the movement of the supporting crest element, with the final damage (at  $N_s=3.49$ ) being repairable and limited at the 4 upper rows of the breakwater.

## 6.2 Recommendations

During this research, additional interesting issues arised. Those are presented in this section, as recommendations for further research, and are divided into two categories: recommendations regarding the single, unsupported Xbloc+ crest units and recommendations regarding the optimised configuration of the Xbloc+ crest units.

### 6.2.1 Recommendations for further research on the single Xbloc+ crest units

The following recommendations regarding further research on the stability of the single Xbloc+ crest units are made:

- The final damage during all tests was repairable and did not endanger the armour layer as a whole, thus, tests with higher waves can be performed, in order to investigate when the failure of the top armour row leads to failure of the armour layer.
- For this research, the model breakwater slope was 3:4, which is the most common slope expected to be applied in practice. Milder slopes, such as 1:2 and 2:3, can be tested, because there is higher probability of occurrence of more energetic breakers - collapsing and even plunging - that increase the wave impact load, especially in the case zero freeboard, when the wave impact is concentrated at the top armour row.
- Waves with  $s_{op}=6\%$  steepness can also be tested, since higher wave steepness is expected to have the same effect on the breaker type, as milder slopes.
- During testing, it was found that the underlayer irregularities play a role in the time of displacement of the Xbloc+ crest units, based on simple measurements of the distances between the tail of the units and the underlayer. The effect of the underlayer can be quantified in a more detailed way by applying methods, such as laser techniques, stereo photography and spherical foot staff.
- Since failure occurred for relative freeboard of 3.4, but not for 5.1, tests with intermediate relative freeboards are recommended, in order to find the exact value of relative freeboard above which no failure occurs.

### 6.2.2 Recommendations for further research on the optimised configuration

The following recommendations regarding further research on the optimised crest configuration are made:

- The function of the optimised configuration (rock backfill and concrete crest element) was to provide nonerodable backwards support, that can resist the rotation of the Xbloc+ crest units. However, such a configuration is not limiting and other alternatives serving the same purpose can be sought.
- The applied fill was of the same grading as the underlayer (11.2 – 16 mm). Heavier grading with larger horizontal and vertical thickness, grouted or not can be tested to

investigate its effectivity in preventing erosion without the presence of the concrete element.

- In the case that the concrete crest element proves essential, different versions of it can be investigated, such as cast in-situ, perforated and with altered dimensions to reach an optimal between cost and contribution to erosion resistance. Furthermore, based on the fact that during the test with  $R_c/D_n=0$  and  $s_{op}=2\%$ , the element moved and failure occurred, this test is advised to be repeated to investigate the occurrence, cause and mitigation of the phenomenon. A possible explanation might be the pressure differences between the bottom and the top of the impermeable concrete crest element, which can be confirmed by pressure measurements.
- Physical modelling on the final optimised configuration can be performed with waves of steepness 2%, 4% and 6%, as well as at a breakwater with slopes of 3:4, 2:3 and 1:2. In the cases of lower wave steepness and steeper structure slopes, it is expected that there will be increased run-up, whereas in the cases of higher wave steepness and milder slopes, more energetic breaking and increased impact forces are probable. The structural integrity of the final configuration can be confirmed by applying numerical modelling.

---

## References

1. Aamer Raza, M. (2017). *Breakwaters* [Power Point Slides]. Retrieved from <https://www.slideshare.net/MAamerRaza/breakwaters-and-types>
2. Allsop, N. W. H., Hettiarachchi, S. S. L. (1988). *CHAPTER 58 Reflections from coastal structures*. 782–794. 21st International Conference on Coastal Engineering. Retrieved from <https://ascelibrary.org/doi/abs/10.1061/9780872626874.059>
3. Andersen, O. H., Burcharth, H. F. (1995). *On the One-Dimensional Steady and Unsteady Porous Flow Equation*. *Coastal Engineering*, (24), 233-257. Retrieved from [https://vbn.aau.dk/ws/files/65299460/On\\_the\\_one\\_dimensional\\_steady\\_and\\_unsteady\\_porous\\_flow\\_equations.pdf](https://vbn.aau.dk/ws/files/65299460/On_the_one_dimensional_steady_and_unsteady_porous_flow_equations.pdf)
4. Baird, W.F., Caldwell J.M., Edge B.L., Magoon O.T., Treadwell D.D. (1980). *Report on the damages to the Sines breakwater, Portugal*. Coastal engineering proceedings, [s.l.], n. 17, jan. 2011. issn 2156-1028. Retrieved from <https://icce-ojs-tamu.tdl.org/icce/index.php/icce/article/view/3610/3292>
5. Battjes, J. A. (1974). *Computation of set-up, longshore currents, run-up and overtopping due to wind-generated waves*, 251. Retrieved from <https://repository.tudelft.nl/islandora/object/uuid:e126e043-a858-4e58-b4c7-8a7bc5be1a44>
6. Bessel's correction. (2019). In *Wikipedia*. Retrieved June 18, 2019, from [https://en.wikipedia.org/wiki/Bessel%27s\\_correction](https://en.wikipedia.org/wiki/Bessel%27s_correction)
7. Brouwer, M. (2013). *The influence of the underlayer on the stability of single layer armour units*. Retrieved from <https://repository.tudelft.nl/islandora/object/uuid%3A6b142495-00d3-4ed4-a73e-65c74e30c577>
8. Burcharth, H. F. (1994). *Reliability evaluation of a structure at sea*. Proc. Int. Workshop on Wave Barriers in Deep Water, 599. Retrieved from <https://repository.tudelft.nl/islandora/object/uuid:22243a72-a728-4649-97c1-bd1013d7f876/datastream/OBJ/download+&cd=1&hl=en&ct=clnk&gl=nl>
9. Burcharth, H. F., Andersen, T. L. (2009). *Scale Effects Related to Small Physical Modelling of Overtopping of Rubble Mound Breakwaters*. In L. Franco, G. R. Tomasicchio, & A. Lamberti (Eds.), *Coastal Structures 2007: Proceedings of the 5th International Conference : Venice, Italy, 2-4 July 2007* (pp. 1532-1541). World Scientific. Retrieved from <https://core.ac.uk/download/pdf/60398304.pdf>
10. Burcharth, H. F., Kramer, M., Lamberti, A., Zanuttigh, B. (2006). *Structural stability of detached low crested breakwaters*. *Coastal Engineering*, 53(4), 381–394. <https://doi.org/10.1016/j.coastaleng.2005.10.023>
11. Burcharth, H.F., Liu, Z., Troch, P. (1999). *Scaling of core material in rubble mound breakwater model tests*. Proceedings 5th International Conference on Coastal and Port Engineering in Developing Countries (COPEDEC), Cape Town, South Africa, pp. 1518-1528. Retrieved from Delta Marine Consultants' archive.
12. CIRIA, CUR, CETMEF (2007). *The Rock Manual. The use of rock in hydraulic engineering (2<sup>nd</sup> edition)*. C683, CIRIA, London. Retrieved from <http://www.kennisbank-waterbouw.nl/DesignCodes/rockmanual/>
13. De Jong, R.J. (1996). *Wave transmissions at low-crested structures. Stability of tetrapods at front, crest and rear of a low-crested breakwater*. Retrieved from



- <https://repository.tudelft.nl/islandora/object/uuid%3Ae091d54b-bffa-44ba-8d5d-850cdc03731a>
14. Delta Marine Consultants (2018). *Guidelines for Xbloc Concept Design*
  15. Dupray, S., Roberts, J. (2010). Review of the use of concrete in the manufacture of concrete armour units. *Coasts, Marine Structures and Breakwaters: Adapting to Change - Proceedings of the 9th International Conference*. 1. 245-259. Retrieved from [https://www.researchgate.net/publication/288661643\\_Review\\_of\\_the\\_use\\_of\\_concrete\\_in\\_the\\_manufacture\\_of\\_concrete\\_armour\\_units](https://www.researchgate.net/publication/288661643_Review_of_the_use_of_concrete_in_the_manufacture_of_concrete_armour_units) (citation by research gate)
  16. Eggeling, T. (2016). *Research on the scaling of core material in rubble mound breakwaters*. [Internal Report from DMC].
  17. Eggeling, T. (2018). *Hydraulic stability and overtopping performance of a new type of regular placed armor unit* [Power Point Slides]. Retrieved from <https://www.xbloc.com/sites/default/files/domain-671/documents/xbloc-hydraulic-stability-and-overtopping-performance-xblocplus-icce-2018-671-1536059849601746306.pdf>
  18. EurOtop, 2016. Manual on wave overtopping of sea defences and related structures. An overtopping manual largely based on European research, but for worldwide application. Van der Meer, J.W., Allsop, N.W.H., Bruce, T., De Rouck, J., Kortenhaus, A., Pullen, T., Schüttrumpf, H., Troch, P. and Zanuttigh, B., [www.overtopping-manual.com](http://www.overtopping-manual.com).
  19. Hald, T. (1998). *Wave Induced Loading and Stability of Rubble Mound Breakwaters*. Aalborg: Hydraulics & Coastal Engineering Laboratory, Department of Civil Engineering, Aalborg University. Series paper, No. 18. Retrieved from [https://vbn.aau.dk/ws/portalfiles/portal/55248437/Wave\\_Induced>Loading\\_and\\_Stability\\_of\\_Rubble\\_Mound\\_Breakwaters.pdf](https://vbn.aau.dk/ws/portalfiles/portal/55248437/Wave_Induced>Loading_and_Stability_of_Rubble_Mound_Breakwaters.pdf).
  20. Heineke, R., Verhagen, H.J. (2007). *On the use of the fictitious wave steepness and related surf-similarity parameters in methods that describe the hydraulic and structural response to waves*. *Coastal Structures 2007: Proceedings of the 5th International Conference, Venice, Italy, 2-4 July 2007*. Retrieved from <https://repository.tudelft.nl/islandora/object/uuid:2b24e555-bfe5-4600-a0da-8147717cd1da?collection=research>
  21. Jacobs, R., Bakker, P., Vos, I., Reedijk, B. (2018). *XblocPlus – Development of a regular placed interlocking armour unit (Abstract)*. Retrieved from <https://www.xbloc.com/sites/default/files/domain-671/documents/xblocplus-development-of-a-regular-placed-interlocking-armour-unit-abstract-2018-671-15360601631294554944.pdf>
  22. Kamali, B., Hashim, R. (2009). *Recent Advances in Stability Formulae and Damage Description of Breakwater Armour Layer*. *Australian Journal of Basic and Applied Sciences*, 3(3), 2817–2827. Retrieved from [http://eprints.um.edu.my/8839/1/Recent\\_advances\\_in\\_stability\\_formulae\\_and\\_damage\\_description\\_of\\_breakwater\\_armour\\_layer.pdf](http://eprints.um.edu.my/8839/1/Recent_advances_in_stability_formulae_and_damage_description_of_breakwater_armour_layer.pdf)
  23. Kramer, M. (2006). *Structural Stability of Low-Crested Breakwaters*. Aalborg: Department of Civil Engineering, Aalborg University. (DCE Thesis; No. 1). Retrieved from <https://core.ac.uk/download/pdf/60345970.pdf>
  24. Latham, J. P., Xiang, J., Anastasaki, E., Guo, L., Karantzoulis, N., Viré, A., & Pain, C. (2014). Numerical modelling of forces, stresses and breakages of concrete armour

- units. In Proceedings of the 34th International Conference on Coastal Engineering, ICCE 2014 (Vol. 2014-January). ASCE. <https://doi.org/10.9753/icce.v34.structures.78>
25. Mansard, E. P. D., Funke, E. R. (1980). *CHAPTER 8 The Measurement of Incident and Reflected Spectra Using a least Squares Method*, 154–172. Int. Conf. on Coastal Engineering (ICCE), Sydney. Retrieved from <https://repository.tudelft.nl/islandora/object/uuid%3A840a64af-b113-4372-8f91-47b4d7a3cc78?collection=research>
  26. Meer, J. W. Van Der. (1998). Application and stability criteria for rock and artificial units. *Dikes and Revetments. Design, Maintenance and Safety Assessment*, (3), 1–24. Retrieved from <http://citeseerx.ist.psu.edu/viewdoc/download?doi=10.1.1.713.5044&rep=rep1&type=pdf>.
  27. Muttray, M., Reedijk, B. (2009). *Design of concrete armour layers*. Hansa International Maritime Journal, 6, 111-118. Retrieved from <https://www.xbloc.com/sites/default/files/domain-671/documents/xbloc-2008-design-of-concrete-armour-layers-muttray-et-al-671-14585724381469179232.pdf>
  28. Muttray, M., Ten Oever, E., Reedijk, B. (2012). *Stability of Low Crested and Submerged Breakwaters with Single Layer Armouring*. Journal of Shipping and Ocean Engineering, 2, 140–152. Retrieved from <https://www.xbloc.com/sites/default/files/domain-671/documents/xbloc-2012-stability-of-low-crested-and-submerged-breakwaters-muttray-et-al-671-14585726531875894758.pdf>
  29. PND Engineers. (2018). Breakwaters including partial penetrating wave barriers. Retrieved September 20, 2018, from <http://www.pndengineers.com/home/showdocument?id=413>
  30. Price, W.A. (1979). *Static stability of rubble mound breakwaters*. Dock & Harbour Authority, vol60, May 1979, pp2-7. Retrieved from <https://repository.tudelft.nl/islandora/object/uuid:0af313f0-1fa0-4311-8d94-50bd331ae7d3?collection=research>
  31. Rada Mora, B. (2017). *Hydraulic performance of Xbloc+ armor unit*. Retrieved from <https://repository.tudelft.nl/islandora/object/uuid%3Afb797ef-5944-4bc1-9d25-e7448dce3d1b>
  32. Schiereck, G.J., Verhagen, H.J. (2016). *Introduction to Bed, bank and shore protection*. Delft Academic Press
  33. Schüttrumpf, H., Van Gent, M. (2004). *Wave Overtopping at Seadikes*. Coastal Structures 2003 - Proceedings of the Conference. 431-443. 10.1061/40733(147)36. Retrieved from [https://www.researchgate.net/profile/Marcel\\_Gent/publication/268598040\\_Wave\\_Overtopping\\_at\\_Seadikes/links/5580339a08ae712be7a15f67.pdf](https://www.researchgate.net/profile/Marcel_Gent/publication/268598040_Wave_Overtopping_at_Seadikes/links/5580339a08ae712be7a15f67.pdf)
  34. Schüttrumpf, Holger & Kortenhaus, Andreas & Bruce, Tom & Franco, Leopoldo. (2009). *Wave Run-Up and Wave Overtopping at Armored Rubble Slopes and Mounds*. Handbook of Coastal and Ocean Engineering. Retrieved from [http://www.vandermeerconsulting.nl/downloads/functional\\_a/2010\\_schuttrumpf\\_vandermeer.pdf](http://www.vandermeerconsulting.nl/downloads/functional_a/2010_schuttrumpf_vandermeer.pdf).
  35. Standard deviation. (2019). In *Wikipedia*. Retrieved June 18, 2019, from [https://en.wikipedia.org/wiki/Standard\\_deviation](https://en.wikipedia.org/wiki/Standard_deviation)
  36. Standard deviation. (2019). In *Wikipedia*. Retrieved June 18, 2019, from [https://en.wikipedia.org/wiki/Standard\\_deviation](https://en.wikipedia.org/wiki/Standard_deviation)

37. Taveira-Pinto, F. (2005). *Analysis of submerged breakwaters stability design*. WIT Transactions on the Built Environment, 78, 15. Retrieved from <https://www.witpress.com/Secure/elibrary/papers/CE05/CE05019FU.pdf>
38. U.S. Army Corps of Engineers (2002). *Coastal Engineering Manual (CEM), Engineer Manual 1110-2-1100*. U.S. Army Corps of Engineers. Washington, D.C. (6 volumes).
39. Van den Berg, I. (2018). *Effect of irregularities in the under layer on the stability of Xbloc<sup>Plus</sup> concrete armour unit*. Retrieved from <https://repository.tudelft.nl/islandora/object/uuid%3Aadd9fc49-b3dd-4e7f-b0a9-91a9caf2ff92?collection=education>
40. Van den Bosch, I., ten Oever, E., Bakker, P., Muttray, M. (2012). *Stability of interlocking armour units on a breakwater crest*. Coastal Engineering Proceedings. Retrieved from [https://icce-ojs-tamu.tdl.org/icce/index.php/icce/article/viewFile/6695/pdf\\_667](https://icce-ojs-tamu.tdl.org/icce/index.php/icce/article/viewFile/6695/pdf_667)
41. Van der Linde, J. P. (2009). *Stability of single layer armour units on low-crested structures*. Retrieved from <https://repository.tudelft.nl/islandora/object/uuid%3A1f995447-3078-4d99-801f-60b19d1116f2>
42. Van der Meer, J.W. (1998). *Geometrical design of coastal structures. Seawalls, Dikes and Revetments*, 1–15. Retrieved from [http://www.vandermeerconsulting.nl/downloads/stability\\_b/1998\\_vandermeer\\_ch\\_9.pdf](http://www.vandermeerconsulting.nl/downloads/stability_b/1998_vandermeer_ch_9.pdf)
43. Van der Meer, J.W., Daemen, I.F.R. (1994). *Stability and Wave Transmission at Low-Crested Rubble-Mound Structures*. Journal of Waterway Port Coastal and Ocean Engineering. Retrieved from [http://www.vandermeerconsulting.nl/downloads/stability\\_e/1994\\_vandermeer\\_daemen.pdf](http://www.vandermeerconsulting.nl/downloads/stability_e/1994_vandermeer_daemen.pdf)
44. Van der Meer, J.W., Pilarczyk, K.W. (1990). *Stability Of Low-Crested And Reef Breakwaters*. Coastal Engineering Proceedings, [S.L.], N. 22, Jan. 2011. Issn 2156-1028. Retrieved from <<https://icce-ojs-tamu.tdl.org/icce/index.php/icce/article/view/4532>>.
45. Van Gent, M.R.A (2001). *Low-exceedance wave overtopping events - Estimates of wave overtopping parameters at the crest and landward side of dikes*. Retrieved from <https://repository.tudelft.nl/islandora/object/uuid%3A75d667f6-7491-4c2c-8829-c3a2be581102>
46. Van Zwicht, B.N.M. (2017). *Wave flume manual – Hydraulic model testing*. Delta Marine Consultants
47. Vanneste, D., Troch, P. (2012). *A Revision of the Scaling Method for Core Material in Rubble-mound Breakwaters Approaches to the Scaling of Core Material*. Coastlab12, 1–10. Retrieved from [https://www.researchgate.net/profile/Dieter\\_Vanneste/publication/279175446\\_A\\_Revision\\_of\\_the\\_Scaling\\_Method\\_for\\_Core\\_Material\\_in\\_Rubble-mound\\_Breakwaters/links/558bc96108ae48b7b56dc2d8/A-Revision-of-the-Scaling-Method-for-Core-Material-in-Rubble-mound-Breakwaters.pdf](https://www.researchgate.net/profile/Dieter_Vanneste/publication/279175446_A_Revision_of_the_Scaling_Method_for_Core_Material_in_Rubble-mound_Breakwaters/links/558bc96108ae48b7b56dc2d8/A-Revision-of-the-Scaling-Method-for-Core-Material-in-Rubble-mound-Breakwaters.pdf).
48. Verhagen, H. J., van den Bos J.P. (2018). *Breakwater Design – Lecture Notes CIE5308 (Edition 2018)*, Department of Hydraulic Engineering, Faculty of Civil Engineering and Geosciences, Delft University of Technology.
49. Vidal, C., Losada, M. A., Mansard, E. P. (1995). *Stability of low-crested rubble-mound breakwater heads*. Journal of waterway, port, coastal, and ocean engineering,

- 
- 121(2), 114-122. Retrieved from [https://www.academia.edu/download/38011741/1995\\_Stability\\_of\\_Low-Crested.pdf](https://www.academia.edu/download/38011741/1995_Stability_of_Low-Crested.pdf)
50. Vos, A. B. (2017). *Exploration into the mechanisms that govern the stability of an Xbloc+ v1 armour unit*. Retrieved from <https://repository.tudelft.nl/islandora/object/uuid%3AAdd61dbae-67ea-4a67-b5f2-b9691240f729?collection=education>
51. Vos-Jansen, L. (2018) . *Physical modelling of reflection on gentle coasts to minimise reflection in a wave flume*. Retrieved from <https://repository.tudelft.nl/islandora/object/uuid%3A2d25af25-f4dc-4537-8153-71408cf22fa0>
52. Wolters, G., van Gent, M., Allsop, W., Hamm, L. and Mühlestein, D. (2007). Guidelines for physical model testing of breakwaters. Rubble mound breakwaters. *Report prepared for Hydralab III*. Retrieved from [https://www.researchgate.net/profile/William\\_Allsop/publication/301298828\\_Guidelines\\_for\\_physical\\_model\\_testing\\_of\\_breakwaters\\_Rubble\\_mound\\_breakwaters/links/5711006f08ae846f4ef05bdd.pdf](https://www.researchgate.net/profile/William_Allsop/publication/301298828_Guidelines_for_physical_model_testing_of_breakwaters_Rubble_mound_breakwaters/links/5711006f08ae846f4ef05bdd.pdf)
53. Wolters, G., van Gent, M., Allsop, W., Hamm, L., & Muhlestein, D. (2010). *HYDRALAB III: Guidelines for physical model testing of rubble mound breakwaters*. *Coasts, Marine Structures and Breakwaters: Adapting to Change*, 2: 559-670. Retrieved from [https://www.researchgate.net/profile/Marcel\\_Gent/publication/259264269\\_HYDRALAB\\_III\\_Guidelines\\_for\\_physical\\_model\\_testing\\_of\\_rubble\\_mound\\_breakwaters/links/0046352a9d90e11aef000000.pdf](https://www.researchgate.net/profile/Marcel_Gent/publication/259264269_HYDRALAB_III_Guidelines_for_physical_model_testing_of_rubble_mound_breakwaters/links/0046352a9d90e11aef000000.pdf)

## Appendix A. Literature Review

### A.1. Breakwaters

#### A.1.1. Breakwater Categories

Different types of breakwaters exist, according to different criteria:

Depending on the structural features, breakwaters can be distinguished into the following categories (Verhagen and van den Bos, 2018):

- Rubble mound: their cross section consists of different layers of quarry material with rock or concrete blocks placed at the outer layer.
- Monolithic, which have a cross section which “behaves like a solid block”.
- Composite, which is a “hybrid” between the rubble mound and monolithic type.
- Special types, such as floating, pneumatic, hydraulic, pile, horizontal plate breakwaters.

Depending on the position of the top of the structure with respect to the still water level, breakwaters can be rarely overtopped by the incoming waves (conventional type with high crest), frequently overtopped (low crested type) or be permanently underwater (submerged) (Kramer, 2006).

Depending on their position relative to the shore, breakwaters can either be connected (attached) or not to the shore (detached).

#### A.1.2. Main Dimensions of a Rubble Mound Breakwater

The main dimensions of a rubble mound breakwater (without filter layer and crown wall superstructure) are shown in Figure A-1. (The Rock Manual, 2007).

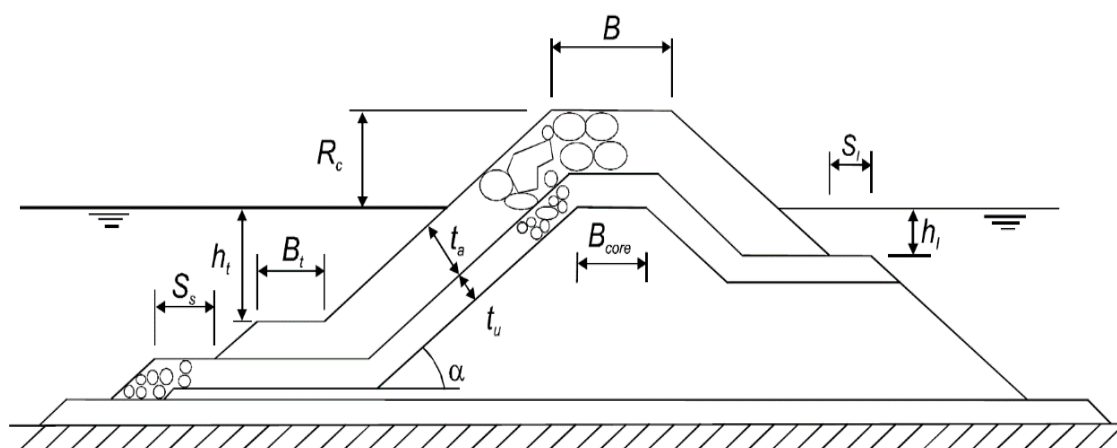


Figure A-1: Main breakwater dimensions without a filter layer and crown superstructure (The Rock Manual, 2007)

Where

$t_a$ : armour layer thickness

$t_u$ : underlayer thickness

$B_{core}$ : width of the breakwater at the top of the core

$B$ : crest width (typically minimum 3-4 armour stones or 3 concrete units)

$h_t, h_l$ : water depth at the sea and lee-side of the toe respectively

$B_t$ : width of the toe at  $h_t$

$\alpha$ : slope angle

$S_s, S_l$ : the width of the sea and lee-side shoulder respectively (typically  $S_s > 2m$  &  $S_l > 0.5t_u$ , but further increased when erosion is present)

$R_c$ : vertical distance between the still water level and the crest (freeboard)

Subsequently, as brief description of the function of the different parts of a breakwater is provided.

### **Core**

The function of the core is to fill the majority of the volume of the breakwater structure. The core material can be primary rockfill, such as quarry run, or dredged sand with gravel (The Rock Manual, 2007).

### **Filter layer**

In view of considerable pressure differences causing outward movement of the finer core material, a filter layer can be placed under the underlayer at the seaward part, to prevent washing of the core material out of the armour layer. The filter layer typically consists of one or more layers of rock, resulting in a geometrically closed filter. Alternatively, geotextile or mattresses can be used at the filter layer (Verhagen and van den Bos, 2018).

### **Underlayer**

The underlayer consists of rock, with weight typically in the range of 1/25 to 1/10 of the weight of the armour layer units. It provides a smooth transition between the armour layer and the core and prevents the washing out of the core material, in the case that no filter layer is constructed.

### **Toe Berm**

The toe berm has a “foundation”-like function for the armour layer and provides support by preventing it from sliding.

### **Crown superstructure**

A crown wall can be constructed in the cases of aiming to lower overtopping discharge and/or access to the breakwater crest. However, attention should be given to the geotechnical and structural design of the crown wall because of potential uneven settlements and high wave impact forces. A “side effect” of the presence of a crown wall is the decrease in the interlocking of the armour stones near the wall. Additionally, since overtopping is minimised, most of the wave energy is focused on the front slope, which leads to the enhancement of the wave forces at the armour units.

### Armour layer of rubble mound breakwaters

The outer layer of a breakwater is the armour layer. The design of the armour layer is crucial, since it resists the wave forces. Underestimation of the required strength of this layer can cause extensive damage or complete failure (Van der Meer, 1998), whereas overestimation leads to unnecessarily high construction costs. Thus, it is important to ensure that the required strength is achieved in an economical way.

#### A.1.3. Rocking

Rocking can be an important failure mechanism, especially in the case of slender armour units, which can be illustrated by the characteristic example of the failure of the Sines breakwater in Portugal. According to Baird et al (1980), the increasing velocity of the incident waves caused rocking of the dolosse of the armour layer, which led to their impact with neighbouring dolosse. The impact stresses exceeded the concrete strength and, resulted to the breakage of the units in smaller pieces. The latter were easily dragged by the waves and caused additional impacts with other units. The gaps that were created, after broken parts of the dolosse were carried away, provided more space for other units to move, which finally resulted in extensive overall damage in the armour layer.

Delta Marine Consultants uses the 2% rocking criterion: not more than 2% of the units should be visually observed to move more than 20 times in 1000 waves. Based on the current research on Xbloc+, rocking for the armour layer was found to fall within the above criterion, so it can be considered limited. Furthermore, the structural stability of Xbloc+ is higher compared to that of slender units, so rocking is more difficult to lead to structural failure. However, rocking of units can be considered as a “warning sign” for failure, because it often occurs well before the start of damage or failure.

#### A.1.4. Stability Formulae for Rock Armour

##### Iribarren’s formula

By taking into account the drag and lift forces, the submerged weight and neglecting the inertia force, Iribarren produced a formula for wave down rush, which was extended by Hedar (1960) for the case of wave uprush:

$$\frac{H}{\Delta * d_n} < N * (\mu * \cos \alpha \pm \sin \alpha)$$

Where,

H: wave height (m)

$$\Delta = \frac{\rho_s - \rho_w}{\rho_s}: \text{relative mass density}; \rho_s: \text{rock density } \left(\frac{\text{kg}}{\text{m}^3}\right); \rho_w: \text{water density } \left(\frac{\text{kg}}{\text{m}^3}\right)$$

$d_n$ : characteristic stone diameter (m)

$\alpha$ : structure slope (–)

$\mu$ : friction coefficient (–)

N: coefficient

(–) or (+) are used for wave run – down or run – up respectively

N is an experimentally determined coefficient, in which all factors not explicitly expressed in the formula (unit shape, damage level etc) are accounted for.

### Hudson's formula

The stability formula proposed by Hudson, in its modified form, reads as follows:

$$W_{50} = \frac{\rho_s g H_{1/10}^3}{K_D \Delta^3 \cot \alpha}$$

Where,

$W_{50}$ : median unit weight (N)

g: gravitational acceleration ( $\frac{m}{s^2}$ )

$H_{\frac{1}{10}}$ : average of the 10% highest waves in the record, at the toe of the structure.

with  $H_{1/10} = 1.27 H_s$  (m)

$K_D$ : stability coefficient

The factor  $K_D$  includes all other factors, such as storm type and acceptable damage degree, that are not explicitly included in Hudson's formula. Values of  $3 < K_D < 6$  and  $K_D > 8$  are typical for rock and concrete armour units respectively.

### Van der Meer's formula

The stability formulas of Iribarren and Hudson have several limitations. The experiments conducted by Iribarren and Hudson concerned wave steepness of 3-4% and relatively permeable structures. Thus, the influence of wave steepness, structure permeability, as well as type of wave breaking and number of waves are not included explicitly in the formulas.

Van der Meer (1988) distinguished between plunging and surging breaking waves and explicitly included more factors of influence, thus, producing the formulas:

$$\frac{H_s}{\Delta D_{n50}} = c_{pl} P^{0,18} \left(\frac{S}{\sqrt{N}}\right)^{0,2} \xi_m^{-0,5}, \quad \text{for plunging type of breaking}$$

$$\frac{H_s}{\Delta D_{n50}} = c_s P^{-0,13} \left(\frac{S}{\sqrt{N}}\right)^{0,2} \sqrt{\cot \alpha} \xi_m^P, \quad \text{for surging type of breaking}$$

Where,

N: number of waves (-)

$$D_{n50} = \sqrt[3]{\frac{M}{\rho_s}}: \text{nominal median diameter (m); } M: \text{unit mass (kg); } \rho_s: \text{unit density } \left(\frac{kg}{m^3}\right)$$

$$\Delta = \frac{\rho_s - \rho_w}{\rho_s}: \text{relative mass density (-); } \rho_w: \text{water density } \left(\frac{kg}{m^3}\right)$$

$H_s$ : significant wave height

$H_s = H_{\frac{1}{3}}$ , if obtained by a time series or  $H_{m0}$ , if obtained by spectral analysis



P: notional permeability coefficient (–)

$S = \frac{A}{D_{n50}^2}$ : damage level (–); A: cross – sectional eroded area (m<sup>2</sup>)

$\alpha$ : structure slope

$\xi_m$ : surf similarity parameter (–)

$c_{pl}, c_s$ : coefficients for plunging and surging waves with values of 6.2 and 1.0 respectively (–)

$\xi_{cr} = \left( \frac{c_{pl}}{c_s} P^{0.31} \sqrt{\tan \alpha} \right)^{\frac{1}{P+0.5}}$ : critical surf similarity parameter (–)

For  $\xi_{m-1,0} < \xi_{cr}$ , waves are plunging and for  $\xi_{m-1,0} > \xi_{cr}$ , waves are surging. At  $\xi_{m-1,0} = \xi_{cr}$ , the minimum stability of the armour layer is observed.

According to the Van der Meer formula, increasing permeability leads to higher stability of the armour layer.

The van der Meer formulas are applicable for irregular, non-breaking and non-depth limited waves. For shallow water, Verhagen and van den Bos (2018) refer to the following relations derived from the Van der Meer (1988) formula modified by Van Gent et al (2004):

$$\frac{H_s}{\Delta D_{n50}} = c_{pl} P^{0.18} \left( \frac{S}{\sqrt{N}} \right)^{0.2} \left( \frac{H_s}{H_{2\%}} \right) \xi_{m-1,0}^{-0.5}, \quad \text{for plunging type of breaking}$$

$$\frac{H_s}{\Delta D_{n50}} = c_s P^{-0.13} \left( \frac{S}{\sqrt{N}} \right)^{0.2} \left( \frac{H_s}{H_{2\%}} \right) \sqrt{\cot \alpha} * \xi_{m-1,0}^P, \quad \text{for surging type of breaking}$$

Where,

$H_s$ : significant wave height

$H_{2\%}$ : wave height exceeded by 2% of the waves

$$s_{m-1,0} = \frac{2\pi H_{2\%}}{g T_{m-1,0}^2}: \text{fictitious wave steepness (–)}$$

$$\xi_{m-1,0} = \frac{\tan \alpha}{\sqrt{s_{m-1,0}}}: \text{surf similarity parameter based on } s_{m-1,0} \text{ (–)}$$

$$T_{m-1,0} = \frac{m_{-1}}{m_0}: \text{spectral mean wave energy period (s)}$$

The critical surf similarity parameter is the same with the original van der Meer formula, but the coefficients for plunging and surging waves,  $c_{pl}$  and  $c_s$ , have the values of 8.4 and 1.3 respectively.

#### A.1.5. Damage definitions and stages of damage

Different damage definitions for the armour layer exist in literature. The damage can be expressed as the quotient of the displaced units over the total number of units initially present in an area of the breakwater:

$$N_d = \frac{\text{number of displaced units in area}}{\text{total number of units in area}}$$

The area can be defined by the limits of a specific vertical distance above and below the still water level. A commonly used distance is  $\pm 1.5H_D$  ( $H_D$ : design wave height).

Van der Meer (1991) proposed to use the number of moving units moving (displaced or rocking) out of a strip of width equal to  $D_n$  extending from the bottom to the top of the armour layer along the slope:

$$N_{omov} = N_{od} + N_{or}$$

Where,

$N_{omov}$ : number of moving units

$N_{od}$ : number of displaced units

$N_{or}$ : number of rocking units

Three damage levels were defined:

- $N_{od}$ : number of units totally displaced out of the layer at a distance more than  $2D_n$ .
- $N_{o>0.5}$ : number of units displaced at a distance more than  $0.5D_n$ .
- $N_{o<0.5}$ : number of units displaced at a distance less than  $0.5D_n$ .

Alternatively, the eroded profile can be measured and the parameter  $S$  (Broderick parameter) can be used as a damage criterion.

$$S = \frac{A_e}{D_{n50}^2}$$

Where,

$A_e$ : cross – sectional eroded area around still water level ( $m^2$ ),

$$D_{n50}: \text{nominal diameter of unit} = \sqrt[3]{\frac{W_{50}}{\rho_s}}$$

This parameter expresses the number of cubic stones with a side of  $D_{n50}$  eroded within a width of one  $D_{n50}$  (Van der Meer, 1988). However, the real number of units eroded differs due to factors, such as the porosity, gradation and shape of the rocks.

The following relation holds between the number of displaced units ( $N_{od}$ ) and the damage parameter ( $S$ ):

$$N_{od} = G(1 - n_v)S$$

Where,

$n_v$ : porosity of armour layer

$G$ : gradation factor (equal to 1 for concrete units)

Vidal et al (1995), when researching the stability of low-crested rubble-mound breakwaters, summarized the different damage stages, after Losada et al (1986) and Vidal et al (1991), as following:

- Initiation of damage: “when a number of armour units are displaced from their original position to a new one at a distance equal to or larger than the unit nominal diameter”. At this stage, the occurring gaps in the armour layer are bigger than the mean size of its pores.
- Irribaren’s damage: “when the extent of the failure area of the outer armour layer is large enough for degrees of waves to act directly on the lower armour layer”.
- Start of destruction: “initiation of damage of the lower layer of the armour, whereby a number of units of the inner armour layer are displaced, causing large holes”.
- Destruction: “material of the secondary (or filter layer) is removed”.

The Rock Manual (2007) presents 3 different stages of damage:

- Start of damage
- Intermediate damage
- Failure

For rock in two layers, damage is initiated for  $S > 2-3$ , intermediate damage for  $S > 3-12$  and failure for  $S > 8-17$ . The ranges of the damage parameter  $S$  are quite large, since there is a strong dependency on the structure slope. The lowest value refers to  $\cot\alpha = 1.5$ , the highest to  $\cot\alpha = 6$  and intermediate values apply for intermediate slopes.

## A.2. Waves

### A.2.1. Wave Statistics

In irregular wave fields, wave characteristics can vary on the short or long term and are described by the short and long term distributions respectively.

#### A.2.1.1 Short Term Distribution

To determine the short term distribution of wave characteristics, a record of 20-30 minutes is typically used. This duration is long enough to include sufficient (typically 1000) number of waves, in order to obtain reliable results from the analysis, but short enough to ensure stationary conditions. In deep water ( $h > 3H_s$ ) and in the short term, the wave heights follow the Rayleigh distribution. The probability of exceedance of a specific wave height is:

$$P\{\underline{H} > H\} = \exp\left[-\left(\frac{H}{H_{\text{rms}}}\right)^2\right] = \exp\left[-2\left(\frac{H}{H_s}\right)^2\right] = \exp\left[-\frac{H^2}{8m_0}\right]$$

Where,

$H_{\text{rms}}$ : root mean square wave height (square root of the mean of the squares of all wave heights)

$H_s$ : significant wave height with various definitions, depending on the derivation method

The following approximate relations hold:

$$H_s \equiv H_{\text{visual}} \equiv H_{1/3} \equiv H_{13.5\%} \equiv H_{m0} \approx 4\sqrt{m_0}$$

With,

$H_{\text{visual}}$ : significant wave height from visual observations;  $H_{1/3}$ : mean wave height of the highest one third of the waves from a wave record;  $H_{m0}$ : significant wave height from spectral analysis, approximately equal to  $4\sqrt{m_0}$ .

Generally,  $H_{1/Q}$  is defined as the average height of the  $1/Q$  highest waves of a record and  $H_{P\%}$  as the height that is exceeded by  $P$  per cent of the waves of a record (The Rock Manual, 2007).

When travelling to shallow waters, wave heights deviate from the Rayleigh distribution and can be described by the composed Weibull distribution proposed by Battjes and Groenendijk (2000). The Rayleigh distribution is valid up to a transitional wave height, which depends on the water depth and can be derived from the wave spectrum.

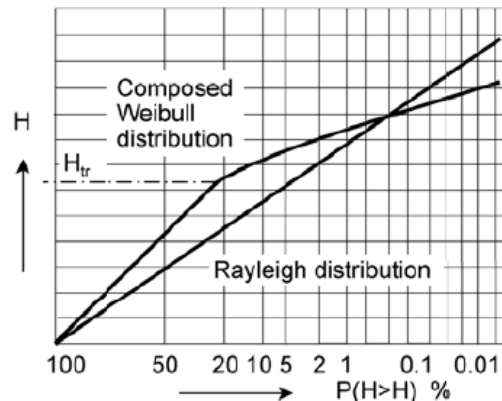


Figure A-2: Wave height probability distributions (from Schiereck (2004) after Battjes and Groenendijk (2000))

#### A.2.1.2 Long Term Distribution

To get the long term characteristics of waves, storms can be distinguished in a given record by defining a minimum wave height as a threshold, above which a storm lasts (Peak over Threshold Analysis). After extrapolating the maximum wave height in each storm, the long term wave height distribution can be constructed (Verhagen and van den Bos, 2018).

#### A.2.2. Wave Spectra

Another method to describe and obtain wave characteristics is spectral analysis. Wave spectra, which are produced by Fourier transformations of a sea-surface record, express the distribution of the wave energy over the wave frequencies. The variances, equal to  $0.5\alpha_i^2$  ( $\alpha_i$ : amplitude of each of the superimposed wave components used to create the irregular wave field) are plotted in the y axis, whereas the frequencies ( $f_i$ ) are plotted in x-axis. From the wave spectra, wave statistical quantities can be derived. When integrating the density spectrum, i.e. calculating the total area under the spectrum, the total variance ( $m_0$ ) is obtained. Higher order moments can be obtained from the following expression:

$$m_n = \int_0^\infty f^n S(f) df, \quad \text{where } S(\omega) = \frac{1}{2} \sum_{\Delta\omega} \frac{\alpha_i^2}{\Delta\omega} \quad \text{and } \omega = 2\pi f$$

In order to include the spreading over the directions, apart from the spreading over the frequencies, the two-dimensional spectrum ( $S(\omega, \theta)$ ) is used.

Different wave spectra can be found in literature with the Pierson Moskowitz and Jonswap spectra are the most common spectra in literature.

The Pierson Moskowitz spectrum describes fully developed sea conditions and the distribution of energy over the frequencies is given by:

$$E_{P-M}(f) = 0.00615 \frac{g^2}{(2\pi)^4 f_p} f^{-4} \exp\left(-\left(\frac{f}{f_p}\right)^{-4}\right)$$

Where,

$$f_p = \frac{0.123g}{U_{10}} : \text{peak frequency } \left(\frac{1}{s}\right)$$

$$g: \text{gravitational acceleration } \left(\frac{m}{s^2}\right)$$

$$U_{10} = \text{wind speed at 10 m altitude } \left(\frac{m}{s}\right)$$

The Jonswap spectrum describes fetch-limited conditions, which is mostly the case in nature. The distribution of energy over the frequencies, in its original form, is:

$$E_J(f) = \frac{ag^2}{(2\pi)^4} f^{-5} \exp\left(-\frac{5}{4}\left(\frac{f}{f_p}\right)^{-4}\right) \gamma^\delta$$

Where,

$$a = 0.076 \left(\frac{gF}{U_{10}^2}\right)^{-0.22} ; F: \text{fetch (m)}; f_p = 3.5 \frac{g}{U_{10}} \left(\frac{gF}{U_{10}^2}\right)^{-0.33} : \text{peak frequency } \left(\frac{1}{s}\right)$$

$$\delta = \exp\left(-\frac{\left(\frac{f}{f_p} - 1\right)^2}{2\sigma^2}\right); \sigma = \sigma_a = 0.07, \text{ for } f \leq f_p \text{ or } \sigma = \sigma_b = 0.09, \text{ for } f > f_p$$

$\gamma$ : peak enhancement factor (from 1 to 7 with mean of 3)

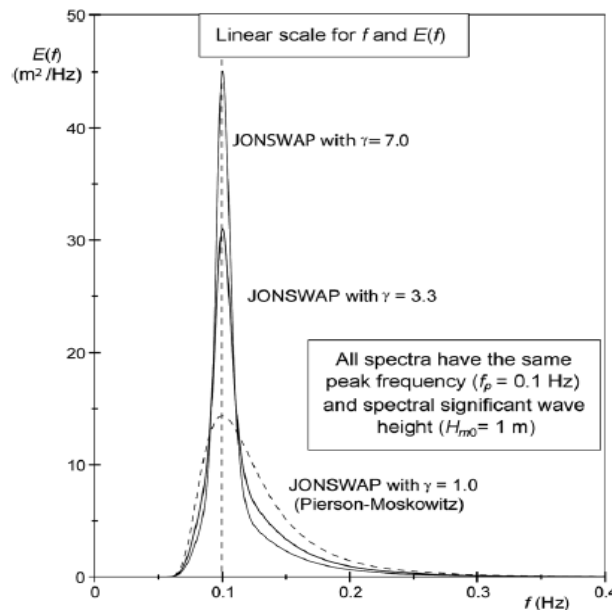


Figure A-3: Jonswap ( $\gamma=7$ ), Jonswap ( $\gamma=3.3$ ) and Jonswap ( $\gamma=1$ ) (Pierson-Moskowitz) spectra. (The Rock Manual, 2007)

The peak enhancement factor determines the amount of energy that is concentrated at the peak frequency. It can be seen from Figure A-3 that for spectra with the same spectral significant wave height and peak period, the larger the  $\gamma$  factor, the more energy is concentrated at the peak of the spectrum.

The shape of the wave spectrum is also affected when moving towards depth limited waters: a new much lower peak is created at lower frequencies, the shape becomes flatter and the area below the spectrum considerably decreases, which corresponds to increased energy dissipation. Subsequently, the relations between the different wave heights also change.

### A.2.3. Breaker Parameter

Different definitions are used for the wave steepness, depending on the definitions chosen for the wave height and period.

For the wave height at the toe of the structure ( $H$ ), the significant height from the wave record ( $H_{1/3}$ ) or from spectral analysis ( $H_{m0}$ ) can be used. For the wave period, different definitions can be used:

- $T_p$ : peak period, calculated at the point of maximum energy from the wave spectrum.
- $T_s$  (or  $T_{1/3}$ ): mean period of the 1/3 highest waves in a wave record and is approximately equal to  $0.95T_p$ .
- $T_m$ : mean period of all waves in a wave record.
- $T_{m-1,0} = m_{-1}/m_0$ : mean energy wave period, derived from the wave energy spectrum.

No universal relationships exist between  $T_m$ ,  $T_{m-1,0}$  and  $T_p$ , as the shape of the wave spectrum determines the relative magnitudes. The relations fall within the following ranges:  $T_m = (0.71-0.85)T_p$  and  $T_m = (0.80-0.95)T_{m-1,0}$ . (Goda (2000) from Heineke and Verhagen (2007)). For the relationship between  $T_p$  and  $T_{m-1,0}$ , it holds that  $T_p = 1.1 T_{m-1,0}$  for conventional single peak spectra. The peak period can be applied for single peak wave spectra, but is not handy to be applied for double-peaked spectra and cannot be applied for multi-peaked or flat spectra, as it can cause inaccuracies (EurOtop, 2016).

Heineke and Verhagen (2007) have summarised the notations of the fictitious wave steepness and surf-similarity parameter, resulting from the definitions of the wave height and period that are combined in the quotient of the wave steepness (Table A-1).

Wave Height	Wave Period	Wave Steepness	Surf Similarity Parameter
$H_s$	$T_m$	$S_{0m}$	$\xi_m$
$H_s$	$T_p$	$S_{0p}$	$\xi_p$
$H_{m0}$	$T_{m-1,0}$	$S_{m-1,0}$	$\xi_{m-1,0}$
$H_s$	$T_{m-1,0}$	$S_{s-1,0}$	$\xi_{s-1,0}$
$H_s$	$T_p$ (associated with the local wave length)	$s_p$ (real steepness at the toe of structure)	$\xi_p$ (surf similarity parameter resulting from real steepness)

Table A-1: Various Notations of Wave Steepness and Surf Similarity Parameter

Battjes (1974), among other researchers, stated the relationship between the wave breaking types and the surf-similarity parameter: as the value of the surf similarity decreases, which is the case when slope decreases and/or steepness increases, the breaking regime changes from surging to collapsing, plunging and spilling. The transition from one regime to another is moderate rather than abrupt, as can be noticed from the limits of  $\xi_{m-1,0}$  in Figure A-4. The breaker parameter plays a major role in how the waves break on the structure slope and, consequently, on the resulting damage on the armour layer.

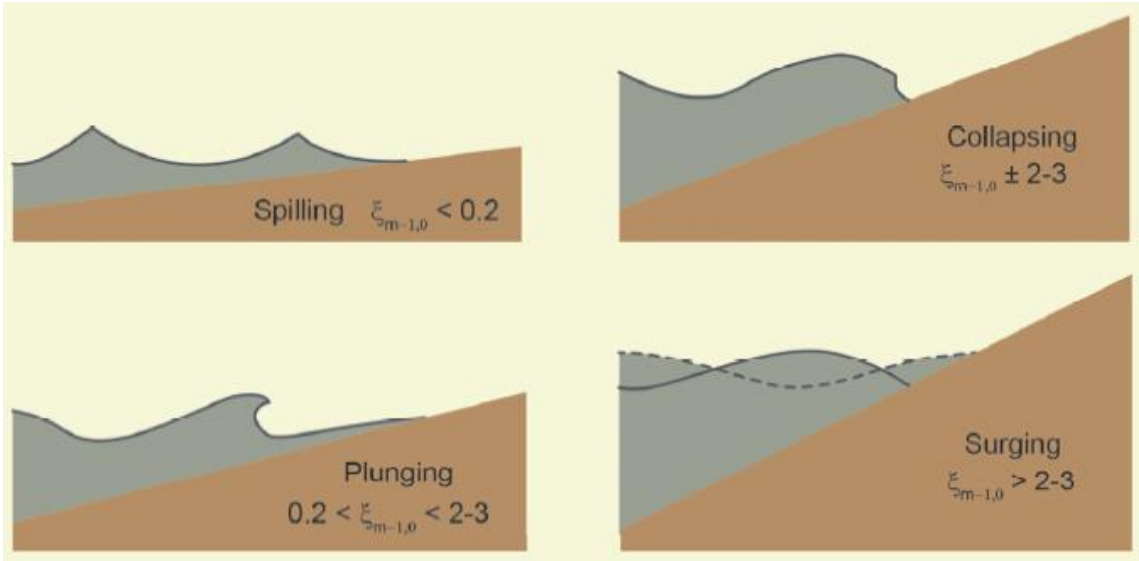


Figure A-4: Breaker types in relation with steepness (EurOtop II, 2016)



## A.2.4. Wave structure interaction

### A.2.4.1 Run-up

According to the Rock Manual (2007), the wave run-up height can be presented in a dimensionless form,  $R_{un\%}/H_s$ . ( $n\%$ : percentage of incoming waves that surpass the defined run-up level;  $H_s$ : significant wave height at the structure. The definition of run-up implies that the water tongue at its highest point still remains lower than the top level of the structure.

Wave run-up is highly influenced by the permeability of the breakwater. Low permeability leads to the interaction being concentrated at the outer slope, thus, increasing the flow velocities on the armour units. High permeability leads to the interaction taking place in a larger area, extending within the structure itself, which results in lower flow velocities at the armour layer. The difference is illustrated in Figure A-5.

Wave run-up changes the water level inside the structure. The stage of wave run-up is characterised by larger inflow period and inflow surface compared to the subsequent stage of run-down (Hald, 1998), which leads to a faster rise in the water level inside the breakwater during wave run-up and a slower lowering during wave run-down. The result is an outward-directed water flow inside the structure. Permeability of the structure is an important parameter also in this phenomenon, since the lower it is, the more difficult it is for the water table inside the breakwater to follow the changes in the “external water table” caused by the wave movement, which results in higher pressure build-up. Both the internal and external velocity fields interact, resulting in a very complex flow around the armour units.

In armoured slopes, the wave run-up is significantly decreased compared to the case of smooth, impermeable slopes, which is the result of the increased roughness of the armour layer and the increased porosity of the armour layer, underlayer and core.

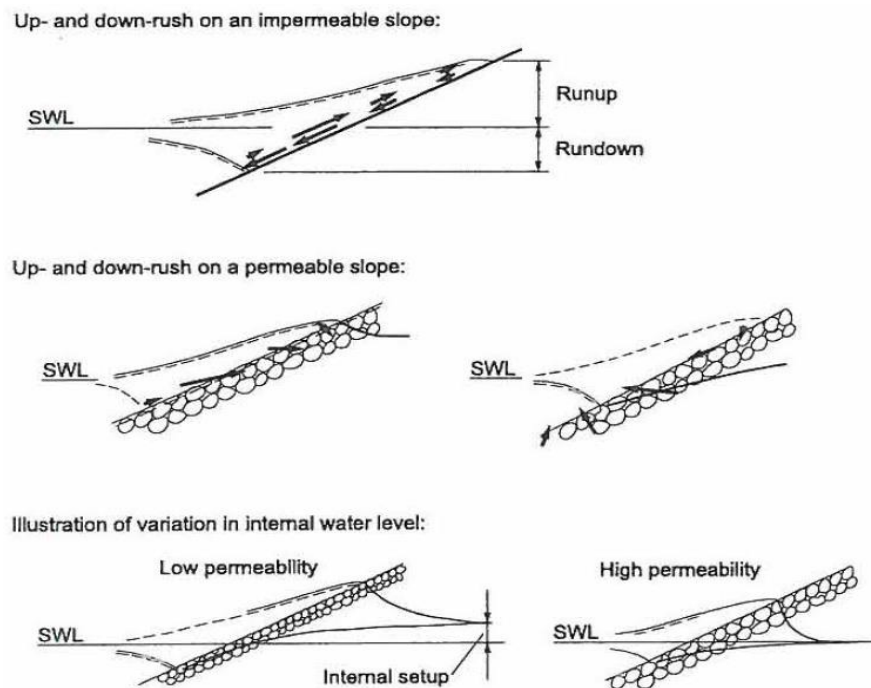


Figure A-5: Top: Velocities during wave run-up and run-down on an impermeable slope. Middle: Velocities during wave run-up (left) and run-down (right) on a permeable slope. Bottom: Effect of permeability on the internal water table (From Hald (1998) after Burcharth (1993))

Wave run-up for irregular waves acting on rock or rough slopes is given by the formula (EurOtop II, 2016):

$$\frac{R_{u2\%}}{H_{m0}} = 1.65 * \gamma_b * \gamma_f * \gamma_\beta * \xi_{m-1,0}$$

With a maximum of

$$\frac{R_{u2\%}}{H_{m0}} = 1.00 * \gamma_{fsurging} * \gamma_\beta * \left(4.0 - \frac{1.5}{\sqrt{\gamma_b * \xi_{m-1,0}}}\right)$$

Where

$R_{u2\%}$ : wave run up height exceeded by 2% of the incoming waves at the toe of the structure (m)

$H_{m0}$ : significant wave height at the toe (m)

$$\xi_{m-1,0} = \frac{\tan\alpha}{\sqrt{s_{m-1,0}}} = \frac{\tan\alpha}{\sqrt{\frac{2\pi H_{m0}}{gT_{m-1,0}^2}}}: \text{surf similarity parameter } (-)$$

$$T_{m-1,0} = \frac{m_{-1}}{m_0}: \text{mean energy wave period at the toe of the structure (s)}$$

$\tan\alpha$ : average slope angle (-)

$\gamma_b$ : reduction factor for berm (-)

$\gamma_\beta$ : reduction factor for oblique wave attack (-)

$\gamma_f$ : surface roughness correction factor (-)

$$\gamma_{fsurging} = \gamma_f + \frac{(\xi_{m-1,0} - 1.8)(1 - \gamma_f)}{8.2} \text{ for } \xi_{m-1,0} < 10 \text{ or } \gamma_{fsurging} = 1.0 \text{ for } \xi_{m-1,0} > 10$$

The equation for the maximum can be used in the cases with a very shallow foreshore with a lot of wave breaking. In this case, the breaker parameter  $\xi_{m-1,0}$  is large, because the wave steepness is very low. The breaker parameter can also be large when there is a very steep slope. The steepness can be used to discern between the former and latter cases. A wave steepness of  $s_{m-1,0} < 0.01$  gives generally conditions of severe wave breaking at a shallow foreshore (except for the case with very low and long swell) (EurOtop, 2016).

The maximum  $R_{u2\%}/H_{m0}$  is 3 and 2 for breakwaters with an impermeable and permeable core respectively. The coefficient 1.65 has a standard deviation of  $\sigma=0.10$ , so the value of 1.75 should be applied for design, whereas the coefficient 1.00 has a standard deviation of  $\sigma=0.07$ , so the value of 1.07 should be applied for design.

#### A.2.4.2 Overtopping

The mean overtopping discharge is given by:

$$\frac{q}{\sqrt{gH_{m0}^3}} = 0.09 * \exp\left(-\left(\frac{1.5R_c}{H_{m0}\gamma_f\gamma_\beta}\right)^{1.3}\right), \text{ for steep slopes 1: 2 to 3: 4}$$

Where,

q: average discharge per linear meter of width (m<sup>3</sup>/s per m)

#### A.2.4.3 Reflection

According to research by Allsop et al (1988) for reflection at slopes armoured with concrete units, reflection increases with increasing surf-similarity parameter. The relation of the reflection coefficient with the surf similarity parameter, as determined experimentally by Battjes (1974) (after Schiereck (2004)), is:

$$K_R = \frac{H_R}{H_I} \approx 0.1\xi^2 \text{ for } \xi < 2.5$$

Where,

$H_R$ : Reflected wave height (m)

$H_I$ : Incoming wave height (m)

$\xi$ : Surf similarity parameter (–)

#### A.2.4.4 Transmission

Important parameters for wave transmission are the permeability, crest freeboard and width, wave height and surf-similarity parameter (The Rock Manual, 2007). As was shown in data analysed by Van der Meer et al (1994), wave transmission becomes higher as wave steepness becomes lower, so more energy is expected to be transmitted to the leeside of the same structure for swell waves compared to a similar case with wind waves. The transmitted, together with the overtopped wave energy, are mainly responsible for the wavy conditions that can occur at the lee side of a breakwater structure.

A relationship for the wave transmission coefficient with the relative freeboard was proposed by De Jong (1996):

$$K_t = -0.4 \frac{R_c}{H_{si}} + A_{str} \left( \frac{B}{H_{si}} \right)^{-0.31} (1 - e^{-0.5\xi})$$

With,

$K_t = \frac{H_{st}}{H_{si}}$ : transmission coefficient

$H_{st}$ : transmitted significant wave height (m)

$H_{si}$ : incoming significant wave height (m)

$R_c$ : crest freeboard (m)

B: crest width (m)

$\xi$ : surf similarity parameter (–)

$A_{str}$ : coefficient ranging from 0.64 for armour layers with rock or concrete units to 0.80 for smooth, impermeable slopes

The equation is valid for  $K_t$  between 0.075 and 0.8, as well as for narrow crested breakwaters ( $B/H_s < 8$ ).

For wide-crested breakwaters ( $B/H_s > 12$ ) the following formula is applicable:

$$K_t = -0.35 \frac{R_c}{H_{si}} + 0.51 \left( \frac{B}{H_{si}} \right)^{-0.65} (1 - e^{-0.41\xi})$$

The lower and upper boundaries for  $K_t$  are 0.05 and  $0.93 - 0.006B/H_s$ .

For  $8 < B/H_s < 12$ , interpolation can be used, since the limits of each formula are not strictly defined.

### A.3. Model Core Scaling

The various methods for core scaling in physical models are summarised below:

- Jensen and Klinting (1983) proposed a method to calculate the scale factor for the core. By using the same value for the hydraulic pressure gradient ( $I = \alpha \frac{(1-n)^3}{n^2} \frac{v}{gd^2} U + \beta \frac{(1-n)}{n^3} \frac{1}{gd} U|U|$ ) in the prototype and the model and by using Froude similarity for the flow velocities ( $\bar{U}^m = \frac{\bar{U}^p}{\sqrt{\lambda}}$ ), they concluded in an expression for the scale factor:

$$\lambda^c = \frac{d^p}{d^m} = \frac{\text{prototype core median grain diameter}}{\text{model core median grain diameter}} = \frac{\xi_p}{2\sqrt{\lambda}} \left\{ \left( 1 + 4\lambda^{\frac{3}{2}} * \frac{1 + \xi_p}{\xi_p^2} \right)^{\frac{1}{2}} - 1 \right\}$$

Where,

$$\xi_p = \frac{\beta}{\alpha} \frac{1}{n(1-n)^2} \frac{U^p d^p}{v}$$

and I: hydraulic pressure gradient (-); U: macroscopic filter velocity through the core material (m/s); n: porosity of the core material (-); g: gravitational acceleration (m/s<sup>2</sup>); v: kinematic viscosity (m<sup>2</sup>/s); d: characteristic grain size (m);  $\alpha, \beta$ : shape factors (-)

This approach requires the knowledge of the in time and space varying prototype flow velocity and assumes that the shape factors and the porosity are the same in the prototype and the model.

- Burcharth et al (1999) proposed to choose the diameter of the model core's material, so that the Froude scaling law is valid for the characteristic pore velocity. The method is summarised by Eggeling (2016):
  1. The shape factors ( $\alpha, \beta$ ) and the porosity (n) for the prototype and the model are chosen.
  2. Geometrical scaling of the breakwater and Froude scaling of the hydraulic parameters is performed.
  3. The prototype and model hydraulic pressure gradient are calculated based on the assumption of an exponential decrease in the core's pore pressure.
  4. The prototype and model core characteristic pore velocity,  $\bar{U}^p$  and  $\bar{U}^m$  respectively, are calculated by averaging the flow velocities in space over 6 locations and in time over half a wave period (Figure A-6) and using the Forchheimer equation for the hydraulic pressure gradients:

$$I = \alpha \frac{(1-n)^2}{n^3} \frac{v}{gD_{50}^2} U + \beta \frac{(1-n)}{n^3} \frac{1}{gD_{50}} U|U|$$

Where, I: hydraulic pressure gradient (-); U: macroscopic filter velocity through the core material (m/s); n: porosity of the core material (-); g: gravitational

acceleration ( $m/s^2$ );  $\nu$ : kinematic viscosity ( $m^2/s$ );  $D_{50}$ : median core grain size (m);  $\alpha, \beta$ : shape factors (-).

5. The target model core velocity is calculated by performing Froude scaling of the prototype core velocity, as per  $\bar{U}_{\text{target}}^m = \frac{\bar{U}^p}{\sqrt{\lambda}}$ .
  6. Steps 3-5 are repeated in an iterative procedure, during which the model median core grain size is being changed. The procedure stops when the model core velocity converges to the target of step 5.
- Vanneste et al. (2012) proposed an alternative method for core scaling. The concept of their method is very similar to Burcharth et al (1999), but the following differences exist. The distribution of the pressure decay was considered to be exponential in zone 2, but not in zone 1. This leads to a different choice of averaging locations, as can be seen in Figure A-6. Furthermore, in this research, the effect of varying hydraulic conditions and varying shape factors on the core scaling factor was studied, which was concluded to be very small.

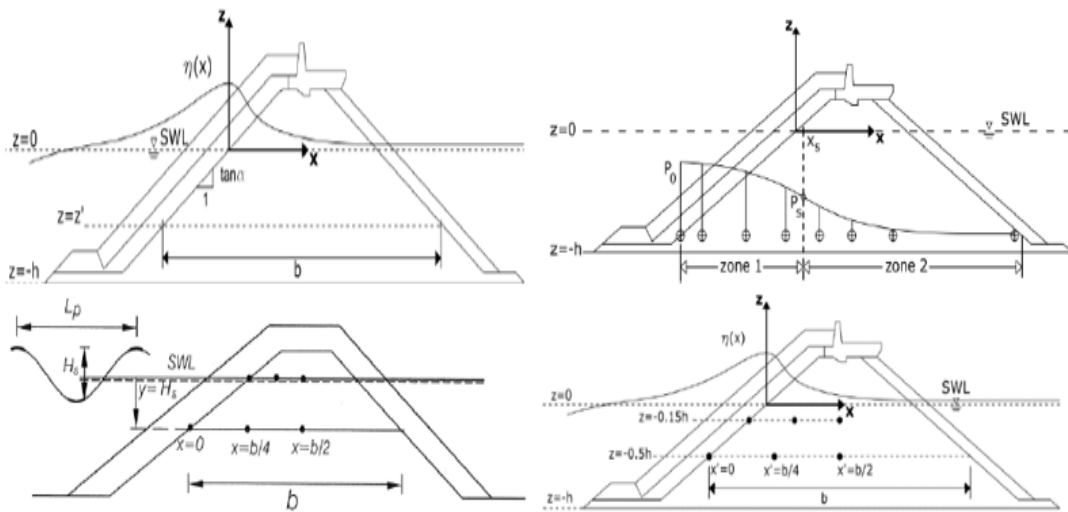


Figure A-6: Top: Pressure distribution after Burcharth (left) and Vanneste (right). Bottom: Locations for averaging of velocity after Burcharth (left) and Vanneste (right)

## Appendix B. Failure Development in Time

The failure development in time at the top armour row is presented in this section. In Figure B-1 & Figure B-2, the failure development in time for the initial and repetition tests on the single Xbloc+ is shown respectively. The cumulative number of failed crest units during each test series (percentage of total Xbloc+ crest units) is plotted in the Y axis, whereas the time of failure (made dimensionless by dividing with the total duration of the test series) is plotted in the X axis.

In Figure B-2, the vertical lines mark the end of the previous test and start of the next and the labels show the stability number of the previous test (top label for 2% steepness, bottom label for 4% steepness).

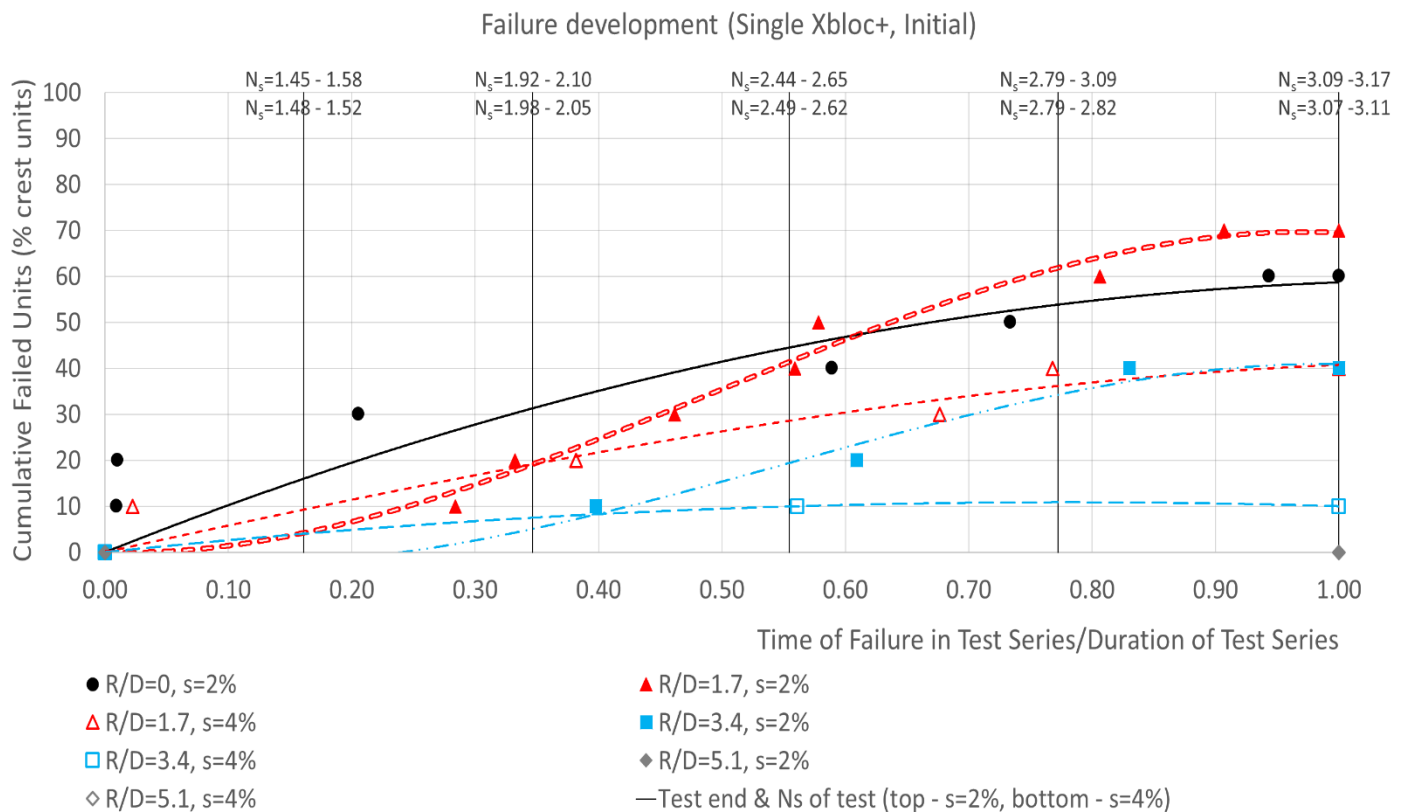


Figure B-1: Failure development in time at the Initial test series on the single Xbloc+.

In Figure B-2, the vertical lines corresponding to the end of the tests with  $H_s=0.50H_{s,d}$  (average  $N_s=1.25$ ) and  $H_s=1.00H_{s,d}$  (average  $N_s=2.46$ ) are shown. Due to the fact that the wave height of the first performed test (lowest of each test series) was different in most test series, the ratio of the end time of each test over the total duration of the test series is not the same for all test series.

Failure development (Single Xbloc+, Repetition)

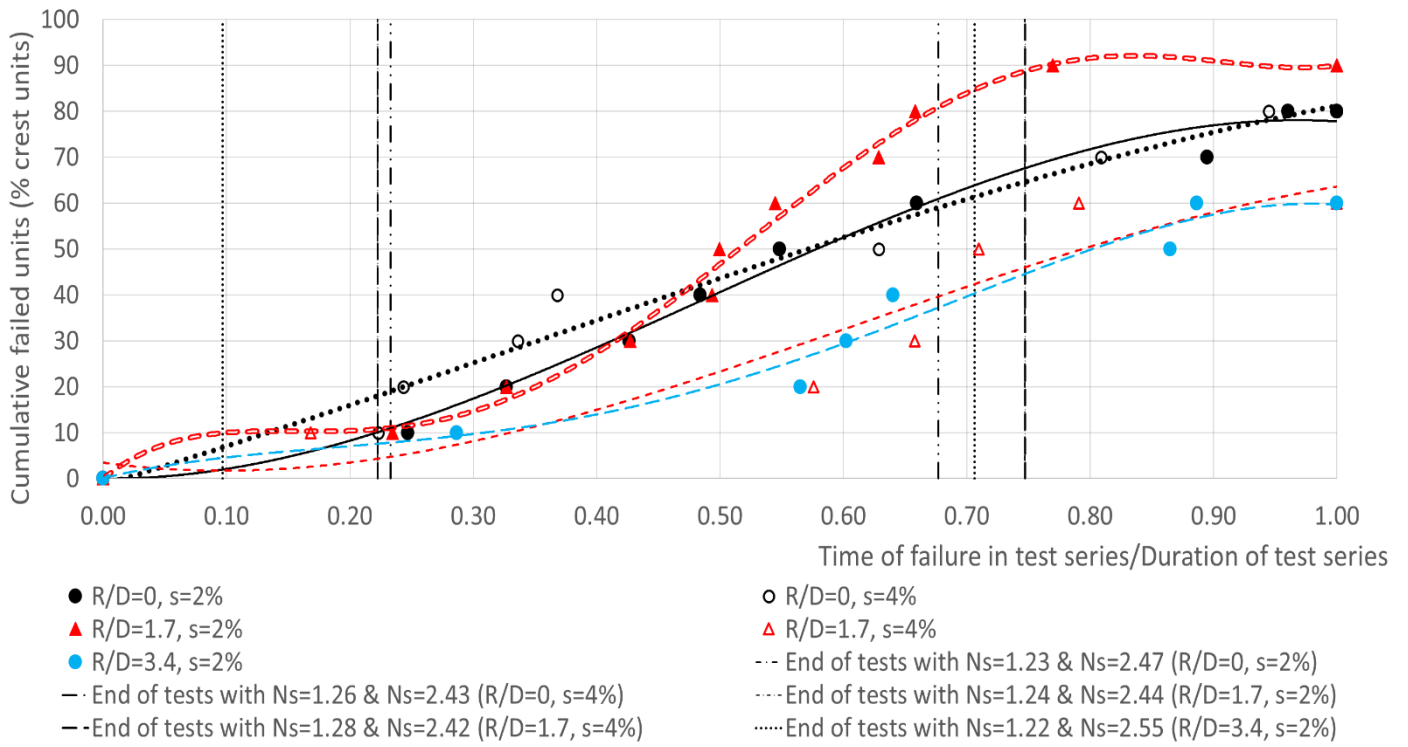


Figure B-2: Failure development in time at the Repetition test series on the single Xbloc+.



## Appendix C. Rocking Before and After Failure Units

In Figure C-1 and Figure C-2 and, the influence of the freeboard and wave steepness is shown for the rocking before and after failure units respectively.

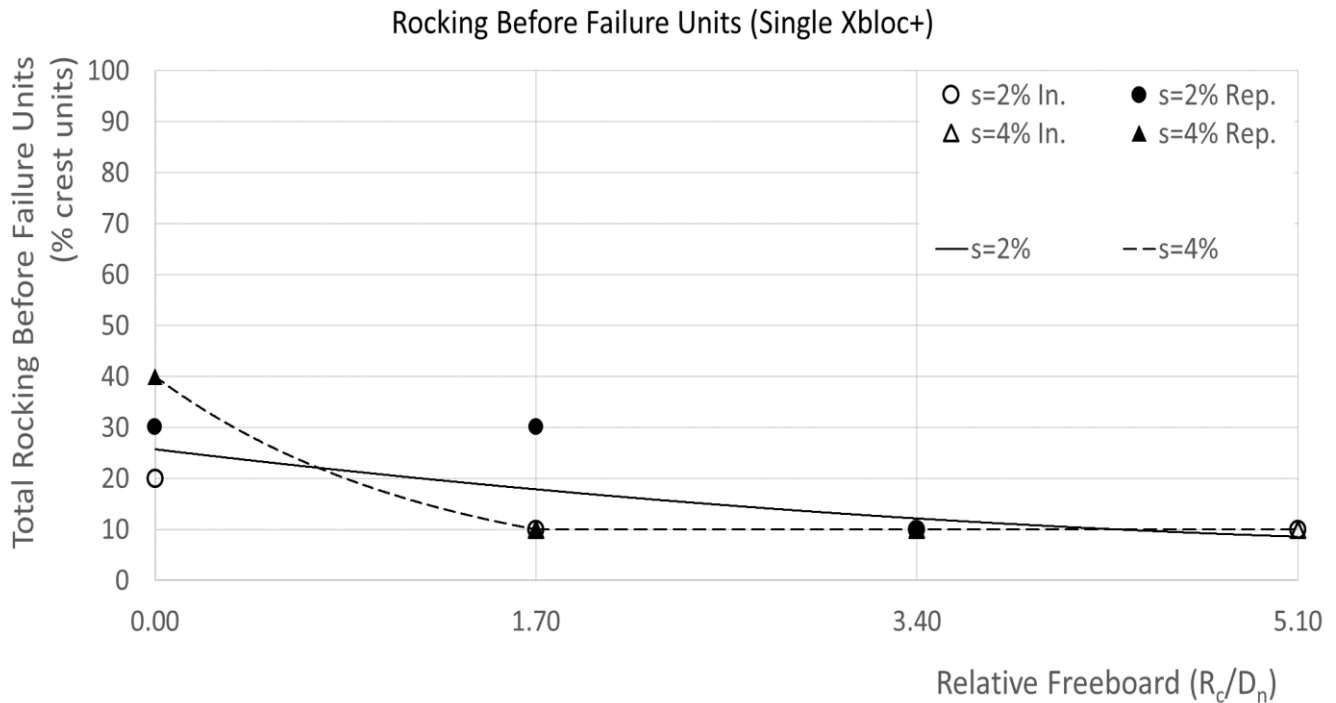


Figure C-1: Rocking Before Failure Units. Initial & Repetition Tests on the Single Xbloc+ (1<sup>st</sup> Test Set)

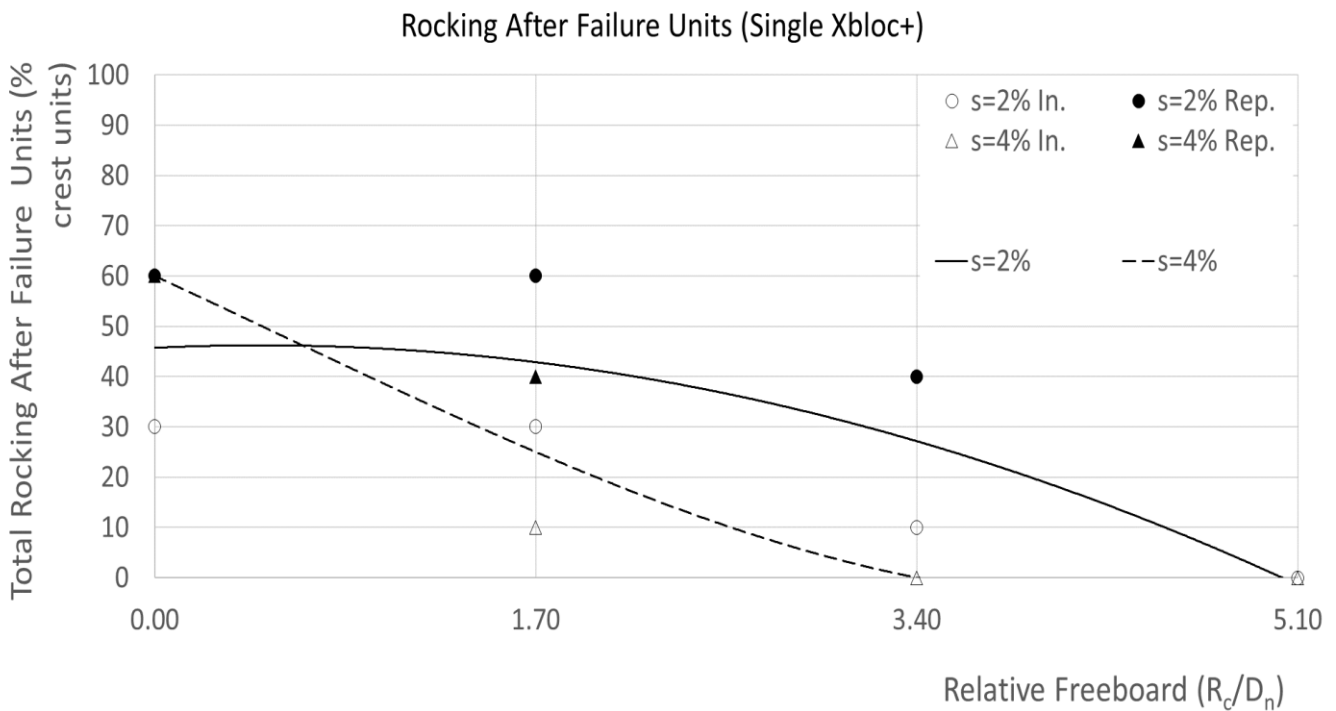


Figure C-2: Rocking After Failure Units. Initial & Repetition Tests on the Single Xbloc+ (1<sup>st</sup> Test Set)

## Appendix D. Standard Deviation (for formulas of freeboard influence on critical stability number)

The standard deviation ( $\sigma$ ), used in the formulas describing the influence of  $R_c/D_n$  on the critical stability numbers ( $N_{s,c}$ ) for failure and partial displacement (section 3.3) was calculated using the following formula:

$$\sigma = \sqrt{\frac{\sum_{i=1}^n (N_{s,c-i} - \overline{N_{s,c}})^2}{n - 1}}$$

Where,

$\sigma$ : standard deviation

$N_{s,c-i}$ : critical stability numbers from experimental data

$\overline{N_{s,c}}$ : value from equations fit to the experimental data

$n$ : number of experimental data

$$n = 4, \quad \text{for } 0 \leq \frac{R_c}{D_n} \leq 1.7 \quad \& \quad n = 6, \quad \text{for } 1.7 \leq \frac{R_c}{D_n} \leq 5.1$$

In the formula,  $n-1$  is used (Bessel's correction).

## Appendix E. Theoretical Background of the Failure Mechanisms

### E.1. Wave Loads

The wave loads can be distinguished in the following categories:

- Quasi-static wave load: “pressure under a wave increases and decreases with the wave cycle as long as the water keeps in touch with the point where the pressure is considered” (Schiereck, 2004). This load is higher, when a crest passes and lower, when a trough passes and is directed inwards (Vos, 2017). This load is more relevant in the cases of propagating waves, before they break and run-up the breakwater slope.
- Dynamic wave load (Wave impact load): “when water from a wave collides with the surface, a very short, very high impact pressure occurs” (Schiereck, 2004). This force is directed inwards (Vos, 2017).
- Wave velocities: the velocity of wave cause drag and lift forces on the armour units, during wave run-up and run-down. The wave velocity is directed upwards, during wave run-up and downwards, during wave run-down.
- Uplift: the hydrostatic pressure build up (resulting from the difference in water level inside and outside the breakwater) and the outward directed flow velocities inside the breakwater cause an outward directed force, the seepage force ( $F_s$ ), which pushes the units out of the armour layer. This force is the largest at the point of the maximum run-down (Hald, 1998), so it can be considered of lesser importance for the loading on the crest units, since the governing situation is wave run-up.

### E.2. Wave Run-up

The relevant parameters to wave run-up are schematised in Figure E-1. Subsequently, the equations from literature (EurOtop (2016), Schuttrumpf and van Gent (2003)) and the values applicable during the physical modelling for the Xbloc+ crest elements are presented.

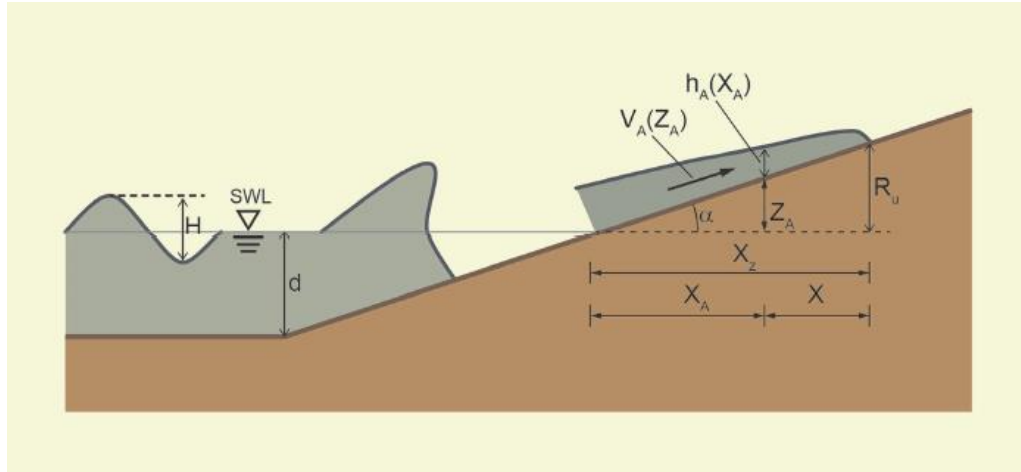


Figure E-1: Wave run-up velocity (EurOtop, 2016)

The run-up height ( $R_u$ ) is given by:

$$\frac{R_{u2\%}}{H_{m0}} = 1.65 * \gamma_b * \gamma_f * \gamma_\beta * \xi_{m-1,0}$$

With a maximum of

$$\frac{R_{u2\%}}{H_{m0}} = 1.00 * \gamma_{fsurging} * \gamma_\beta * \left(4.0 - \frac{1.5}{\sqrt{\gamma_b * \xi_{m-1,0}}}\right)$$

Where

$R_{u2\%}$ : run – up height exceeded by 2% of the up – rushing waves (m)

$$\gamma_{fsurging} = \gamma_f + \frac{(\xi_{m-1,0} - 1.8)(1 - \gamma_f)}{8.2} \quad \text{for} \quad \xi_{m-1,0} \leq 10$$

$\gamma_f$  = roughness factor (0.45 for Xbloc +)

$\gamma_b$  = reduction factor for berm (1.00 – no berm)

$\gamma_\beta$  = reduction factor for oblique wave action (1.00 – waves perpendicular)

$$\xi_{m-1,0} = \frac{\tan \alpha}{\sqrt{s_{m-1,0}}} \quad (\text{breaker parameter – lower than 10 in all tests})$$

$\tan \alpha$  = breakwater slope (3:4)

$$s_{m-1,0} = \frac{2\pi H_{m0}}{g T_{m-1,0}^2}$$

$$T_{m-1,0} = \frac{T_p}{1.1} \quad (\text{s}) \quad (\text{for conventional single peaked spectra})$$

$$T_p = \sqrt{\frac{2\pi H_{m0}}{g s_{op}}}$$

$$s_{op} = \text{wave steepness (corresponding to peak period } (T_p) \text{ and } H_{m0}) = \frac{2\pi H_{m0}}{g T_p^2}$$

The maximum run-up velocity at a specific location on the seaward breakwater slope is given by (Schüttrumpf and Van Gent (2004)):

$$\frac{u_{2\%}}{\sqrt{gH_s}} = c'_{\alpha,u} \left( \frac{R_{u2\%} - z}{\gamma_f H_s} \right)^{0.5}$$

Where

$u_{2\%}$ : wave run – up velocity exceeded by 2% of the incoming waves

$z$ : vertical position on the seaward slope with respect to the still water level (SWL)

$H_s$ : significant wave height (m)

$\gamma_f$  = roughness factor (0.45 for Xbloc +)

$g$  = acceleration of gravity ( $\frac{m}{s^2}$ )

$c'_{\alpha,u}$ : empirical coefficient

Different values for the empirical coefficient have been proposed by different researchers (Table E-1). The empirical coefficient does not influence the comparison of the effect of the parameters on run-up, since it is constant during all tests, therefore,  $c'_{\alpha,u}$  is chosen equal to 1.37.

	Schüttrumpf (2002)	Van Gent (2002)
$c'_{\alpha,u}$	1.37	1.30

Table E-1: Empirical coefficients for the equations of wave run-up velocity and flow thickness

The run-up height is given by:

$$R_{u2\%} = 0.51 \frac{H_{m0}}{\sqrt{s_{op}}}$$

With a maximum of

$$R_{u2\%} = H_{m0} \left( 1.28 - 0.59 * s_{op}^{0.25} + \frac{0.2}{s_{op}^{0.5}} - \frac{0.09}{s_{op}^{0.25}} \right)$$

The run-up velocity is given by:

$$u_{A,2\%} = 6.40(R_{u2\%} - R_c)^{0.5}$$

## Appendix F. Wave Parameters

The theoretical wave parameters calculated before testing and the generated wave parameters during testing are presented in this Appendix.

Table F-1: Theoretical Wave Parameters

Test No.	$H_{m0}$ (m)	% $H_{m0,d}$	$S_{op}$ (-)	$T_p$ (s)	$R_c/H_{m0}$	Test duration (min/sec)
<u>Test series 1.1.1 Initial (single element, <math>s_{op}=2\%</math>, <math>R_c/H_{m0,d}=0.0</math> (<math>h=0.635m</math>))</u>						
1	0.0595	60	0.02	1.38	0.00	23 min 0 sec
2	0.0793	80	0.02	1.59	0.00	26 min 34 sec
3	0.0991	100	0.02	1.78	0.00	29 min 42 sec
4	0.1090	110	0.02	1.87	0.00	31 min 9 sec
5	0.1190	120	0.02	1.95	0.00	32 min 32 sec
<u>Test series 1.2.1 Initial (single element, <math>s_{op}=4\%</math>, <math>R_c/H_{m0,d}=0.0</math> (<math>h=0.635m</math>))</u>						
1	0.0595	60	0.04	0.98	0.00	16 min 16 sec
2	0.0793	80	0.04	1.13	0.00	18 min 47 sec
3	0.0991	100	0.04	1.26	0.00	21 min 0 sec
4	0.1090	110	0.04	1.32	0.00	22 min 1 sec
5	0.1190	120	0.04	1.38	0.00	23 min 0 sec
<u>Test series 1.1.2 Initial (single element, <math>s_{op}=2\%</math>, <math>R_c/H_{m0,d}=0.5</math> (<math>h=0.585m</math>))</u>						
1	0.0595	60	0.02	1.38	0.83	23 min 0 sec
2	0.0793	80	0.02	1.59	0.63	26 min 34 sec
3	0.0991	100	0.02	1.78	0.50	29 min 42 sec
4	0.1090	110	0.02	1.87	0.45	31 min 9 sec
<u>Test series 1.2.2 Initial (single element, <math>s_{op}=4\%</math>, <math>R_c/H_{m0,d}=0.5</math> (<math>h=0.585m</math>))</u>						
1	0.0595	60	0.04	0.98	0.83	16 min 16 sec
2	0.0793	80	0.04	1.13	0.63	18 min 47 sec
3	0.0991	100	0.04	1.26	0.50	21 min 0 sec
4	0.1090	110	0.04	1.32	0.45	22 min 1 sec
5	0.1190	120	0.04	1.38	0.42	23 min 0 sec
<u>Test series 1.1.3 Initial (single element, <math>s_{op}=2\%</math>, <math>R_c/H_{m0,d}=1.0</math> (<math>h=0.536m</math>))</u>						
1	0.0595	60	0.02	1.38	1.67	23 min 0 sec
2	0.0793	80	0.02	1.59	1.25	26 min 34 sec
3	0.0991	100	0.02	1.78	1.00	29 min 42 sec
4	0.1090	110	0.02	1.87	0.91	31 min 9 sec
5	0.1190	120	0.02	1.95	0.83	32 min 32 sec
<u>Test series 1.2.3 Initial (single element, <math>s_{op}=4\%</math>, <math>R_c/H_{m0,d}=1.0</math> (<math>h=0.536m</math>))</u>						
1	0.0595	60	0.04	0.98	1.67	16 min 16 sec
2	0.0793	80	0.04	1.13	1.25	18 min 47 sec
3	0.0991	100	0.04	1.26	1.00	21 min 0 sec
4	0.1090	110	0.04	1.32	0.91	22 min 1 sec
5	0.1190	120	0.04	1.38	0.83	23 min 0 sec

Test series 1.1.4 Initial (single element, $s_{op}=2\%$ , $R_c/H_{m0,d}=1.5$ ( $h=0.486m$ ))						
1	0.0595	60	0.02	1.38	2.50	23 min 0 sec
2	0.0793	80	0.02	1.59	1.88	26 min 34 sec
3	0.0991	100	0.02	1.78	1.50	29 min 42 sec
4	0.1090	110	0.02	1.87	1.36	31 min 9 sec
Test series 1.2.4 Initial (single element, $s_{op}=4\%$ , $R_c/H_{m0,d}=1.5$ ( $h=0.486m$ ))						
1	0.0595	60	0.04	0.98	2.50	16 min 16 sec
2	0.0793	80	0.04	1.13	1.88	18 min 47 sec
3	0.0991	100	0.04	1.26	1.50	21 min 0 sec
4	0.1090	110	0.04	1.32	1.36	22 min 1 sec
5	0.1190	120	0.04	1.38	1.25	23 min 0 sec
Test series 1.1.1 Repetition (single element, $s_{op}=2\%$ , $R_c/H_{m0,d}=0.0$ ( $h=0.635m$ ))						
1	0.0297	30	0.02	0.98	0.00	16 min 16 sec
2	0.0397	40	0.02	1.13	0.00	18 min 47 sec
3	0.0496	50	0.02	1.26	0.00	21 min 0 sec
4	0.0595	60	0.02	1.38	0.00	23 min 0 sec
5	0.0694	70	0.02	1.49	0.00	24 min 51 sec
6	0.0793	80	0.02	1.59	0.00	26 min 34 sec
7	0.0892	90	0.02	1.69	0.00	28 min 10 sec
8	0.0991	100	0.02	1.78	0.00	29 min 42 sec
9	0.1090	110	0.02	1.87	0.00	31 min 9 sec
10	0.1190	120	0.02	1.95	0.00	32 min 32 sec
Test series 1.2.1 Repetition (single element, $s_{op}=4\%$ , $R_c/H_{m0,d}=0.0$ ( $h=0.635m$ ))						
1	0.0198	20	0.04	0.56	0.00	9 min 23 sec
2	0.0297	30	0.04	0.69	0.00	11 min 30 sec
3	0.0397	40	0.04	0.80	0.00	13 min 17 sec
4	0.0496	50	0.04	0.89	0.00	14 min 51 sec
5	0.0595	60	0.04	0.98	0.00	16 min 16 sec
6	0.0694	70	0.04	1.05	0.00	17 min 34 sec
7	0.0793	80	0.04	1.13	0.00	18 min 47 sec
8	0.0892	90	0.04	1.20	0.00	19 min 55 sec
9	0.0991	100	0.04	1.26	0.00	21 min 0 sec
10	0.1090	110	0.04	1.32	0.00	22 min 1 sec
11	0.1190	120	0.04	1.38	0.00	23 min 0 sec
Test series 1.1.2 Repetition (single element, $s_{op}=2\%$ , $R_c/H_{m0,d}=0.5$ ( $h=0.585m$ ))						
1	0.0297	30	0.02	0.98	1.67	16 min 16 sec
2	0.0397	40	0.02	1.13	1.25	18 min 47 sec
3	0.0496	50	0.02	1.26	1.00	21 min 0 sec
4	0.0595	60	0.02	1.38	0.83	23 min 0 sec
5	0.0694	70	0.02	1.49	0.71	24 min 51 sec
6	0.0793	80	0.02	1.59	0.63	26 min 34 sec
7	0.0892	90	0.02	1.69	0.56	28 min 10 sec
8	0.0991	100	0.02	1.78	0.50	29 min 42 sec
9	0.1090	110	0.02	1.87	0.45	31 min 9 sec

10	0.1190	120	0.02	1.95	0.42	32 min 32 sec
<u>Test series 1.2.2 Repetition (single element, <math>s_{op}=4\%</math>, <math>R_c/H_{m0,d}=0.5</math> (<math>h=0.585m</math>))</u>						
1	0.0297	30	0.04	0.69	1.67	11 min 30 sec
2	0.0397	40	0.04	0.80	1.25	13 min 17 sec
3	0.0496	50	0.04	0.89	1.00	14 min 51 sec
4	0.0595	60	0.04	0.98	0.83	16 min 16 sec
5	0.0694	70	0.04	1.05	0.71	17 min 34 sec
6	0.0793	80	0.04	1.13	0.63	18 min 47 sec
7	0.0892	90	0.04	1.20	0.56	19 min 55 sec
8	0.0991	100	0.04	1.26	0.50	21 min 0 sec
9	0.1090	110	0.04	1.32	0.45	22 min 1 sec
10	0.1190	120	0.04	1.38	0.42	23 min 0 sec
<u>Test series 1.1.3 Repetition (single element, <math>s_{op}=2\%</math>, <math>R_c/H_{m0,d}=1.0</math> (<math>h=0.536m</math>))</u>						
1	0.0496	50	0.02	1.26	2.00	21 min 0 sec
2	0.0595	60	0.02	1.38	1.67	23 min 0 sec
3	0.0694	70	0.02	1.49	1.43	24 min 51 sec
4	0.0793	80	0.02	1.59	1.25	26 min 34 sec
5	0.0892	90	0.02	1.69	1.11	28 min 10 sec
6	0.0991	100	0.02	1.78	1.00	29 min 42 sec
7	0.1090	110	0.02	1.87	0.91	31 min 9 sec
8	0.1190	120	0.02	1.95	0.83	32 min 32 sec
<u>Test series 2.2.1 (Orientation with Tail upwards, <math>s_{op}=4\%</math>, <math>R_c/H_{m0,d}=0.0</math> (<math>h=0.635m</math>))</u>						
1	0.0595	60	0.04	0.98	0.00	16 min 16 sec
<u>Test series 2.2.1 (Orientation with Nose upwards, <math>s_{op}=4\%</math>, <math>R_c/H_{m0,d}=0.0</math> (<math>h=0.635m</math>))</u>						
1	0.0595	60	0.04	0.98	0.00	16 min 16 sec
<u>Test series 3.2.1 (Configuration with Xblocs A, <math>s_{op}=4\%</math>, <math>R_c/H_{m0,d}=0.0</math> (<math>h=0.635m</math>))</u>						
1	0.0595	60	0.04	0.98	0.00	16 min 16 sec
<u>Test series 4.2.1 (Configuration with Xblocs B, <math>s_{op}=4\%</math>, <math>R_c/H_{m0,d}=0.0</math> (<math>h=0.635m</math>))</u>						
1	0.0595	60	0.04	0.98	0.00	16 min 16 sec
2	0.0793	80	0.04	1.13	0.00	18 min 47 sec
3	0.0991	100	0.04	1.26	0.00	21 min 0 sec
4	0.1090	110	0.04	1.32	0.00	22 min 1 sec
5	0.1190	120	0.04	1.38	0.00	23 min 0 sec
<u>Test series 5.2.1 (Configuration with Xblocs &amp; Crown Wall, <math>s_{op}=4\%</math>, <math>R_c/H_{m0,d}=0.0</math> (<math>h=0.635m</math>))</u>						
1	0.0595	60	0.04	0.98	0.00	16 min 16 sec
2	0.0793	80	0.04	1.13	0.00	18 min 47 sec
3	0.0991	100	0.04	1.26	0.00	21 min 0 sec
4	0.1090	110	0.04	1.32	0.00	22 min 1 sec
5	0.1190	120	0.04	1.38	0.00	23 min 0 sec
6	0.1388	140	0.04	1.49	0.00	24 min 51 sec
<u>Test series 6.2.1 (Configuration with Underlayer filling &amp; Crown Wall, <math>s_{op}=4\%</math>, <math>R_c/H_{m0,d}=0.0</math> (<math>h=0.635m</math>))</u>						
1	0.0595	60	0.04	0.98	0.00	16 min 16 sec
2	0.0793	80	0.04	1.13	0.00	18 min 47 sec
3	0.0991	100	0.04	1.26	0.00	21 min 0 sec



4	0.1090	110	0.04	1.32	0.00	22 min 1 sec
5	0.1190	120	0.04	1.38	0.00	23 min 0 sec
6	0.1388	140	0.04	1.49	0.00	24 min 51 sec
<b>Test series 7.2.1 (Configuration with Underlayer filling at top of crest, <math>s_{op}=4\%</math>, <math>R_c/H_{m0,d}=0.0</math> (<math>h=0.635m</math>))</b>						
1	0.0595	60	0.04	0.98	0.00	16 min 16 sec
2	0.0793	80	0.04	1.13	0.00	18 min 47 sec
3	0.0991	100	0.04	1.26	0.00	21 min 0 sec
4	0.1090	110	0.04	1.32	0.00	22 min 1 sec
<b>Test series 6.1.1 (Configuration with Underlayer filling &amp; Crown Wall, <math>s_{op}=2\%</math>, <math>R_c/H_{m0,d}=0.0</math> (<math>h=0.635m</math>))</b>						
1	0.0595	60	0.02	1.38	0.00	23 min 0 sec
2	0.0793	80	0.02	1.59	0.00	26 min 34 sec
3	0.0991	100	0.02	1.78	0.00	29 min 42 sec
4	0.1090	110	0.02	1.87	0.00	31 min 9 sec
5	0.1190	120	0.02	1.95	0.00	32 min 32 sec
6	0.1388	140	0.02	2.11	0.00	35 min 8 sec
<b>Test series 6.1.2 (Configuration with Underlayer filling &amp; Crown Wall, <math>s_{op}=2\%</math>, <math>R_c/H_{m0,d}=0.5</math> (<math>h=0.585m</math>))</b>						
1	0.0595	60	0.02	1.38	0.83	23 min 0 sec
2	0.0793	80	0.02	1.59	0.63	26 min 34 sec
3	0.0991	100	0.02	1.78	0.50	29 min 42 sec
4	0.1190	120	0.02	1.95	0.42	32 min 32 sec
<b>Test series 6.2.2 (Configuration with Underlayer filling &amp; Crown Wall, <math>s_{op}=4\%</math>, <math>R_c/H_{m0,d}=0.5</math> (<math>h=0.585m</math>))</b>						
1	0.0595	60	0.04	0.98	0.83	16 min 16 sec
2	0.0793	80	0.04	1.13	0.63	18 min 47 sec
3	0.0991	100	0.04	1.26	0.50	21 min 0 sec
4	0.1190	120	0.04	1.38	0.42	23 min 0 sec
5	0.1388	140	0.04	1.49	0.36	24 min 51 sec

Table F-2: Generated Wave Parameters during the Experiments

Test No.	H <sub>mo</sub> (m)	Waves (%H <sub>mo,d,generated</sub> )	Waves (%H <sub>mo,d,theoretical</sub> )	S <sub>op</sub> (-)	T <sub>p</sub> (s)
<u>Test series 1.1.1 Initial (single element, s<sub>op</sub>=2%, R<sub>c</sub>/H<sub>m0,d</sub>=0.0 (h=0.635m))</u>					
1	0.0627	60	63	0.0216	1.36
2	0.0834	79	84	0.0219	1.56
3	0.1050	100	106	0.0213	1.78
4	0.1125	107	113	0.0215	1.83
5	0.1257	120	127	0.0214	1.94
<u>Test series 1.2.1 Initial (single element, s<sub>op</sub>=4%, R<sub>c</sub>/H<sub>m0,d</sub>=0.0 (h=0.635m))</u>					
1	0.0598	58	60	0.0408	0.97
2	0.0815	78	82	0.0414	1.12
3	0.1038	100	105	0.0422	1.26
4	0.1114	107	112	0.0418	1.31
5	0.1232	119	124	0.0425	1.36
<u>Test series 1.1.2 Initial (single element, s<sub>op</sub>=2%, R<sub>c</sub>/H<sub>m0,d</sub>=0.5 (h=0.585m))</u>					
1	0.0575	59	58	0.0198	1.36
2	0.0761	78	77	0.0210	1.52
3	0.0969	100	98	0.0186	1.83
4	0.1224	126	123	0.0234	1.83
<u>Test series 1.2.2 Initial (single element, s<sub>op</sub>=4%, R<sub>c</sub>/H<sub>m0,d</sub>=0.5 (h=0.585m))</u>					
1	0.0586	59	59	0.0423	0.94
2	0.0787	80	79	0.0428	1.09
3	0.0989	100	100	0.0402	1.26
4	0.1108	112	112	0.0399	1.33
5	0.1216	123	123	0.0420	1.36
<u>Test series 1.1.3 Initial (single element, s<sub>op</sub>=2%, R<sub>c</sub>/H<sub>m0,d</sub>=1.0 (h=0.536m))</u>					
1	0.0590	59	60	0.0204	1.36
2	0.0796	79	80	0.0209	1.56
3	0.1001	100	101	0.0203	1.78
4	0.1108	111	112	0.0200	1.88
5	0.1229	123	124	0.0209	1.94
<u>Test series 1.2.3 Initial (single element, s<sub>op</sub>=4%, R<sub>c</sub>/H<sub>m0,d</sub>=1.0 (h=0.536m))</u>					
1	0.0601	60	61	0.0397	0.98
2	0.0783	79	79	0.0370	1.16
3	0.0996	100	100	0.0405	1.26
4	0.1117	112	90	0.0403	1.33
5	0.1217	122	100	0.0420	1.36
<u>Test series 1.1.4 Initial (single element, s<sub>op</sub>=2%, R<sub>c</sub>/H<sub>m0,d</sub>=1.5 (h=0.486m))</u>					
1	0.0619	58	62	0.0214	1.36
2	0.0858	80	87	0.0225	1.56
3	0.1066	100	108	0.0216	1.78
4	0.1178	111	119	0.0226	1.83

Test series 1.2.4 Initial (single element, $s_{op}=4\%$ , $R_c/H_{m0,d}=1.5$ ( $h=0.486m$ ))					
1	0.0623	62	63	0.0412	0.98
2	0.0789	79	80	0.0373	1.16
3	0.0999	100	101	0.0406	1.26
4	0.1209	121	122	0.0417	1.36
5	0.1320	132	133	0.0456	1.36
Test series 1.1.1 Repetition (single element, $s_{op}=2\%$ , $R_c/H_{m0,d}=0.0$ ( $h=0.635m$ ))					
1	0.0292	30	29	0.0193	0.98
2	0.0388	40	39	0.0183	1.16
3	0.0489	50	49	0.0199	1.26
4	0.0585	60	59	0.0211	1.33
5	0.0700	72	71	0.0202	1.49
6	0.0824	84	83	0.0217	1.56
7	0.0877	90	88	0.0208	1.64
8	0.0978	100	99	0.0198	1.78
9	0.1080	110	109	0.0195	1.88
10	0.1195	122	121	0.0204	1.94
Test series 1.2.1 Repetition (single element, $s_{op}=4\%$ , $R_c/H_{m0,d}=0.0$ ( $h=0.635m$ ))					
1	0.0195	20	20	0.0275	0.674
2	0.0292	30	29	0.0395	0.688
3	0.0390	40	39	0.0371	0.821
4	0.0499	52	50	0.0394	0.901
5	0.0594	62	60	0.0392	0.985
6	0.0669	69	67	0.0364	1.085
7	0.0755	78	76	0.0357	1.164
8	0.0893	93	90	0.0377	1.231
9	0.0965	100	97	0.0392	1.255
10	0.1082	112	109	0.0374	1.362
11	0.1202	125	121	0.0433	1.333
12	0.1230	128	124	0.0443	1.333
Test series 1.1.2 Repetition (single element, $s_{op}=2\%$ , $R_c/H_{m0,d}=0.5$ ( $h=0.585m$ ))					
1	0.0287	30	29	0.0190	0.985
2	0.0386	40	39	0.0182	1.164
3	0.0491	51	50	0.0200	1.255
4	0.0596	62	60	0.0215	1.333
5	0.0709	73	72	0.0205	1.488
6	0.0819	85	83	0.0215	1.561
7	0.0906	94	91	0.0194	1.730
8	0.0968	100	98	0.0196	1.778
9	0.1106	114	112	0.0200	1.882
10	0.1255	130	127	0.0214	1.939
Test series 1.2.2 Repetition (single element, $s_{op}=4\%$ , $R_c/H_{m0,d}=0.5$ ( $h=0.585m$ ))					
1	0.0300	31	30	0.0405	0.688
2	0.0402	42	41	0.0383	0.821

3	0.0509	53	51	0.0401	0.901
4	0.0585	61	59	0.0386	0.985
5	0.0671	70	68	0.0365	1.085
6	0.0776	81	78	0.0367	1.164
7	0.0908	95	92	0.0398	1.208
8	0.0958	100	97	0.0390	1.255
9	0.1055	110	106	0.0364	1.362
10	0.1178	123	119	0.0425	1.333
<u>Test series 1.1.3 Repetition (single element, <math>s_{op}=2\%</math>, <math>R_c/H_{m0,d}=1.5</math> (<math>h=0.536m</math>))</u>					
1	0.0485	48	49	0.0197	1.255
2	0.0590	58	60	0.0204	1.362
3	0.0698	69	70	0.0202	1.488
4	0.0816	81	82	0.0225	1.524
5	0.0901	89	91	0.0193	1.730
6	0.1010	100	102	0.0205	1.778
7	0.1119	111	113	0.0202	1.882
8	0.1246	123	126	0.0212	1.939
<u>Test series 2.2.1 (Orientation with Tail upwards, <math>s_{op}=4\%</math>, <math>R_c/H_{m0,d}=0.0</math> (<math>h=0.635m</math>))</u>					
1	0.0579	-	58	0.0382	0.985
<u>Test series 2.2.1 (Orientation with Nose upwards, <math>s_{op}=4\%</math>, <math>R_c/H_{m0,d}=0.0</math> (<math>h=0.635m</math>))</u>					
1	0.0579	-	58	0.0382	0.985
<u>Test series 3.2.1 (Configuration with Xbloccs A, <math>s_{op}=4\%</math>, <math>R_c/H_{m0,d}=0.0</math> (<math>h=0.635m</math>))</u>					
1	0.0576	-	58	0.0381	0.985
<u>Test series 4.2.1 (Configuration with Xbloccs B, <math>s_{op}=4\%</math>, <math>R_c/H_{m0,d}=0.0</math> (<math>h=0.635m</math>))</u>					
1	0.0584	59	59	0.0386	0.985
2	0.0772	79	78	0.0379	1.143
3	0.0982	100	99	0.0399	1.255
4	0.1092	111	110	0.0410	1.306
5	0.1206	123	122	0.0435	1.333
<u>Test series 5.2.1 (Configuration with Xbloccs &amp; Crown Wall, <math>s_{op}=4\%</math>, <math>R_c/H_{m0,d}=0.0</math> (<math>h=0.635m</math>))</u>					
1	0.0589	60	59	0.0389	0.985
2	0.0775	79	78	0.0380	1.143
3	0.0982	100	99	0.0399	1.255
4	0.1087	111	110	0.0408	1.306
5	0.1195	122	121	0.0431	1.333
6	0.1405	143	142	0.0406	1.488
<u>Test series 6.2.1 (Configuration with Underlayer filling &amp; Crown Wall, <math>s_{op}=4\%</math>, <math>R_c/H_{m0,d}=0.0</math> (<math>h=0.635m</math>))</u>					
1	0.0585	60	59	0.0386	0.985
2	0.0775	79	78	0.0380	1.143
3	0.0979	100	99	0.0398	1.255
4	0.1077	110	109	0.0404	1.306
5	0.1188	121	120	0.0428	1.333
6	0.1394	142	141	0.0403	1.488

Test series 7.2.1 (Configuration with Underlayer filling at top of crest, $s_{op}=4\%$ , $R_c/H_{m0,d}=0.0$ ( $h=0.635m$ ))					
1	0.0590	60	60	0.0390	0.985
2	0.0780	79	79	0.0382	1.143
3	0.0990	100	100	0.0403	1.255
4	0.1091	110	110	0.0410	1.306
Test series 6.1.1 (Configuration with Underlayer filling & Crown Wall, $s_{op}=2\%$ , $R_c/H_{m0,d}=0.0$ ( $h=0.635m$ ))					
1	0.0609	60	61	0.0220	1.333
2	0.0821	81	83	0.0216	1.561
3	0.1009	100	102	0.0204	1.778
4	0.1104	109	111	0.0211	1.829
5	0.1209	120	122	0.0206	1.939
6	0.1382	137	139	0.0208	2.065
Test series 6.1.2 (Configuration with Underlayer filling & Crown Wall, $s_{op}=2\%$ , $R_c/H_{m0,d}=0.5$ ( $h=0.585m$ ))					
1	0.0599	56	60	0.0216	1.333
2	0.0814	76	82	0.0214	1.561
3	0.1066	100	108	0.0216	1.778
4	0.1340	126	135	0.0228	1.939
Test series 6.2.2 (Configuration with Underlayer filling & Crown Wall, $s_{op}=4\%$ , $R_c/H_{m0,d}=0.5$ ( $h=0.585m$ ))					
1	0.0588	60	59	0.0388	0.985
2	0.0791	80	80	0.0374	1.164
3	0.0985	100	99	0.0401	1.255
4	0.1200	122	121	0.0433	1.333
5	0.1407	143	142	0.0407	1.488

## Appendix G. Observations during the Experiments

The observations made and noted down during the experiments are presented in this Appendix.

Test	Time (hr:min:sec)	Observations
<b>Initial tests on the single Xbloc+ (1<sup>st</sup> test set)</b>		
1.1.1 - 60%	00:00:55	Unit 2R moves backwards, more at right wing.
	00:01:08	Unit 5R starts <b>rocking</b> .
	00:01:19	Unit 3L <b>rocks</b> once, then rotates and <i>fails</i>
	00:01:26	Unit 5R stops <b>rocking</b> and <i>fails</i> . 5R <b>rocked</b> approx. 5 times
	00:11:32	By this time, units 2L, 4L, 5L, 2R, 4R have slid backwards considerably, but still maintaining contact with units underneath. Units 1R, 3R have also slid backwards, but only a little. Unit 1L has not moved.
	00:16:48	Observations made on 0:11:32 still valid.
	00:23:00	End test 60%
1.1.1 - 80%	00:29:21	4L <i>fails</i> . It rotates and loses contact at the nose and right wing.
	00:32:16	4L, while having already failed, starts <b>rocking</b> .
	00:32:31	4L, <b>stops rocking</b> , when it finds a new position on the crest. Subsequently, it gets displaced even more. 4L <b>rocked</b> approx. 11 times for 15 s.
	00:40:55	2nd row of Xbloc+'s from top does not show signs of damage.
	00:49:34	End test 80%
1.1.1 - 100%	00:52:53	Unit 4L moved while having already failed and found a new position on crest.
	00:59:41	Unit 3L (already failed) <b>rocked</b> 2 times and stopped.
	01:00:01	Unit 3L (already failed) <b>rocked</b> again 2 times and stopped.
	01:00:31	Unit 3L (already failed) <b>rocked</b> again 3 times for 10 s and stopped.
	01:01:11	Unit 3L <b>is rocking</b> many times and keeps rocking during the passing of a train of high waves.
	01:02:08	Unit 3L <b>stops rocking</b> , when it finds new position. It has rocked approx. 17 times.
	01:04:41	Unit 3L does not rock, although a train of high waves passes.
	01:15:11	Unit 4L from 2nd row of Xbloc+'s from top slid backwards
01:19:16	End test 100%	
1.1.1 - 110%	01:24:13	Unit 2L <i>failed</i> by losing contact at right side
	01:40:30	Unit 4L is <b>rocking</b> continuously for approx. 20 s, when already failed.
	01:40:50	Unit 4L <b>stops rocking</b> , after having rocked for approx. 8 times.
	01:44:55	Unit 2R <i>fails</i> .
	01:50:25	End test 110%
1.1.1 - 120%	01:58:11	No changes observed since start of test (at 1:48:47)
	01:59:01	Unit 3L <b>rocked</b> 2 times (while already failed)
	02:14:53	Unit 1R <i>fails</i> (it maintains contact only a little at left side, whereas nose and right wing are lifted). Unit 2R (already failed) <b>starts rocking</b> .
	02:15:20	Unit 2R <b>stops rocking</b> after approx. 30 s of rocking (during pass of high waves train)

	02:16:44	Unit 2R <b>starts rocking</b> (under the attack of lower waves than previously) and rocks continuously for approx. 2-3 min
	02:22:57	End of test 120%. End test series.
Test	Time (hr:min:sec)	Observations
1.2.1 - 60%	00:00:56	Unit <u>1R fails</u> after sliding more and more backwards during consecutive waves
	00:01:04	Unit <u>5L fails</u> after successive rotational motions
	00:02:11	Unit <u>5R fails</u>
	00:02:16	Unit 4L slides back sideways
	00:03:56	Unit <u>4L fails</u> , by losing contact under right wing
	00:16:16	End test 60%
1.2.1 - 80%	00:20:11	Unit 1L has not moved
	00:21:56	Unit <u>3L fails</u> with nose tilted downwards and tail tilted upwards.
	00:28:11	Units 4L, 5L, 6L from 2nd row of Xbloc+'s have slid backwards, especially unit 5L
	00:29:16	Unit <u>3R fails</u> sideways by losing contact at right wing, after having moved backwards sideways
	00:29:26	Unit <u>4R fails</u> sideways by losing contact at left wing, after having moved backwards sideways
	00:33:16	Unit <u>2L fails</u> sideways by losing contact at right wing, after having moved backwards sideways
	00:33:56	Failed units 5L, 6L remain slanted with nose upwards; 3L with nose downwards
	00:35:03	End test 80%
1.2.1 - 100%	00:35:43	Unit 1R <b>rocked</b> once, while already failed.
	00:36:02	Unit 1R <b>rocked</b> again
	00:37:22	Unit 1R <b>rocked</b> again
	00:39:30	Unit 1R <b>rocked</b> again and keeps rocking continuously for 30 s approx., then stops.
	00:40:23	Unit 6L from 2nd row of Xbloc+'s starts rocking
	00:41:03	Unit 1R <b>rocked</b> once
	00:41:29	Unit 6L from 2nd row of Xbloc+'s starts rocking continuously
	00:43:03	Unit 6L from 2nd row of Xbloc+'s keeps rocking
	00:45:33	Unit 6L from 2nd row of Xbloc+'s touches with upper left Xbloc+ and stops rocking
	00:47:18	Unit 6L from 2nd row of Xbloc+'s is rocking again
	00:56:03	Unit 6L from 2nd row of Xbloc+'s keeps rocking continuously until end of test
00:56:03	End test 100%	
1.2.1 - 110%	01:02:34	Unit 6L from 2nd row of Xbloc+'s rocks 3 times
	01:03:24	Unit <u>1L fails</u> by losing contact at right wing
	01:12:30	Unit 6L from 2nd row of Xbloc+'s rocks 5 times
	01:16:07	Unit 6L from 2nd row of Xbloc+'s rocks once
	01:17:14	Unit 1L loses also contact at left wing, after having failed
	01:18:04	At the end of this test, unit 4L has failed and only its right wing touches a bit the left part of the tail of the underneath element of the 2nd row

		located at the right. Unit 3R has failed and only its left wing touches a bit the right part of the tail of the underneath element of the 2nd row located at the left. Unit 4R has failed and only its right wing touches the right part of the tail of the underneath element of the 2nd row located at the right. The only unit that has not failed is 2R, which has slid backwards more under the right than the left wing, but keeps contact with underneath elements at both sides.
	01:18:04	End test 110%
1.2.1 - 120%	01:22:16	Unit 4R (already failed) <b>starts rocking.</b>
	01:25:22	Unit 4L (already failed) <b>starts rocking</b>
	01:25:51	Unit 4L <b>stops rocking</b> and finds itself in a new position. It has rocked approx. 16 times for approx. 30 s
	01:26:01	Unit 4L <b>starts rocking</b> in its new position
	01:26:11	Unit 4L <b>stops rocking</b> and gets displaced into a new position.
	01:26:16	Unit 4L <b>starts rocking</b> in its new position. Unit 4L keeps going on the above "cycle" of rocking and changing positions.
	01:29:01	Unit 4R finds a more stable position and <b>stops rocking.</b>
	01:31:10	Unit 1L <b>rocks.</b>
	01:31:31	Unit 4L <b>stops rocking.</b> It finds a new position and does not rock or gets displaced any more until the end of the test.
	01:31:57	Unit 5L from 2nd row of Xbloc+'s rocks several times.
	01:34:01	Unit 1L <b>rocks again.</b>
	01:35:31	Unit <u>2R fails</u> by losing contact at right wing with unit underneath
	01:41:04	End test 120%. End test series.
<b>Test</b>	<b>Time (hr:min:sec)</b>	<b>Observations</b>
1.1.2 - 60%	00:00:22	Unit 2R slides backwards horizontally
	00:01:47	Unit 4L slides backwards sideways at left wing
	00:14:31	No elements have failed yet
	00:19:27	The noses of units 3L and 4R are noticed to have been lifted up (at some point during this test)
	00:22:05	Unit 4R move a lot backwards more at right wing than left. It is clearly observed to have moved backwards much more than the other units. 4R still maintains contact at both wings.
	00:23:00	End test 60%
1.1.2 - 80%	00:27:00	From beginning of test until that time, unit 4L has moved moves backwards sideways intensively and more under left wing than right wing. This movement has started from previous test.
	00:31:20	Unit <u>2R failed.</u>
	00:36:40	Unit <u>4L fails</u> by losing contact at left wing.
	00:39:30	Rock of underlayer at crest behind unit 5R is rocking for approx. 2.5 min.
	00:49:34	End test 80%
1.1.2 - 100%	00:50:57	Unit 5R <b>rocks</b> once, then makes a larger rotational motion and gets displaced backwards, then another even larger rotational motion which leads to <u>failure</u>
	00:53:07	Unit 4L is rotated sideways even more, after having already failed
	00:54:57	Rocks of underlayer at crest behind unit 2L are rocking



	00:56:37	Unit 4L (already failed) <b>rocks</b> once
	00:57:12	Unit 4L (already failed) <b>rocks</b> once more
	01:01:44	Unit <u>3L fails</u> with nose tilted downwards and tail tilted upwards.
	01:03:52	Unit <u>4R fails</u> . The unit has lost contact at right side and its nose is tilted upwards.
	01:19:16	End test 100%
1.1.2 - 120%	01:23:20	Unit 5R (already failed) <b>rocked once</b> .
	01:27:26	Unit 4R (already failed) <b>rocked</b> once.
	01:29:01	Unit <u>3R fails</u> sideways by losing contact at left wing, but maintaining contact at right wing.
	01:40:08	Unit <u>5L fails</u> by losing contact under right wing.
	01:50:25	End test 110% (or 120%). End test series
<b>Test</b>	<b>Time (hr:min:sec)</b>	<b>Observations</b>
1.2.2 - 60%	00:00:25	Units 3L, 4L slide backwards
	00:02:15	Unit 3L <b>rocks</b> once and then <u>fails</u> after a larger rotational motion. Unit 2L rotates and its nose is tilted up. Contact is lost at the nose, but maintained under both wings. Unit 2R moves backwards mainly at right wing
	00:04:23	Unit 3L (already failed) <b>rocks</b> once
	00:16:16	At the end of this test, unit 3L is seen to have contact again with the two units of the second row underneath at right side, despite that this contact was lost at 02:15, when unit 3L practically failed. This may imply that the unit was brought back near its original position due to an opposite motion to the one that led to its failure. Indeed, at 6:25, the unit is brought back during wave downrush.
	00:16:16	End test 60%
1.2.2 - 80%		No significant observations during this test. Generally, units keep moving backward, so the gap between the front vertical parts of their wings and the back vertical parts of the units of the 2nd row underneath becomes larger. Units 1L and 5R have not moved. Units 2L,3L stay in the same positions that they have acquired during the previous test.
	00:35:03	End test 80%
1.2.2 - 100%	00:38:36	Unit <u>5R fails</u> . From stable position (unit 5R has not moved before), it makes two large rotational motion and eventually gets displaced.
	00:47:46	The right wing of unit 3L loses contact with unit underneath and ends up at a lower position, at the left of the right neighbouring unit of the 2nd row. At some point later in the test, 3L right wing goes again on the top of the latter unit and, then, loses contact again. In the end, 3L makes only contact with unit 3L of the 2nd row with the nose of 3L being on top of this unit.
	00:56:03	End test 100%
1.2.2 - 110%	01:08:21	Unit <u>2L fails</u> by losing contact at right wing.
	01:17:37	Unit <u>5L fails</u> .
	01:18:04	End test 110%
1.2.2 - 120%		No significant changes
	01:41:04	End test 120%. End test series.
<b>Test</b>	<b>Time (hr:min:sec)</b>	<b>Observations</b>

1.1.3 - 60%	00:01:25	No visible movement
	00:02:55	Unit 5L's nose is tilted up and loses contact with elements of 2nd row below.
	00:03:05	Unit 3L slides backwards sideways. Its right wing gets displaced, but left wing does not move.
	00:23:00	End test 60%
1.1.3 - 80%	00:25:17	Unit 3L's right wing gets displaced even more, but contact is maintained.
	00:26:36	Unit 1R slides backwards at both sides.
	00:31:22	Unit 4R slides slightly backwards at both sides.
	00:49:34	End test 80%
1.1.3 - 100%	00:55:06	Unit 5L moves slightly backwards at the right wing.
	00:56:54	Unit <u>1R fails</u>
		Unit 4L moves slightly backwards at both sides
01:19:16	End test 100%	
1.1.3 - 110%	01:27:04	Unit <u>5R fails</u> after too rotational motions. Then, 5R <b>rocks</b> a lot during the whole test, while already failed.
		Unit 3L <b>rocks</b> once
	01:50:25	End test 110%
1.1.3 - 120%	01:58:42	Units <u>3L &amp; 5L failed</u> .
	02:25:57	End test 120%. End test series.
<b>Test</b>	<b>Time (hr:min:sec)</b>	<b>Observations</b>
1.2.3 - 60%	00:16:16	No damage or movement observed in this test
		End test 60%
1.2.3 - 80%	00:18:50	Unit 3L slides backwards considerably at right wing. Unit 4L slides backwards a bit at right wing. Unit 5L's nose is tilted up.
	00:20:44	Unit 1R moves backwards and its nose is tilted up.
		Unit 3L <b>rocks</b> for 2 times
00:35:03	End test 80%	
1.2.3 - 100%	00:39:01	Noses of units 3R and 4R are tilted up.
	00:40:07	Unit 2R rotates and its nose is tilted up. Contact is still maintained under the wings.
	00:56:03	End test 100%
1.2.3 - 110%	00:56:42	<u>1R fails</u> . Its right wing loses contact and unit is tilted sideways.
	01:18:04	End test 110%
1.2.3 - 120%	01:23:56	Unit 4R slides backwards a lot, but maintains contact under both wings.
	01:41:04	End test 120%. End test series.
<b>Test</b>	<b>Time (hr:min:sec)</b>	<b>Observations</b>
1.1.4 - 60%		No damage or movement observed in this test
	00:23:00	End test 60%
1.1.4 - 80%	00:24:28	Wave run-up reaches top row
	00:28:28	No damage has been caused yet
	00:29:23	Unit 3L slides backwards at both wings, but a bigger gap is created at the right wing. Unit 4L slides slightly backwards at left wing
	00:36:40	Unit 3L <b>rocks</b> once and subsequently slides more backwards.

	00:46:53	Unit 1R rotates, its nose is tilted up and the unit slides also backwards. Contact is maintained
	00:49:34	End test 80%
1.1.4 - 100%	00:53:34	Unit 4R moves horizontally backwards.
	00:56:41	Unit 2R rotates, its nose is tilted up and the unit slides also backwards. Contact is maintained
	01:19:16	End test 100%
1.1.4 - 110%	01:35:19	Unit 3L starts <b>rocking</b> . 3L rocks every now and then, mainly during the passing of high waves, until the end of the test
	01:50:25	End test 110% (End test series)
<b>Test</b>	<b>Time (hr:min:sec)</b>	<b>Observations</b>
1.2.4 - 60%		No damage or movement during this test. Run-up reaches up to 3rd row from top.
	00:16:16	End test 60%
1.2.4 - 80%		Run up reaches the top row only for the high waves. No damage or movement.
	00:35:03	End test 80%
1.2.4 - 100%	00:40:08	Unit 2R's nose gets tilted up and unit also slides slightly backwards
	00:42:23	Unit 1R's nose gets tilted up and unit also slides slightly backwards
	00:56:03	End test 100%
1.2.4 - 110%	01:00:00	Unit 3L moves backwards, more at right wing than left. Unit 4L's nose get tilted up.
	01:03:35	Unit 3L <b>rocks</b> once. 3L keeps <b>rocking</b> occasionally.
	01:11:20	Unit 3L <b>stops rocking</b> .
	01:18:04	End test 110%
1.2.4 - 120%	01:25:34	Unit 3L <b>rocks</b> once. Unit 5L slides backwards at both sides.
	01:31:54	Unit 3L <b>rocks</b> once again.
		Breaking of some of the highest waves in deep water is observed
	01:41:04	End test 120% (End test series)
<b>Tested Configurations (2<sup>nd</sup> test set)</b>		
<b>Test</b>	<b>Time (hr:min:sec)</b>	<b>Observations</b>
2.2.1 - 60%	00:00:15	Units <b>1L starts rocking</b> .
	00:00:25	Unit <u>2L failed</u> by losing contact at right wing.
	00:00:55	Unit <b>1L stops rocking</b> . It has rocked for approx. 15 times.
	00:00:57	Unit <u>3L failed</u> by losing contact at left wing. Before failing, <b>3L rocked once</b> and then made larger subsequent rotational motions that led to its failure.
	00:02:15	Units <u>2R and 3R and 4R failed</u> .
	00:02:24	Unit <b>2R starts rocking and rocks continuously</b> .
	00:02:45	Units <b>3R rocked 3 times</b> . Then got displaced a bit, then <b>rocked again</b> , then got displaced in a new position, where it started rocking again.
	00:03:00	Unit <u>5R fails</u> by rotating 180°. Units 3R, 4R move to the left towards the gap that was created. <b>3R stops rocking</b> at new position.
	00:04:20	Unit 4R made one large rotational motion and returned almost to its previous position.
	00:05:10	Unit <u>1L fails</u> .

		Unit 4R is rotated 180° and ends up next to 5R with same orientation (similar type of failure).
	00:06:09	Unit <b>2R rocking observed again.</b>
	00:10:35	Unit <b>2L</b> (already failed) starts <b>rocking</b> and rocks continuously.
	00:13:42	Unit <b>3L rocked once</b> again.
	00:14:25	Unit <b>2R rocked once</b> again.
	00:16:16	End test 60% (End test series)
		No more tests were conducted, because failure already very extensive at wave height of 5.79 cm.
<b>Test</b>	<b>Time (hr:min:sec)</b>	<b>Observations</b>
3.2.1 - 60%	00:00:28	Xblocs at left and right sides of the crest are displaced and gaps are created between them.
	00:01:07	Units 2L and 3L move backwards.
	00:01:25	3 Xblocs at the left side of the crest rock for 3 times.
	00:02:17	The same 3 Xblocs and an additional one rock.
Units 3R, 4R, 5R slide backwards.		
	00:03:55	7 Xblocs at left side move more backwards in the crest, gaps are created between them and the blocks subsequently rock.
	00:03:58	Unit <u>4L fails.</u>
	00:13:55	Unit <u>2R fails</u> by losing contact at right wing.
	00:16:16	End test 60% (End test series)
No more tests were conducted, because already 2 units fail and there is also extensive damage to the Xblocs.		
<b>Test</b>	<b>Time (hr:min:sec)</b>	<b>Observations</b>
4.2.1 - 60%	00:01:38	No damage observed yet.
	00:16:16	End test 60%.
		No obvious damage to Xbloc+ units and no obvious damage to Xblocs.
4.2.1 - 80%	00:17:45	No damage observed yet.
	00:18:45	Xblocs at left side get rearranged.
	00:20:50	Units 3L, 4L, 5R slide backwards.
	00:21:16	2 Xblocs at right side get displaced at the crest area.
	00:21:45	2 additional Xblocs at right side get displaced at the crest area.
	00:22:10	2 Xblocs at left side (near the edge of the structure) fall down the front slope. Remaining Xblocs there move and rearrange.
	00:24:20	1 Xbloc near 1L Xbloc+ rocked some times.
	00:26:05	Another Xbloc near 1L Xbloc+ rocked some times.
00:35:03	End test 80%.	
4.2.1 - 100%	00:39:14	1 Xbloc at left of 1L Xbloc+ making large rotational motions and displaced a bit from position.
	00:40:06	Unit <u>2L failed.</u>
	00:41:25	Unit <b>2L rocked once.</b>
	00:42:03	Unit <b>2L started rocking again.</b>
	00:43:05	Xblocs start rocking.
00:48:43	Xblocs stop rocking. In the meantime, different Xblocs and for different amount of time rocked.	

	00:55:05	Unit <b>2L stopped rocking</b> . It has rocked for the majority of the waves.
	00:56:03	End test 100%.
4.2.1 - 110%	00:56:56	Unit <b>2L started rocking</b> . (already failed)
	01:00:01	Unit <b>2L stopped rocking</b> . (already failed)
	01:01:56	Xblocs at center of the crest (behind 5L, 5R) moved, rearranged and created more space.
	01:02:31	Unit <b>1R rocked</b> (already failed).
	01:03:46	Units <u>5L and 5R failed</u> . Can be a consequence of the more space created behind them after the movement of the Xblocs.
	01:18:04	End test 110%.
4.2.1 - 120%	01:32:40	Unit <u>1L failed</u> .
	01:41:04	End test 120% (End test series)
<b>Test</b>	<b>Time (hr:min:sec)</b>	<b>Observations</b>
5.2.1 - 60%	00:02:11	Underlayer material behind crown wall rocked, moved and rearranged.
	00:02:17	Unit 5R slid backwards at left wing.
	00:16:16	End test 60%.
5.2.1 - 80%	00:19:03	Unit 3L slides backwards at left wing. Units 4R, 5R slide backwards more.
	00:35:03	End test 80%.
5.2.1 - 100%	00:35:36	1 Xbloc at the middle of crest rocked once.
	00:36:52	The Xbloc mentioned at 00:35:36 rocked once more and moved.
	00:37:56	Same Xbloc was dragged over the crown wall and ended up at the crest.
	00:40:06	3 more Xblocs were dragged over the crown wall and ended up at the crest.
	00:56:03	End test 100%.
5.2.1 - 110%	00:58:06	1 Xbloc, initially at the left part of the crest, was dragged over the crown wall and ended up at the crest.
	01:00:11	1 Xbloc, mentioned in 00:58:06, rocked.
	01:00:26	Another Xbloc gets dragged over the crown wall and ends up at the crest.
	01:07:11	1 Xbloc, which previously moved at the back of the crest, rocked.
	01:18:04	End test 110%.
5.2.1 - 120%	01:21:17	1 Xbloc at crest rocked.
	01:26:27	The same Xbloc, mentioned in 01:21:17, rocked more intensively and moved a bit.
	01:32:27	The same Xbloc and also another one, rocked some times.
	01:41:04	End test 120%.
5.2.1 - 140%	01:46:59	"Most left" Xbloc at crest gets dragged down the rear slope.
	01:47:08	Units <u>4R and 5R failed</u>
	02:02:01	One Xbloc was dragged over the crown wall, all over the crest and went down the rear slope.
	02:05:55	End test 140% (End test series).
<b>Test</b>	<b>Time (hr:min:sec)</b>	<b>Observations</b>
7.2.1 - 60%		Not much movement of the Xbloc+ units during this test series. Underlayer material rocks a bit and gets rearranged.
	00:16:16	End test 60%.

7.2.1 - 80%	00:35:03	End test 80%.
		By the end of test 80%, no item has failed yet, but all items have slid backwards. Sliding is horizontal.
7.2.1 - 100%	00:38:47	One big stone of the underlayer, initially between 1L & 2L Xbloc+ units, got dragged all the way to the back of the crest, where it rocked.
	00:40:04	Units <u>3R, 4R, 5R, 1L, 2L failed</u> simultaneously.
	00:56:03	End test 100%.
7.2.1 - 110%	01:01:47	Units <u>4L &amp; 5L failed</u> .
	01:07:27	Unit <u>2R fails</u> by losing contact at left wing.
	01:03:53	Unit <b>5L rocked (already failed)</b> . 5L rocked for many times for approx. 6 minutes.
	01:09:42	Unit <u>3L failed</u> .
	01:15:24	Unit <u>1R failed</u> .
	01:18:04	End test 110%.
<b>Test</b>	<b>Time (hr:min:sec)</b>	<b>Observations</b>
6.2.1 - 60%	00:00:53	1 stone behind 3R unit's left wing rocked.
	00:01:01	1 stone between 5R & 5L units dragged & went over the crown wall element.
	00:01:37	1 stone behind 5R unit's tail rocked, moved & "climbed" at the crown wall element.
		1 stone behind 2L unit's tail rocked.
	00:03:07	No damage observed yet.
	00:07:37	1 stone between 4L & 5L rocked.
	00:08:07	The stone between 4L & 5L rocked again.
	00:10:37	No damage observed yet.
	00:16:16	End test 60%
6.2.1 - 80%	00:18:53	Passing of high waves "train". No damage observed.
	00:22:13	1 stone behind unit 1L rocked & changed position. Another stone, next to it, rocked.
	00:30:13	1 stone between 4L & 5L units rocked some times.
	00:35:03	End test 80%. No movement of Xbloc+ was observed.
6.2.1 - 100%	00:36:58	No damage yet.
	00:37:55	Passing of high waves "train". No damage observed.
	00:40:10	Passing of high waves "train". No damage observed.
	00:52:40	Stones between 1L & 2L rocking.
	00:56:03	End test 100%.
6.2.1 - 110%	01:00:56	1R moved backwards slightly under right wing
	01:02:01	1 stone behind unit 1L rocked
	01:13:51	1 stone behind 5L unit rocked, got rearranged & ended up above the tail of 5L
	01:18:04	End test 110%.
6.2.1 - 120%	01:31:14	Piece of "glued rock" at right side moved & went down the rear slope.
	01:41:04	End test 120%. Only units 1R & 2R have been partially displaced so far.
		Some units slid back a bit.

6.2.1 - 140%		No rocking of units observed, not even when looking from the side of the flume and during high wave "trains".
	02:05:55	End test 140%. End test series.
<b>Test</b>	<b>Time (hr:min:sec)</b>	<b>Observations</b>
6.1.1 - 60%	00:00:23	1 stone of the underlayer got displaced to the back of the crest between the crown wall element and the gabion.
	00:01:58	More stones of the underlayer got displaced to the back of the crest between the crown wall element and the gabion.
	00:03:58	Stone above tail of unit 3L left and went to the back of the crest between the crown wall element and the gabion.
	00:05:18	Stones at the right of unit 1R rock.
	00:05:33	Passing of high waves "train". No damage observed.
		Gabion behind crown wall element was dragged and went down the rear slope.
	00:23:00	End test 60%.
6.1.1 - 80%		No damage observed.
	00:49:34	End test 80%.
6.1.1 - 100%	00:54:41	One stone left from the backfill & went over the crown wall element.
		During this test, some units slide backwards horizontally.
		At the end of test series, unit 3R slid back towards right wing, 2R at both sides
	01:19:16	End test 100%.
6.1.1 - 110%	01:25:03	1 big stone between units 4L & 5L rocked, got rearranged & then kept on rocking.
	01:40:20	The right wing of unit 1R went up and lost contact with the tail of the underneath row's right unit. Nose went up at right side. At left side, contact both at the nose and the wing is maintained.
	01:49:17	Unit <u>1R failed</u> .
		Crown wall element has moved backwards during this test. Wall could have moved due to underpressure & because gabion behind has also moved.
	01:50:25	End test 110%.
6.1.1 - 120%		Before this test, the gabion was placed again to stop erosion there & movement of crown wall element. Nothing else was moved (or changed) in the cross-section.
	01:54:45	Unit <b>1R rocked</b> once (already failed).
	01:56:15	Unit 1R got displaced to a new position while already displaced.
	01:56:52	Unit 1R got displaced to new (second) position while already displaced.
	01:57:10	Unit <b>1R rocked once</b> and then got displaced to a new (third) position.
	01:58:22	Unit 1R flipped over at the top of units 1R & 2R of the 2nd row, then moved two times and finally fell down the front slope.
	02:22:57	End test 120%.
6.1.1 - 140%	02:30:06	No units have failed from the start of the test (except 1R that failed during 110% test)
	02:46:43	Units <u>3L &amp; 3R failed</u> .
	02:52:16	Unit <u>4L failed</u> .

	02:56:48	Units 3L and 4L got carried above the crown wall element and down the rear slope.
		Unit <u>2R failed</u>
	02:56:50	Unit 2R was displaced to a new position just after it failed.
	02:56:58	Units <u>1L &amp; 2L failed</u> . Unit 4L from 2nd row failed (toppled over)
	02:58:05	End test 140%. End test series.
<b>Test</b>	<b>Time (hr:min:sec)</b>	<b>Observations</b>
6.1.2 - 60%		No damage observed.
	00:23:00	End test 60%
6.1.2 - 80%	00:26:23	No damage observed yet.
	00:26:30	High wave passed, but no damage is observed.
	00:49:34	End test 80%
6.1.2 - 100%	01:07:14	Subsequent high waves pass, but no damage is observed.
	01:19:16	End test 100%.
6.1.2 - 120%		During the 100% conditions test, the generated wave height was 10.66 cm, equal to 1.08*9.91 cm (design wave height, corresponding to a stability number of 2.5). Thus, 110% conditions test was not performed.
	01:23:38	High wave train passed, but no damage and no rocking is observed.
	01:24:23	One stone left from the backfill.
	01:36:08	Passing of high waves "train". No damage observed. No rocking. No obvious rearrangement of the underlayer.
	01:51:48	End test 120%. No damage. End test series.
		During the 120% conditions test, the generated wave height was 13.40 cm, equal to 1.35*9.91 cm (design wave height, corresponding to a stability number of 2.5). Thus, 140% conditions test was not performed.
<b>Test</b>	<b>Time (hr:min:sec)</b>	<b>Observations</b>
6.2.2 - 60%		No movement is observed during the test series.
	00:16:16	End test 60%.
6.2.2 - 80%	00:18:51	First high wave attack, but no damage.
		Also no movement is observed during the test series.
	00:35:03	End test 80%.
6.2.2 - 100%	00:40:06	1 stone initially located behind 3L left from the underlayer backfill.
	00:56:03	End test 100%.
6.2.2 - 120%		110% conditions test was not performed.
	00:59:15	High wave train passed, but no damage and no rocking is observed.
	01:19:03	End test 120%.
6.2.2 - 140%	01:22:25	High wave train passed, but no damage and no rocking is observed.
	01:26:45	Stone between units 1L & 2L rocking for approx. 5 sec.
	01:35:50	Stone between units 1L & 2L rocking again.
	01:43:54	End test 140%. End test series.
<b>Repetition tests on the single Xbloc+ (1<sup>st</sup> test set)</b>		
<b>Test</b>	<b>Time (hr:min:sec)</b>	<b>Observations</b>
	00:06:16	No damage or movement visible.



1.1.1 R - 30%	00:12:04	No damage or movement visible.
	00:16:16	End test 30%. No failure, displacement or rocking observed.
1.1.1 R - 40%		During this test, only unit 4L has slid backwards. No other movements of units or rocking happened.
	00:35:03	End test 40%.
1.1.1 R - 50%	00:40:07	Unit 5L slid backwards under both wings.
	00:42:17	Unit <b>3L rocked</b> for 3 times.
	00:42:52	Unit <b>3L rocked</b> again.
	00:43:17	Unit <b>3L rocked</b> again.
	00:44:07	Unit <b>3L rocked</b> again.
	00:44:57	Unit <b>3L rocked</b> again.
		Unit <b>3L rocks</b> for almost every wave.
	00:49:37	Unit <b>2L rocked</b> .
	00:52:37	Unit <b>2L rocked</b> .
	00:55:22	Unit <b>2L rocked</b> 2 times. Unit <b>3L rocked</b> .
00:56:03	End test 50%.	
1.1.1 R - 60%	00:57:16	Unit <b>2L rocked</b> approx. 5 times.
	00:58:01	Unit <b>2L rocked</b> once.
	01:02:16	Unit <b>1L rocked</b> approx. 5 times, then made a larger rotational motion & <u>1L failed</u> . Then, it stopped rocking.
	01:03:16	Unit <b>2L rocked</b> 2 times.
	01:04:01	Unit <b>2L rocked</b> .
	01:04:11	Unit <b>2L rocked</b> .
		Unit <b>2L</b> seen to be rocking in same manner many times. The rocking is not exactly rotational, but the unit makes more of a horizontal backwards motion, during wave run-up, & then a horizontal forward motion, during wave run-down, after which it returns to the initial position.
01:19:03	End test 60%.	
1.1.1 R - 70%	01:20:33	Unit <b>2L rocked</b> 2 times.
	01:21:17	Unit <b>2L rocked</b> again.
	01:22:23	Unit <u>5L failed</u> .
	01:25:03	Unit <b>2L rocked</b> again 2 times.
	01:41:28	Unit <b>2L rocked</b> again 6 times.
	01:43:54	End test 70%.
1.1.1 R - 80%	01:44:26	Unit <b>2L rocked</b> approx. 4 times.
	01:47:26	Unit <b>2L rocked</b> 3 times & unit <u>4R failed</u> .
	01:50:16	Unit <b>2L rocked</b> .
	02:01:56	Unit <u>4L failed</u> .
	02:10:28	End test 80%.
1.1.1 R - 90%	02:18:11	Unit <u>2L failed</u> .
	02:18:31	Unit <b>5L rocked</b> many times (almost at all waves) for approx. 1 min.
	02:35:51	Unit <b>2L rocked</b> once, after failure.
	02:38:38	End test 90%.
1.1.1 R - 100%	02:41:33	Unit <b>2L rocked</b> after failure.
	02:42:38	Unit <b>3L rocked</b> once, before failure.

	02:45:48	Unit <b>2L rocked</b> after failure.
	02:46:08	Unit <u>3L failed</u> .
	03:08:20	End test 100%.
1.1.1 R - 110%	03:15:53	Unit 4L, after having already failed, gets displaced to a new position.
	03:16:02	Unit <b>4L rocks once</b> , at new position & already failed.
	03:16:08	Unit <b>4R starts rocking</b> , after it has failed. It is rocking continuously for almost all waves.
	03:20:23	Unit <b>4R stops rocking</b> .
	03:24:33	Unit <b>4L rocks once</b> again.
	03:38:23	Unit <b>4L rocks several times</b> .
		Unit <b>4L also observed rocking</b> during lower waves at the end of the test.
	03:39:29	End test 110%.
1.1.1 R - 120%	03:43:18	Unit <b>4L rocked</b> , after failure.
	03:45:30	Unit <u>3R failed</u> .
	03:47:19	Units 2L & 3R got displaced at a new position, while already failed.
	03:47:24	Unit <b>4L rocked</b> , after failure.
	03:47:54	Unit <b>2L rocked</b> .
	03:48:04	Unit <b>4L rocked</b> for approx. 5 times during subsequent waves.
	03:53:44	Unit 3R (already failed), roated/flipped to a new position at the crest & then returned near to its initial position.
	03:54:24	Unit 3R rotated again, but remained flipped over at a new position at the crest. At the new position, <b>3R rocked</b> several times.
	03:54:44	Unit <b>4L rocked</b> again.
	03:55:04	Units <b>3R &amp; 4L rocked</b> .
	03:55:44	Unit <b>4L rocked</b> , after failure.
	03:56:19	Unit <b>3R rocked</b> .
	03:56:39	Unit <b>4L rocked</b> .
	03:56:59	Units <b>4L &amp; 3R rocked</b> .
	03:57:24	Units <b>4L &amp; 3R rocked</b> .
	03:57:49	<b>3R</b> is observed <b>rocking again</b> .
	04:02:04	Unit <u>5R failed</u> .
	04:02:19	<b>3R</b> is still <b>rocking</b> continuously.
	04:05:49	<b>3R rocked</b> .
	04:12:01	End test 120%. End test series.
<b>Test</b>	<b>Time (hr:min:sec)</b>	<b>Observations</b>
1.2.1 R - 20%	00:06:15	No movements observed yet.
	00:09:23	End test 20%. No rocking, displacement or failure observed.
1.2.1 R - 30%	00:15:28	Unit 4L slid backwards.
	00:20:53	End test 30%. Only one unit was displaced. No rocking was observed.
1.2.1 R - 40%	00:22:49	Unit 3L slid backwards under both wings.
	00:24:09	Unit <b>1L rocked</b> & then slid backwards at left wing.
		Unit 2L slid backwards at both wings

	00:26:19	Unit <b>2R rocked</b> . Unit <b>2R rocks continuously</b> until end of test.
	00:34:10	End test 40%.
1.2.1 R - 50%	00:34:35	Unit <b>2R starts rocking</b> . Unit <b>2R rocks continuously</b> until end of test series.
	00:46:56	Unit <u>2L failed</u> .
	00:49:01	Unit <b>2L rocked</b> some times, after it failed.
	00:49:01	End test 50%.
1.2.1 R - 60%	00:49:21	Unit <b>2R rocked</b> .
	00:50:08	Unit <b>2R rocked</b> .
	00:51:13	Unit <u>1L failed</u> .
	00:51:58	Unit <b>5R rocked</b> (tilted at the horizontal plane)
	00:52:38	Unit <b>2R rocked</b> .
	00:52:58	Unit <b>2L rocked once</b> . (already failed)
	01:05:17	End test 60%.
1.2.1 R - 70%	01:05:37	Unit <b>2L rocked</b> (already failed)
	01:07:42	Unit <b>2L rocked</b> (already failed)
	01:09:27	Unit <b>2L rocked</b> (already failed)
	01:10:47	Unit <u>3L failed</u> .
	01:11:22	Unit <b>2L rocked</b> (already failed)
	01:12:32	Unit <b>2L rocked</b> (already failed)
	01:13:02	Unit <b>2L rocked</b> (already failed)
	01:14:25	Unit <b>5L rocked once</b> .
	01:16:02	Unit <b>2L rocked</b> (already failed)
	01:16:17	Unit <b>2L rocked</b> (already failed). 2L keeps rocking many times until the end.
	01:17:30	Unit <u>5R failed</u> .
	01:22:51	End test 70%.
1.2.1 R - 80%	01:23:16	Unit <b>2L rocked</b> (already failed)
	01:25:37	Unit <b>2L rocked</b> (already failed)
	01:31:53	Unit <b>2L rocked</b> (already failed)
	01:40:56	Unit <b>2L rocked</b> (already failed)
	01:41:38	End test 80%.
1.2.1 R - 90%	01:42:58	Unit <b>2L rocked</b> (already failed)
	01:50:23	Unit <b>2L rocked</b> (already failed)
	01:57:33	Unit <b>2L rocked</b> (already failed). Unit <b>3L rocked</b> once (already failed).
	01:59:53	Unit <b>2L rocked</b> (already failed). Unit 2L is rocking continuously during the test.
	02:01:33	End test 90%.
1.2.1 R - 100%	02:03:30	Unit <b>2L rocked</b> (already failed)
	02:11:30	Unit <b>2L rocked</b> (already failed)
	02:12:20	Unit <u>4R failed</u> .
		Unit 5R from 2nd row moved a lot.
	02:13:28	Unit <b>2L rocked</b> (already failed)
	02:16:30	Unit <b>2L rocked</b> (already failed)
	02:22:33	End test 100%.
	02:33:19	Unit <b>3L rocked</b> . (already failed)

1.2.1 R - 110%	02:33:59	Unit <b>3L rocked</b> . (already failed)
	02:43:19	Unit <b>2L rocked</b> . (already failed)
	02:43:59	Unit <b>2L rocked</b> . (already failed)
	02:44:34	End test 110%.
1.2.1 R - 120%	02:45:16	Unit <b>2L rocked</b> . (already failed)
	02:46:06	Unit <b>2L rocked</b> & got displaced to a new position while already failed.
	02:49:06	Unit <b>2L rocked</b> . (already failed)
	02:50:20	Units <u>2R &amp; 5L failed</u> .
	02:52:46	Unit <b>2L rocked</b> . (already failed)
	02:53:56	Unit <b>2L rocked</b> . (already failed)
	03:00:30	Unit <b>2L rocked</b> . (already failed)
	03:07:34	Damage at 2nd row is extensive. One of the units of the 2nd row has failed. End test 120%.
1.2.1 R - 120% EXTRA		After 120% conditions test, the generated wave height was 12.02 cm, so an additional test with higher wave height is performed.
	03:08:52	Unit <b>3L rocked</b> , while already failed.
	03:13:07	High wave passes, units at 1st & 2nd row get displaced. Unit 5L from 1st row changes position, while already failed. Unit 4L from 1st row & unit 5L from 2nd row got dragged once but returned to their original position.
	03:13:32	Unit <b>5L rocked</b> approx. 5 times, while already failed.
	03:14:07	Unit <b>2R rocked</b> .
	03:14:27	Unit <b>5L rocked</b> , while already failed.
	03:15:07	Unit <b>5L rocked</b> , while already failed.
	03:15:27	Unit <b>2R rocked</b> , while already failed.
	03:15:47	Units <b>2R &amp; 5L rocked</b> , while already failed.
	03:16:12	Unit <b>2R is rocking</b> .
	03:18:17	Unit <b>2R is rocking</b> .
	03:18:57	Unit <u>4L failed</u> .
	03:19:29	Unit <b>4R rocked</b> .
	03:20:27	Unit <b>4R rocked</b> .
	03:20:47	Units <b>2R &amp; 4R</b> (both already failed) <b>rocked</b> approx. 5 times.
	03:22:07	Unit <b>1L rocked</b> .
	03:22:45	Unit <b>1L rocked</b> .
	03:23:02	Unit <b>1L rocked</b> .
03:24:22	Unit <b>1L rocked</b> .	
03:25:07	Unit <b>1L rocked</b> .	
03:30:34	End test 120% EXTRA. End test series.	
<b>Test</b>	<b>Time (hr:min:sec)</b>	<b>Observations</b>
1.1.2 R - 30%	00:01:02	Run-up reaches 2nd row. No movements.
	00:02:22	Run-up reaches 1st row. No movements.
	00:16:16	End test 30%. No failure, displacement or rocking observed.
1.1.2 R - 40%	00:18:54	Run-up reaching & "covering" the 1st row. No movements yet.
	00:33:24	Unit 1R is noticed to have slid backwards
	00:35:03	End test 40%.

1.1.2 R - 50%		Some units are seen to have slid backwards.
	00:44:24	1 stone of the underlayer behind unit 3L rocked.
	00:56:03	End test 50%.
1.1.2 R - 60%	00:59:08	Unit <u>3R failed</u> .
	01:19:03	End test 60%.
1.1.2 R - 70%	01:22:20	Unit <b>4R rocked</b> , before failure.
	01:22:25	Unit <u>2L failed</u> .
	01:25:00	Unit <b>2L rocked</b> , after having failed.
	01:25:35	Unit <b>4R rocked</b> , before failure.
	01:33:55	Unit <b>4R rocked once</b> , before failure. Rocking motion was large, but unit returned to initial position.
	01:36:55	Unit <b>4R rocked</b> , before failure.
	01:37:10	Unit <b>4R rocked</b> , before failure.
	01:41:25	Unit <b>4R rocked</b> , before failure.
	01:43:54	End test 70%.
1.1.2 R - 80%	01:45:00	Unit <b>4R rocked</b> , before failure.
	01:45:16	Unit <b>4R rocked</b> , before failure.
	01:46:10	Unit <b>4R rocked</b> , before failure.
	01:46:35	Unit <b>4R rocked</b> , before failure.
	01:47:39	Unit <u>4R failed</u> . Subsequently, got displaced a bit, <b>rocked once</b> & then got displaced to a new position at the crest.
	01:50:50	Unit <b>3R</b> , which has already failed, was displaced to a new position, then to another position at the crest, where it <b>rocked twice</b> .
	01:51:17	Unit <b>3R rocked</b> again (already failed).
	02:04:20	Unit <u>1R failed</u> .
	02:05:06	Unit <b>4L rocked</b> , before failure.
	02:05:15	Unit <b>4L rocked</b> , before failure.
	02:05:25	Unit <b>4L rocked</b> , before failure.
	02:05:30	Unit <b>4L rocked</b> , before failure.
	02:05:55	Unit <u>4L failed</u> .
	02:07:55	Unit <b>4L rocked twice</b> , after having already failed.
	02:08:14	Unit <b>4L rocked</b> , after having already failed.
02:08:50	Unit <b>4L rocked</b> , after having already failed.	
02:09:30	Unit <b>4L rocked</b> , after having already failed.	
02:10:28	End test 80%.	
1.1.2 R - 90%	02:10:35	Unit <b>4L rocked twice</b> , after having already failed.
	02:11:00	Unit <b>4L rocked</b> , after having already failed.
	02:11:50	Unit <b>4L rocked</b> , after having already failed.
	02:12:05	Unit <b>4L rocked</b> , after having already failed.
	02:12:50	Unit <b>4R rocked once</b> (already failed) & then got displaced to a new position at the crest.
	02:15:55	Units 4R & 5L of 2nd row have been displaced.
	02:17:15	Unit <u>3L failed</u> .
		Unit 2L (already failed), was displaced to a new position, then was displaced again to a newer position.

	02:17:45	Unit <b>2L rocked 3 times</b> , at the latest position it has acquired after failure.
	02:18:00	Unit <b>2L rocked</b> .
	02:18:45	Units 2L & 4L rocked. Unit <b>2L rocked</b> for approx. 4 times, unit <b>4L</b> for approx. 3 times, while failed.
	02:19:20	Units <b>2L &amp; 4L rocked</b> .
	02:20:15	Unit <b>2L rocked</b> .
	02:22:55	Unit <b>2L rocked</b> approx. 2 times & then got displaced to a new position, close to the previous one.
	02:23:09	Unit <b>2L rocked</b> twice at its new position.
	02:38:27	Unit <u>2R failed</u> .
	02:38:33	Unit <b>5R rocked once</b> , before failure.
	02:38:38	End test 90%.
1.1.2 R - 100%	02:40:51	Unit <b>2R rocked</b> (already failed).
	02:45:53	Unit <u>5L failed</u> .
	02:46:23	Unit <b>5L</b> , which has failed a bit before, <b>rocked</b> .
	02:51:05	Unit 5L has been displaced to a new position at the crest. Before that larger displacement, 5L was being slightly displaced to new positions, near the initial position it acquired when it failed.
	02:56:13	Unit <b>5L rocked</b> at the new position it has moved before.
	02:57:53	Unit <b>5L rocked</b> .
	02:58:33	Unit <b>5L rocked</b> .
	03:05:13	Unit <b>5R rocked</b> , then made a larger rotational motion & displaced at a new position without failing.
	03:08:20	End test 100%.
1.1.2 R - 110%	03:13:58	Unit <u>5R failed</u> .
	03:39:29	End test 110%.
1.1.2 R - 120%	03:47:17	Unit 4R from 2nd row has failed (lost contact with underlying units of 3rd row).
		Units at 2nd row are displaced.
	04:12:01	End test 120%. End test series.
<b>Test</b>	<b>Time (hr:min:sec)</b>	<b>Observations</b>
1.2.2 R - 30%	00:11:30	End test 30%. No failure, displacement or rocking observed.
1.2.2 R - 40%	00:12:21	No movements observed yet.
	00:15:56	Nose of units 1L & 2R are noticed to have been tilted up (happened at some point before).
	00:24:47	End test 40%.
1.2.2 R - 50%	00:29:32	Unit 1L made a larger rotational motion & ended up displaced without losing contact with underlying unit.
	00:29:57	Unit 1L made another large rotational motion & ended up more displaced, then made another rotational motion & failed. <u>1L failed</u> .
	00:39:38	End test 50%.
1.2.2 R - 60%		No rocking & no movements are observed during this test.
	00:55:54	End test 60%.
1.2.2 R - 70%		No rocking & no failures are observed during this test.
	01:13:05	End test 70%.

1.2.2 R - 80%	01:16:05	Unit <b>1L</b> (already failed) <b>rocked once</b> , then made a larger motion & got displaced to another position.
	01:32:15	End test 80%.
1.2.2 R - 90%	01:37:30	Unit <b>1L</b> <b>rocked twice</b> (already failed).
	01:42:35	Unit <u>2L failed</u> .
	01:52:10	End test 90%.
1.2.2 R - 100%	01:57:14	Unit <u>4L failed</u> .
	02:06:26	Units <u>5L &amp; 4R failed</u> . Before failing, units were maintaining slight contact with the units underneath.
	02:06:59	Unit <b>4R</b> <b>rocked</b> (already failed).
	02:07:19	Unit <b>4R</b> <b>rocked</b> (already failed).
	02:07:29	Unit <b>4R</b> <b>rocked</b> (already failed).
	02:07:44	Unit <b>4R</b> <b>rocked</b> (already failed).
	02:09:49	Unit <b>4R</b> <b>rocked</b> 2 times (already failed).
	02:10:02	Units <b>5L &amp; 4R</b> <b>rocked twice</b> during same waves.
	02:10:04	Unit 5L toppled over & gets displaced to a new position at the crest. Unit <b>4R</b> <b>rocks once</b> . Subsequently, units 5L & 4R get displaced to new positions by the same wave.
	02:11:09	Unit <b>2L</b> moves a bit, then <b>rocks a couple of times</b> at new position (while already failed)
02:13:10	End test 100%.	
1.2.2 R - 110%	02:15:19	Unit <b>5L</b> (already failed) <b>rocked</b> .
	02:16:14	Unit 4R was displaced to a new position at the back of the crest near the gabion. Then, <b>4R</b> <b>rocked once</b> .
	02:16:39	Unit 4R moved to another position at the crest. Then, <b>4R</b> <b>rocked once</b> .
	02:20:04	Unit <b>5R</b> <b>rocked once</b> , before failure.
	02:20:54	Unit <u>5R failed</u> .
	02:35:11	End test 110%.
1.2.2 R - 120%		No rocking observed. No additional units failed.
	02:58:11	End test 120%. End test series.
<b>Test</b>	<b>Time (hr:min:sec)</b>	<b>Observations</b>
1.1.3 R - 50%	00:02:48	No movements observed yet.
	00:21:00	End test 50%. No rocking, displacement or failure is observed.
1.1.3 R - 60%	00:23:02	Run up reaches top row. No movements yet.
	00:44:00	End test 60%. No rocking, displacement or failure is observed.
1.1.3 R - 70%	00:47:18	Unit 5L slid backwards under right wing.
		Unit 4L rotated & its nose is tilted up.
	00:48:48	Unit 3L slid backwards under both wings.
	00:54:18	More units are observed to have been partially displaced.
	00:59:38	No rocking is observed yet. No units have failed yet.
	01:02:08	Unit <u>4L failed</u> .
	01:08:51	End test 70%.
1.1.3 R - 80%		No important observations were made. No rocking or failures were observed.
	01:34:59	End test 80%.

1.1.3 R - 90%	01:42:08	Unit <b>1L rocked once</b> before failure.
	02:02:35	Unit <u>2L failed</u> .
	02:03:35	End test 90%.
1.1.3 R - 100%	02:07:02	Unit <b>1L rocked once</b> before failure.
	02:10:42	Unit <u>1L failed</u> . It lost contact at left wing with left unit underneath, but maintained contact at right wing.
	02:12:27	Unit <b>1L rocked once</b> after failure.
	02:13:27	Unit <b>1L rocked once</b> after failure.
	02:13:52	Unit <b>1L rocked once</b> after failure.
	02:15:57	Unit <b>1L rocked once</b> after failure.
	02:18:55	Unit <u>3L failed</u> . Just after failure, it was displaced to a new position. (1st position)
	02:18:59	Unit <b>3L rocked</b> , at new position (1st position), after failure.
	02:19:12	Unit <b>3L rocked</b> , after failure.
	02:20:02	Unit 3L moved to a new position. (2nd position)
	02:20:17	Unit 3L moved to a new position. (3rd position)
	02:21:21	Unit 3L moved to a new position. (4th position) Then, at new position, <b>3L rocked</b> .
	02:21:36	Unit <b>3L rocked. (already failed)</b>
02:21:42	Unit <b>3L rocked</b> , then moved to a new position (5th position), where it stopped rocking.	
02:33:17	End test 100%.	
1.1.3 R - 110%	02:33:52	Unit <b>1L rocked twice</b> (already failed).
	02:40:42	Unit 3R was displaced forward & subsequently backwards again by the next wave. Unit 3R has not failed.
	03:04:26	End test 110%.
1.1.3 R - 120%	03:07:38	Unit <u>3R failed</u> . It lost contact at left wing.
	03:12:18	Unit <u>4R failed</u> . Subsequently, <b>4R rocked twice</b> . Unit <b>2L</b> (already failed) <b>rocked once</b> .
	03:12:33	Units <b>2L &amp; 4R rocked once</b> . (both have already failed). Subsequently, unit 2L made a larger rotational motion & displaced to a new position at the crest, close to the initial position.
	03:12:43	Units <b>2L &amp; 4R rocked twice</b> . (both have already failed).
	03:12:53	Unit <b>2L rocked twice</b> & then got displaced to a new position at the crest, close to its previous position.
	03:13:23	Unit <b>4R rocked once</b> .
	03:14:03	Unit <b>2L rocked twice</b> , then made a larger rotational motion, that led to a new position & then another larger rotational motion that led to a newer position at the crest.
	03:14:48	Unit <b>2L is rocking &amp; moving</b> during subsequent waves.
	03:15:43	Unit <b>2L rocked once</b> .
	03:16:23	Unit <b>2L rocked once</b> .
	03:19:03	Unit <b>4R rocked once</b> .
	03:19:23	Unit <b>2L</b> (already failed) <b>rocked twice</b> .
	03:21:13	Unit 4R makes a larger rotational motion & gets displaced to a new position at the crest. Then, <b>4R rocks</b> .
	03:21:33	Unit <b>4R rocks twice</b> .



	03:22:23	Unit <b>4R rocks once</b> .
	03:23:03	Unit 4R makes a larger rotational motion & gets displaced to a new position at the crest. Then, <b>4R rocks once</b> .
	03:25:33	Unit <b>4R rocked once</b> .
	03:26:19	Unit <b>4R rocked once</b> .
	03:35:48	Unit <b>2L (already failed) rocked 4 times</b> . Rocking happened during subsequent waves of high wave height "train".
	03:36:58	End test 120%. End test series.

## Appendix H. Experiment Photos

The photos taken before and after the tests are included in this Appendix.

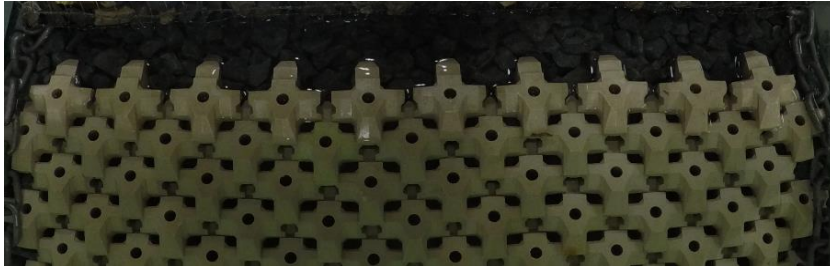


Figure H-1: Test series 1.1.1 Initial – Before Test with  $N_s=1.58$  (60% design conditions)

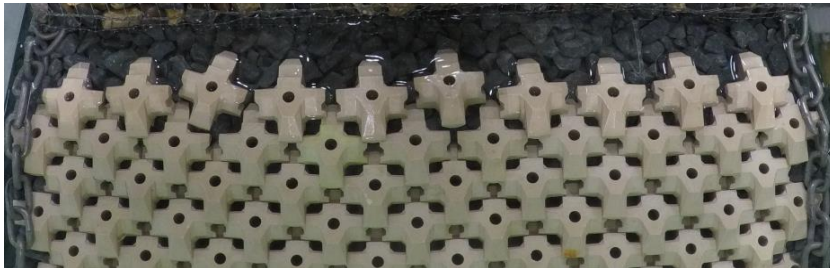


Figure H-2: Test series 1.1.1 Initial – Before Test with  $N_s=2.10$  (80% design conditions)



Figure H-3: Test series 1.1.1 Initial – Before Test with  $N_s=2.65$  (100% design conditions)



Figure H-4: Test series 1.1.1 Initial – Before Test with  $N_s=2.84$  (110% design conditions)



Figure H-5: Test series 1.1.1 Initial – Before Test with  $N_s=3.17$  (120% design conditions)



Figure H-6: Test series 1.1.1 Initial – After Test with  $N_s=3.17$  (120% design conditions)

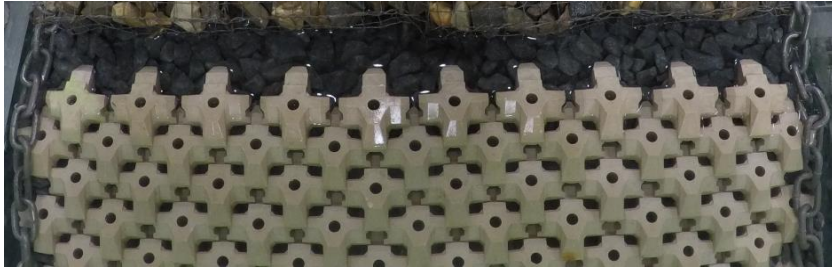


Figure H-7: Test series 1.2.1 Initial – Before Test with  $N_s=1.51$  (60% design conditions)



Figure H-8: Test series 1.2.1 Initial – Before Test with  $N_s=2.05$  (80% design conditions)



Figure H-9: Test series 1.2.1 Initial – Before Test with  $N_s=2.62$  (100% design conditions)



Figure H-10: Test series 1.2.1 Initial – Before Test with  $N_s=2.81$  (110% design conditions)



Figure H-11: Test series 1.2.1 Initial – Before Test with  $N_s=3.11$  (120% design conditions)



Figure H-12: Test series 1.2.1 Initial – After Test with  $N_s=3.11$  (120% design conditions)



Figure H-13: Test series 1.1.2 Initial – Before Test with  $N_s=1.45$  (60% design conditions)



Figure H-14: Test series 1.1.2 Initial – Before Test with  $N_s=1.92$  (80% design conditions)



Figure H-15: Test series 1.1.2 Initial – Before Test with  $N_s=2.44$  (100% design conditions)



Figure H-16: Test series 1.1.2 Initial – Before Test with  $N_s=3.09$  (120% design conditions)



Figure H-17: Test series 1.1.2 Initial – After Test with  $N_s=3.09$  (120% design conditions)



Figure H-18: Test series 1.2.2 Initial – Before Test with  $N_s=1.48$  (60% design conditions)



Figure H-19: Test series 1.2.2 Initial – Before Test with  $N_s=1.99$  (80% design conditions)



Figure H-20: Test series 1.2.2 Initial – Before Test with  $N_s=2.49$  (100% design conditions)



Figure H-21: Test series 1.2.2: Initial – Before Test with  $N_s=2.80$  (110% design conditions)



Figure H-22: Test series 1.2.2 Initial – Before Test with  $N_s=3.07$  (120% design conditions)



Figure H-23: Test series 1.2.2 Initial – After Test with  $N_s=3.07$  (120% design conditions)



Figure H-24: Test series 1.1.3 Initial – Before Test with  $N_s=1.49$  (60% design conditions)



Figure H-25: Test series 1.1.3 Initial – Before Test with  $N_s=2.01$  (80% design conditions)



Figure H-26: Test series 1.1.3 Initial – Before Test with  $N_s=2.52$  (100% design conditions)



Figure H-27: Test series 1.1.3 Initial – Before Test with  $N_s=2.79$  (110% design conditions)



Figure H-28: Test series 1.1.3 Initial – Before Test with  $N_s=3.10$  (120% design conditions)



Figure H-29: Test series 1.1.3 Initial – After Test with  $N_s=3.10$  (120% design conditions)



Figure H-30: Test series 1.2.3 Initial – Before Test with  $N_s=1.52$  (60% design conditions)



Figure H-31: Test series 1.2.3 Initial – Before Test with  $N_s=1.98$  (80% design conditions)



Figure H-32: Test series 1.2.3 Initial – Before Test with  $N_s=2.51$  (100% design conditions)



Figure H-33: Test series 1.2.3 Initial – Before Test with  $N_s=2.82$  (110% design conditions)



Figure H-34: Test series 1.2.3 Initial – Before Test with  $N_s=3.07$  (120% design conditions)





Figure H-35: Test series 1.2.3 Initial – After Test with  $N_s=3.07$  (120% design conditions)



Figure H-36: Test series 1.1.4 Initial – Before Test with  $N_s=1.56$  (60% design conditions)



Figure H-37: Test series 1.1.4 Initial – Before Test with  $N_s=2.16$  (80% design conditions)



Figure H-38: Test series 1.1.4 Initial – Before Test with  $N_s=2.69$  (100% design conditions)



Figure H-39: Test series 1.1.4 Initial – Before Test with  $N_s=2.97$  (120% design conditions)



Figure H-40: Test series 1.1.4 Initial – After Test with  $N_s=2.97$  (120% design conditions)



Figure H-41: Test series 1.2.4 Initial – Before Test with  $N_s=1.57$  (60% design conditions)



Figure H-42: Test series 1.2.4 Initial – Before Test with  $N_s=1.99$  (80% design conditions)



Figure H-43: Test series 1.2.4 Initial – Before Test with  $N_s=2.52$  (100% design conditions)



Figure H-44: Test series 1.2.4 Initial – Before Test with  $N_s=3.05$  (110% design conditions)



Figure H-45: Test series 1.2.4 Initial – Before Test with  $N_s=3.33$  (120% design conditions)



Figure H-46: Test series 1.2.4 Initial – After Test with  $N_s=3.33$  (120% design conditions)

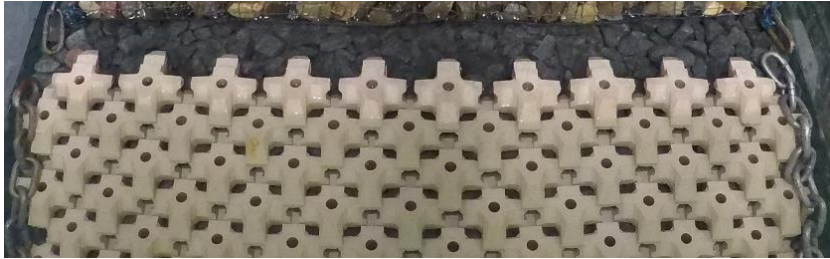


Figure H-47: Test series 1.1.1 Repetition – Before Test with  $N_s=0.74$  (30% design conditions)



Figure H-48: Test series 1.1.1 Repetition – Before Test with  $N_s=0.98$  (40% design conditions)



Figure H-49: Test series 1.1.1 Repetition – Before Test with  $N_s=1.23$  (50% design conditions)



Figure H-50: Test series 1.1.1 Repetition – Before Test with  $N_s=1.48$  (60% design conditions)



Figure H-51: Test series 1.1.1 Repetition – Before Test with  $N_s=1.77$  (70% design conditions)

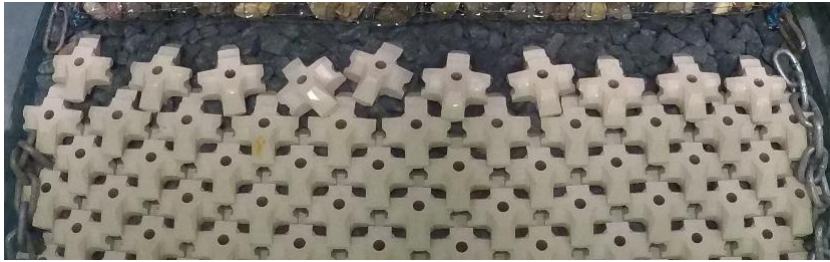


Figure H-52: Test series 1.1.1 Repetition – Before Test with  $N_s=2.08$  (80% design conditions)



Figure H-53: Test series 1.1.1 Repetition – Before Test with  $N_s=2.21$  (90% design conditions)



Figure H-54: Test series 1.1.1 Repetition – Before Test with  $N_s=2.47$  (100% design conditions)

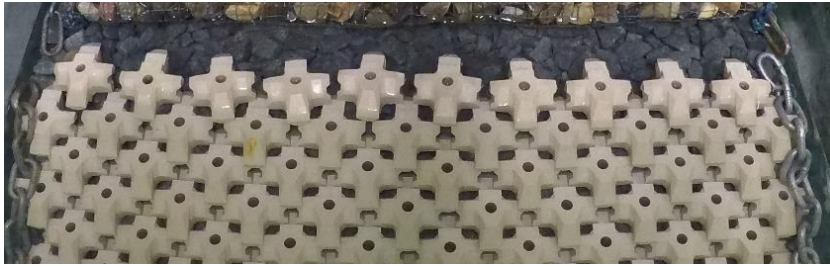


Figure H-55: Test series 1.1.1 Repetition – Before Test with  $N_s=2.72$  (110% design conditions)

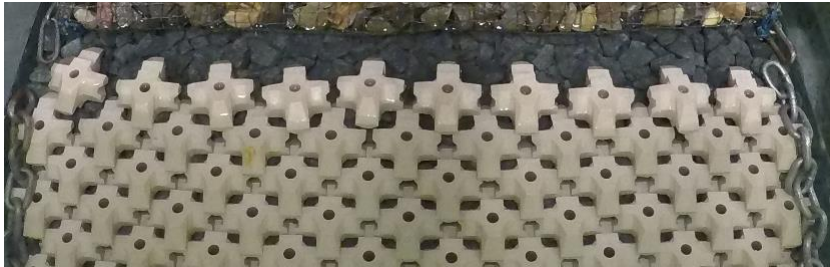


Figure H-56: Test series 1.1.1 Repetition – Before Test with  $N_s=3.01$  (120% design conditions)



Figure H-57: Test series 1.1.1 Repetition – After Test with  $N_s=3.01$  (120% design conditions)

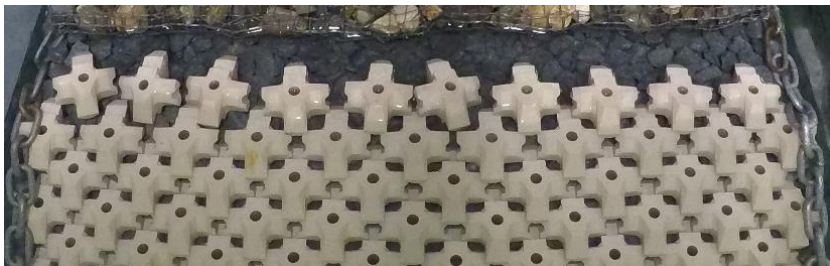


Figure H-58: Test series 1.2.1 Repetition – Before Test with  $N_s=0.49$  (20% design conditions)



Figure H-59: Test series 1.2.1 Repetition – Before Test with  $N_s=0.74$  (30% design conditions)

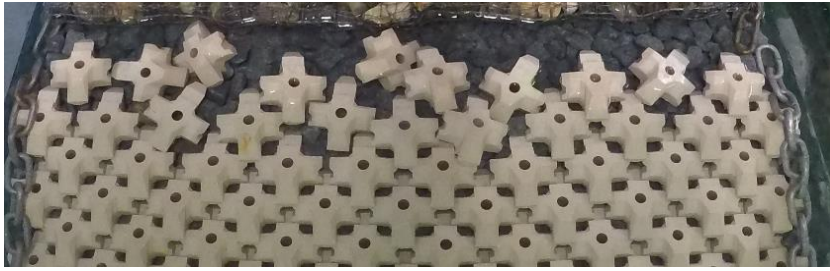


Figure H-60: Test series 1.2.1 Repetition – Before Test with  $N_s=0.98$  (40% design conditions)



Figure H-61: Test series 1.2.1 Repetition – Before Test with  $N_s=1.26$  (50% design conditions)



Figure H-62: Test series 1.2.1 Repetition – Before Test with  $N_s=1.50$  (60% design conditions)

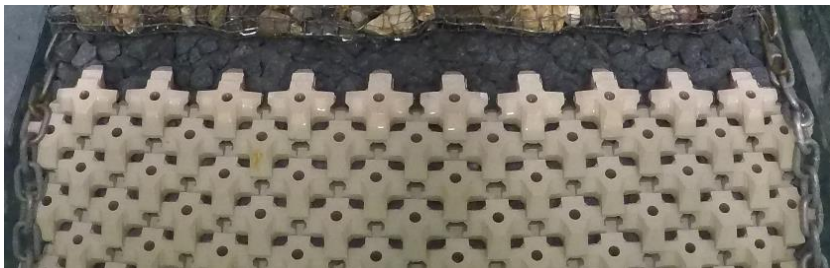


Figure H-63: Test series 1.2.1 Repetition – Before Test with  $N_s=1.69$  (70% design conditions)



Figure H-64: Test series 1.2.1 Repetition – Before Test with  $N_s=1.90$  (80% design conditions)



Figure H-65: Test series 1.2.1 Repetition – Before Test with  $N_s=2.25$  (90% design conditions)

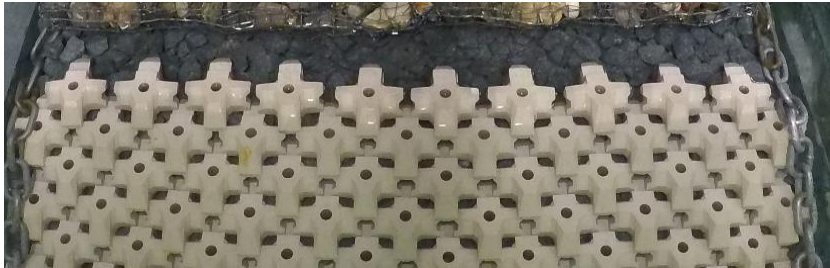


Figure H-66: Test series 1.2.1 Repetition – Before Test with  $N_s=2.43$  (100% design conditions)

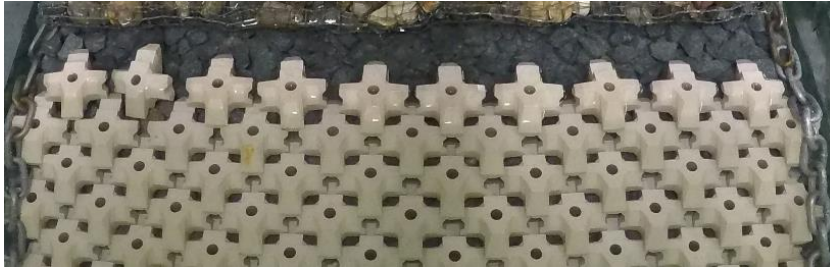


Figure H-67: Test series 1.2.1 Repetition – Before Test with  $N_s=2.73$  (110% design conditions)

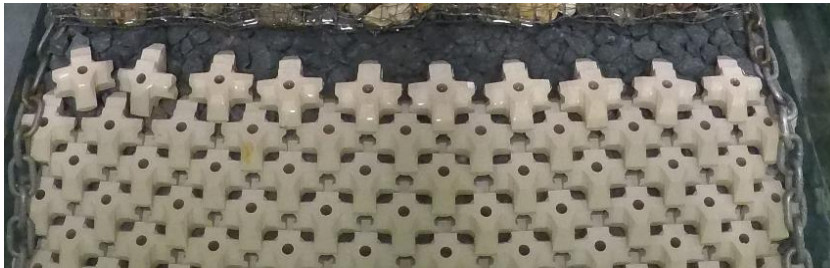


Figure H-68: Test series 1.2.1 Repetition – Before Test with  $N_s=3.03$  (120% design conditions)



Figure H-69: Test series 1.2.1 Repetition – Before Additional Test with  $N_s=3.10$  (120% design conditions)



Figure H-70: Test series 1.1.2.1 Repetition – Before Additional Test with  $N_s=3.10$  (120% design conditions)



Figure H-71: Test series 1.1.2 Repetition – Before Test with  $N_s=0.73$  (30% design conditions)

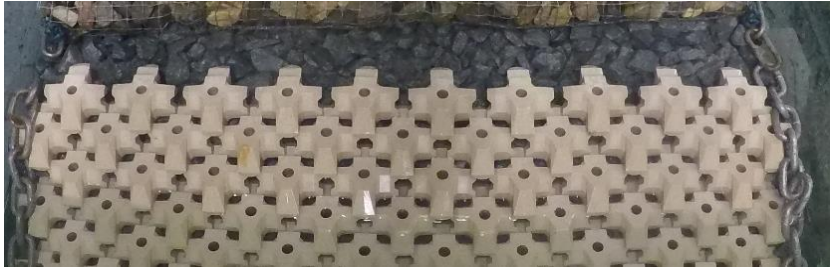


Figure H-72: Test series 1.1.2 Repetition – Before Test with  $N_s=0.97$  (40% design conditions)

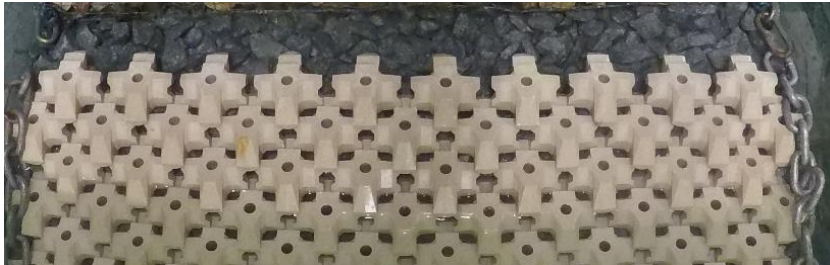


Figure H-73: Test series 1.1.2 Repetition – Before Test with  $N_s=1.24$  (50% design conditions)



Figure H-74: Test series 1.1.2 Repetition – Before Test with  $N_s=1.50$  (60% design conditions)



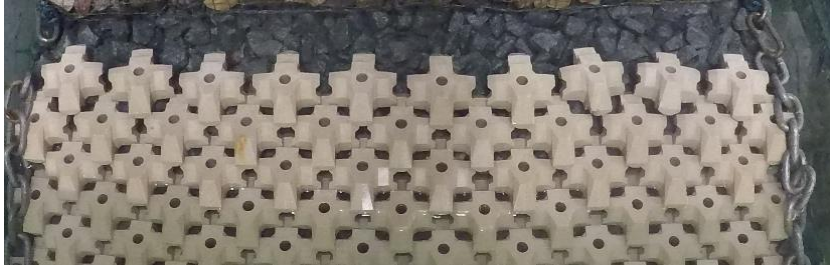


Figure H-75: Test series 1.1.2 Repetition – Before Test with  $N_s=1.79$  (70% design conditions)

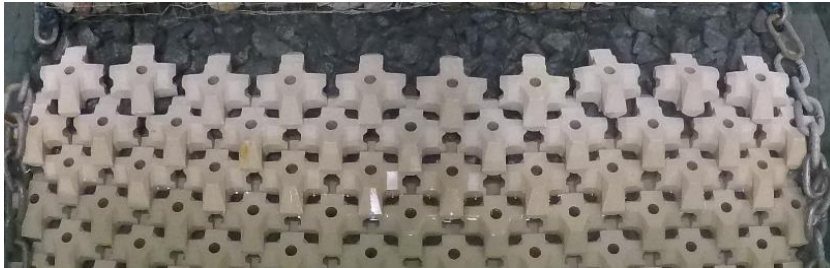


Figure H-76: Test series 1.1.2 Repetition – Before Test with  $N_s=2.06$  (80% design conditions)



Figure H-77: Test series 1.1.2 Repetition – Before Test with  $N_s=2.28$  (90% design conditions)



Figure H-78: Test series 1.1.2 Repetition – Before Test with  $N_s=2.44$  (100% design conditions)

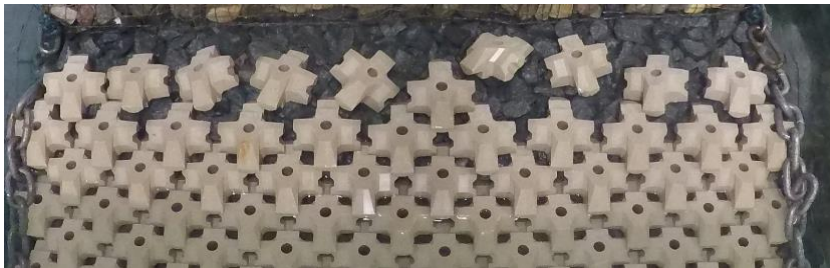


Figure H-79: Test series 1.1.2 Repetition – Before Test with  $N_s=2.79$  (110% design conditions)



Figure H-80: Test series 1.1.2 Repetition – Before Test with  $N_s=3.17$  (120% design conditions)



Figure H-81: Test series 1.1.2 Repetition – After Test with  $N_s=3.17$  (120% design conditions)

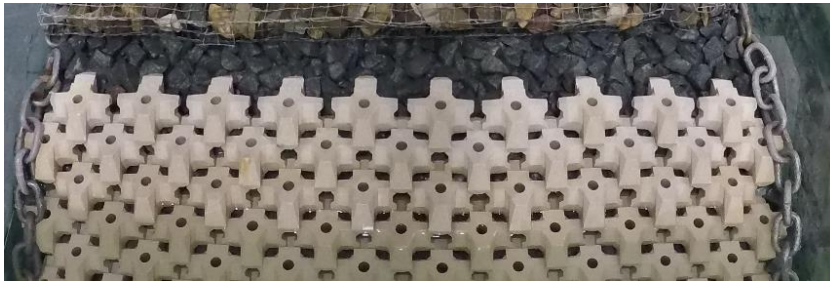


Figure H-82: Test series 1.2.2 Repetition – Before Test with  $N_s=0.76$  (30% design conditions)

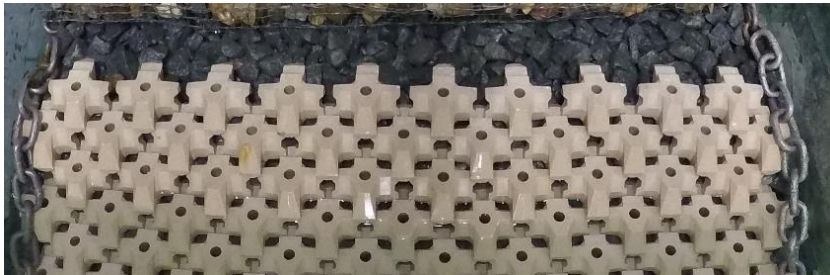


Figure H-83: Test series 1.2.2 Repetition – Before Test with  $N_s=1.01$  (40% design conditions)



Figure H-84: Test series 1.2.2 Repetition – Before Test with  $N_s=1.28$  (50% design conditions)



Figure H-85: Test series 1.2.2 Repetition – Before Test with  $N_s=1.48$  (60% design conditions)



Figure H-86: Test series 1.2.2 Repetition – Before Test with  $N_s=1.69$  (70% design conditions)



Figure H-87: Test series 1.2.2 Repetition – Before Test with  $N_s=1.96$  (80% design conditions)



Figure H-88: Test series 1.2.2 Repetition – Before Test with  $N_s=2.29$  (90% design conditions)



Figure H-89: Test series 1.2.2 Repetition – Before Test with  $N_s=2.42$  (100% design conditions)



Figure H-90: Test series 1.2.2 Repetition – Before Test with  $N_s=2.66$  (110% design conditions)



Figure H-91: Test series 1.2.2 Repetition – Before Test with  $N_s=2.97$  (120% design conditions)



Figure H-92: Test series 1.2.2 Repetition – After Test with  $N_s=2.97$  (120% design conditions)



Figure H-93: Test series 1.1.3 Repetition – Before Test with  $N_s=1.22$  (50% design conditions)



Figure H-94: Test series 1.1.3 Repetition – Before Test with  $N_s=1.49$  (60% design conditions)

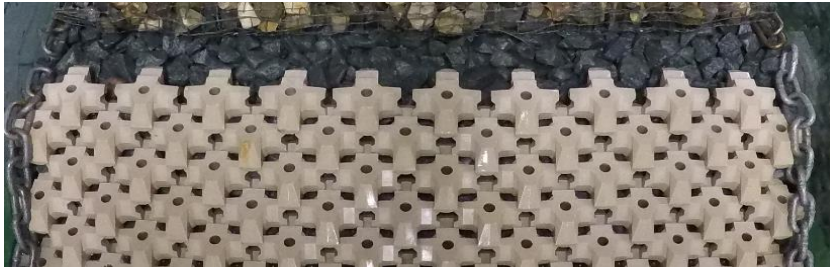


Figure H-95: Test series 1.1.3 Repetition – Before Test with  $N_s=1.76$  (70% design conditions)



Figure H-96: Test series 1.1.3 Repetition – Before Test with  $N_s=2.06$  (80% design conditions)

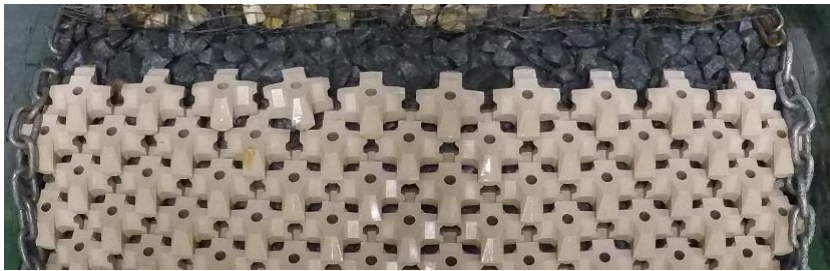


Figure H-97: Test series 1.1.3 Repetition – Before Test with  $N_s=2.27$  (90% design conditions)



Figure H-98: Test series 1.1.3 Repetition – Before Test with  $N_s=2.55$  (100% design conditions)



Figure H-99: Test series 1.1.3 Repetition – Before Test with  $N_s=2.82$  (110% design conditions)

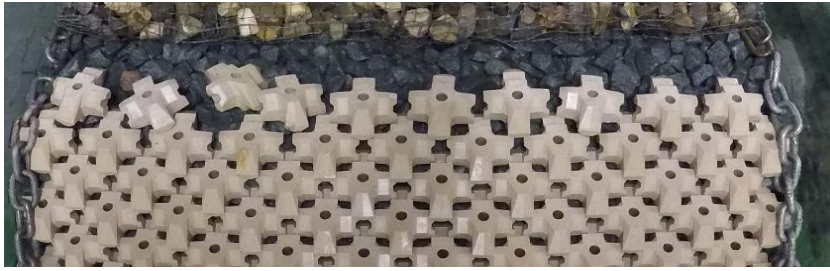


Figure H-100: Test series 1.1.3 Repetition – Before Test with  $N_s=3.14$  (120% design conditions)



Figure H-101: Test series 1.1.3 Repetition – After Test with  $N_s=3.14$  (120% design conditions)

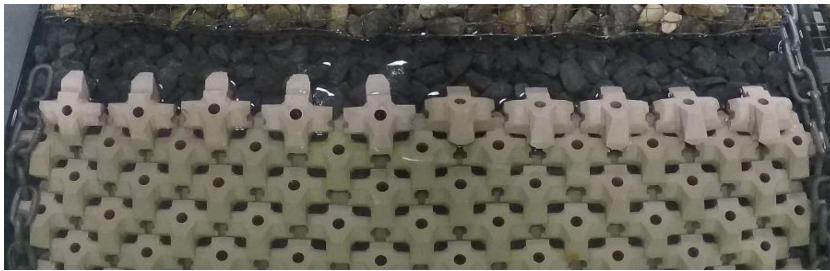


Figure H-102: Test series 2.2.1 – Before Test with  $N_s=1.46$  (60% design conditions)



Figure H-103: Test series 2.2.1 – After Test with  $N_s=1.46$  (60% design conditions)



Figure H-104: Test series 3.2.1 – Before Test with  $N_s=1.45$  (60% design conditions)

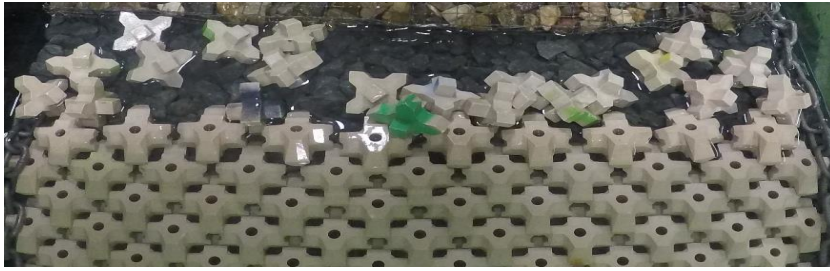


Figure H-105: Test series 3.2.1 – After Test with  $N_s=1.45$  (60% design conditions)



Figure H-106: Test series 4.2.1 – Before Test with  $N_s=1.47$  (60% design conditions)

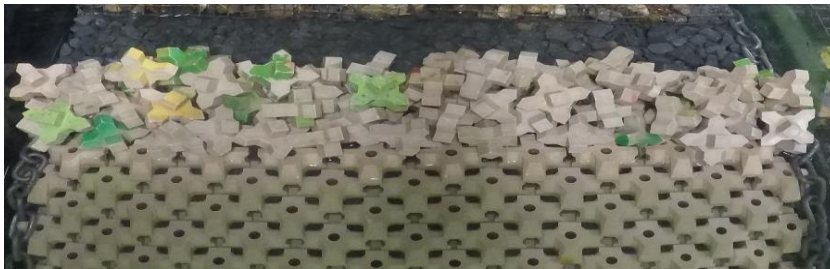


Figure H-107: Test series 4.2.1 – Before Test with  $N_s=1.95$  (80% design conditions)



Figure H-108: Test series 4.2.1 – Before Test with  $N_s=2.48$  (100% design conditions)



Figure H-109: Test series 4.2.1 – Before Test with  $N_s=2.75$  (110% design conditions)



Figure H-110: Test series 4.2.1 – Before Test with  $N_s=3.04$  (120% design conditions)



Figure H-111: Test series 4.2.1 – After Test with  $N_s=3.04$  (120% design conditions)

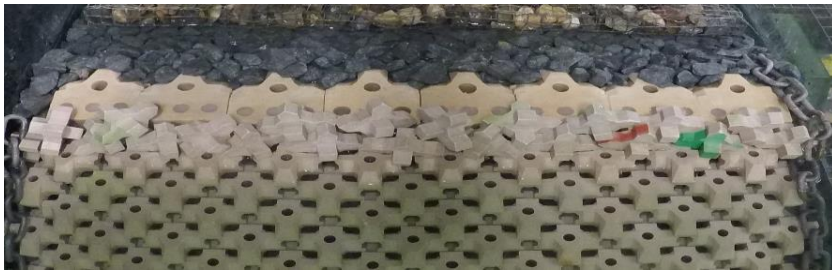


Figure H-112: Test series 5.2.1 – Before Test with  $N_s=1.49$  (60% design conditions)

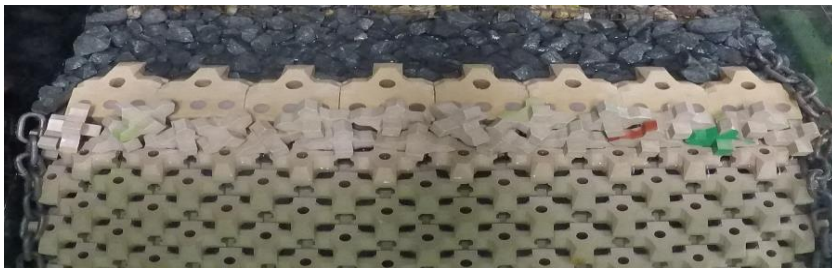


Figure H-113: Test series 5.2.1 – Before Test with  $N_s=1.96$  (80% design conditions)

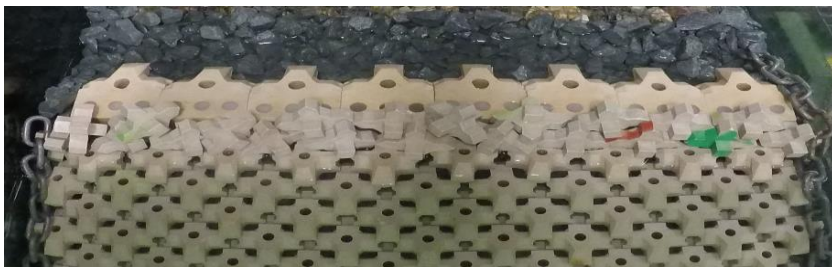


Figure H-114: Test series 5.2.1 – Before Test with  $N_s=2.48$  (100% design conditions)





Figure H-115: Test series 5.2.1 – Before Test with  $N_s=2.74$  (110% design conditions)



Figure H-116: Test series 5.2.1 – Before Test with  $N_s=3.01$  (120% design conditions)



Figure H-117: Test series 5.2.1 – Before Test with  $N_s=3.54$  (140% design conditions)



Figure H-118: Test series 5.2.1 – After Test with  $N_s=3.54$  (140% design conditions)



Figure H-119: Test series 7.2.1 – Before Test with  $N_s=1.49$  (60% design conditions)

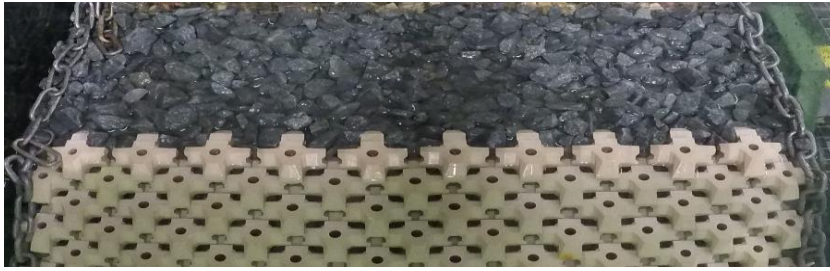


Figure H-120: Test series 7.2.1 – Before Test with  $N_s=1.97$  (80% design conditions)



Figure H-121: Test series 7.2.1 – Before Test with  $N_s=2.50$  (100% design conditions)

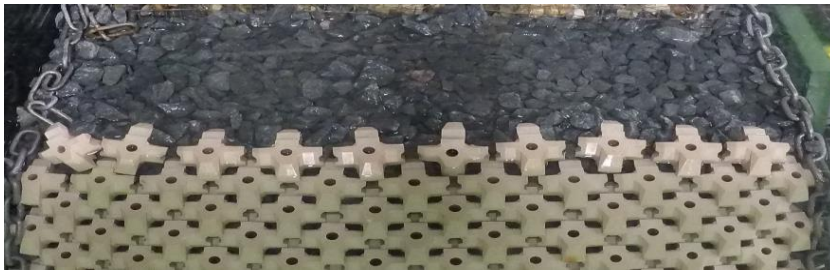


Figure H-122: Test series 7.2.1 – Before Test with  $N_s=2.75$  (110% design conditions)



Figure H-123: Test series 7.2.1 – After Test with  $N_s=2.75$  (110% design conditions)



Figure H-124: Test series 6.1.1 – Before Test with  $N_s=1.54$  (60% design conditions)



Figure H-125: Test series 6.1.1 – Before Test with  $N_s=2.07$  (80% design conditions)



Figure H-126: Test series 6.1.1 – Before Test with  $N_s=2.55$  (100% design conditions)



Figure H-127: Test series 6.1.1 – Before Test with  $N_s=2.78$  (110% design conditions)



Figure H-128: Test series 6.1.1 – Before Test with  $N_s=3.05$  (120% design conditions)



Figure H-129: Test series 6.1.1 – Before Test with  $N_s=3.49$  (140% design conditions)

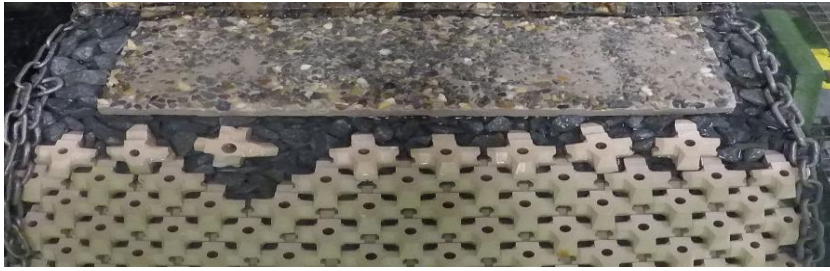


Figure H-130: Test series 6.1.1 – After Test with  $N_s=3.49$  (140% design conditions)



Figure H-131: Test series 6.2.1 – Before Test with  $N_s=1.48$  (60% design conditions)



Figure H-132: Test series 6.2.1 – Before Test with  $N_s=1.96$  (80% design conditions)



Figure H-133: Test series 6.2.1 – Before Test with  $N_s=2.47$  (100% design conditions)



Figure H-134: Test series 6.2.1 – Before Test with  $N_s=2.72$  (110% design conditions)



Figure H-135: Test series 6.2.1 – Before Test with  $N_s=3.00$  (120% design conditions)



Figure H-136: Test series 6.2.1 – Before Test with  $N_s=3.52$  (140% design conditions)



Figure H-137: Test series 6.2.1 – After Test with  $N_s=3.52$  (140% design conditions)



Figure H-138: Test series 6.2.1 – Before Test with  $N_s=1.51$  (60% design conditions)



Figure H-139: Test series 6.2.1 – Before Test with  $N_s=2.05$  (80% design conditions)



Figure H-140: Test series 6.2.1 – Before Test with  $N_s=2.69$  (110% design conditions)



Figure H-141: Test series 6.2.1 – Before Test with  $N_s=3.38$  (140% design conditions)



Figure H-142: Test series 6.2.1 – After Test with  $N_s=3.38$  (140% design conditions)



Figure H-143: Test series 6.2.2 – Before Test with  $N_s=1.48$  (60% design conditions)



Figure H-144: Test series 6.2.2 – Before Test with  $N_s=1.99$  (80% design conditions)



Figure H-145: Test series 6.2.2 – Before Test with  $N_s=2.48$  (100% design conditions)



Figure H-146: Test series 6.2.2 – Before Test with  $N_s=3.03$  (120% design conditions)



Figure H-147: Test series 6.2.2 – Before Test with  $N_s=3.55$  (140% design conditions)



Figure H-148: Test series 6.2.2 – After Test with  $N_s=3.55$  (140% design conditions)

## Table of Figures

Figure 1.1: Left to right: 3D, Front, Back, Left, Right, Top and Bottom view of the Xbloc+ (Delta Marine Consultants) .....	1
Figure 1.2: Main dimensions of Xbloc+ (DMC Guidelines for Xbloc Concept Design, 2018) ....	2
Figure 1.3: Xbloc+ crest element concept for the Afsluitdijk .....	2
Figure 1.4: Thesis Outline .....	3
Figure 1.5: Methodology for physical modelling.....	5
Figure 1.6: Typical cross section of a rubble mound breakwater without filter layer and crown superstructure (Hald, 1998) .....	6
Figure 1.7: Failure modes of a rubble mound breakwater with crown superstructure (Burcharth, 1994) .....	7
Figure 1.8: Armour layer failure modes (Hald, 1998).....	7
Figure 1.9: Forces acting on a stone at slope during wave run-down (left) and run-up (right) (Hald, 1998).....	8
Figure 1.10: Contribution of interlocking, friction and own weight to stability plotted against the structure's slope angle for complex interlocking armour units (left) and bulky units (right). (CEM, 2002) .....	9
Figure 1.11: Concrete Armor Units Categories (Muttray and Reedijk, 2008) .....	10
Figure 1.12: Main wave-structure hydraulic interactions (The Rock Manual, 2007).....	15
Figure 1.13: Freeboard for emerged (left) and submerged (right) breakwater (Burcharth et al, 2005).....	17
Figure 1.14: Stability number of different parts of a breakwater trunk and head as a function of the normalised freeboard. (From Vidal et al. (1992, 1995). (Burcharth et al, 2005).....	17
Figure 1.15: Stability number of different parts of a breakwater trunk as a function of the normalised freeboard, from Burger (1995). (Burcharth et al, 2005) .....	18
Figure 2.1: Top (top of image) and side view (bottom of image) of wave flume (Delta Marine Consultants).....	26
Figure 2.2: Experimental set-up cross section .....	28
Figure 2.3: Model breakwater cross section .....	31
Figure 2.4: Test series 2.2.1 Crest configuration.....	34
Figure 2.5: Test series 3.2.1 Crest configuration.....	35
Figure 2.6: Test series 4.2.1 Crest configuration.....	35
Figure 2.7: Test series 5.2.1 Crest configuration.....	36
Figure 2.8: Test series 6.2.1 Crest configuration.....	37
Figure 2.9: Test series 7.2.1 Crest configuration.....	37
Figure 2.10: Top left: Stable unit; Top right: Stage 1 of partial displacement; Bottom left: Stage 2 of partial displacement; Bottom right: Stage 3 of partial displacement .....	41
Figure 2.11: Examples of failed units .....	41
Figure 3.1: Failed units - Initial & Repetition tests on the single Xbloc+ (1 <sup>st</sup> test set).....	43
Figure 3.2: Failed units at the end of each test series on the single Xbloc+ – Initial and Repetition .....	44
Figure 3.3: Rocking units - Initial & Repetition tests on the Single Xbloc+ (1 <sup>st</sup> test set) .....	46
Figure 3.4: Failed unit at position that facilitates rocking.....	49
Figure 3.5: Total number of Rocking Before failure and Rocking After failure units per test series - Initial and Repetition tests on the single Xbloc+ (1 <sup>st</sup> test set) .....	50
Figure 3.6: Influence of Freeboard & Wave Steepness on Start of Movement .....	51



Figure 3.7: Failed units at 1 <sup>st</sup> , 2 <sup>nd</sup> , 3 <sup>rd</sup> , 4 <sup>th</sup> upper rows - Initial and Repetition tests on the Single Xbloc+ (1 <sup>st</sup> test set).....	53
Figure 3.8: Displaced units at 1 <sup>st</sup> , 2 <sup>nd</sup> , 3 <sup>rd</sup> , 4 <sup>th</sup> upper rows - Initial and Repetition tests on the single Xbloc+.....	54
Figure 3.9: Armour layer at the end of test series 1.1.2 – Repetition.....	54
Figure 3.10: Distances from unit to the underlayer measured before the repetition of the test series on the single Xbloc+ crest elements (dimension in cm) .....	55
Figure 3.11: Points at which the distances from unit to the underlayer were measured .....	55
Figure 3.12: Stability Number at Failure and Distance from Underlayer .....	56
Figure 3.13: Stability Number at Initial Partial Displacement and Distance from Underlayer .....	57
Figure 4.1: Failed units during the Tested Configurations .....	58
Figure 4.2: Failed units at 1 <sup>st</sup> , 2 <sup>nd</sup> , 3 <sup>rd</sup> , 4 <sup>th</sup> upper rows during the Tested Configurations .....	59
Figure 4.3: Displaced units at 1 <sup>st</sup> , 2 <sup>nd</sup> , 3 <sup>rd</sup> , 4 <sup>th</sup> upper rows during the Tested Configurations .	59
Figure 4.4: Rocking units during the Tested Configurations .....	60
Figure 4.5: Optimised configuration from 2 <sup>nd</sup> test set .....	61
Figure 4.6: Failed units during testing on the Optimised Configuration .....	62
Figure 4.7: Crown Element Before movement (Left) and After movement (Right).....	62
Figure 4.8: Rocking units during testing on the Optimised configuration .....	64
Figure 4.9: Failed units at 1 <sup>st</sup> , 2 <sup>nd</sup> , 3 <sup>rd</sup> , 4 <sup>th</sup> upper rows - Optimised Configuration .....	65
Figure 4.10: Displaced units at 1 <sup>st</sup> , 2 <sup>nd</sup> , 3 <sup>rd</sup> , 4 <sup>th</sup> upper rows - Optimised Configuration.....	65
Figure 4.11: Armour layer at the end of test series 6.1.1 .....	66
Figure 5.1: Crest Xbloc+ at stable position, prior to wave action. ....	68
Figure 5.2: Crest Xbloc+ during the initial rotational movement.....	68
Figure 5.3: Crest Xbloc+ during the combined rotational, vertical and horizontal movement. ....	68
Figure 5.4: Crest Xbloc+ at final failed position, after wave action.....	69
Figure 5.5: Various positions acquired by failed units. ....	69
Figure 5.6: Collapsing breaker at the top armour row.....	70
Figure 5.7: Forces during Wave run-up. Single Xbloc+ (left) and Optimised Configuration (right).....	73

---

## Table of Tables

Table 1.1: Forces' Ratios and Scale Numbers .....	23
Table 1.2: Reynolds number above which no viscous scale effects occur .....	25
Table 2.1: Dimensions of Xbloc+ model units .....	28
Table 2.2: Relative freeboard formulations .....	34
Table 2.3: Characteristics of Xblocs used for configurations .....	35
Table 2.4: All tests overview .....	38
Table 3.1: Duration ratio and Failed units ratio (Repetition/Initial) .....	45
Table 3.2: Relation of Rocking before failure and Failed units (All test series) .....	48
Table 3.3: Relation of Rocking after Failure and Failed units (All test series) .....	49
Table 4.1: Failed units - Optimised Configuration & Single Xbloc+ .....	63
Table 4.2: Stable units - Optimised Configuration & Single Xbloc+ .....	63
Table 4.3: Rocking units - Optimised Configuration & Single Xbloc+ .....	63